

# **Transgenic winter wheat – Increased sucrose uptake capacity accelerates plant development and enhances grain yield**

## **Dissertation**

zur Erlangung des akademischen Grades  
Doctor rerum naturalium (Dr. rer. nat.)



vorgelegt an der  
Naturwissenschaftlichen Fakultät I-Biowissenschaften  
der Martin-Luther-Universität Halle-Wittenberg  
Fachbereich Biologie

von

Frau María Isabel Mora Ramírez  
geboren am 08.04.1982 in Cartago, Costa Rica

Gutachter:

1. Prof. Dr. Thomas Altmann
2. Prof. Dr. Uwe Ludewig
3. Prof. Dr. Bettina Hause

Halle (Saale), den 06.10.2016

**This work was supported by:  
German Academic Exchange Service (DAAD), the Leibniz Institute of  
Plant Genetics and Crop Plant Research (IPK) Gatersleben and the  
University of Costa Rica**

# Table of contents

Table of contents .....	iii
List of Figures .....	v
List of Tables .....	vii
Abbreviations .....	ix
Summary .....	1
<b>I. General Introduction.....</b>	<b>3</b>
<b>i. Wheat production: actual situation and effects of climate change.....</b>	<b>3</b>
<b>ii. Wheat yield potential.....</b>	<b>4</b>
<b>iii. Yield components and their importance for yield potential.....</b>	<b>5</b>
<b>iv. Sink strength: important component for plant development and grain filling .....</b>	<b>5</b>
<b>v. Sucrose transporters and their importance for grains' sink strength.....</b>	<b>6</b>
<b>vi. Transgenic HOSUT winter wheat lines .....</b>	<b>8</b>
<b>II. Hypothesis and aim of this study.....</b>	<b>10</b>
<b>1. Chapter. Plant phenology and grain yield of HOSUT lines .....</b>	<b>11</b>
<b>1.1. Introduction.....</b>	<b>11</b>
<b>1.2. Materials and methods .....</b>	<b>12</b>
1.2.1. Plant material, greenhouse conditions and chlorophyll measurements .....	12
1.2.2. Phenological stages of HOSUT lines in comparison with Certo .....	13
1.2.3. Yield-related parameters and grain morphology .....	13
1.2.4. Analysis of grain composition: sucrose, starch, C, N and amino acids .....	13
<b>1.3. Results.....</b>	<b>14</b>
1.3.1. Developmental and phenotypical differences between HOSUT and Certo plants .....	14
1.3.1.1. HOSUT development differs from that of Certo .....	14
1.3.1.2. Apices of HOSUT show accelerated development under field-like conditions .....	15
1.3.1.3. Earlier flowering of HOSUT lines .....	16
1.3.1.4. Increased chlorophyll content of HOSUT plants .....	18
1.3.2. Influence of diminished fertilization on grain yield of HOSUT.....	18
1.3.3. Morphology and composition of fully developed grains of HOSUT and Certo grown under different fertilization conditions .....	20
1.3.3.1. Analysis of sucrose, N and C content .....	21
1.3.3.2. Free amino acid content.....	22
<b>1.4. Discussion .....</b>	<b>23</b>
1.4.1. Accelerated development of HOSUT lines under field-like conditions .....	24
1.4.2. HOSUT lines conserved their yield advantage under limiting nutritional conditions .....	25
1.4.3. Diminished fertilization does not affect the N content in the grains of HOSUT24 .....	26
1.4.4. Altered amino acid content in ripe grains of HOSUT plants.....	26
<b>2. Chapter. Seedling development of HOSUT lines .....</b>	<b>28</b>
<b>2.1. Introduction.....</b>	<b>28</b>
<b>2.2. Materials and Methods.....</b>	<b>29</b>
2.2.1. Plant material and establishment of the <i>in vitro</i> system .....	29
2.2.2. Determination of root dry mass, number of primary roots and length of the root system of seedlings grown <i>in vitro</i> .....	30
2.2.2.1. N- deprived: XS medium.....	30
2.2.2.2. N- supplied XS medium .....	31
2.2.3. Biomass accumulation during early seedling development.....	31
2.2.4. 2D- imaging and analysis of the early root development .....	32
2.2.5. Seedling phenotype of plants grown under field-like conditions .....	33
2.2.6. Evaluation of chlorophyll content .....	33
2.2.7. Determination of C/N, starch, sugar and amino acids content of seedling tissues .....	34
2.2.8. Metabolite and hormone analysis of dried root tissues of HOSUT and Certo plants: GC-MS and UPLC-MSMS profiling.....	35
2.2.8.1. Metabolite analysis by GC-MS.....	35
2.2.8.2. Hormone profiling by UPLC-MS .....	35
<b>2.3. Results.....</b>	<b>36</b>
2.3.1. Grain weight influences early seedling vigour.....	36
2.3.1.1. Frequency distribution of grain weight differs in HOSUT .....	36
2.3.1.2. Effect of same grain weight on seedling vigour.....	36
2.3.1.2.1. High grain weight (54-56 mg) .....	37
2.3.1.2.2. Low grain weight (40-45 mg) .....	38
2.3.1.2.3. Typical grain weight distribution for both lines.....	38
2.3.1.2.4. Effect of grain weight on seedling development and vigour under field-like conditions.....	39

2.3.2.	HOSUT seedling vigour under different growing conditions .....	40
2.3.2.1.	Evaluation under field-like conditions of HOSUT's seedling vigour .....	40
2.3.2.1.1.	Seedling root and shoot biomass.....	41
2.3.2.1.2.	Chlorophyll content in seedlings under field-like conditions.....	42
2.3.2.2.	Analysis of seedling growth under <i>in vitro</i> N-supplied conditions .....	42
2.3.2.2.1.	Chlorophyll content of seedlings under <i>in vitro</i> N-supplied conditions.....	43
2.3.2.2.2.	Root biomass under N-supplied <i>in vitro</i> conditions.....	43
2.3.2.3.	Seedling phenotyping under N-deprived conditions.....	44
2.3.2.3.1.	Root biomass .....	44
2.3.2.3.2.	Number of lateral roots.....	45
2.3.2.3.3.	Chlorophyll content in seedlings grown under <i>in vitro</i> N-deprived conditions .....	46
2.3.3.	Metabolites and hormone profiling in HOSUT and Certo seedlings grown under different growth conditions.....	47
2.3.3.1.	N, C and CHO analyses of <i>in vitro</i> and field-like seedlings at 12-13BBCH.....	47
2.3.3.2.	Metabolite analysis of roots at 12-13BBCH grown <i>in vitro</i> .....	48
2.3.3.3.	Free amino acids in the root system of seedlings under <i>in vitro</i> and field-like conditions.....	49
2.3.3.4.	Auxin and cytokinin content in HOSUT seedlings under N-deprived <i>in vitro</i> conditions .....	50
<b>2.4.</b>	<b>Discussion .....</b>	<b>52</b>
2.4.1.	Influence of the increased HOSUT grain weight on the early seedling phenotype .....	52
2.4.2.	HOSUT performance under <i>in vitro</i> nutritional limiting conditions .....	54
2.4.3.	Changes in HOSUT seedlings' metabolism during early development .....	54
2.4.3.1.	Altered content of sucrose and glucose and their putative effect on the shikimate pathway of HOSUT24 seedlings .....	54
2.4.3.2.	Change in HOSUT's C/N ratio might be involved in lateral root formation.....	56
<b>3.</b>	<b>Chapter. Influence of HvSUT1 on the transcriptome of early developing roots.....</b>	<b>57</b>
<b>3.1.</b>	<b>Introduction.....</b>	<b>57</b>
<b>3.2.</b>	<b>Materials and methods .....</b>	<b>58</b>
3.2.1.	qRT-PCR analysis of HvSUT1 expression in wheat seedlings at distinct developmental stages....	58
3.2.1.1.	Plant material .....	58
3.2.1.2.	RNA isolation .....	58
3.2.1.2.1.	<i>In vitro</i> seedlings .....	58
3.2.1.2.2.	Developing grains.....	59
3.2.1.2.3.	Developing spikes.....	60
3.2.1.3.	cDNA synthesis and qRT-PCR.....	60
3.2.2.	Transcriptome analysis of seedling's root tissue grown under control climatic conditions .....	61
3.2.2.1.	RNA-labelling and array hybridization.....	61
<b>3.3.</b>	<b>Results.....</b>	<b>62</b>
3.3.1.	HvSUT1 expression is also found in vegetative tissues of HOSUT24.....	62
3.3.2.	Comparative gene expression analysis in the root system of seedlings.....	62
3.3.2.1.	Altered carbohydrate metabolism and cell division in roots of HOSUT.....	64
3.3.2.2.	Ca <sup>2+</sup> and G-protein signalling pathways in HOSUT .....	66
3.3.2.3.	Entities of the amino acid metabolism with changed gene expression .....	69
3.3.2.4.	Hormone metabolism is altered in HOSUT24 .....	70
3.3.2.5.	Transcription factors with altered expression levels in HOSUT24 .....	71
3.3.2.6.	Changes in gene expression of entities involved in transport processes .....	73
<b>3.4.</b>	<b>Discussion .....</b>	<b>74</b>
3.4.1.	HvSUT1 expression in vegetative tissues leads to metabolic changes in the seedling.....	75
3.4.2.	Enhanced sucrose-mediated signalling in HOSUT24 activates cell division in roots.....	75
3.4.3.	Sucrose-dependent auxin signalling triggers GTPase and Ca <sup>2+</sup> signalling pathways in HOSUT wheat roots.....	78
3.4.4.	LONESOME HIGHWAY (LHW) and auxin signalling and transport .....	79
<b>III.</b>	<b>General discussion .....</b>	<b>80</b>
<b>i.</b>	<b>Seedling vigour in HOSUT goes beyond from a grain size effect.....</b>	<b>80</b>
<b>ii.</b>	<b>HOSUT vigour and photosynthetic efficiency.....</b>	<b>81</b>
<b>iii.</b>	<b>Better HOSUT performance under limiting conditions might be related to increased N use efficiency .....</b>	<b>82</b>
<b>iv.</b>	<b>Sucrose-induced tryptophan-dependent auxin biosynthetic pathway in HOSUT24 .....</b>	<b>85</b>
<b>v.</b>	<b>Altered sucrose signalling in HOSUT root system plays a role in lateral root branching .....</b>	<b>86</b>
<b>IV.</b>	<b>References.....</b>	<b>90</b>
<b>V.</b>	<b>Supplemental Data.....</b>	<b>103</b>
<b>VI.</b>	<b>Curriculum vitae.....</b>	<b>132</b>
<b>VII.</b>	<b>Declaration (Eklärung).....</b>	<b>134</b>
<b>VIII.</b>	<b>Acknowledgments .....</b>	<b>135</b>

## List of Figures

- Figure 1. FAO statistics on wheat production placement in the global market. A: Top 5 commodities produced worldwide, average of years 2003 – 2013. B: Wheat production shared by regions, average of years 2003 – 2013. Wheat production since the green revolution until present. C: World production of Wheat 1961-2013. Data available at: <http://faostat3.fao.org/>. .....4
- Figure 2. Schematic model of sucrose transport, symplastic and apoplastic pathways from source cells to the sink. Modified from Sauer (2007) and Schroeder et al. (2013). .....7
- Figure 3. The HOSUT construct used for wheat transformation as described in Weichert et al. 2010. HorB1 promoter, accession no. X87232, HorB1 terminator accession no. FN643080 and HvSUT1 cDNA accession no. AJ272309. ....9
- Figure 4. Representation of winter wheat development in relation to the BBCH growth scale (Meier, 2001).14
- Figure 5. Phenological scale showing the growth differences of HOSUT24 and Certo plants according to the BBCH scale during the 2012-2013 season. Red boxes indicate a determinate stage of development. ....15
- Figure 6. Developing apices of HOSUT24 and Certo plants grown under field-like conditions, harvested during the growing season 2012-2013. Apex staging according to (Vahamidis et al., 2014). Plants analysed at A. 23-24BBCH, leaf formation/early tillering. B. 24-25BBCH tillering. C. 29-30BBCH end of tillering/beginning of stem elongation. D. 30-32BBCH stem elongation. ....16
- Figure 7. Flowering time of the three HOSUT lines and Certo grown under field-like conditions. Growing season 2012/2013. Data evaluated in June 2013. A. HOSUT24 and Certo under diminished fertilization. B. HOSUT24 and Certo under complete fertilization. C and D. HOSUT20 and HOSUT12 complete fertilization. ....17
- Figure 8. Free amino acid concentration in ripe grains of HOSUT24 and Certo grown under two distinct fertilization conditions at field-like conditions A. Diminished fertilization, B. Normal fertilization. Grains from the growing season 2012/2013. Vertical bars = means of 6 repetitions  $\pm$  SD.  $P < 0.05$  (\*),  $P < 0.01$  (\*\*),  $P < 0.001$  (\*\*\*) according to T-test. ....23
- Figure 9. Photographs taken from HOSUT20 and Certo plants in spring 2011. A, difference in growth behaviour. B, difference of the early root system. ....29
- Figure 10. Grain characteristics. Frequency distribution pattern of grain weight of 1000 individual grains harvested in 2011, results published in Saalbach et al. (2014). .....36
- Figure 11. Biomass comparison of seedlings emerging from grains of similar grain weight in Certo and HOSUT24 (54-56 mg). Data given per experimental sample (pot=5 plants of each line). Bars  $\pm$  SD. A: Grain rest dry mass. B: Shoot dry mass. C: Number of roots per seedling. D: Root dry mass. ....37
- Figure 12. Biomass comparison of seedlings emerging from grains of similar grain weight in Certo and HOSUT24 (40-45 mg). Data given per experimental sample (pot=5 plants of each line). Bars  $\pm$  SD. A: Grain rest dry mass. B: Shoot dry mass. C: Number of roots per seedling. D: Root dry mass. ....38
- Figure 13. Biomass of seedlings emerging from grains with a weight range of 40-45 mg for Certo and 55-60 mg for HOSUT (median grain weight-distribution pattern). Bars  $\pm$  SD. A: Grain rest dry mass. B: Shoot dry mass. C: Number of roots per seedling. D: Root dry mass. ....39
- Figure 14. Seedling vigour characteristics at 12-13BBCH stage of HOSUT24 and Certo plants grown under field-like conditions. A. Vigour parameters of seedlings grown from similar grain weight (50-55 mg). B. Vigour parameters of seedlings growing from unsorted grains corresponding to the typical grain weight. C. Seedling of the experiment with same grain weight (50-55 mg) for both lines growing under field-like conditions. T-Test  $P < 0.05$  (\*),  $P < 0.01$  (\*\*),  $P < 0.001$  (\*\*\*) . Season 2013-2014. ....40
- Figure 15. Seedling vigour parameters of HOSUT plants grown under field-like conditions at 12BBCH. Values in percentages (Certo = 100%). Kruskal-Wallis Test  $P < 0.05$  (\*),  $P < 0.01$  (\*\*),  $P < 0.001$  (\*\*\*) .41
- Figure 16. Differences detected in SPAD units between three HOSUT lines and Certo (100%, red line). Plants were grown under field-like conditions. Vertical bars:  $\pm$  SD. T-Test  $P < 0.05$  (\*),  $P < 0.01$  (\*\*),  $P < 0.001$  (\*\*\*) . Season 2012-2013. ....42
- Figure 17. Root dry mass evaluated under *in vitro* conditions with depletion or supply of N. A: Root dry mass of HOSUT and Certo plants grown in XS N-deprived medium and XS + 165 mg/l  $\text{NH}_4\text{NO}_3$ . ANOVA  $P < 0.05$  (\*),  $P < 0.01$  (\*\*),  $P < 0.001$  (\*\*\*) . ....43
- Figure 18. Examples of 2-D images used for acquisition of data reflecting root branching at the two leaves

stage (12BBCH). <i>In vitro</i> plants were grown with N-free medium. ....	45
Figure 19. Difference between HOSUT24 and Certo in the number of branching points in the root system at the 12 BBCH stage. Stars show significant differences according to the Kruskal-Wallis test. P<0.05 (*), P<0.01(**), P<0.001(***).....	46
Figure 20. Auxin and cytokinin content in root and shoot tissue of HOSUT24 and Certo at 11BBCH and 12BBCH grown under <i>in vitro</i> N-depleted conditions. T-test P<0.05 (*), P<0.01(**), P<0.001(***). Vertical bars $\pm$ SD. Values given in percentages of Certo = 100% marked with a red dotted line.....	51
Figure 21. Metabolites involved in the auxin biosynthetic pathway found in increased contents in HOSUT seedlings (colour boxes). Modified from Maeda and Dudareva (2012). Dotted lines correspond to several steps in the metabolic pathway. ....	56
Figure 22. Relative expression of HvSUT1 in distinct tissues of HOSUT24. Vertical bars: $\pm$ SD.....	62
Figure 23. Differentially expressed transcripts between HOSUT24 and Certo. T-test P<0.05, FC 1.5. Multiple testing correction: Westfall and Young. A. Venn diagram showing the number of transcripts differentially expressed in Certo and HOSUT24 evaluated at the 11, 12 and 13 BBCH stage of development. B. Percentage of differentially expressed transcripts of known function according to their Bincode classification. Partial list with top 460 significantly different entities available in Supplemental data Table 19.....	63
Figure 24. Differences in gene expression of Carbohydrate metabolism entities. Comparison of HOSUT: Certo (Values in Log <sub>2</sub> of the gene expression fold change). ....	65
Figure 25. Differences in gene expression of transcripts related to processes in cellular organization and cell division. Comparison of HOSUT: Certo (Values in Log <sub>2</sub> of the gene expression fold change). ....	65
Figure 26. Differences in gene expression of transcripts related to signalling processes (A) calmodulin/Ca <sup>2+</sup> (B) G-proteins and GTPase (C) Inositol-Lipid/DAG/ signalling (D) Protein kinases. Comparison of HOSUT:Certo (Values in Log <sub>2</sub> of the gene expression fold change).....	68
Figure 27. Differences in gene expression in the Amino acid metabolism. Comparison of HOSUT:Certo (Values in Log <sub>2</sub> of the gene expression fold change). ....	70
Figure 28. Differences in gene expression of transcripts involved in hormone metabolism. Comparison of HOSUT:Certo (Values in Log <sub>2</sub> of the gene expression fold change). ....	71
Figure 29. Transcription factors differentially expressed in HOSUT24 and Certo at least in one developmental stage. Comparison of HOSUT:Certo (Values in Log <sub>2</sub> of the gene expression fold change). ....	72
Figure 30. Expression pattern of entities involved in transport processes with differences in gene expression. Comparison of HOSUT:Certo (Values in Log <sub>2</sub> of the gene expression fold change). ....	73
Figure 31. Proposed model for the shikimate pathway and auxin biosynthesis altered entities and metabolites in HOSUT roots. Red boxes are transcripts with higher expression at 11-13BBCH. Blue boxes metabolites found in higher concentration in roots or shoots. Small boxes describe higher expression in HOSUT according to developmental stage. Red, higher expression in HOSUT, white same level of expression and blue lower expression in HOSUT. Modified from Ljung (2013); Maeda and Dudareva (2012) and Tzin and Galili (2010).....	86
Figure 32. Proposed model of signalling pathways with changed expression in root tissues of HOSUT plants at the seedling stage under N limiting growing conditions. Metabolites in blue-framed boxes found in higher amounts in HOSUT plants. Transcripts are in red-framed boxes. Inner boxes describe expression in HOSUT according to developmental stage. Red boxes higher expressed in HOSUT, white same level of expression and blue lower expressed in HOSUT. Modified from (Dodd et al., 2010; Rolland et al., 2006; Ruan, 2014).....	88
Figure 33. Distribution pattern of TGW. Growing season <b>2009-2010</b> . Certo grain weight distribution: Median value 44 mg, average value 42.6 mg. HOSUT24 grain weight distribution: Median value 52 mg, average value 50 mg.....	103
Figure 34. Shoot dry mass and plant height at 13 BBCH stage of development in three HOSUT lines. Comparison to Certo (100%, red dotted line). Plants were grown under near-field conditions. Vertical bars: $\pm$ SE, P<0.05 (*), P<0.01(**), P<0.001(***).....	103
Figure 35. Free amino acids measured in lyophilised roots of HOSUT lines 24, 20 and 12 in comparison to Certo at the 13BBCH grown <i>in vitro</i> with N-deprived medium (XS medium). Certo =100% marked by a red dotted line. Vertical bars: $\pm$ SD. ....	105

- Figure 36. Biomass of above ground tissue of HOSUT24 and Certo plants during the growth cycle in the growing season 2012-2013. A. Complete fertilization. B. Diminished fertilization. Vertical bars:  $\pm$ SD. ....108
- Figure 37. Phenological scale of HOSUT lines grown under field-like conditions with complete fertilization in comparison to their wild type Certo. A. HOSUT20 and 12, growing season 2012/2013. B. HOSUT24, growing season 2013/2014. Phenological phases given in the BBCH scale. ....109

## List of Tables

- Table 1. Yield-related parameters evaluated for three HOSUT lines during consecutive harvest periods. Significant differences: P < 0.05(\*), P < 0.01(\*\*), P < 0.001(\*\*\*). Values in percentages of Certo =100%. ....11
- Table 2. Chlorophyll content (SPAD) of plants grown under field-like conditions, diminished and complete fertilization at booting and grain filling stage. Certo =100%. Season 2012-2013. Abs. Absolute value. T-Test \*P < 0.05, \*\*P < 0.01, \*\*\*P < 0.001. ....18
- Table 3. Yield parameters of line HOSUT24 compared to Certo. Plants were grown under field-like conditions under two fertilization conditions. T-Test \*P < 0.05, \*\*P < 0.01, \*\*\*P < 0.001. Values in percentages of Certo (100%)  $\pm$  SD. ....19
- Table 4. Yield parameters calculated for HOSUT20 and HOSUT12 in comparison with Certo. Plants were grown under complete fertilization at field-like conditions during the growing season 2012/2013. T-Test \*P < 0.05, \*\*P < 0.01, \*\*\*P < 0.001. Values in percentages of Certo (100%)  $\pm$  SD. ....20
- Table 5. Evaluation of grain morphology of transgenic line HOSUT24 grown under field-like conditions with two different fertilization conditions. T-Test \*P < 0.05, \*\*P < 0.01, \*\*\*P < 0.001. Values in percentages of Certo (100%)  $\pm$  SD. ....20
- Table 6. Grain morphology of transgenic lines HOSUT12 and HOSUT20 grown under field-like conditions with complete fertilization during the growing season 2012/2013. Values in percentages of Certo (100%)  $\pm$  SD. P<0.05 (\*), P<0.01(\*\*), P<0.001(\*\*\*) according to T-test. ....21
- Table 7. Grain Composition of transgenic line HOSUT24 grown under field-like conditions with two different fertilization conditions during two growing seasons. Values in percentages of Certo (100%)  $\pm$  SD. P<0.05 (\*), P<0.01(\*\*), P<0.001(\*\*\*) according to T-test. ....22
- Table 8. Composition of the XS medium used for cultivation of seedlings under controlled *in vitro* conditions .....29
- Table 9. Seedling root parameters under *in vitro* conditions with N-deprived XS medium. Values in percentages of Certo (100%)  $\pm$  SD. P<0.05 (\*), P<0.01(\*\*), P<0.001(\*\*\*). Root dry mass and number of seminal roots was analysed with ANOVA. Root length data analysis performed with Kruskal-Wallis test. ....44
- Table 10. Chlorophyll content measured in SPAD units at 11, 12 and 13BBCH from seedlings growing *in vitro* in XS medium without N. Values in SPAD units (Abs) and in percentages (Certo = 100%). P<0.05 (\*), P<0.01(\*\*), P<0.001(\*\*\*) .....46
- Table 11. N, C and sugars concentration in roots and shoots of HOSUT24 seedlings at 12-13BBCH in comparison to Certo  $\pm$  SD. T-test P<0.05 (\*), P<0.01(\*\*), P<0.001(\*\*\*) .....48
- Table 12. Metabolites significantly altered in HOSUT24 and HOSUT20 roots in comparison to Certo. The plantlets were grown *in vitro* in N-deprived XS medium, values are given in percentages (Certo= 100%). P-values are corrected according to Bonferroni. ....49
- Table 13. Content of free amino acids in lyophilized shoots and roots of HOSUT24 in comparison to Certo (100%) grown *in vitro* with N-supplied medium (165 mg/L) and *in vitro* with N-deprived medium and field-like conditions, harvested at 13BBCH (values: percentages calculated with Certo as 100%  $\pm$ SD. T-test: P<0.05 (\*), P<0.01(\*\*), P<0.001(\*\*\*)). ....50
- Table 14. Specific forward (F) and reverse (R) primers for qRT-PCR (5' - 3') oriented. ....60
- Table 15. Percentage of N, C and C/N in roots, shoots and grain rest during early seedling development of *in vitro* plants under N-deprived conditions. Comparison of HOSUT24 and Certo (Certo=100%).  $\pm$  SD. Analysis performed until the 13BBCH. ....104
- Table 16. N, C and sugars concentration in roots and shoots of HOSUT20 and HOSUT12 seedlings in comparison to Certo.  $\pm$  SD. T-test. P<0.05 (\*), P<0.01(\*\*), P<0.001(\*\*\*) .....105

Table 17. Free amino acids in lyophilised shoots of HOSUT24 and Certo at the 13BBCH grown <i>in vitro</i> with N-supplied medium, <i>in vitro</i> with N-free medium and under field-like conditions (values: nmol/DWmg $\pm$ SD, percentages are calculated with Certo as 100% T-test . P<0.05 (*), P<0.01(**), P<0.001(***)). .....	106
Table 18. Free amino acids in lyophilised root system of HOSUT24 and Certo at the 13BBCH grown <i>in vitro</i> with N-supplied medium, <i>in vitro</i> with N-free medium and under field-like conditions (values: nmol/DWmg $\pm$ SD, percentages are calculated with Certo as 100% T-test . P<0.05 (*), P<0.01(**), P<0.001(***)). .....	107
Table 19. Partial list of entities with statistical significant differences between HOSUT24 and Certo in root transcriptome analysis at 11, 12 and 13BBCH stage of development. (T-test P-value < 0.05, Multiple testing correction performed: Westfall and Young). Values correspond to the Log <sub>2</sub> of the gene-expression fold change between both lines. 460 entities with the highest values are presented. Coloured cells indicate statistical differences between the lines. Light blue significant differences at 11BBCH, medium blue at 12BBCH and dark blue at 13BBCH.....	110
Table 20. Top 48 entity list with a correlation >0.90 to LHW and a value of Log <sub>2</sub> Fold Change higher than 1.0 at the 11BBCH and lower than -2 at 13BBCH. All entities shown have significant differences between HOSUT24 and Certo at least in one developmental stage according to the transcriptome analysis. Coloured cells indicate statistical differences between the lines. Light blue significant differences at 11BBCH, medium blue at 12BBCH and dark blue at 13BBCH.....	129



## Abbreviations

<b>ABA:</b>	Abcisic acid	<b>min</b>	minute
<b>ABC:</b>	ATP-binding cassette	<b>ml</b>	millilitre
<b>AFL:</b>	Aberrant lateral root formation	<b>mm:</b>	millimetre
<b>ANK:</b>	Ankyrin	<b>mM:</b>	millimolar
<b>ANOVA</b>	Analysis of Variance	<b>MS:</b>	Mass spectrometry
<b>ARF:</b>	Auxin response factor protein	<b>MYB:</b>	Myeloblastosis family of transcription factors
<b>bp:</b>	Base pair	<b>nm:</b>	nanometre
<b>°C:</b>	Degree Celsius	<b>nmol:</b>	nano mol
<b>Ca<sup>2+</sup>:</b>	Calcium	<b>NRT:</b>	nitrate transporter
<b>CaLB:</b>	Calcium-dependent lipid-binding	<b>P:</b>	p-value ('probability')
<b>CaM:</b>	Calmodulin	<b>PCR:</b>	Polymerase chain reaction
<b>cDNA</b>	complementary DNA	<b>pH:</b>	'power of hydrogen', measure of the acidity or basicity of an aqueous solution
<b>CML:</b>	Calmodulin-like	<b>PIN:</b>	PINFORMED protein
<b>CRLK2:</b>	Calmodulin-regulated receptor-like kinase 2	<b>RBR:</b>	Retinoblastoma-related
<b>CWINV:</b>	Cell wall invertases	<b>RKL1:</b>	Receptor-like kinase 1
<b>DAG:</b>	1,2-diacylglycerol	<b>RNA:</b>	ribonucleic acid
<b>DNA:</b>	Desoxyribonucleic acid	<b>rpm:</b>	Revolutions per minute
<b>DW:</b>	Dry weight	<b>RT:</b>	Retention time
<b>e.g.:</b>	<i>exempli gratia</i> (from Latin: per example)	<b>SA:</b>	Salicylic acid
<b>ERF</b>	Ethylene-responsive transcription factor	<b>SAUR:</b>	Small Auxin Up Regulated RNA
<b>EtOH</b>	Ethanol	<b>SD:</b>	Standard deviation
<b>FDR:</b>	False discovery rate	<b>SE:</b>	Standard error
<b>FW:</b>	Fresh weight	<b>Tre-6-P:</b>	trehalose-6-phosphate
<b>g:</b>	gram	<b>T-DNA</b>	transfer-DNA
<b>GDP:</b>	Glutathione diphosphate	<b>TGW:</b>	Thousand grain weight
<b>GFP:</b>	Green fluorescent protein	<b>t-test:</b>	Student's t distribution test
<b>GTP:</b>	Glutathione triphosphate	<b>UPLC:</b>	Ultrahigh performance liquid chromatography
<b>i.e.:</b>	<i>id est</i> (from Latin: that is)	<b>UPLC-ESI-MS:</b>	UPLC-electrospray-ionization-mass spectroscopy
<b>JA:</b>	Jasmonic acid	<b>UV:</b>	Ultra-violet light
<b>JAZ:</b>	Jasmonate-zim-domain protein	<b>WHO:</b>	World health organization
<b>LC-ESI-MS:</b>	Liquid chromatography-electrospray-ionization-mass spectroscopy	<b>WSC:</b>	water soluble carbohydrates
<b>m/z:</b>	mass-to-charge	<b>WT:</b>	Wild type
<b>M:</b>	molar	<b>μ:</b>	micro
<b>m:</b>	milli	<b>μg:</b>	microgram
<b>MAPKKK:</b>	Mitogen-activated protein kinase kinase kinase	<b>μl:</b>	microliter
<b>MATE:</b>	Multi drug and toxic compound extrusion proteins	<b>μM:</b>	micro molar
<b>mg:</b>	milligram		

## Summary

Sucrose is the major photoassimilate that is translocated throughout the plant. It is considered not only as bricks for biomass synthesis, but also is an important signalling molecule, as itself or through the products of its cleavage. Consequently, changes in its transport play an important role in the partitioning of sucrose throughout the plant.

Transgenic winter wheat lines (HOSUT) expressing the barley sucrose transporter HvSUT1(SUT) (Weschke et al. 2000) under control of the barley hordein B1 promoter (HO) increases the sucrose uptake capacity of the developing grains (Weichert et al. 2010) resulting in increased grain yield (Saalbach et al. 2014).

The comparative analyses of yield-related parameters between HOSUT24 and the wild type Certo, performed under field-like conditions with diminished fertilization during two consecutive seasons, indicated better performance of HOSUT24 in grain yield and TGW during consecutive growing seasons.

Comprehensive analyses of the seedling development of three HOSUT lines under *in vitro* and field-like conditions reported enhanced seedling vigour, with more biomass in both roots and shoots compared to their wild type. Increased root biomass in HOSUT corresponded to an increase in the number of later roots formed at early stages. Increased chlorophyll content was determined under different conditions throughout the crop's life cycle. Furthermore, HOSUT lines grown under field-like conditions presented faster growth and earlier flowering.

Seedlings and mature grains of HOSUT24 had a changed biochemical profile in comparison with those of Certo. Free amino acid and untargeted metabolite analyses, determined higher amounts of aromatic amino acids in HOSUT (especially Trp). Roots and shoots of young HOSUT seedlings had increased amounts of sucrose and glucose. Additionally, UPLC-MS/MS hormone analysis on these tissues evidenced differences in the content of IAA and its precursors in both 11 and 12BBCH stage of development; moreover, also lower amounts of cis-zeatin in shoots of HOSUT seedlings.

Through qRT-PCR, high expression of HvSUT1 was detected in the seedlings' vegetative tissues grown under *in vitro* N-depleted conditions. Transcriptome analysis by an 8×60K array, performed on root tissues of *in vitro* HOSUT24 and Certo seedlings grown under N-depleted conditions, identified 2,649 transcripts with significantly different expression levels between both lines, in at least one of the three developmental stages analysed.

From those entities, an important number were involved in CHO metabolism, cell organization and cell division, hormone metabolism, signalling and transport.

Data of increased transcript levels of high and low affinity nitrate transporters during N-depleted conditions suggest a sucrose-glucose-mediated increased nitrogen use efficiency in HOSUT plants. Furthermore, during those stress conditions, the enhanced lateral root formation in HOSUT plants could be product of an altered signalling that changes the shikimate pathway producing increased content of free IAA as well as storage forms. Results in this study suggest a possible sucrose-triggered Trp-dependent pathway of auxin biosynthesis in young wheat roots.

## **I. General Introduction**

### **i. Wheat production: actual situation and effects of climate change**

Since ancient times cereals represent one of the most important food sources in the world (Morris and Bryce, 2000). Nowadays, cultivated wheat corresponds in 95% to bread wheat (*Triticum aestivum* L) and 5% to durum wheat (*T. turgidum* spp) (Shewry, 2009).

FAO statistics (<http://faostat3.fao.org/>) rank wheat at the fifth place in the most produced commodities worldwide (Figure 1A). Wheat production represents 25.4% of the total cereal market (FAO, Cereal Supply and Demand Brief, March 2015), and is the second major food crop, occupying more than 50% of the world's crop-destined area, being Europe and Asia the mayor producers (<http://faostat3.fao.org/>). Consequently, wheat represents an important component of food security discussions around the world.

During the Green Revolution, major changes in the agricultural production systems were originated and crop breeding was importantly enhanced by introduction of dwarf varieties and improved vigour, among other characteristics (Slafer and Araus, 2007). However, in views of climate changes and a growing world population (estimated to reach 9 billion in 2050), future challenges for increasing wheat production are constantly debated.

The climate change brings increased average temperatures, changed rainfall patterns and subsequently aridity. This changes affect crop production, and their effect is evident in present times (Araus et al. 2008; FAO, 2015; Lizana and Calderini, 2013).

According to FAO statistics, wheat production is reaching a plateau and is severely affected by climate change, as has been registered in the last decade, due to a slowdown of the yield potential increase to only 0.50% per year (Fisher, 2007) (Figure 1C). This reality represents a major threat for food security and a challenge for crop breeders and crop scientists.

Asia alone generates 44% of the world's wheat production (Figure 1B). Temperature increases in South Asia and Africa may result in a decline in crop yield and in the case of wheat it could drop 17% (Wheeler and von Braun, 2013), in this way diminishing food availability, especially in climate change-affected areas, which are already economically vulnerable. Diverse strategies are needed, in order to overcome future food requirements and guarantee its availability and stability of prices.

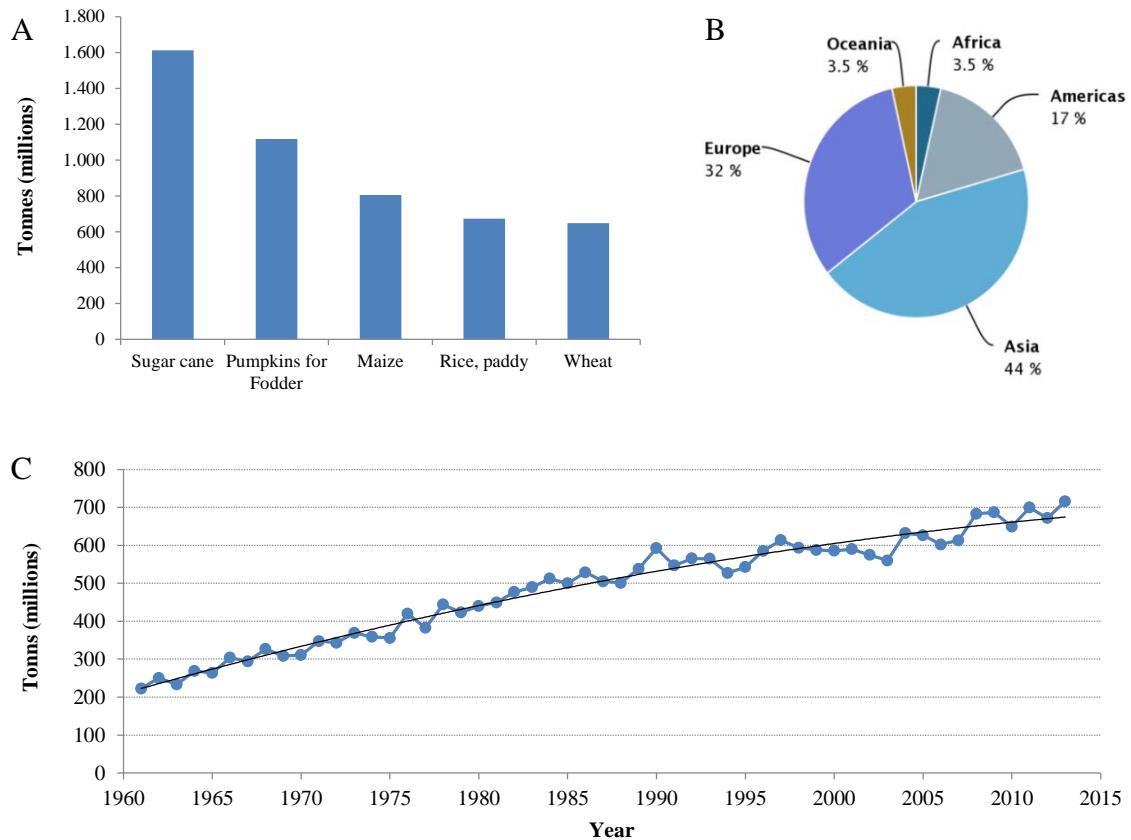


Figure 1. FAO statistics on wheat production placement in the global market. A: Top 5 commodities produced worldwide, average of years 2003 – 2013. B: Wheat production shared by regions, average of years 2003 – 2013. C: World production of Wheat 1961-2013. Data available at: <http://faostat3.fao.org/>.

## ii. Wheat yield potential

Yield potential is defined as the maximal production capacity of a given crop genotype under its optimal environmental conditions (Hawkesford et al., 2013), without limitations in nutrition or water supply and controlled pests, diseases and other types of stresses (Evans and Fischer, 1999). Increased yield potential can also be associated to increased yield under moderate stress conditions (Araus et al. 2008; Hawkesford et al. 2013).

Grain number per area ( $m^2$ ) and grain weight, are important components of yield potential in wheat. In the last century, breeding programs have made great efforts to increase grain number per spike, through improvements in the floret survival in the spikelet. However, a down side was the decrease in grain weight obtained in parallel (Araus et al., 2008; Reynolds et al., 2009, 2012; Slafer and Araus, 2007).

Foulkes et al. (2011) and Reynolds et al. (2012) discussed breeding approaches to rise wheat yield, ranging from increasing photosynthetic capacity and  $CO_2$  fixation,

optimization of phenology and partitioning of assimilates to maximize spike fertility and grain yield. They also mentioned the importance of an adequate root system for resource capture and improving lodging resistance.

Nowadays China is the largest wheat producer. Its production represents ca. 22% of the total produced worldwide (<http://faostat3.fao.org/>). Their punctual strategies to improve yield potential follow, in most of the cases, the discussions in Foulkes et al. (2011) and Reynolds et al. (2012).

Efforts have been made to increase the number of grains per m<sup>2</sup>, grain weight per spike, harvest index, chlorophyll content, stem water soluble carbohydrate (WSC) content at anthesis and to potentiate photosynthesis at grain filling (Hawkesford et al., 2013). In that direction, Dreccer et al. (2009) determined a tendency of wheat genotypes with increased WSC to produce heavier grains with the positive outcome of increased yield in those genotypes.

### **iii. Yield components and their importance for yield potential**

Grain yield per m<sup>2</sup> is the product of grain number and grain weight. The number of spikes per m<sup>2</sup> and the number of grains per spike define the grain number per m<sup>2</sup>. The latter can also be divided into number of spikelets per spike and number of grains per spikelet (Slafer et al. 1996). Additionally, spikelet number and fertile floret number per spike also play an important role in determining yield potential (Dreccer et al., 2014; González et al., 2011; Guo and Schnurbusch, 2015).

Grain weight is limited by its sink strength also under optimal assimilate supply (Serrago et al. 2013). Handling one of the yield components, *e.g.* grain number per spike (Slafer et al. 1996) or grain weight, will undoubtedly affect yield (Blanco et al., 2012; Slafer and Andrade, 1993; Hawkesford et al., 2013; Reynolds et al., 2009).

### **iv. Sink strength: important component for plant development and grain filling**

Carbon partitioning is the process in which photoassimilates, mainly in the form of sucrose, are distributed throughout the plant. This process is driven by the strength of sink and source tissues (Braun and Slewinski, 2009; Reynolds et al., 2012). Higher sink strength in plants refers to the increased ability of an organ or tissue in capturing and storing assimilates from photosynthesis. Sink strength will be determined by cell number

(sink size) and the physiological process for uptake in the cells (sink activity) (Bihmidine et al., 2013; Blum et al., 1988; Herbers and Sonnewald 1998; Marcelis 1996; Serrago et al., 2013; Weichert et al., 2010).

Sink organs can be grouped into sinks for development and sinks for storage. The latter ones typically emerge at later developmental stages and are organs such as stems, tubers, fruits and grains, which are involved in the temporal storage of photoassimilates for later use. The former ones are organs that, due to their active growth, demand an important amount of assimilates and nutrients, *i.e.* meristems and developing leaves and roots (Herbers and Sonnewald, 1998). Therefore dynamics of source and sink capacities will change during crop development (Reynolds et al., 2012).

In cereals, during the vegetative growth, the root system is the main sink of the plant; later on, this role is taken over by the reproductive tissues. The developing spike requires high amounts of assimilates for fast cell division and development. During pre-anthesis, developing anthers are the main sink followed by the ovary and finally the developing grain (Gupta et al. 2006; Ji et al., 2010; Peleg et al. 2011).

Grain filling is a key period, during which, grain size and weight are determined. Therefore, the capacity of the grain to attract assimilates and to store them will be responsible for yield production. Manipulation of the grain sink strength is a promising approach to improve different yield parameters such as harvest index, which in turn will influence grain yield. Weichert et al. (2010) determined in winter wheat, that enhancing the sink strength in developing grains by increasing sucrose uptake capacity has a positive effect on grain weight and therefore yield of winter wheat lines.

Lines with increased assimilate supply towards developing tissues might also be advantageous under changing climate conditions, *e.g.* the evaluation of a number of wheat lines with increased amounts of soluble carbohydrates performed by Dreccer et al. (2014), which presented increased floret survival after treating them with increased temperatures and longer photoperiods.

## **v. Sucrose transporters and their importance for grains' sink strength**

Photosynthesis transforms sunlight energy and atmospheric CO<sub>2</sub> into chemical energy in the form of carbohydrates. Sucrose is the major form in which carbon (therefore energy) is transported over long distances across the plant. This is due to the chemical stability of

the molecule, which can be split up into glucose and fructose by invertases once it reached its destiny (Sauer, 2007). Sucrose is transported throughout the plant from photosynthetically active source tissues towards sink tissues such as developing roots, developing grains and other storage tissues (Sauer 2007; Truernit 2001; Wind et al. 2010).

Sucrose translocation throughout the plant can be symplastic through the plasmodesmata, or apoplastic through membrane transporters as presented in Figure 2. Sucrose translocation starts at the mesophyll source cells and is directed towards the phloem for later distribution. Initially, sucrose is transported out of the mesophyll cells through SWEET transporters (Braun, 2012; Chen et al., 2012; Schroeder et al., 2013). Then, sucrose is imported into the phloem's companion cells (CC) through membrane localized  $H^+$ /symporters called sucrose transporters, which are necessary for sucrose import from the apoplast to the phloem as symplastic continuity is missing between the mesophyll cells and the CC/sieve element complex. Sucrose then will be transported through the phloem towards sink organs *i.e.* young vegetative tissues, roots, developing grains, etc. (Aoki et al., 2004; Sauer, 2007).

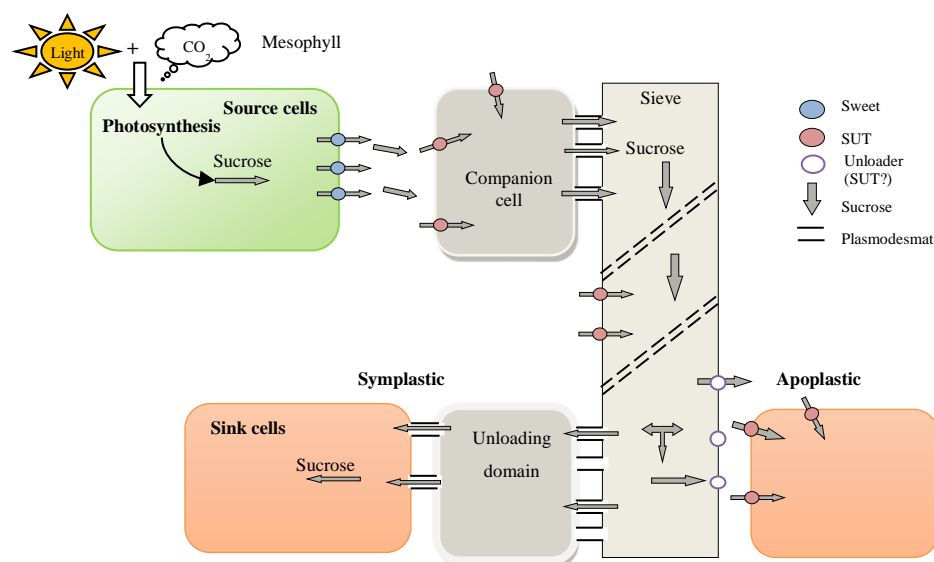


Figure 2. Schematic model of sucrose transport, symplastic and apoplastic pathways from source cells to the sink. Modified from Sauer (2007) and Schroeder et al. (2013).

Once in the sink tissues, sucrose is unloaded from the vascular parenchyma and can be transported either symplastically or apoplastically or by a combination of both as mentioned in Kühn and Grof (2010).

Sucrose transporters are crucial elements, especially in symplastically isolated tissues



such as developing pollen, pollen tubes, guard cells and the developing grains, which depend on sucrose import for their development (Weschke et al., 2000; Sauer, 2007).

Sucrose transporters are classified according their affinity into high affinity transporters, sensors or low affinity transporters (Kühn, 2003). In wheat, three sucrose transporters have been identified. Each member of the gene family is represented in the A, B and D genome (Aoki et al., 2004).

The sucrose transporters: HvSUT1, TaSUT1 (wheat), OsSUT1 (rice) and ZmSUT1 (maize) share sequence similarities. Different phylogenetic analysis also reported their proximity (Kühn and Grof, 2010; Sauer, 2007). ZmSUT1 is highly expressed in source leaves functioning in phloem loading. TaSUT1 transcripts accumulate in sieve elements of the phloem of wheat leaves, as well as in developing and germinating grains (Aoki et al. 2002; 2004; 2006).

High levels of HvSUT1 mRNA have been detected in developing seeds during grain filling. The transcripts accumulate in the maternal nucellar projection and in the endosperm transfer cells (Weschke et al., 2000). These tissues are crucial for assimilate transfer from maternal to filial tissues during development and endosperm filling.

Manipulation of the CHO metabolism by increasing the transport of sucrose is a promising approach, which positively alters plant development. Sucrose has to be considered not only as an energy source and building block for starch synthesis, but also as a signalling molecule, either directly or indirectly through the signalling effects of glucose (Gibson, 2005; Rolland et al., 2006; Rosche et al., 2002; Yadav et al., 2015).

Sucrose and glucose levels and fluxes have been linked to the timing and determination of given events such as root formation in Arabidopsis or tuber development in potato modulating tuber production and seedling development. A cross talk with hormones and significant influences on gene expression have been documented (Gibson 2005; LeCLere et al. 2010; MacGregor et al. 2008).

## **vi. Transgenic HOSUT winter wheat lines**

HOSUT lines express the barley sucrose transporter HvSUT1 (SUT) under the control of the promoter and terminator from Hordein B1 (HO) of barley (Figure 3). The transgenic lines were established in the winter wheat Certo cultivar (Weichert et al., 2010). Regulatory elements from a storage protein gene in cereals (Hordein B1) were used for

endosperm expression of the transgene. Three independent homozygous lines carrying one copy of the transgene were established. The lines are marker-gene free.

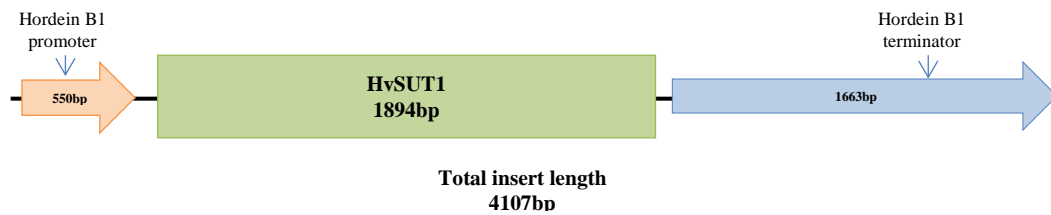


Figure 3. The HOSUT construct used for wheat transformation as described in Weichert et al. 2010. HorB1 promoter, accession no. X87232, HorB1 terminator accession no. FN643080 and HvSUT1 cDNA accession no. AJ272309.

Hordeins are grain storage proteins, that are highly expressed in the developing endosperm of barley (Furtado et al., 2009; Shewry et al., 2001; Weichert et al., 2010). Hordeins belong to the prolamin storage-protein group. In wheat, these proteins are gliadins and glutenins (high molecular weight glutenins, HMW, and low molecular weight glutenins, LMW). They are crucial determinants of grain quality. Moreover, prolamin levels in the grain reflect the N status of the plant. Prolamin gene expression is regulated by N and S availability in the plant and had been detected exclusively in the developing endosperm (Shewry et al., 2001).

Furtado et al. (2008) used rice as a model to evaluate the specificity of prolamin promoters. They evaluated one HMW glutenin promoter from wheat and two hordein promoters of barley, among them the promoter from Hordein B1. The authors concluded that in the heterologous system that was used (rice) those promoters are leaky, expressing the GFP marker also in vegetative tissues. Furtado et al. (2009) performed a similar experiment in barley. In this case, the wheat HMW glutenin promoter was also endosperm specific in barley. No studies using barley hordein promoters in wheat were presented.

In developing barley grains, HvSUT1 is expressed in the endosperm transfer cells, the nucellar projection, and in the integument/nucellar epidermis region (Weschke et al., 2000). Weichert et al. (2010) performed an initial evaluation of the HOSUT lines. In that study, the authors showed that, high expression of the transgene in developing grains is related to an enhanced sucrose uptake capacity during grain development. In addition, diverse changes in the developing grain metabolism were detected such as in the central carbon metabolism and amino acid biosynthesis. Changes in signalling involving both sugars and hormones were suggested by the authors.

## II. Hypothesis and aim of this study

Adequate food supply in the next decades has become a major topic of discussion due to the climate change effects on crop production. Genetically new crop plants, with higher grain yield, showing also high efficiency in their assimilate-usage under changing climate conditions, will be helpful not only as tools to overcome this problem but also as models to elucidate the metabolic pathways determining higher yield and overall better plant performance.

HOSUT lines produce grains of increased weight and size, which results in an augmented yield. Additionally, there had been evidences of better performance of the early HOSUT shoot and root system in comparison to the wild type control.

In this study, **analyses of the yield potential were performed also under different soil fertilization regimes in order to assess the potential of these novel lines under nutrient limitation growth.** Analysis of HOSUT expression at the whole-plant level is one part of these studies.

Sucrose is a signalling molecule that has been correlated with cell division, differentiation and expansion. It is hypothesized that the cross-talk between sucrose and other signalling pathways -that includes hormone signalling- might be altered in the HOSUT lines due to an enhanced sucrose transport to developing tissues, enhancing seedling development and overall performance of the HOSUT lines.

Consequently, **this study aims to uncover the positive effects of HOSUT expression not only in developing grains but also in other sink tissues like seedling roots, shoots, developing leaves and developing spikes.** Differences in plant performance were characterized by comprehensive phenotyping of three HOSUT lines and their non-transformed wild type control Certo, focusing first on early seedling development under distinct *in vitro* growth conditions and later under field-like conditions.

Expression of the transgene alters the carbohydrate metabolism in developing grains as shown by Weichert et al. (2010). Moreover, sugars are known to be signalling molecules involved in triggering diverse developmental processes. **In its last part, this work aimed to identify regulators responsible for the enhanced performance of HOSUT plants by omics analyses.** Specifically, by analysing the transcriptome of HOSUT seedling roots, the relationship between sucrose transporter expression and accelerated development was uncovered.

# 1. Chapter. Plant phenology and grain yield of HOSUT lines

## 1.1. Introduction

Assuring basic food supply for an increasing world population, puts enormous pressure on the environment; either more lands are needed, more fertilization input is required or more efficient lines must be developed. The latter is the most environment friendly solution.

Increasing the yield potential in cereals and particularly in wheat has been a topic of discussion since previous years (Reynolds et al., 2012). Climate change and global warming influence cereal performance. Temperatures before and during anthesis become important for grain weight at maturity, *i.e.* the higher the temperatures, the lighter the grain (Calderini et al., 2001).

Extensive evaluation of novel HOSUT lines was carried out under field-like conditions and were published in Saalbach et al. (2014). Three transgenic winter wheat lines (HOSUT24, 20 and 12) harbouring one homozygous copy of the transgene at independent genomic loci were developed by *Agrobacterium*-mediated transformation of the winter wheat cultivar Certo and evaluated over three vegetation periods (Table 1). HOSUT lines were grown together with the respective control (non-transgenic winter wheat Certo) under field-like conditions in non-heated glasshouses.

Under these conditions, the HOSUT lines had a better performance than their non-transgenic counterpart Certo (Table 1).

Table 1. Yield-related parameters evaluated for three HOSUT lines during consecutive harvest periods. Significant differences: P < 0.05(\*), P < 0.01(\*\*), P < 0.001(\*\*\*). Values in percentages of Certo =100%.

Line	Year of harvest	Yield (%)	TGW (%)	N-yield per plot (%)
HOSUT20	2009	123.8*	129.3***	121.5***
	2010	117.8	120.7***	114.9
	2011	135.1**	122.1***	121.7
HOSUT24	2010	120.9**	133.7***	130.8***
	2011	128.0**	119.5***	112.1
HOSUT12	2010	139.6*	116.7	139.2***

Source: Saalbach et al., 2014.

In this chapter, a detailed phenological comparison between HOSUT and the non-transgenic control Certo is described, assessing the differences in vegetative development

and growth parameters, which might be responsible for an increase in HOSUT source capacity. Furthermore, detailed yield parameters evaluation of three HOSUT lines was performed in order to bring a better and complete comprehension of the parameters determining the increased yield in HOSUT lines.

The potential of the lines under challenging environmental conditions was not evaluated in Saalbach et al. (2014); therefore, evaluation of HOSUT potential under diminished fertilization during two growing seasons was performed.

## **1.2. Materials and methods**

### ***1.2.1. Plant material, greenhouse conditions and chlorophyll measurements***

Grains of the transgenic lines HOSUT20 and 12 together with the wild type Certo were planted in natural soil in two non-heated glass houses in field-like planting densities during mid October 2012 for growing season 2012/2013. Grains were sown directly into the soil in a depth of 2 cm in 16 plots of 0.5 m width x 1.0 m length. Each plot contained 200 seeds distributed in five rows with spacing of 12.5 cm between rows and 2.5 cm between grains. Plots of each line were set in a randomized design. Complete fertilization was applied during the crop's life cycle (ca. 200kg of N/ha) applied at two distinct time points, half of the amount before sowing and the rest during early spring.

Following the abovementioned greenhouse and sowing conditions, HOSUT24 and Certo were exclusively sown in two houses. One of these two houses received complete fertilization during the crop life cycle, applied as mentioned before. In order to evaluate the yield potential of the transgenic line under diminished fertilization, the second house received only the initial fertilization at sowing, ca. 100kg of N/ha. This experiment was performed during two growing seasons: 2012/2013 and 2013/2014.

Chlorophyll measurements of the developing plants growing under field-like conditions were performed at booting and at grain filling stages. Measurements were performed using the Chlorophyll meter SPAD-502 from Minolta. 20 plants per plot were evaluated, each plot corresponded to one biological replication per line per developmental stage for a total of 8 biological replications. Statistical analysis was performed with InfoStat vr. 2011, InfoStat Group ([www.infostat.com.ar](http://www.infostat.com.ar)).

### ***1.2.2. Phenological stages of HOSUT lines in comparison with Certo***

During the growing seasons 2012/2013 and 2013/2014, a comparative phenology analysis of HOSUT and Certo was performed under field-like conditions. For the first crop period all three HOSUT lines were compared with Certo, in addition line HOSUT24 was also evaluated under diminished fertilization. During the second growing season only HOSUT24 was evaluated under complete fertilization and diminished fertilization. In both cases, comparisons were performed with their corresponding Certo.

For identification and standardization of the phenological stages in the development of wheat, the BBCH scale was used as detailed in Meier (2001).

### ***1.2.3. Yield-related parameters and grain morphology***

Yield-related parameters were evaluated comparing HOSUT lines with Certo. Parameters such as grain yield per plot, thousand grain weight (TGW), number of spikes per plot, tiller number per plant at the early stem elongation stage, number of grains per spike and number of spikelets per spike and N-yield per plot were measured.

For grain morphology the width, length and area of HOSUT24 and Certo ripe grains were analysed after harvest. Harvested grains of cropping season 2012-2013 and 2013-2014 were analysed for HOSUT24. HOSUT20 and 12 were analysed only during 2012-2013.

HOSUT24 grains obtained under both diminished and complete fertilization were used for these analyses. For HOSUT20 and 12 only grains of complete fertilization conditions were evaluated. A random sample of 50g of pooled harvested grains per plot was used for analysis with the digital seed analyser MARVIN ([www.gta-sensorik.com](http://www.gta-sensorik.com)).

Statistical analyses were performed with InfoStat vr 2011, InfoStat Group ([www.infostat.com.ar](http://www.infostat.com.ar)).

### ***1.2.4. Analysis of grain composition: sucrose, starch, C, N and amino acids***

Ripe grains were used for these analyses. Samples of each plot were thoroughly mixed in order to obtain a representative sample of the plot. Then, 5 g per plot was grinded using a Retsch® MM400 mill. The resulting powder was used in following analyses. Each plot corresponded to a biological replication. Three technical repetitions per plot were analysed.

Total carbon (C) and nitrogen (N) were determined with a Vario EL Elementar analyser ([www.elementar.de](http://www.elementar.de)). C/N ratio was also calculated. Sucrose and starch were determined

according to Weichert et al. (2010). The data was analysed by a T-test performed with InfoStat vr. 2011, InfoStat Group (www.infostat.com.ar).

For extraction of free amino acids, a powdered sample of ca. 15 mg was incubated with 80% EtOH for 60 min at 60°C under constant agitation; 150 nmol of internal standard was added to each sample. Probes were centrifuged by 15 min and 50 µl of each extract were taken for derivatization with a AccQ-Tag derivatization kit from Waters according to the manufacturer's instructions. Further analysis was performed by an Acquity UPLC system for amino acid analysis from waters, using column AccQ-Tag Ultra RP 1.7 µm particles. Mobile-phase A corresponded to AccQ-Tag Ultra Eluent A and mobile-phase B to AccQ-Tag Ultra Eluent B both from Waters. Flow rate was set to 700 µl/min and the detection was UV@260nm. Standards used for calibration were the amino acid standard solutions from Waters® to which asparagine (132.12 g/mol), glutamine (146.15 g/mol), tryptophan (204.23g/mol), GABA (103.12 g/mol) and norvalin (117.15 g/mol) were added fresh according to the manufacturer's recommendation. Data acquisition and chromatogram analysis were performed with Waters EMPOWER 2 software. Statistical analysis was performed with T-Test through InfoStat vr. 2011. InfoStat Group (www.infostat.com.ar).

### 1.3. Results

#### 1.3.1. Developmental and phenotypical differences between HOSUT and Certo plants

##### 1.3.1.1. HOSUT development differs from that of Certo

Faster growth of HOSUT plants was observed during their entire life cycle; though, the differences with respect to the BBCH phenological scale are not clearly pronounced during early seedling stages such as 11-13BBCH, differences in biomass indicated enhanced seedling vigour of HOSUT (detailed information in Chapter 2). A representation of wheat development in relation to the BBCH scale is given in Figure 4.

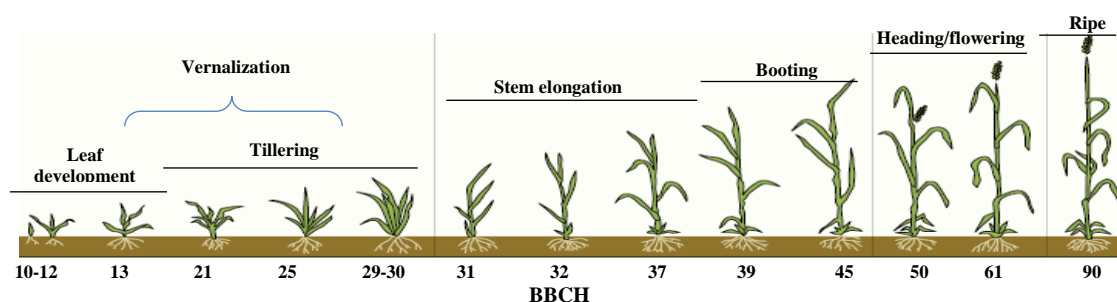


Figure 4. Representation of winter wheat development in relation to the BBCH growth scale (Meier, 2001).

After the vernalization period, differences in development between HOSUT24 and Certo become evident and are quantifiable with the BBCH scale (Figure 4 and Figure 5). HOSUT20 and HOSUT12 showed the same accelerated growth that was observed for HOSUT24 plants (Figure 37 in Supplemental data).

The same accelerated development was observed for HOSUT24 plants growing under diminished fertilization.

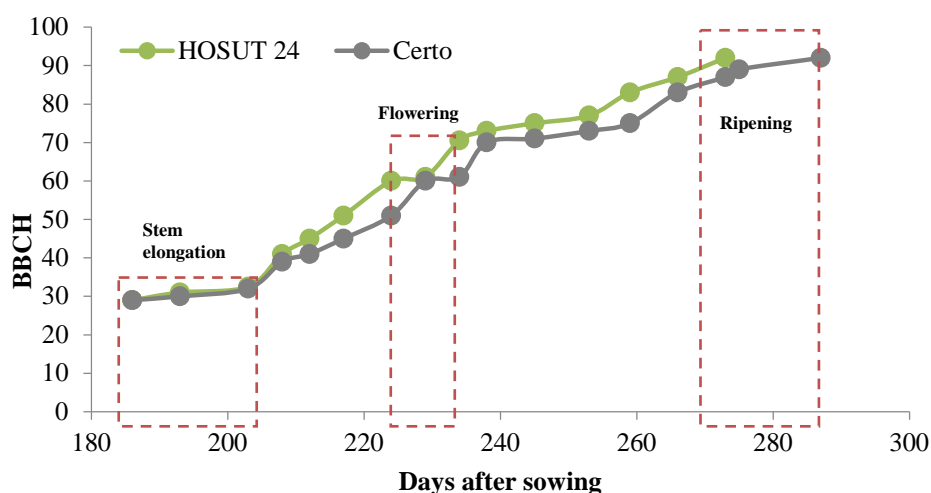


Figure 5. Phenological scale showing the growth differences of HOSUT24 and Certo plants according to the BBCH scale during the 2012-2013 season. Red boxes indicate a determinate stage of development.

### 1.3.1.2. Apices of HOSUT show accelerated development under field-like conditions

Developing apices of the main stem of both HOSUT24 and Certo were harvested in parallel at four developmental stages between the tillering stage and initiation of the stem elongation (Figure 6). At the whole plant level, the BBCH scale differences between the end of tillering and initiation of the stem elongation are not evident. However, photographs taken from HOSUT and Certo meristems harvested at the same time point after sowing highlighted accelerated HOSUT development.



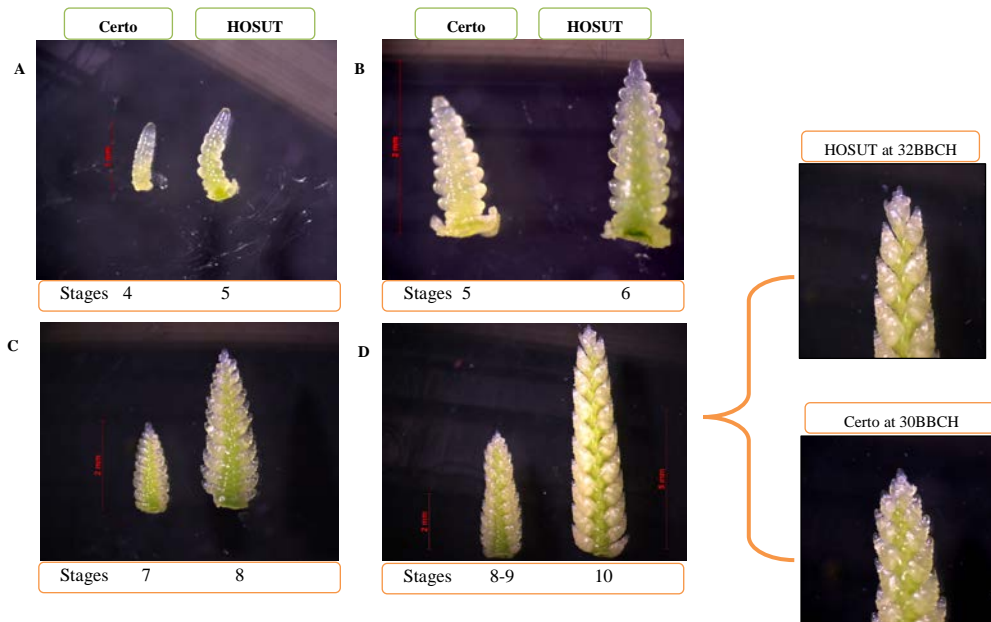


Figure 6. Developing apices of HOSUT24 and Certo plants grown under field-like conditions, harvested during the growing season 2012-2013. Apex staging according to (Vahamidis et al., 2014). Plants analysed at A. 23-24BBCH, leaf formation/early tillering. B. 24-25BBCH tillering. C. 29-30BBCH end of tillering/beginning of stem elongation. D. 30-32BBCH stem elongation.

### 1.3.1.3. Earlier flowering of HOSUT lines

Under complete fertilization conditions, detailed evaluation of the flowering time in all three HOSUT lines and Certo indicated an earlier flowering of HOSUT plants. This trait was confirmed in HOSUT24 under diminished fertilization, when flowering began 7 days earlier than Certo.

HOSUT20 and 12 also flowered earlier, in a range from 4 to 6 days before Certo. Figure 7 shows results of a detailed evaluation of the daily progression in flowering time for all three lines.

The earlier flowering time detected also in HOSUT plants under diminished fertilization, indicated a connection of this trait with the HOSUT genotype independently from the fertilization provided during the crop's life cycle.

Flowering spikes at the 61-65 BBCH stage

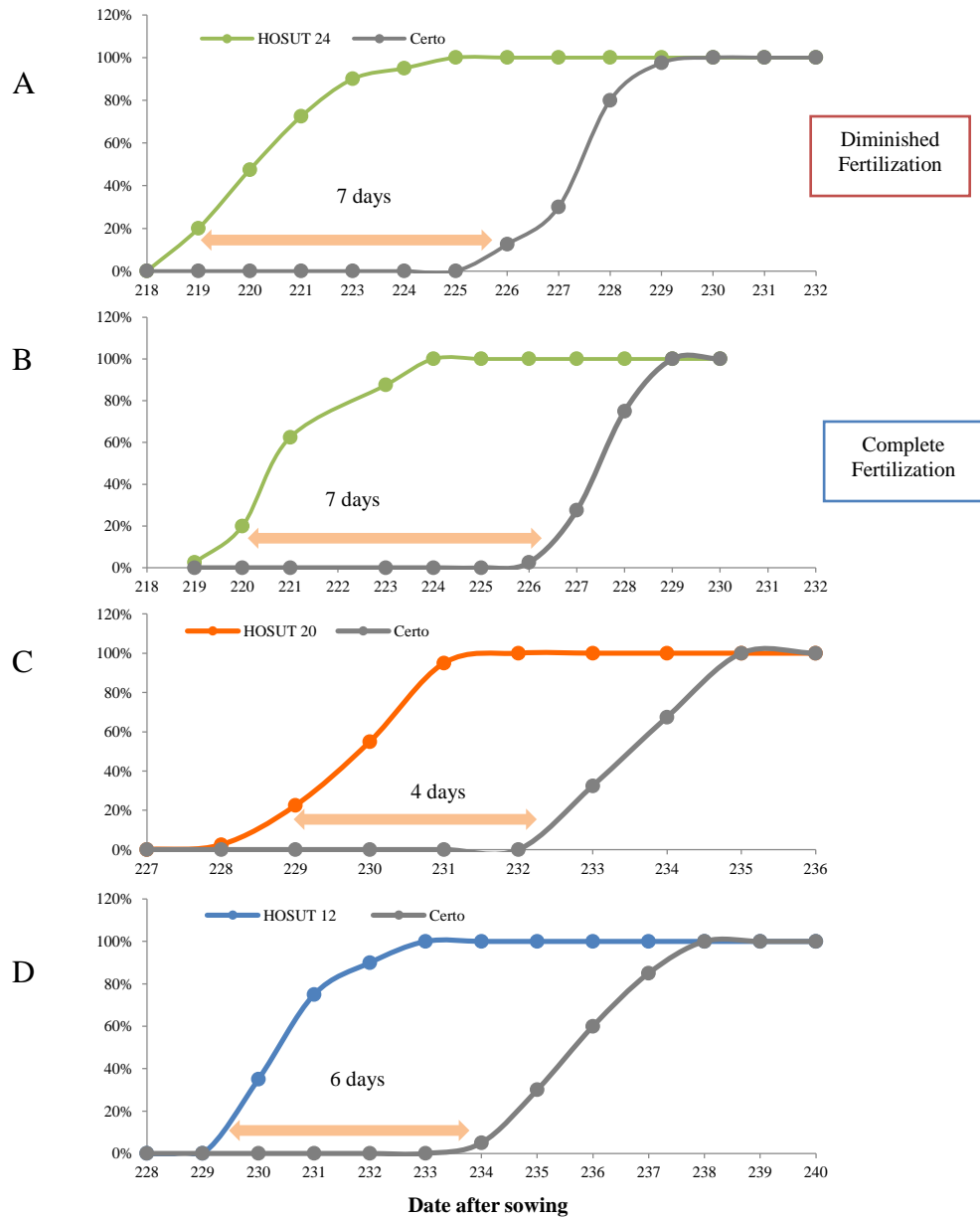


Figure 7. Flowering time of the three HOSUT lines and Certo grown under field-like conditions. Growing season 2012/2013. Data evaluated in June 2013. A. HOSUT24 and Certo under diminished fertilization. B. HOSUT24 and Certo under complete fertilization. C and D. HOSUT20 and HOSUT12 complete fertilization.

Environmental conditions determine the flowering time in winter cereals. Vernalization is important for winter cereals, changes during the years in vernalization temperatures and time have an effect on flowering time (Greenup et al., 2011). Evaluation of phenological stages of HOSUT24 during the growing season 2013/2014 indicated differences in flowering time between HOSUT and Certo from up to 5 days in full fertilization conditions (Figure 37B in Supplemental data). This might indicate that early flowering of HOSUT lines depend on interaction between transgene influence and environmental conditions. This observation needs further evaluation.

#### 1.3.1.4. Increased chlorophyll content of HOSUT plants

Chlorophyll measurements performed at booting and grain filling stage revealed increased values in HOSUT24, even when the plants were developing under diminished fertilization (Table 2). However, chlorophyll content of both HOSUT and Certo plants is reduced under diminished fertilization.

Table 2. Chlorophyll content (SPAD) of plants grown under field-like conditions, diminished and complete fertilization at booting and grain filling stage. Certo =100%. Season 2012-2013. Abs. Absolute value. T-Test \*P < 0.05, \*\*P < 0.01, \*\*\*P < 0.001.

Line	Complete fertilization				Diminished fertilization			
	Booting		Grain filling		Booting		Grain filling	
	SPAD	% of Certo	SPAD	% of Certo	SPAD	% of Certo	SPAD	% of Certo
HOSUT24	48.8±1.2	107.2%**	52.8±1.4	105.2%***	40.6±1.0	105.3%**	38.3±2.7	102.4%
Certo	45.5±1.4		50.3±0.9		38.6±1.5		37.4±1.7	

#### 1.3.2. Influence of diminished fertilization on grain yield of HOSUT

Performance of line HOSUT24 was evaluated under diminished and complete fertilization during the growing seasons 2010-2013 and 2013-2014 under field-like conditions.

Although diminished fertilization had a strong effect on the final yield of both lines, the yield of HOSUT24 was significantly higher than Certo under both fertilization conditions (Table 3).

Diminished fertilization did not seem to affect the TGW of both lines. The difference of TGW between HOSUT24 and Certo was stable during both evaluated growing seasons, even under these limiting fertilization conditions *i.e.* HOSUT24 had grain ca. 20% heavier (Table 3).

The number of spikes per plot was significantly increased for HOSUT24 under complete fertilization in the growing season 2012-2013. In the following season, increase number of spikes per plot in HOSUT27 was also documented; however, differences were not statistically significant for that trait.

Under diminished fertilization, HOSUT24 showed a slight decrease in the number of tillers per plant when compared to Certo; nevertheless, the number of spikes per plot had a tendency to be higher in HOSUT (Table 3), even if, they were not statistically different.

Table 3. Yield parameters of line HOSUT24 compared to Certo. Plants were grown under field-like conditions under two fertilization conditions. T-Test \*P < 0.05, \*\*P < 0.01, \*\*\*P < 0.001. Values in percentages of Certo (100%)  $\pm$  SD.

Parameter	Complete fertilization		Diminished Fertilization	
	2012/2013	2013/2014	2012/2013	2013/2014
<b>Yield</b>	119.8 $\pm$ 5.8% **	119.2 $\pm$ 6.5% **	118.8 $\pm$ 11.6% *	115.3 $\pm$ 6.9% **
<b>TGW</b>	123.6 $\pm$ 2.4% **	118.5 $\pm$ 1.7% **	125.5 $\pm$ 3.4% **	127.5 $\pm$ 2.8% **
<b>N-yield per plot</b>	112.2 $\pm$ 2.6% *	113.1 $\pm$ 7.3% **	120.2 $\pm$ 5.7% *	112.1 $\pm$ 7.2%
<b>Spikes per plot</b>	124.0 $\pm$ 6.9% **	107.3 $\pm$ 8.1%	104.9 $\pm$ 6.1%	100.3 $\pm$ 6.3%
<b>Grains per spike</b>	96.6 $\pm$ 4.1%	nd	88.5 $\pm$ 8.5%	nd
<b>Spikelets per spike</b>	94.9 $\pm$ 0.8 %	nd	91.8 $\pm$ 5.2%	nd
<b>Tillers per plant</b>	99.8 $\pm$ 4.3%	97.9 $\pm$ 2.1%	90.3 $\pm$ 8.8%	98.9 $\pm$ 6.0%

The germination rate of both lines was analysed early in the sowing season 2013-2014 and it ranged between 95% and 98% in both lines (data not shown). This information together with the results of number tillers per plant and the spikes per plot suggest a lesser rate of tiller abortion in HOSUT24 under complete fertilization and also the same tendency under diminished fertilization. The tendency to increased biomass also pointed out to this hypothesis (Figure 36A and B in Supplemental data).

Under complete fertilization, lines HOSUT20 and 12 also showed increased yield parameters (Table 4). As in HOSUT24, TGW was significantly increased in HOSUT20 and HOSUT12 as the number of spikes per plot.

The number of grains per spike in all three lines is similar to that of Certo. The number of spikelets per spike had a tendency to be reduced in HOSUT; however, in all three lines this effect was never statistically significant.

Table 4. Yield parameters calculated for HOSUT20 and HOSUT12 in comparison with Certo. Plants were grown under complete fertilization at field-like conditions during the growing season 2012/2013. T-Test \*P < 0.05, \*\*P < 0.01, \*\*\*P < 0.001. Values in percentages of Certo (100%)  $\pm$  SD.

Parameter	HOSUT20	HOSUT12
<b>Yield</b>	107.0 $\pm$ 8.9%	122.4 $\pm$ 6.8%
<b>TGW</b>	140.6 $\pm$ 2.9%***	133.4 $\pm$ 3.6%**
<b>Spikes per plot</b>	126.8 $\pm$ 6.0%**	144.1 $\pm$ 11.5%*
<b>Grains per spike</b>	104.9 $\pm$ 4.3%	100.6 $\pm$ 11.6%
<b>Spikelets per spike</b>	97.7 $\pm$ 0.4%	94.9 $\pm$ 3.6%
<b>Tillers per plant</b>	106.2 $\pm$ 6.9%	100.4 $\pm$ 2.2%

Grain weight has been documented to be inversely related to the number of grains per spike (Dreccer et al. 2009; Fischer 2008; Sinclair and Jamieson 2008). In accordance to that, HOSUT spikes with bigger grains produced slightly lower number of grains per spike; however, in HOSUT24 plants, this effect was buffered by the production of more spikes per plot as by the increased TGW.

### ***1.3.3. Morphology and composition of fully developed grains of HOSUT and Certo grown under different fertilization conditions***

Grain width, length and area were determined using the digital seed analyser MARVIN (www.gta-sensorik.com). Highly significant differences were found for all evaluated parameters. The area of HOSUT grains is increased by 13-15% when compared to Certo regardless of the fertilization conditions (Table 5).

Table 5. Evaluation of grain morphology of transgenic line HOSUT24 grown under field-like conditions with two different fertilization conditions. T-Test \*P < 0.05, \*\*P < 0.01, \*\*\*P < 0.001. Values in percentages of Certo (100%)  $\pm$  SD.

Parameter	Complete fertilization		Diminished Fertilization	
	2012/2013	2013/2014	2012/2013	2013/2014
<b>Width (mm)</b>	108.7 $\pm$ 0.6%**	107.6 $\pm$ 0.9%**	109.8 $\pm$ 1.8%**	111.4 $\pm$ 1.3%**
<b>Length (mm)</b>	105.0 $\pm$ 0.6%**	103.1 $\pm$ 0.9%**	105.9 $\pm$ 0.9%**	104.6 $\pm$ 0.4%**
<b>Area (mm<sup>2</sup>)</b>	113.2 $\pm$ 1.0%**	109.7 $\pm$ 0.9%**	115.3 $\pm$ 2.3%**	114.8 $\pm$ 1.3%**

HOSUT20 and 12 also show significantly larger grains (Table 6) confirming the positive effect of the HOSUT genotype on the grain size. In HOSUT20, the increase in area is due to both increased width and length. The increase in area of HOSUT12 is due only to a significant increase in the width of its grains.

Table 6. Grain morphology of transgenic lines HOSUT12 and HOSUT20 grown under field-like conditions with complete fertilization during the growing season 2012/2013. Values in percentages of Certo (100%)  $\pm$  SD. P<0.05 (\*), P<0.01(\*\*), P<0.001(\*\*\*) according to T-test.

Parameter	HOSUT12	HOSUT20
<b>Width (mm)</b>	108.2 $\pm$ 10.6%***	108.4 $\pm$ 6.7%***
<b>Length (mm)</b>	98.6 $\pm$ 6.6%	102.8 $\pm$ 7.7%***
<b>Area (mm<sup>2</sup>)</b>	106.0 $\pm$ 12.9%***	113.7 $\pm$ 10.1%***

#### 1.3.3.1. Analysis of sucrose, N and C content

In Saalbach et al. (2014), the evaluation of the grain composition of three HOSUT lines determined that the sucrose content of mature HOSUT grains was diminished. During the seasons 2012-2013 and 2013-2014, HOSUT24 grains grown with complete fertilization showed similar results (Table 7). This trend was also evident when the plants were grown under diminished fertilization; the sucrose content in the grains from both seasons was 89.4% and 84.0% of the value of Certo.

Under complete fertilization, HOSUT24 had the tendency to accumulate more starch than Certo during the first evaluated growing season (113.2%). This tendency remained in grains harvested from the experiment with diminished fertilization, although it was not statistically significant.

N content in the grain was slightly diminished in the complete fertilization experiments. Grains of the experiments with diminished fertilization had a N content similar to that of Certo and also similar raw protein content.

C concentration in HOSUT24 and Certo under both normal and diminished fertilization was not statistically different. As a result, C/N ratio of ripe grains indicates significant differences between HOSUT24 and Certo only for grains harvested from plants grown under normal N fertilization. For those grains, HOSUT24 C/N ratio is 107.1%.

Table 7. Grain Composition of transgenic line HOSUT24 grown under field-like conditions with two different fertilization conditions during two growing seasons. Values in percentages of Certo (100%)  $\pm$  SD.  $P < 0.05$  (\*),  $P < 0.01$  (\*\*),  $P < 0.001$  (\*\*\*) according to T-test.

Variable	Complete fertilization				Diminished fertilization			
	2012-2013		2013-2014		2012-2013		2013-2014	
	abs	(%)	abs	(%)	abs	(%)	abs	(%)
<b>sucrose</b> ( $\mu\text{mol/gDW}$ )	27.2 $\pm$ 1.9	74.2 %***	30.3 $\pm$ 2.1	78.9 %***	28.7 $\pm$ 1.8	89.4%**	31.8 $\pm$ 1.7	84.0%***
<b>Starch (mg/gDW)</b>	640.3 $\pm$ 26.3	113.2%**	637.0 $\pm$ 15.9	101.9%	659.7 $\pm$ 34.1	104.0%	677.6 $\pm$ 22.4	103.5%
<b>C (% of total mass)</b>	44.4 $\pm$ 0.2	99.8%	44.3 $\pm$ 0.8	99.9%	43.9 $\pm$ 0.3	99.9%	44.2 $\pm$ 0.8	99.9%
<b>N (% of total mass)</b>	2.22 $\pm$ 0.03	93.7%**	2.36 $\pm$ 0.04	94.8%**	1.35 $\pm$ 0.04	100.7%	2.05 $\pm$ 0.07	97.2%
<b>C/N</b>	20.1 $\pm$ 0.3	107.1%**	18.8 $\pm$ 0.3	105.2%**	32.7 $\pm$ 0.9	99.2%	21.58 $\pm$ 0.74	102.7%
<b>Grain raw protein</b> (% of total mass) <b>Nx5.7</b>	12.63 $\pm$ 0.17	93.3%**	13.46 $\pm$ 0.20	94.9%**	7.68 $\pm$ 0.22	100.9%	11.70 $\pm$ 0.39	97.3%

### 1.3.3.2. Free amino acid content

Free amino acids were measured in ripe grains of plants grown under field-like conditions with normal and diminished fertilization.

Contents of free amino acids in the grains harvested from the diminished fertilization experiments were reduced in HOSUT24 as well as in Certo when compared to grains from the normal fertilization experiment. The decrease in HOSUT amino acid concentration was more pronounced under diminished fertilization (Figure 8).

The measurements in HOSUT24 indicated that under both fertilization conditions there was a decreased content of most of the amino acids in comparison to Certo with the exception of Tryptophan (Trp), which was significantly increased in HOSUT24 in both cases (150.6% and 126.2% in comparison to Certo:100%, Figure 8). This is related to results obtained from vegetative tissues of seedlings (Chapter 2).

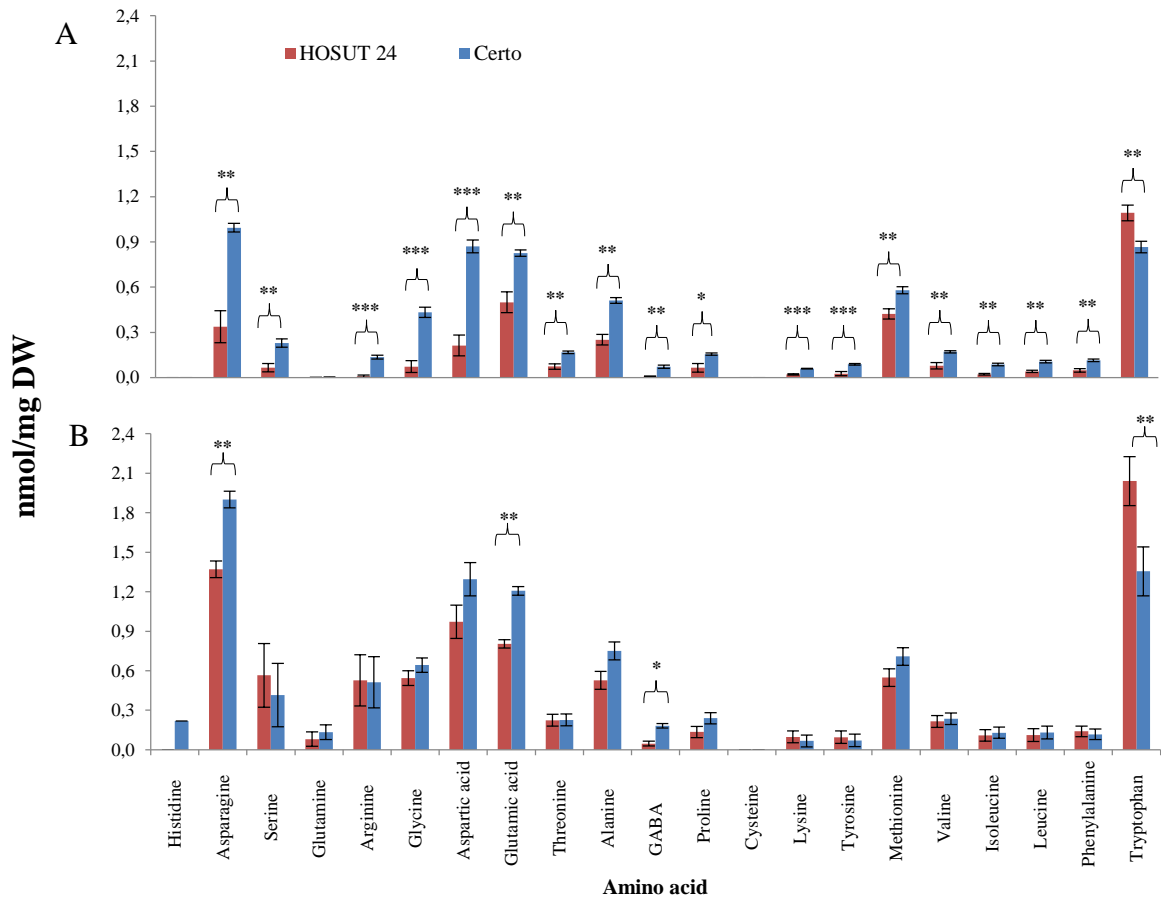


Figure 8. Free amino acid concentration in ripe grains of HOSUT24 and Certo grown under two distinct fertilization conditions at field-like conditions A. Diminished fertilization, B. Normal fertilization. Grains from the growing season 2012/2013. Vertical bars = means of 6 repetitions  $\pm$  SD.  $P < 0.05$  (\*),  $P < 0.01$  (\*\*),  $P < 0.001$  (\*\*\*) according to T-test.

## 1.4. Discussion

Yield potential is influenced by grain filling and the ratio of harvested grains to biomass production, also called Harvest Index (Semenov et al., 2014). Climate change brings higher temperatures, changes in rainfall, and therefore, also in the N cycle and N soil fixation, which ultimately affects crops' production and food supply.

Fertilization represents an important input during a crop's cycle; however, increasing N fertilization in agricultural systems without careful planning to avoid the leaching of residual waters has strong environmental repercussions (Galloway et al., 2008). Good agronomical practices, enhancement of yield potential and higher N use efficiency in the crops could help achieve the challenge of enhancing food supply and diminish the environment repercussions (Semenov et al. 2014). Better yields with less input are a trait to look forward.



HOSUT lines have an increased sucrose uptake capacity in the developing grains, and so, an increased grain sink strength (Weichert et al. 2010). Saalbach et al. (2014) determined increased grain yield of HOSUT lines. However, neither the differences in phenology nor the response of HOSUT to limiting fertilization under field-like conditions were evaluated.

#### ***1.4.1. Accelerated development of HOSUT lines under field-like conditions***

In-depth analysis of phenology differences between HOSUT lines and Certo, as well as the analysis of the apex development during early stem growth placed in evidenced that HOSUT wheat develops faster than its wild type Certo. Preliminary biomass analyses of HOSUT plants at the booting stage, indicated a tendency of HOSUT to accumulate more shoot biomass. Tendency that was also evident under limiting nutritional conditions (Figure 36 in Supplemental data).

The acceleration of HOSUT development was especially evident by earlier flowering. HOSUT lines at season 2012-2013 flowered up to 7 days earlier than Certo. In the following season HOSUT24 flowered 5 days earlier. This accelerated development was also detected when HOSUT was grown under diminished fertilization, making this, a nutritional-independent effect, reinforcing the hypothesis of a positive influence of the transgene in accelerating plant development and hence flowering time.

Winter cereals require vernalization periods in order to induce flowering. *VERNALIZATION 1 (VRNI)* promotes the transition of the apex from vegetative to reproductive development (Trevaskis et al., 2007). Increase in the length of the cold periods, *i.e.* longer periods at temperatures under 10°C (up to a saturation point), makes plants have a higher expression of *VRNI*. Because this gene will promote the transition from vegetative development in the apex to reproductive (Greenup et al. 2011), earlier flowering will be induced by longer periods of cold temperatures.

Considering that last statement, together with the result that HOSUT lines develop faster than their wild type Certo, it is possible that HOSUT lines have an enhanced expression of *VRNI* gene, since their entire development was faster in comparison to Certo. Because of temperatures and length of vernalization influences flowering time, differences in temperature between two growing seasons should affect flowering time in both lines, in that way, the difference between HOSUT and Certo shortens.

In-depth transcriptome analysis of the developing spikes is in progress to clarify the differences in apex development, which might be related to sucrose effects on gene expression and spike metabolism.

#### ***1.4.2. HOSUT lines conserved their yield advantage under limiting nutritional conditions***

Sink strength is a major limiting factor in wheat grain yield (Bihmidine et al. 2013; Reynolds et al. 2012). Increasing the sink strength of the grain as in HOSUT lines, has proven to be a promising approach to elevate significantly the yield in winter wheat.

HOSUT lines were evaluated during a series of growing seasons (Saalbach et al. 2014) and revealed increased values of several yield parameters, showing that, the previously reported increase in sucrose uptake in the grains (Weichert et al., 2010) is translated into increased grain filling and therefore higher TGW.

The grains' width is related to the filling of the grain. In HOSUT, the increase in grain weight is mainly due to an increase in the width of HOSUT grains that could be up to 11% higher than that of Certo even under diminished fertilization, indicating that the enhanced grain sink strength, previously reported for this line, is stable enough to withhold strong nutrient stress.

Productivity in cereals could be visualized as 1) amount of grains/m<sup>2</sup> and 2) the weight of those grains (Ferrante et al. 2010; García et al. 2013; Gupta et al. 2006). Grains are organs that depend on assimilate and nutrient supply to fill up. Weichert et al. (2010) detected longer grain-filling time in HOSUT plants. The tendency of HOSUT plants to produce more vegetative biomass even when growing under limiting conditions (Figure 36B in Supplemental data), together with an enhanced sucrose uptake seems to be of advantage in production to overcome a nutritional shortage.

Tiller number of all HOSUT lines is similar to Certo. The higher spike number found for the HOSUT lines implies less tiller-abortion, possibly due to an enhanced assimilate remobilization to the sink tissue, in this case, the tiller and the developing spike. More spikes per plot is an important yield trait, that together with increased TGW represent a major yield advantage of HOSUT lines over their no-transgenic counterpart.

The fact that HOSUT lines retain their advantage in yield production even under limiting fertilization conditions might indicate that HOSUT lines require less amounts of fertilizer and therefore N for vegetative development and yield production; this could mean that

they have higher N use efficiency (NUE) when compared to Certo. NUE refers to the amount of biomass produced (yield) versus the N input put in the soil (Chardon et al., 2012; Kichey et al., 2007; Pask et al., 2012). This characteristic is of high relevance in breeding programs, since it could help reduce the fertilizer input in the crop without jeopardizing the production or quality of the grains.

#### ***1.4.3. Diminished fertilization does not affect the N content in the grains of HOSUT24***

Results of the compositional analysis of ripe grains of HOSUT24 plants grown under complete fertilization showed a trend to accumulate lower N than Certo, as previously reported in Saalbach et al. (2014). In this study, in the evaluation during two growing seasons, the amount of total N, and in consequence the grain raw protein content, had the tendency to be lower or comparable to that of Certo, in opposition to starch content which had the tendency to increase in HOSUT24. This is also evident in the C/N ratios.

Different scenario was shown under diminished fertilization, where the amount of N in the ripe grains of both lines was comparable. Vegetative remobilization of assimilates and nutrients is important during grain filling. After anthesis, assimilates are remobilized into the developing grain from the senescing tissue, therefore reserves in vegetative tissues play an important role in the yield potential (Howarth et al., 2008).

Under diminished fertilization, HOSUT plants produced more biomass. This increase in biomass could later be remobilized towards the major sink in the plant, which at this stage is the developing grain, hence influencing yield as was described by Foulkes et al. (2011), where it is pointed out the importance of designing strategies to increase photosynthesis and biomass, and the combination of them both with improvements in partitioning.

Wheat crops with increased biomass, tested under medium-drought conditions had the tendency to endure abiotic stress conditions contributing to maintain the yield under such conditions (Dolferus et al., 2011). The increase in biomass, together with an enhanced uptake capacity of the grain, proved beneficial to overcome limiting nutritional conditions that might otherwise lead to a reduction in the yield and nutritional content of the grain.

#### ***1.4.4. Altered amino acid content in ripe grains of HOSUT plants***

Ripe grains of HOSUT24 have the tendency of reduced amino acid amounts when compared to Certo. Most evident were the differences in asparagine (Asn), GABA and glutamic acid (Glu), which were found in significantly reduced amounts in grains of HOSUT24 grown under both fertilization conditions. On the other hand, Trp was found in

significantly elevated amounts. Similar results were reported in Weichert et al. (2010) where Trp, tyrosine (Tyr) and phenylalanine (Phe) also had the tendency to increased values as was found in the present study. When plants are grown under limiting fertilization, the only amino acid product from the Shikimate pathway that has increased values in HOSUT is Trp.

Wakasa et al. (2006) transformed rice lines with a feedback-insensitive  $\alpha$  subunit of anthranilate synthase, in order to enhance the production of precursors of Trp and enhance its accumulation in the rice grains. They obtained, not only increased amounts of this amino acid, but also increased amounts of free IAA and ester forms of IAA. Deeper analyses of the influence of the transgene on the embryo development as well as analysis of hormone content in the embryo would be of great interest in HOSUT lines for acquiring a more complete view of the developmental differences between HOSUT and their wild type Certo.

Detailed analysis of the seedling growth, biochemical analyses and transcriptome is presented in Chapters 2 and 3.

## **2. Chapter. Seedling development of HOSUT lines**

### **2.1. Introduction**

Seedling vigour is important for the early establishment of any crop. High seedling vigour is translated into increased biomass of both root and shoot, and it is also reflected by accelerated seedling growth (Aparicio et al., 2002; Cisse and Ejeta, 2003; Cui et al., 2002, 2013; Evans and Bhatt, 1977).

In both dicot- and monocotyledonous species, increased seed size is correlated with an enhanced survival rate during seedling establishment. This is also true for cereals (Evers and Millar, 2002), since an increase in grain size is translated into higher amounts of remobilized assimilates and nutrients for proper embryo development (Milberg et al., 2014). Under natural conditions, species with large seeds possess increased seedling survival in comparison with species with smaller seeds, as the latter ones are unequivocally more dependant from nutrient uptake from the soil (Cui et al., 2002; Moles and Westoby, 2004; Milberg et al., 2014). In wheat, seedling vigour is influenced not only by seed size but also by seed protein content (Evans and Bhatt, 1977).

In the HOSUT lines, the effect of the transgene results in higher grain yield, TGW is the most enhanced and stable yield parameter found in this lines, in parallel, grain size is increased (Chapter 1). Together with the expected positive effect of the increased HOSUT grain size on seedling growth, also expression of the HOSUT transgene might have positive impact on seedling development.

In winter wheat seedlings, early and proper establishment before vernalization is highly important, since they must endure and survive winter temperatures. Because soil penetration takes place very early, the young root system is essential for proper seedling development (Jansen et al., 2010; Manske and Vlek, 2002). A preliminary experiment showed faster seedling development and a more extensive early root system of line HOSUT20 when compared to Certo under field-like conditions (Figure 9B).



Figure 9. Photographs taken from HOSUT20 and Certo plants in spring 2011. A, difference in growth behaviour. B, difference of the early root system.

In this chapter, results from analysis of the seedling vigour of HOSUT lines under different growing conditions were presented as compared to the non-transgenic winter wheat variety Certo (wild type control).

## 2.2. Materials and Methods

### 2.2.1. Plant material and establishment of the *in vitro* system

An *in vitro* system using vermiculite ([www.kakteen-schwarz.de](http://www.kakteen-schwarz.de)) as substrate was established. This system allowed controlled nutrient supply to the seedlings. Due to the physical characteristics of Vermiculite, extraction of the root system can be done with minimal damage to the tissue. Three independent homozygous HOSUT lines (24, 20 and 12) were used for evaluation.

The liquid medium used for the *in vitro* cultivation corresponds to a nitrogen-deprived (N-deprived) medium (XS) used by Song et al. (2007) (Table 8).

Table 8. Composition of the XS medium used for cultivation of seedlings under controlled *in vitro* conditions

Component	Molarity in XS medium	
<b>CaCl<sub>2</sub> · 2H<sub>2</sub>O</b>	1	mM
<b>KH<sub>2</sub>PO<sub>4</sub></b>	0.5	mM
<b>Fe-citrat C<sub>6</sub>H<sub>5</sub>FeO<sub>7</sub></b>	10	μM
<b>MgSO<sub>4</sub> · 7H<sub>2</sub>O</b>	0.25	mM
<b>K<sub>2</sub>SO<sub>4</sub></b>	0.25	mM
<b>MnSO<sub>4</sub> · H<sub>2</sub>O</b>	1	μM
<b>H<sub>3</sub>BO<sub>3</sub></b>	2	μM
<b>ZnSO<sub>4</sub> · 7H<sub>2</sub>O</b>	0.5	μM
<b>CuSO<sub>4</sub> · 5H<sub>2</sub>O</b>	0.1	μM
<b>CoCl<sub>2</sub> · 6H<sub>2</sub>O</b>	0.1	μM
<b>Na<sub>2</sub>MoO<sub>4</sub> · 2H<sub>2</sub>O</b>	0.1	μM

The seedlings were evaluated at the three leaves stage (13BBCH) according to the phenological development described by Meier (2001). Root dry mass, number of primary roots, and root length were analysed.

### ***2.2.2. Determination of root dry mass, number or primary roots and length of the root system of seedlings grown in vitro***

#### ***2.2.2.1. N- deprived: XS medium***

Grains from the three HOSUT lines and Certo were pre-soaked in water and kept at 4°C for 3 days. Pots of 14.5 x 17.5 cm were used for each experiment. Each line was grown in parallel with Certo.

Every experiment consisted of eight pots. In each pot, five grains of the transgenic line and five Certo grains were sown. Per line, the experiments were performed in triplicated. In total 720 plants were analysed.

The plantlets were grown under greenhouse conditions at 16°C/14°C, 16-h/8-h day/night. XS medium (Table 8) was applied to the substrate in equal volumes every second day.

When plants reached the 13 BBCH stage, the total root system from each pot was harvested separately for each line. The plants of each line were separated carefully from vermiculite and from the plants of the other line. The root system of each plantlet was washed carefully with water. The remaining vermiculite was separated from the tissue.

Root system and shoot were separated with a scalpel; the water excess was eliminated carefully with a tissue paper; number of primary roots was determined for each plant.

The root tissue belonging to the five plants of the same line and the same pot was carefully placed into 50 mL Conical Centrifuge Tubes, frozen in liquid N and lyophilized over three days. The dry weight was measured afterwards. Lyophilized material was stored until further biochemical analyses were performed.

To estimate root length, plants were grown in long pots, each of them 41.5cm in length (11 x 41.5 cm) to provide sufficient elongation space to the roots. Four previously imbibed grains from each HOSUT line and Certo were sowed in each pot, 15 pots per line was used. Each experiment was performed in triplicate. Plants were grown under greenhouse conditions with N-deprived XS medium as described above.

When plants reached the adequate stage for analysis (13 BBCH, 3-leaf stage), they were harvested and the roots were cleaned as previously described. Root length and root

number were evaluated.

The complete data set regarding root mass and length was evaluated using ANOVA statistical analysis with InfoStat vr. 2011. InfoStat Group ([www.infostat.com.ar](http://www.infostat.com.ar)). Results for the transgenic lines are given in percentages of the wild type Certo (WT = 100%). For the number of primary roots, data was analysed performing a Kruskal-Wallis test with InfoStat vr. 2011. InfoStat Group ([www.infostat.com.ar](http://www.infostat.com.ar)).

#### 2.2.2.2. *N- supplied XS medium*

HOSUT24 was chosen as a model representing the transgenic HOSUT lines. The vermiculite *in vitro* system was used to analyse the phenotype of the HOSUT24 root system under N- supply conditions in comparison to Certo. The pre-soaking as well as the growing conditions mentioned above were used. The culture medium corresponds to the described XS medium (Table 8) supplied with  $\text{NH}_4\text{NO}_3$  in a concentration of 165 mg/L. For comparison of plants growth in parallel, XS without  $\text{NH}_4\text{NO}_3$  was used.

Plants grown in both N-free and N-supplied media were kept under the same growing conditions until they reached the 13 BBCH stage. Shoot tissue was also collected for evaluation. Harvesting and cleaning of the root material was performed as described. Two repetitions of each experiment were performed.

Lyophilized material of both tissue types was analysed for dry weight and stored until use for biochemical analyses.

The number of primary roots was analysed through a Kruskal-Wallis test. Statistical analysis was performed with InfoStat vr. 2011, InfoStat Group ([www.infostat.com.ar](http://www.infostat.com.ar)).

For dry mass evaluation, a factorial ANOVA was performed using STATISTICA vr 8.0 StatSoft, Inc. (2008), [www.statsoft.com](http://www.statsoft.com). Results for the transgenic lines are given in percentages relative to Certo (Certo = 100%).

#### 2.2.3. *Biomass accumulation during early seedling development*

In order to determine the differences in biomass accumulation between HOSUT and Certo, a growth curve showing the early differences in biomass accumulation was established. HOSUT24 was chosen as a model for comparison with Certo. The seedlings were grown under *in vitro* conditions in a climatic chamber, at 14°C day and 12°C night using vermiculite as a substrate and XS medium. The photoperiod was set at 12h.

The biomass of dry grains (0 days after imbibition, DAI), imbibed grains (3 DAI) and



growing plantlets at 7, 10, 14, 17, 21, 24, 28, and 35 DAI, the latter corresponding to 13BBCH, of Certo and HOSUT24 were evaluated. For this set of experiments, grains which had a mass close to the median of their respective TGW distribution (HOSUT24: 55-60 mg and Certo: 40-45 mg) were sown.

At each time point, plantlets were harvested and separated into shoot, grain residue and roots. Each tissue sample was lyophilized, weighted and grinded for further amino acid analysis. Experiments were performed in duplicate.

Grain weight has influence on early seedling vigour and early settlement. Having this in mind a comparison of biomass accumulation was performed based on HOSUT and Certo seedlings originating from grains of the same weight. Two sets of experiments were performed. At first, HOSUT and Certo grains with a mass between 54-56 mg were sorted out and sown *in vitro*. Second grains with a mass in the range of 40-45 mg were selected. In all cases, grains were individually weighted. Grains for these experiments were developed under field-like conditions in 2011.

#### ***2.2.4. 2D- imaging and analysis of the early root development***

With the purpose to achieve an automatized and accurate counting of the lateral roots, collaboration was established with the Biosystems Engineering group at the Fraunhofer Institut für Fabrikbetrieb und -automatisierung (IFF) Magdeburg.

With this purpose, 20 plants of HOSUT24 and 20 plants of Certo were grown under the above mentioned N-deprived *in vitro* conditions up to 12 BBCH (2-leaves stage). Once this stage was reached, the plants were harvested and 10 plants of each line were randomly chosen for the analysis. The chosen plants were cleaned and placed individually on glass plates in order to spread the root system for evaluation. The roots dried out for 2 hours, and then a second anti-reflective glass was placed on top and pressed gently against the tissue in order to fix the position of the single roots on the glass surface.

High definition pictures from each root system were taken. Visible vermiculite particles were digitally removed. High-resolution images were sent to the Biosystems Engineering group, Fraunhofer IFF Magdeburg, for root analysis.

A specified analytical tool quantified root parameters. The algorithm calculates at any given distance from the root origin, the branching points, root end points as well as crossing visible in the root system image. T-test analysis was performed for the total of branching points, for analysis of individual distances a Kruskal-Wallis test was

performed. The statistical software used was InfoStat vr. 2011, InfoStat Group (www.infostat.com.ar).

### ***2.2.5. Seedling phenotype of plants grown under field-like conditions***

In order to evaluate root development under field like conditions, grains of the three transgenic lines and Certo were planted at mid-October 2012 in natural soil in non-heated glass houses with field-like planting densities. Grains were sown in rows directly in the soil in at depth of 2 cm with a distance of 2.5 cm between grains. Each row was 1.0 m in length. Adjacent rows of a transgenic line and Certo were sown at a distance of 12.5 cm. Each row with a transgenic line was sown adjacent to a row of Certo in order to minimize the possible effect of soil differences on plant metabolism.

Plants were carefully harvested at 12BBCH taken special care in not breaking the root system and extracting it completely from the soil. The roots were cleansed with water to eliminate any soil residue. Number of primary roots was counted for each plant. Shoot and root tissue were separated with a scalpel. Each biological replication corresponded to 5 plants of the same row. Root and shoot tissues were separately lyophilized and weighted.

During the growing season 2013-2014, grains of 50-55 mg of weight for both HOSUT and Certo as well as unsorted grains representing the usual difference in TGW were sown at the field-like planting densities mentioned in Chapter 1. Roots and shoots of seedlings at 12-13BBCH were harvested as previously mentioned. The seedling characteristics and vigour parameters root and shoot biomass, chlorophyll in SPAD units, plant height, number of primary roots and root system length were evaluated.

### ***2.2.6. Evaluation of chlorophyll content***

Chlorophyll measurements were performed using the Chlorophyll meter SPAD-502 from Minolta. Seedlings growing under *in vitro* conditions in N-deprived medium as well as under N-supplied conditions were evaluated. Furthermore, seedlings growing under field-like conditions were analysed.

For the *in vitro* plants, one biological replication corresponds to the average value of five plants of the same line contained in the same pot up to the 13BBCH stage; in total 20 pots were analysed. Two-way ANOVA was performed with InfoStat vr. 2011, InfoStat Group (www.infostat.com.ar), mean comparison was performed according to Tukey.

Chlorophyll measurements of the developing plants in the green houses under field-like conditions were also performed during the early developmental stages of the seedling until 13 BBCH. The average value of five plants was calculated per biological replication for a total of 5-8 biological replicates per line per developmental stage. Statistical analysis was performed with InfoStat vr. 2011, InfoStat Group ([www.infostat.com.ar](http://www.infostat.com.ar)).

#### **2.2.7. Determination of C/N, starch, sugar and amino acids content of seedling tissues**

Lyophilized root and shoot tissues of seedlings at 12-13BBCH grown *in vitro* in N-deprived and N-supplied media as well as under field-like conditions were grinded using a Retsch® MM400 mill. The resulting powder of each sample was used to estimate starch, sucrose, glucose, fructose, C/N and free amino acid concentration.

Total C and N were determined with a Vario EL Elementar analyser ([www.elementar.de](http://www.elementar.de)). Data was analysed through ANOVA or T-test. Each HOSUT line was compared to the corresponding Certo material from each experiment. Statistical tests were performed using InfoStat vr. 2011. InfoStat Group ([www.infostat.com.ar](http://www.infostat.com.ar)). Results for the transgenic lines are given in percentages relative to the value of Certo (Certo = 100%).

Starch and the sugars glucose, fructose and sucrose, were determined as described in Weichert et al. (2010). Data was analysed with a T-test through InfoStat vr. 2011. InfoStat Group ([www.infostat.com.ar](http://www.infostat.com.ar)).

For free amino acids extraction, samples were incubated with 80% EtOH for 60 min at 60°C under constant agitation; 150nmol of internal standard was added to each sample. Probes were centrifuged by 15 min and 50µl of each was taken for derivatization with a AccQ-Tag derivatization kit from Waters according to the manufacturer's instructions. Further analysis was performed by an Acquity UPLC system for amino acid analysis from waters, using column AccQ-Tag Ultra RP 1.7µm particles. Mobile-phase A corresponded to AccQ-Tag Ultra Eluent A and mobile-phase B to AccQ-Tag Ultra Eluent B both from Waters.

Flow rate was set to 700µl/min and the detection was UV@260nm. Standards used for calibration were the amino acid standard solutions from Waters® to which asparagine (132.12g/mol), glutamine (146.15g/mol), tryptophan (204.23g/mol), GABA (103.12 g/mol) and norvalin (117.15g/mol) were added fresh according to the manufacturer's recommendation.

Data acquisition and chromatogram analysis was performed with Waters EMPOWER 2 software. Statistical analysis was performed with T-Test through InfoStat vr. 2011. InfoStat Group ([www.infostat.com.ar](http://www.infostat.com.ar)).

### **2.2.8. Metabolite and hormone analysis of dried root tissues of HOSUT and Certo plants: GC-MS and UPLC-MSMS profiling**

#### **2.2.8.1. Metabolite analysis by GC-MS**

Lyophilized root tissue from HOSUT lines 20 and 24 and Certo at the 13 BBCH stage was used for untargeted metabolite analysis. Ten biological replicates were extracted and analysed using an Agilent 7890 gas chromatograph coupled to a LECO Pegasus HT mass spectrometer (LECO Corporation, St Joseph, MI, USA). Peaks were annotated using the ChromaTOF software Statistical compare package and the Golm metabolome database library (<http://gmd.mpimp-golm.mpg.de/download>).

Quantitative analysis was performed using R software. ANOVA analysis was applied to the normalized  $\log_{10}$  data.

#### **2.2.8.2. Hormone profiling by UPLC-MS**

In order to identify and quantify differences between HOSUT24 and Certo regarding hormone levels, auxin, auxin conjugates, and cytokinins and its conjugates were analysed. Fresh tissue of in-vitro grown roots and shoots of developing seedlings was used. Early developmental stages were analysed: 8 days after imbibition (DAI) corresponding to 11BBCH and 20 DAI (12 BBCH).

Initial trials were performed to determine the appropriate extraction method which is a modification of the protocol described by Kojima et al. (2009). Briefly, ca. 250 mg of fresh material is grinded in liquid N and extracted with ice-cold extraction buffer (methanol: formic acid: water in a ratio of 15:1:4) and incubated 16h at  $-20^{\circ}\text{C}$ .

The supernatant was vacuum dried at  $38^{\circ}\text{C}$  for ca. 2 h. The sample was re-suspended in 0.1% Formic acid and to remove interfering compounds, the samples were passed through an Oasis HLB 1cc (10 mg) cartridges (Waters). After collection, samples were vacuum dried and re-suspended 100  $\mu\text{l}$  methanol 80%, 900  $\mu\text{l}$  of 1 M Formic acid was added to the samples prior their loading in to the Oasis MCX 1cc (30 mg) cartridge. Elution of ABA and auxins is performed with MeOH, cytokinins are eluted with 0.35M  $\text{NH}_{3(\text{aq})}$  in 60% MeOH. Both fractions were vacuum dried and kept at  $-20^{\circ}\text{C}$  until analysis.

Samples were reconstituted in 50 µl 20%MeOH and subjected to UPLC-MS analysis, using the positive ion mode for auxins and the negative one for cytokinins.

Analysis of the samples was performed with an Agilent Technologies 1290 Infinity UPLC chromatograph coupled with an Agilent Technologies 6490 Triple Quad LC/MS. Data analysis was performed with QQQ Quantitative Analysis vr. B.04.00 software.

## 2.3. Results

### 2.3.1. Grain weight influences early seedling vigour

Seedling reserves are essential for seedling emergence and early vigour. Increases in the aleurone and endosperm mass might influence this processes. In the following sections the evaluation of such influence on HOSUT seedling development is presented.

#### 2.3.1.1. Frequency distribution of grain weight differs in HOSUT

To study the distribution of grain weight frequency of HOSUT24 and Certo grains, 1000 grains of both lines randomly collected from the Season 2010-2011 were individually weighted. The resulting histograms (Figure 10) show that the grain-weight frequency distribution of HOSUT24 (red bars) is shifted to higher values. In the 1000 grains analysed of HOSUT24, 510 grains had a weight between 51 and 65 mg. On the other hand, in Certo, grains of that same range are only 285. Similar behaviour was documented for the 2009-2010 harvest (Figure 33 in Supplemental data).

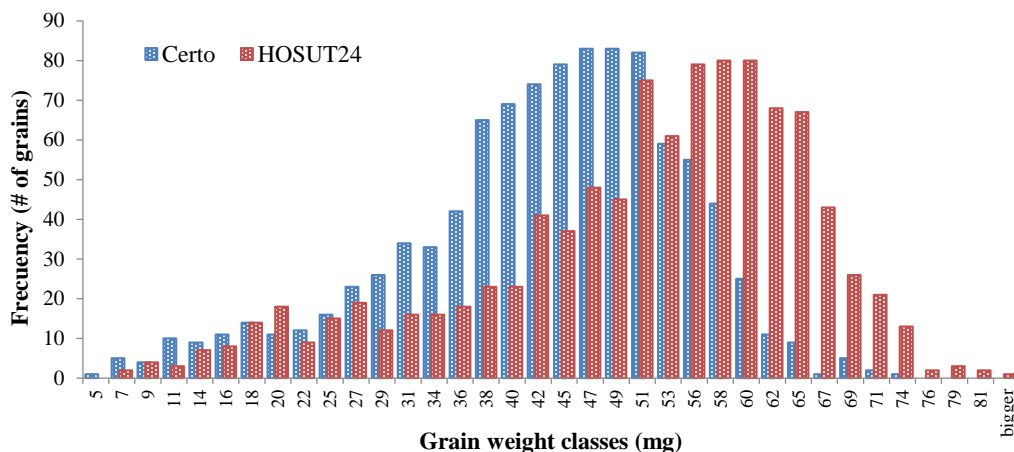


Figure 10. Grain characteristics. Frequency distribution pattern of grain weight of 1000 individual grains harvested in 2011, results published in Saalbach et al. (2014).

#### 2.3.1.2. Effect of same grain weight on seedling vigour

Influence of the grain mass on the seedling growth was evaluated through three grain-weight experiments under *in vitro* N-deprived conditions. For these comparisons,

HOSUT24 was chosen as a representative for the transgenic phenotype.

From HOSUT24 and Certo grains of the same grain weight range were sorted out and sown. The weight range 54-56 mg was considered as high grain weight and grains of 40-45 mg were used for the low weight range. The third experiment was performed using grains with the median value of the grain weight distribution of each line *i.e.* 40-45 mg for Certo and 55-60 for HOSUT.

### 2.3.1.2.1. High grain weight (54-56 mg)

Measurement of the grain depletion indicated that by 21 DAI, the nutrients and assimilates stored in the grain and available for the seedlings were exhausted. Seedlings' biomass until the end of the evaluation was similar for both lines when grains of similar mass were used (Figure 11).

Although there was no difference in biomass between the two lines when grains of similar weight were used, there was a tendency of the HOSUT line for an increased number of primary roots (Figure 11).

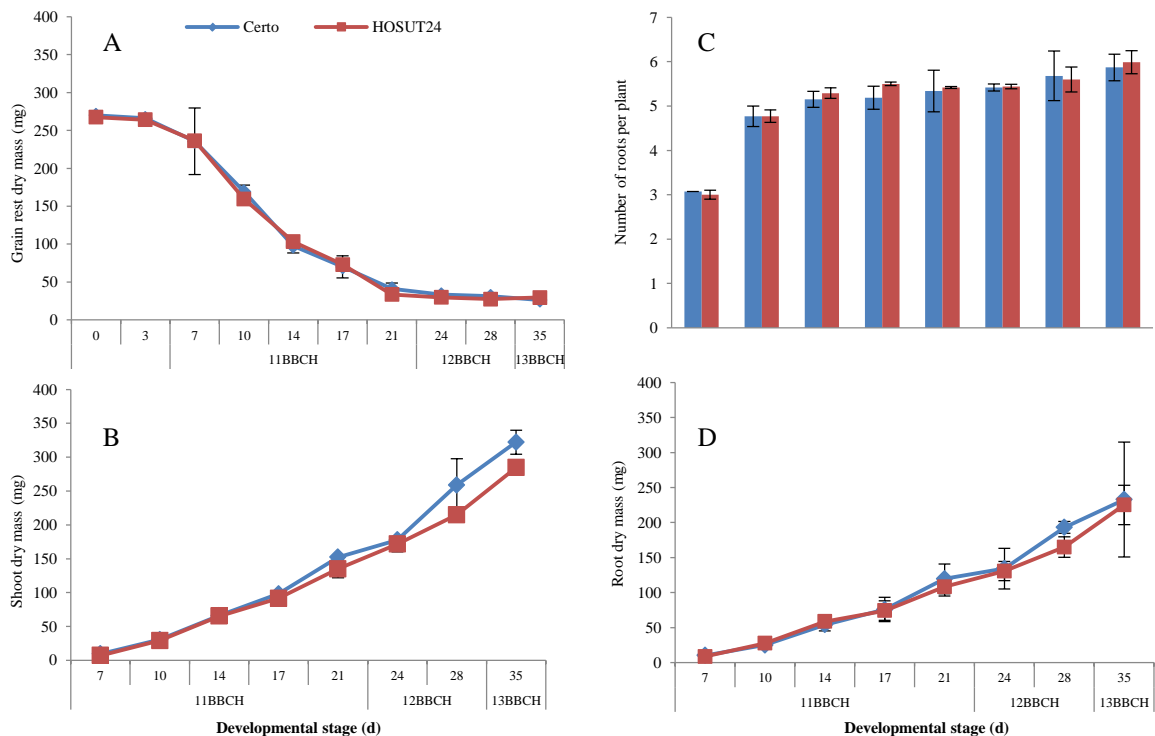


Figure 11. Biomass comparison of seedlings emerging from grains of similar grain weight in Certo and HOSUT24 (54-56 mg). Data given per experimental sample (pot=5 plants of each line). Bars  $\pm$  SD. A: Grain rest dry mass. B: Shoot dry mass. C: Number of roots per seedling. D: Root dry mass.

### 2.3.1.2.2. Low grain weight (40-45 mg)

In order to confirm the effect of same grain weight on biomass accumulation during seedling development, experiments with low grain weight were also performed. In these experiments, the depletion of the grain reserves was documented between 17-21 DAI, earlier than in grains of higher weight.

As in the previous case, seedlings' biomass was similar in both lines with a tendency to increased number of roots in HOSUT (Figure 12C).

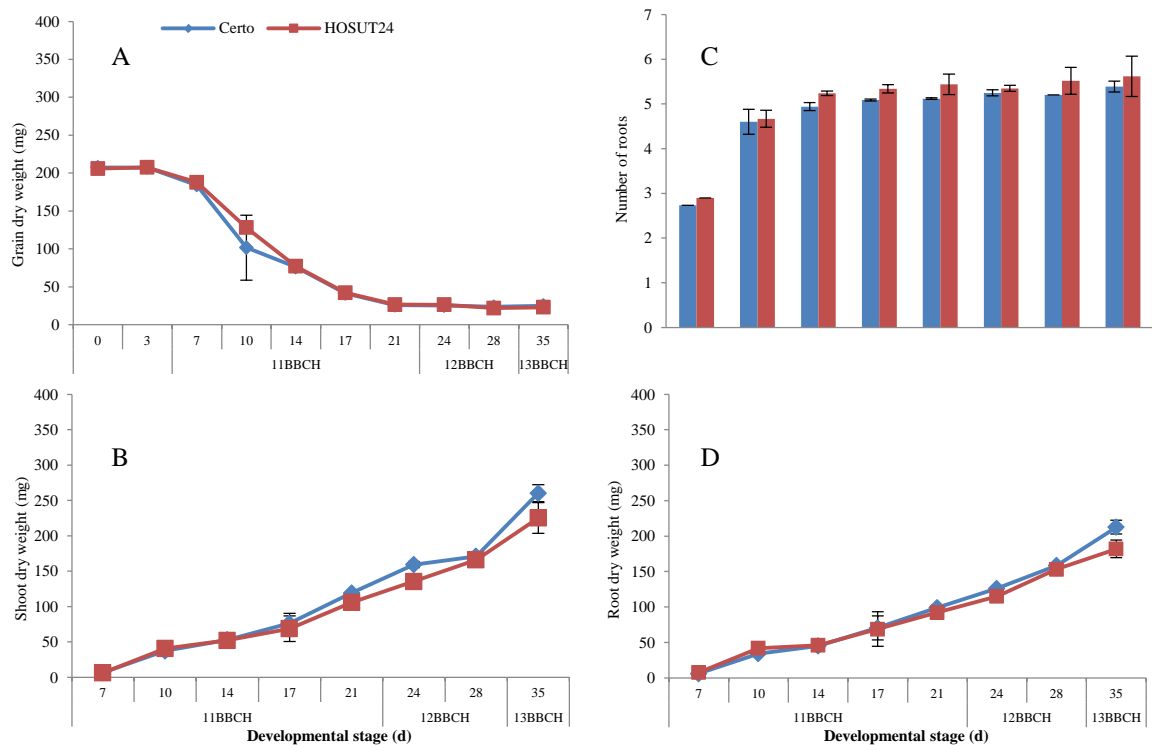


Figure 12. Biomass comparison of seedlings emerging from grains of similar grain weight in Certo and HOSUT24 (40-45 mg). Data given per experimental sample (pot=5 plants of each line). Bars  $\pm$  SD. A: Grain rest dry mass. B: Shoot dry mass. C: Number of roots per seedling. D: Root dry mass.

### 2.3.1.2.3. Typical grain weight distribution for both lines

The typical grain weight distribution refers to the median value of the grain weight distribution of each line.

Under the evaluated N-depleted *in vitro* conditions, seedlings emerging from grains with the typical grain weight difference between the lines show a tendency to have higher shoot and especially root dry mass. Analysis of grain depletion showed, that at 21 DAI the resources of the grain were depleted (Figure 13A). Moreover, there was also the tendency for higher number of seminal roots in HOSUT seedlings.

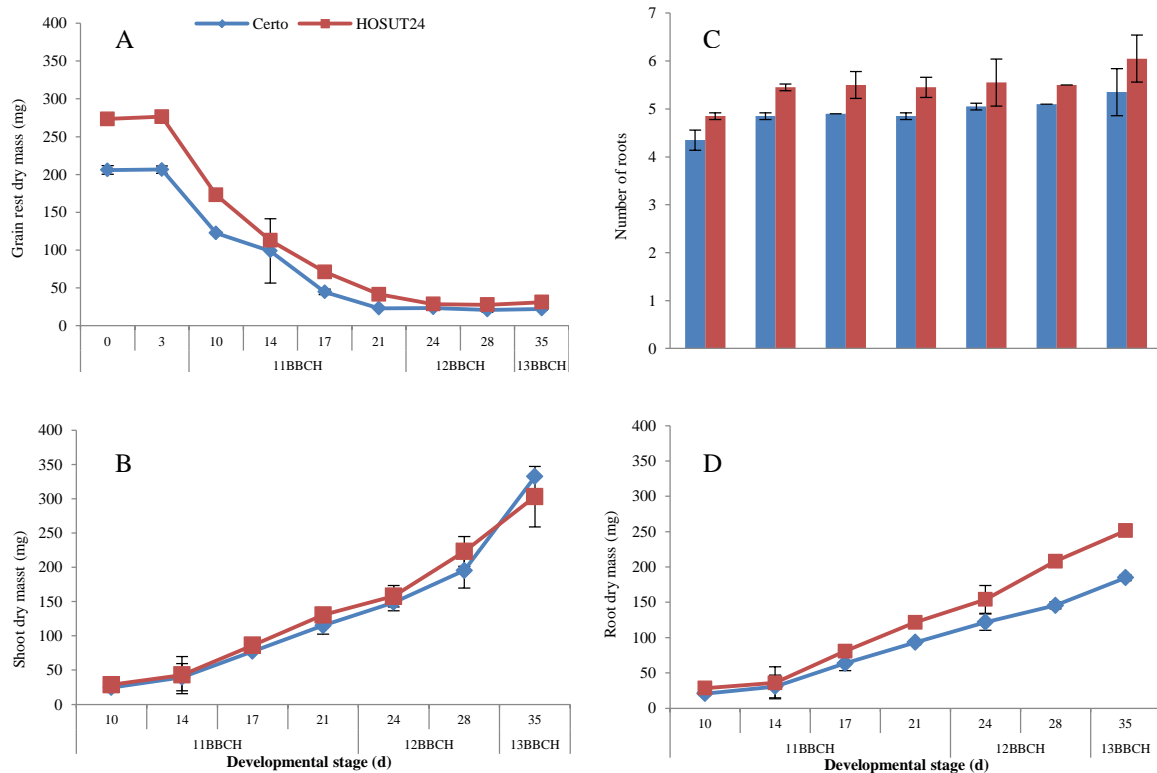


Figure 13. Biomass of seedlings emerging from grains with a weight range of 40-45 mg for Certo and 55-60 mg for HOSUT (median grain weight-distribution pattern). Bars  $\pm$  SD. A: Grain rest dry mass. B: Shoot dry mass. C: Number of roots per seedling. D: Root dry mass.

#### 2.3.1.2.4. Effect of grain weight on seedling development and vigour under field-like conditions

In order to assess whether the differences obtained in the previous analysis was also evident under field-like conditions, seedlings from grains of a weight ranging from 50 to 55 mg and from the typical grain weight distribution for both HOSUT24 and Certo were grown and harvested in parallel at 12-13BBCH during the growing season 2013-2014. The early seedling vigour parameters shoot dry mass, plant height, number of seminal roots and chlorophyll measurements (SPAD values).

Grain weight seemed to affect seedling height. When grains of similar weight were sown, seedlings of both lines had no difference on height as was found in seedlings emerging from grains with the typical weight distribution (Figure 14).

However, the influence of the transgene could be measureable in parameters such as shoot dry mass and SPAD values in which HOSUT24 seedlings presented significantly increased values regardless of the grain weights (55-56 mg and typical distribution) used in the experiment (Figure 14).



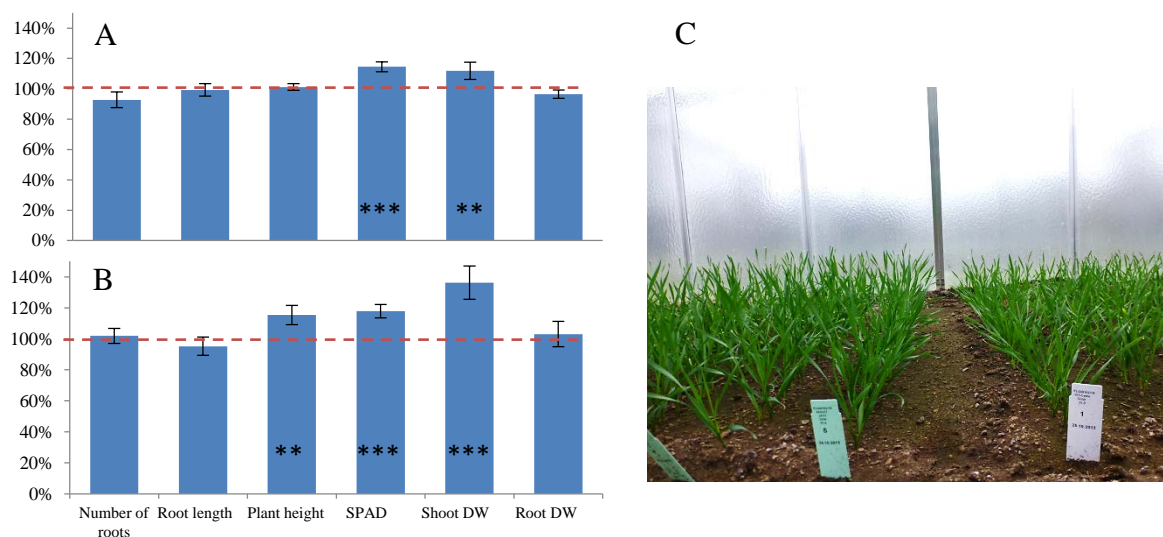


Figure 14. Seedling vigour characteristics at 12-13BBCH stage of HOSUT24 and Certo plants grown under field-like conditions. A. Vigour parameters of seedlings grown from similar grain weight (50-55 mg). B. Vigour parameters of seedlings growing from unsorted grains corresponding to the typical grain weight. C. Seedling of the experiment with same grain weight (50-55 mg) for both lines growing under field-like conditions. T-Test  $P < 0.05$  (\*),  $P < 0.01$  (\*\*),  $P < 0.001$  (\*\*\*) . Season 2013-2014.

The grain weight distribution typically found in HOSUT and Certo seed lots (Figure 10) reflects the positive influence of transgene expression on seed development that seems to be continued during germination and seedling development. This influence is independent of the weight of the grain, since in grains of Certo and HOSUT24 with similar weights, HOSUT24 seedlings still develop a more vigorous phenotype.

In agriculture, seed lots are used without any pre-selection. Thus, the positive impact of higher TGW on seedling vigour is an intrinsic property of this new winter wheat line. Having this in consideration, in-depth analysis of the HOSUT seedling phenotype using grains with typical grain weight distribution for HOSUT and Certo is presented in the following sections.

### 2.3.2. *HOSUT seedling vigour under different growing conditions*

Comprehensive phenotypization of HOSUT's seedling vigour, with focus on the root system was performed under three different growing conditions: N-deprived and N-supplied *in vitro* conditions and field-like conditions.

#### 2.3.2.1. *Evaluation under field-like conditions of HOSUT's seedling vigour*

For field-like evaluation of the seedling's phenotype of HOSUT lines under field-like conditions, three of the transgenic lines were sown. Evaluation was performed at one leaf

(11BBCH), two leaves (12BBCH) and three leaves (13BBCH) stages of development.

At 11BBCH, no clear difference was visible between HOSUT lines and Certo in the dry mass of both shoot and root; moreover, no lateral root emergence was detected in either line. For these reasons, the analysis was focused on 12BBCH for both roots and shoots. Analysis at 13BBCH was performed only for shoot development.

#### 2.3.2.1.1. Seedling root and shoot biomass

At 12BBCH, the height of the shoot was increased in all HOSUT lines when compared to Certo. HOSUT lines 24 and 12 showed significantly increased root and shoot mass in comparison to Certo. HOSUT20 root mass was 3% higher than that of Certo; yet this difference was not significant (Figure 15).

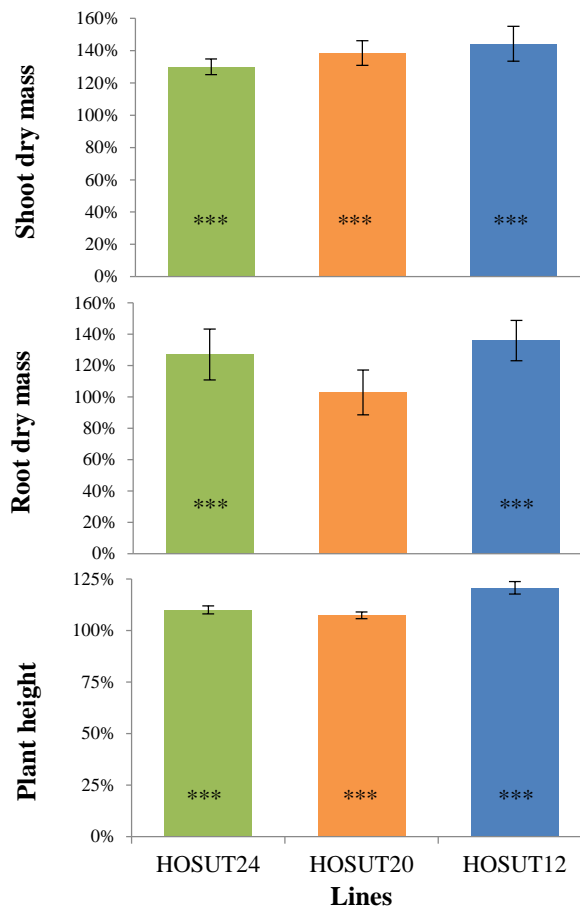


Figure 15. Seedling vigour parameters of HOSUT plants grown under field-like conditions at 12BBCH. Values in percentages (Certo = 100%). Kruskal-Wallis Test  $P < 0.05$  (\*),  $P < 0.01$  (\*\*),  $P < 0.001$  (\*\*\*)

Further biomass measurements performed at 13BBCH indicated that the shoots of all HOSUT plants have increased dry mass in comparison to Certo (Figure 34 in

Supplemental data). Plant height of HOSUT lines 24 and 12 was also significantly increased. HOSUT20's height was in average comparable to Certo.

At 12 and 13BBCH, no difference was found in the number of seminal roots of the transgenic lines.

#### 2.3.2.1.2. Chlorophyll content in seedlings under field-like conditions

SPAD measurements were performed from early seedling development, until the stem elongation phase (from 11 to 32 BBCH), during the growing season 2012-2013. These evaluations indicated that the chlorophyll content of leaves of all three transgenic lines was different from that of Certo with the exception at 13 and 21 BBCH, which corresponds to the vernalization period (Figure 16). According to T-Tests, at stages 11 and 12 BBCH, there was a statistically significant increase in the chlorophyll content. At 13 and 21 BBCH, no difference was registered. From 25 BBCH chlorophyll content was about 20 % higher in HOSUT. Once the plants entered the stem elongation stage the difference in SPAD values between the three HOSUT lines and Certo was stable and significantly higher in the transgenic lines.

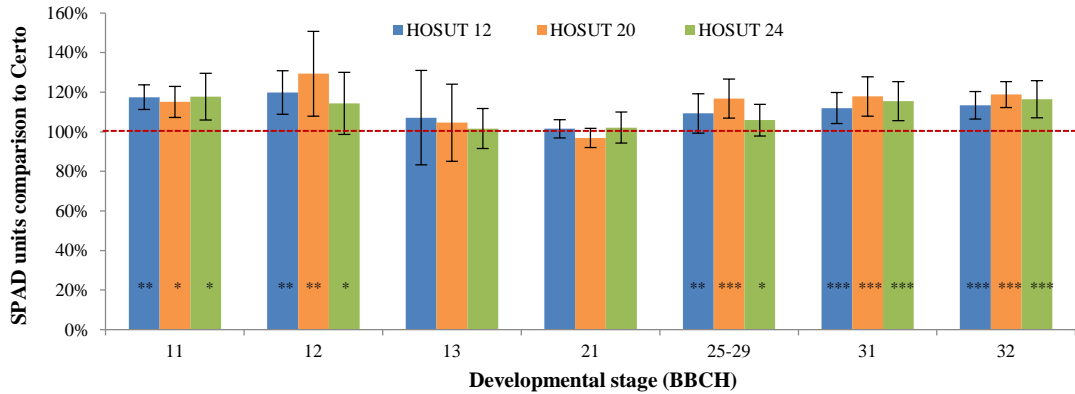


Figure 16. Differences detected in SPAD units between three HOSUT lines and Certo (100%, red line). Plants were grown under field-like conditions. Vertical bars:  $\pm$  SD. T-Test  $P < 0.05$  (\*),  $P < 0.01$  (\*\*),  $P < 0.001$  (\*\*\*) Season 2012-2013.

#### 2.3.2.2. Analysis of seedling growth under *in vitro* N-supplied conditions

The *in vitro* system established in the frame of this PhD thesis was shown to be a useful tool for root analysis. The vermiculite substrate allowed efficient extraction and washing of the root system. Since it is an inert substrate and due to the physical characteristics of its surface it allows a controlled nutrition to the plants and assured that all the liquid volume added to the system will be available for the growing plants.

### 2.3.2.2.1. Chlorophyll content of seedlings under *in vitro* N-supplied conditions

HOSUT24 was used as a model for comparison to Certo. An increase in the chlorophyll content was also evident when *in vitro* seedlings were grown under N-supplied conditions, where the SPAD units in HOSUT had a value of  $107.6 \pm 3.3\%$  (Certo = 100%, T-Test  $P > 0.001$ ) at 13BBCH. In this way showing the stability of this trait also under *in vitro* conditions.

### 2.3.2.2.2. Root biomass under N-supplied *in vitro* conditions

HOSUT24 was chosen as representative of the transgenic phenotype. Both HOSUT24 and the wild type Certo were grown under *in vitro* conditions in XS-media containing 165 mg/l  $\text{NH}_4\text{NO}_3$ . For comparison, biomass accumulation was evaluated at 13BBCH in parallel under conditions where no additional N was used (N-deprived XS medium).

As obtained in the results under field-like conditions, the ANOVA analysis indicated that HOSUT plants grown in XS media supplied with N also developed a root system with increased biomass (Figure 17). Moreover, the difference between the lines was similar under both *in vitro* conditions, in the system with the N-supplied medium the increase is 119.2% and in XS N-deprived medium 113.1%.

Additionally, biomass measurements of HOSUT24 and Certo plants grown on N-supplied medium, indicated that plants were in general shorter and developed lower root biomass than those grown on N-deprived medium ( $P < 0.0001$ ).

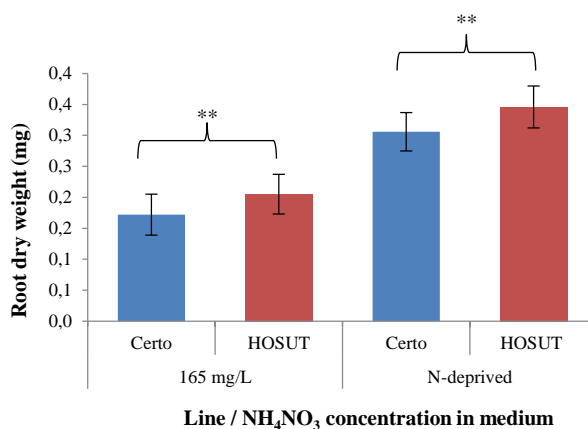


Figure 17. Root dry mass evaluated under *in vitro* conditions with depletion or supply of N. A: Root dry mass of HOSUT and Certo plants grown in XS N-deprived medium and XS + 165 mg/l  $\text{NH}_4\text{NO}_3$ . ANOVA  $P < 0.05$  (\*),  $P < 0.01$ (\*\*),  $P < 0.001$ (\*\*\*).

HOSUT24 and Certo plants grown in N-supplied medium developed similar amount of seminal roots, comparable to the results obtained under field-like conditions. In contrast, on N-deprived conditions, HOSUT24 plants developed significantly more seminal roots ( $P < 0.0001$ ) than Certo.

Also under N-supply, the root system of Certo was in average longer than that of HOSUT24. However, the difference was not statistically significant. The slight reduction in root length and yet increase in root biomass leads to the conclusion that the higher biomass might be due to an increased number of lateral roots and/or an increase in the thickness of the individual roots. Further analysis of the number of lateral roots under N-deprived conditions will be presented in following sections.

### 2.3.2.3. Seedling phenotyping under N-deprived conditions

#### 2.3.2.3.1. Root biomass

To analyse further the root system of the HOSUT phenotype, the three HOSUT lines analysed previously were also tested under *in vitro* nutrient-limiting conditions. Root phenotyping of the transgenic lines showed that all three HOSUT lines develop a highly significant increase in root dry mass in comparison to Certo. The biomass of the HOSUT root system increased from 13% to 30% in comparison to Certo. Moreover, the number of seminal roots was increased in the HOSUT lines (Table 9).

Table 9. Seedling root parameters under *in vitro* conditions with N-deprived XS medium. Values in percentages of Certo (100%)  $\pm$  SD.  $P < 0.05$  (\*),  $P < 0.01$ (\*\*),  $P < 0.001$ (\*\*\*). Root dry mass and number of seminal roots was analysed with ANOVA. Root length data analysis performed with Kruskal-Wallis test.

Line	Root dry mass	No. of primary roots per seedling	Root length
<b>HOSUT24</b>	109.3 $\pm$ 11.9*	113.1 $\pm$ 9.6***	93.6 $\pm$ 8.0**
<b>HOSUT20</b>	111.7 $\pm$ 16.9 **	119.7 $\pm$ 6.9***	88.4 $\pm$ 10.9***
<b>HOSUT12</b>	141.3 $\pm$ 13.5***	128.6 $\pm$ 9.6***	97.7 $\pm$ 11.9

It was evident that the root system of lines 20 and 24 is significantly shorter than that of Certo; however, line 12 produces increased root biomass and a root system similar in length to Certo (Table 9).

#### 2.3.2.3.2. Number of lateral roots

In order to determine the number of lateral roots, root systems of HOSUT and Certo plantlets at 12BBCH were dried and high quality pictures were taken (Figure 18), which were sent to the Biosystems Engineering group at the Fraunhofer IFF Magdeburg.

The new tool and algorithm developed by this group allowed quantification of root parameters such as the number of branching points.

Branching points were analysed in the upper 20cm of the root system. The analysis was performed starting from the point of the origin of the root system (distance 0mm). Results are given as the total number of branching points at every 20mm.

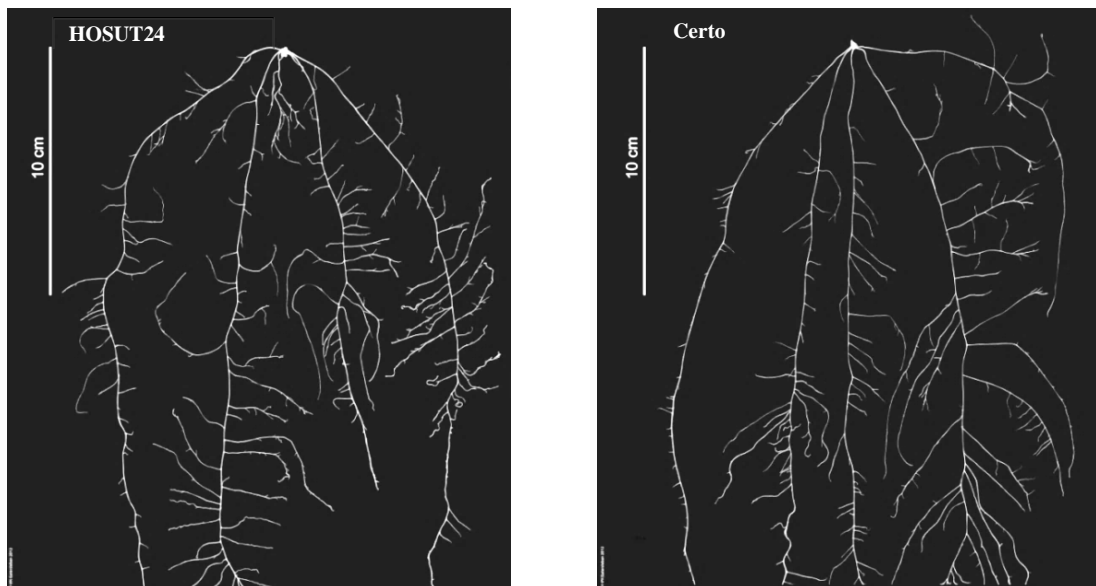


Figure 18. Examples of 2-D images used for acquisition of data reflecting root branching at the two leaves stage (12BBCH). *In vitro* plants were grown with N-free medium.

T-test analysis of the total branching points showed that line HOSUT24 has an increased ( $P < 0.05$ ) number of lateral roots in the upper 20cm of its root system (40.3% more branching points than Certo). Analysis of data allowed identifying differences at any distance from the root origin. Figure 19 details the differences between the two lines at every 2 cm. Significantly increased root branching is visible in the upper and lower part of the root system but surprisingly not in 60 to 100mm distance from the root origin.

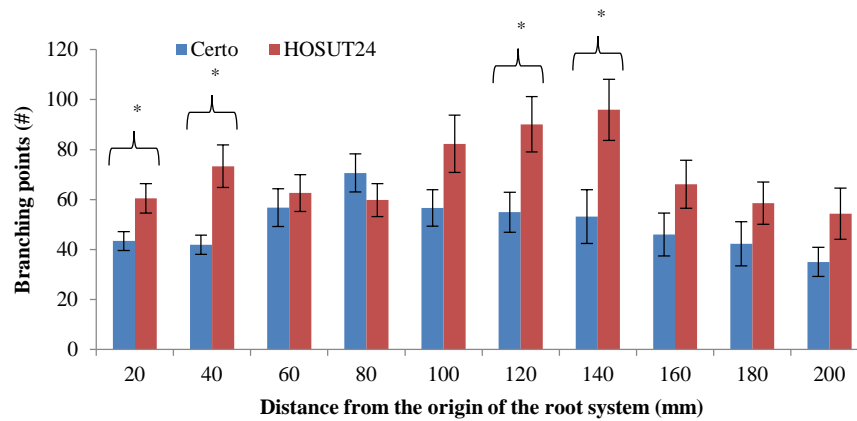


Figure 19. Difference between HOSUT24 and Certo in the number of branching points in the root system at the 12 BBCH stage. Stars show significant differences according to the Kruskal-Wallis test. P<0.05 (\*), P<0.01(\*\*), P<0.001(\*\*\*)

The results from this phenotypization indicated that the increase in biomass under *in vitro* conditions is due the augmented number of lateral roots formed by HOSUT plants.

#### 2.3.2.3.3. Chlorophyll content in seedlings grown under *in vitro* N-deprived conditions

Chlorophyll measurements during early seedling development under *in vitro* conditions were performed in plants growing in XS medium without N. Evaluations at 11, 12 and 13BBCH by SPAD measurements showed increased chlorophyll content in the transgenic lines (Table 10).

Table 10. Chlorophyll content measured in SPAD units at 11, 12 and 13BBCH from seedlings growing *in vitro* in XS medium without N. Values in SPAD units (Abs) and in percentages (Certo = 100%). P<0.05 (\*), P<0.01(\*\*), P<0.001(\*\*\*)

Line	Developmental stage					
	11BBCH		12BBCH		13BBCH	
	SPAD	% of Certo	SPAD	% of Certo	SPAD	% of Certo
<b>HOSUT24</b>	38.7 ± 2.1	117.7%*	40.8 ± 3.7	114.3%*	42.7 ± 9.5	101.6%
<b>HOSUT20</b>	37.9 ± 2.6	115.1%*	44.0 ± 7.3	129.3%**	41.7 ± 7.8	104.6%
<b>HOSUT12</b>	38.7 ± 3.9	117.5%**	38.9 ± 5.3	119.9%**	40.5 ± 4.0	107.1%
<b>Certo</b>	32.9 ± 2.7	100%	34.0 ± 3.6	100.0%	39.9 ± 8.6	100.0%

Phenotypization of HOSUT seedlings indicated that during early growth HOSUT plants developed an enhanced seedling vigour under both *in vitro* and field-like conditions. This

characteristic seemed to be stable in the three HOSUT lines evaluated.

Further biochemical phenotypization was performed in order to determine putative metabolic changes in HOSUT lines responsible for the enhanced performance of the lines.

### ***2.3.3. Metabolites and hormone profiling in HOSUT and Certo seedlings grown under different growth conditions***

#### ***2.3.3.1. N, C and CHO analyses of in vitro and field-like seedlings at 12-13BBCH***

Analysis of seedlings' CHO content on *in vitro* N-deprived conditions indicated that HOSUT24 had higher content of sucrose in shoots and roots. In comparison to Certo, as early as at 11BBCH in these two tissues, sucrose content in HOSUT24 was 110.6% and 114.0%, respectively. At 12BBCH, shoots of HOSUT24 contained 140.9% sucrose, the roots 99.2%. For this reason, deeper analysis of N, C and CHO in three different growing conditions at 13BBCH was performed.

Roots and shoots of HOSUT24 seedlings grown *in vitro* upon XS N-deprived medium have a higher sucrose concentration than those of Certo (Table 11). Similar scenario was documented for HOSUT12 and 20, which also have an increased amount of sucrose though it was not statically significant (Table 16 in Supplemental data). C concentration in both roots and shoots is different between HOSUT and Certo. However, N content in both roots and shoots is not different between HOSUT and Certo. However, N content in both roots and shoots is slightly increased; consequently, C/N ratio in HOSUT24 seedlings was diminished in both roots and shoots, but the difference was statistically significant only in the latter.

The presence of N in the growth media, whether under *in vitro* or field-like conditions, changed the CHO and N contents in comparison to Certo mostly in the root tissue. HOSUT24 root tissue had decreased N but increased C content. Thus, the C/N ratio in roots of this transgenic line was increased to 129.8% (Certo 100%). The corresponding shoot tissue of HOSUT24 seedlings had a similar N content; however, the C/N ratio was significantly higher in HOSUT24 than Certo (Table 11).



Table 11. N, C and sugars concentration in roots and shoots of HOSUT24 seedlings at 12-13BBCH in comparison to Certo  $\pm$  SD. T-test  $P < 0.05$  (\*),  $P < 0.01$  (\*\*),  $P < 0.001$  (\*\*\*)

Growth conditions	Metabolite	Root		Shoot	
		HOSUT24 abs	% of Certo	HOSUT24 abs	% of Certo
<i>In vitro</i> N-deprived	Glucose ( $\mu\text{mol/gDW}$ )	14.8 $\pm$ 4.4	107.6%	33.6 $\pm$ 6.5	157.7%**
	Fructose ( $\mu\text{mol/gDW}$ )	12.9 $\pm$ 3.5	109.4%	63.9 $\pm$ 13.8	82.1%
	Sucrose ( $\mu\text{mol/gDW}$ )	120.5 $\pm$ 6.3	135.1%*	108.3 $\pm$ 11.5	121.5%*
	Starch (mg/gDW)	26.2 $\pm$ 0.9	102.3%	42.9 $\pm$ 3.2	101.4%
	C (% of total mass)	40.8 $\pm$ 0.6	101.0%	39.6 $\pm$ 0.2	99.6%
	N (% of total mass)	0.63 $\pm$ 0.03	105.0%	1.0 $\pm$ 0.1	107.8%
	C/N	64.8 $\pm$ 3.4	96.3%	41.0 $\pm$ 3.3	92.0%*
<i>In vitro</i> N-supplied	Glucose ( $\mu\text{mol/gDW}$ )	23.9 $\pm$ 4.0	91.3%	21.1 $\pm$ 3.4	117.6%**
	Fructose ( $\mu\text{mol/gDW}$ )	19.3 $\pm$ 4.4	95.6%	20.8 $\pm$ 5.3	110.4%
	Sucrose ( $\mu\text{mol/gDW}$ )	27.7 $\pm$ 8.5	93.7%	22.8 $\pm$ 6.2	125.9%*
	Starch (mg/gDW)	35.9 $\pm$ 2.4	98.7%	19.8 $\pm$ 1.1	98.0%
	C (% of total mass)	36.6 $\pm$ 0.4	103.2%***	40.3 $\pm$ 0.2	102.9%***
	N (% of total mass)	2.79 $\pm$ 0.12	79.5%***	5.5 $\pm$ 0.1	99.6%
	C/N	13.1 $\pm$ 0.6	129.8%***	7.3 $\pm$ 0.2	103.1%*
Field-like	Glucose ( $\mu\text{mol/gDW}$ )	10.6 $\pm$ 2.1	105.3%	51.6 $\pm$ 5.2	146.7%**
	Fructose ( $\mu\text{mol/gDW}$ )	14.9 $\pm$ 3.0	75.5%*	134.9 $\pm$ 9.4	124.2%**
	Sucrose ( $\mu\text{mol/gDW}$ )	70.7 $\pm$ 5.0	98.0%	26.3 $\pm$ 3.6	116.1%
	Starch (mg/gDW)	22.8 $\pm$ 3.5	97.1%	11.8 $\pm$ 1.5	97.6%
	C (% of total mass)	35.1 $\pm$ 0.4	103.2%***	40.7 $\pm$ 0.3	100.3%
	N (% of total mass)	3.5 $\pm$ 0.1	93.3%***	5.0 $\pm$ 0.1	94.1%***
	C/N	10.1 $\pm$ 0.5	110.6%***	8.1 $\pm$ 0.2	106.5%***

Fructose in general was found in reduced amounts in HOSUT root tissues grown under all three growing conditions (Table 11). Moreover, analyses performed in HOSUT12 and 20 grown under field-like conditions also showed diminished content of fructose in root tissue (Table 16 in Supplemental data).

### 2.3.3.2. Metabolite analysis of roots at 12-13BBCH grown *in vitro*

Metabolites from seedling roots at 12-13 BBCH grown under *in vitro* N-deprived conditions were analysed by GC-mass spectrometry. 170 compounds were detected, out of which seven showed significant differences between the HOSUT lines 24, 20 and Certo. The major difference was found for Trp (Table 12).

Table 12. Metabolites significantly altered in HOSUT24 and HOSUT20 roots in comparison to Certo. The plantlets were grown *in vitro* in N-deprived XS medium, values are given in percentages (Certo= 100%). P-values are corrected according to Bonferroni.

Compound	HOSUT24 (%)	HOSUT20 (%)	ANOVA p-value (Bonferroni corrected)	Tukey (HOSUT24, 20, Certo)
<b>Tryptophan</b>	221.9 ± 18.3	260.7 ± 19.9	8.78E-07	a,a,b
<b>Tyrosine</b>	126.1 ± 8.4	122.5 ± 10.2	4.53E-04	a,a,b
<b>Phenylalanine</b>	118.6 ± 9.0	139.9 ± 18.7	4.28E-03	a,b,c
<b>Lysine</b>	136.3 ± 25.4	124.8 ± 9.7	8.24E-03	a,a,b
<b>Glucose-6-phosphate</b>	135.8 ± 9.4	115.2 ± 14.8	2.79E-02	a,ab,b
<b>Adipic acid, 2-amino</b>	223.9 ± 19.4	122.8 ± 5.8	3.14E-02	a,bc,c
<b>Citric acid</b>	65.7 ± 8.3	82.9 ± 12.9	3.53E-02	c,ab,a

Also Lysine, Glucose-6-phosphate and 2-aminoadipic acid are significantly increased in HOSUT roots. Citric acid shows a decrease in its concentration in both analysed lines.

### 2.3.3.3. Free amino acids in the root system of seedlings under *in vitro* and field-like conditions

Due to the increased aromatic amino acid levels found in HOSUT roots through the GC-MS, further analysis of free amino acids by UPLC was performed in root tissue at 13BBCH in all HOSUT lines in comparison to Certo, all lines grown under N-depleted conditions. The results of this analysis indicated, for all three lines, a stable increase in the Trp content (Figure 35 in Supplemental data). Further analyses were performed comparing HOSUT24 and Certo root and shoot tissues grown under three different growth conditions (Table 13, and in Supplemental data Table 17 and Table 18).

The results suggested that Asn and glutamine (Gln) levels are lower in HOSUT in both roots and shoots tissues especially when grown under N-supplied and field-like conditions.

Consistently with previous results, the aromatic amino acids Trp, Tyr and Phe had higher values in HOSUT24 roots grown under both *in vitro* conditions (Table 13). Though the Trp content detected in roots grown under field-like conditions was similar to that of Certo, the value obtained in the seedling's shoots grown under all three conditions was higher in HOSUT24.

Table 13. Content of free amino acids in lyophilized shoots and roots of HOSUT24 in comparison to Certo (100%) grown *in vitro* with N-supplied medium (165 mg/L) and *in vitro* with N-deprived medium and field-like conditions, harvested at 13BBCH (values: percentages calculated with Certo as 100%  $\pm$ SD. T-test: P<0.05 (\*), P<0.01(\*\*), P<0.001(\*\*\*)).

Tissue	Amino acid	Growing condition		
		N-deprived (%)	N-Supplied (%)	Field-like (%)
Roots	Asparagine	78.6 $\pm$ 23.2	81.8 $\pm$ 8.1**	38.4 $\pm$ 14.8*
	Glutamine	87.7 $\pm$ 9.6	80.0 $\pm$ 6.7**	78.8 $\pm$ 28.1
	Phenylalanine	112.6 $\pm$ 14.1	114.8 $\pm$ 11.5	120.0 $\pm$ 18.3*
	Tryptophan	175.9 $\pm$ 36.7***	149.2 $\pm$ 28.0*	95.8 $\pm$ 27.4
	Tyrosine	119.2 $\pm$ 17.0	90.5 $\pm$ 0.1	127.8 $\pm$ 52.2
Shoots	Asparagine	100.0 $\pm$ 24.0	68.1 $\pm$ 24.6*	16.5 $\pm$ 4.7***
	Glutamine	85.7 $\pm$ 9.5	74.7 $\pm$ 11.1**	65.5 $\pm$ 16.6**
	Phenylalanine	112.2 $\pm$ 12.9	97.8 $\pm$ 28.3	117.2 $\pm$ 8.8*
	Tryptophan	147.4 $\pm$ 9.4***	113.7 $\pm$ 40.0	170.8 $\pm$ 20.3***
	Tyrosine	128.5 $\pm$ 14.5	99.45 $\pm$ 18.9	117.9 $\pm$ 17.8**

Note: complete data of measured free amino acids is available in Supplemental data (Table 17 and Table 18).

This change in the content of aromatic amino acids in the shoots and roots of HOSUT24 in comparison to Certo suggests an alteration in their biosynthetic pathway and possibly in the metabolites that originate from that as well. These results together with the increased formation of lateral roots in HOSUT24 indicated that changes in the Trp pool in both shoots and roots could influence auxin and cytokinin contents.

#### 2.3.3.4. Auxin and cytokinin content in HOSUT seedlings under N-deprived *in vitro* conditions

By using a UPLC-MS/MS analysis approach, it was possible to detect and quantify indole-3-acetic acid (IAA), IAA-Ala (storage), indole-3-acetamide (IAM) and indole-3-acetonitrile (IAN) (precursors), IAA-Glu (inactivation conjugate) and oxindole-3-acetic acid (OxIAA) which is the non-active oxidized form (Bajguz and Piotrowska, 2009; Korasick et al., 2013; Ludwig-Müller, 2011). Furthermore, cis- and trans-zeatin as well as their ribosides were also measured.

At 11BBCH, when no lateral roots were visible in neither line, the HOSUT24 content of IAM and IAA-Ala in root tissues were similar to that of Certo. However, differences were detected in the shoot tissue, in which already at this stage the precursor IAM was significantly higher in HOSUT24 (Figure 20A).

Differences in the IAA content become more evident at 12BBCH in both tissues, most remarkably in shoots, where the detected amount of IAA in HOSUT24 doubled that found in Certo (Figure 20A). Congruently, at this developmental stage, lateral roots are grown and the difference in lateral root number between both lines is evident as shown in Figure 19.

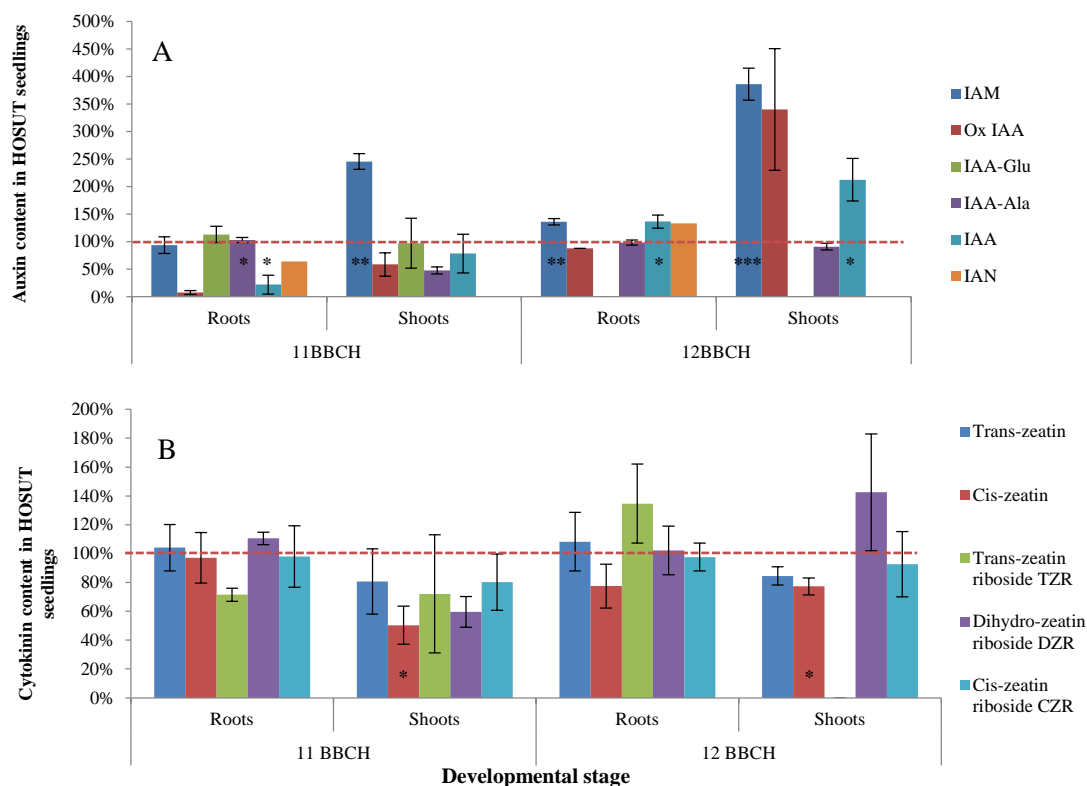


Figure 20. Auxin and cytokinin content in root and shoot tissue of HOSUT24 and Certo at 11BBCH and 12BBCH grown under *in vitro* N-depleted conditions. T-test  $P < 0.05$  (\*),  $P < 0.01$  (\*\*),  $P < 0.001$  (\*\*\*). Vertical bars  $\pm$  SD. Values given in percentages of Certo = 100% marked with a red dotted line.

Auxin biosynthesis in a Trp-dependent way, can be found in three different pathways: the IAM, the IAOx (out of which IAN is an intermediate) and the indole-3-pyruvic acid (Korasick et al., 2013). The results of this study indicate that in HOSUT24 IAA might be synthesized from two Trp-dependent pathways: the IAM and IAOx/IAN pathway. However, the latter was only detected in roots (Figure 20), possibly indicating that the IAM pathway might be the only active in wheat shoots.

Active cytokinins are trans-zeatin and cis-zeatin, the riboside forms are for transport and/or storage (Sakakibara, 2006). Cytokinins and their ribosides were detected with altered values in HOSUT24 tissues at early stages. At 11 and 12 BBCH shoots of HOSUT24 presented significantly decreased values of cis-zeatin, trans-zeatin in shoots

was also diminished in HOSUT24 although in this case these values were not statistically different from Certo (Figure 20).

Riboside forms TZR, DZR and CZR were detected in similar amounts in roots of both lines. In shoots, the riboside forms had the tendency to lower values in HOSUT24 during 11BBCH and slightly increased at 12BBCH.

## **2.4. Discussion**

### **2.4.1. Influence of the increased HOSUT grain weight on the early seedling phenotype**

The grain weight-frequency analysis shows that the increased TGW of HOSUT is due to a greater amount of grains that are 15-20% heavier than those of Certo. By increasing seed/grain size, endosperm and aleurone reserves are also increased, and are able to supply higher nutrient and assimilate amounts to the developing and germinating embryo (Aparicio et al., 2002). Correlation between grain weight and seminal root number in barley, seedling development and vigour, seed viability and proper germination, as well as seedling survival have already been discussed and analysed by Li and Li (2014) and Manske and Vlek (2002) and previously by Evans and Bhatt (1977).

Grain weight is of great importance for grain yield in cereals, and throughout domestication, crop plants were selected for larger seed size and consequently greater seed or grain weight (Aparicio et al., 2002; Boyd et al., 1971; Evans and Bhatt, 1977; Gupta et al., 2006).

In this study, the influence of the grain weight on seedling vigour was evaluated through a series of *in vitro* and field-like experiments, where the effect of similar and different grain weight for both lines were analysed. In all *in vitro* experiments, the grains of both lines were depleted by the end of 11BBCH, at this moment, the direct influence of the grain on the seedling development ends; however, during these early stages, the positive influence of the grain weight might contribute to the enhanced seedlings' vigour observed in HOSUT24. Aparicio et al. (2002) found in their experiments that the leaf appearance rate was associated to the grain weight before the 13BBCH stage.

In experiments with grains of similar weight, either low (40-45 mg) or high (54-56 mg) under N-depleted conditions, there was a tendency to an increased primary root number in HOSUT24, which cannot be explained on a basis of grain size.

It was clear through the *in vitro* experiments that the increased TGW of HOSUT gives an

advantage to the seedlings enhancing their vigour through an increase availability of nutrients for the early seedling development. Assimilate partitioning along the spike is not homogenous to all the grains; those in the middle part of the spike develop first, are best supplied with assimilates and tend to be bigger. Therefore, differences in the composition of the grains are expected between grains of HOSUT and Certo with similar weight. This could be especially evident when grains of the low-weight range were used (40-45 mg), grains of such weight are grown in the middle part of Certo's spike in contrast to grains of the same weight in HOSUT, which developed at a position in the spike that might be related to reduced supply of assimilates.

The early developmental advantage of HOSUT could influence later seedling stages, although, this is not completely clear. In a large accession of spring barley cultivars, Neumann et al. (submitted) found significant correlation, yet of medium-strength ( $R=0.41$ ), between TGW and seedling biomass during early development. However, such correlation decreased its magnitude and statistical significance in time.

In HOSUT lines at the end of 11BBCH, the grain was already depleted. Further phenotypical or metabolic changes in later stages cannot be a simple consequence of an earlier increase due to grain weight. This influence was evident when the effect of grain weight over the seedling vigour was evaluated under field-like conditions; where seedling vigour parameters such as chlorophyll content and shoot biomass were higher in HOSUT24 regardless of the initial grain weight (Figure 14). Nonetheless, the biggest differences between the lines were found in seedlings emerging from grains that represent the typical grain weight distribution *i.e.* not sorted out.

Analysis under field-like conditions of the HOSUT24 and Certo plants that emerged from grains of similar weight included the determination of grain morphology and yield parameters (data not shown). Increased TGW as well as other typical positive morphological characteristics of HOSUT grains were also found in that harvest, *i.e.* HOSUT grains continued having a median value of 55-57 mg and Certo of 44 mg in their TGW. The fact that bigger Certo grains were sown, did not affect the average grain size and weight in Certo's offspring and therefore its yield.

The higher seedling vigour of HOSUT cannot be attributed only to the effect of bigger grains, the increased chlorophyll content throughout the life cycle and the increase in shoot biomass under field-like conditions at early stages cannot be explained by that.

After the depletion of the grain, direct effect of the grains reserves over the plant are not expected.

#### **2.4.2. HOSUT performance under *in vitro* nutritional limiting conditions**

*In vitro* analysis of biomass differences between Certo and HOSUT lines during early seedling development showed that under N-deprived conditions HOSUT lines develop a more vigorous root system in terms of biomass and seminal root number at 13BBCH (Table 9). This increase in biomass in HOSUT could be explained by the significantly increased number of lateral roots already present at the 12BBCH stage (Figure 19) analysed through a 2D-imaging system.

Enhanced lateral root formation under limiting nutritional conditions is a strong advantage for the developing seedling, it allows it to better explore the substrate for nutrients and water. This characteristic of HOSUT lines help ensuring early establishment of the plantlets, which is particularly important to survive winter.

Furthermore, the increased chlorophyll content in HOSUT, also detected under *in vitro* N-depleted conditions as early as at 11BBCH, might indicate an increased photosynthesis capacity in these lines also during such limiting nutritional conditions.

#### **2.4.3. Changes in the metabolism of HOSUT seedlings during early development**

##### **2.4.3.1. Altered content of sucrose and glucose and their putative effect on the shikimate pathway of HOSUT24 seedlings**

HOSUT24 and Certo *in vitro* plants grown under N-supplied conditions tend to have similar amounts of sugars (sucrose, glucose and fructose) in root tissues; however, the total C content is significantly higher in roots of HOSUT24. On the other hand, shoots of HOSUT24 grown under this condition have increased amounts of glucose and sucrose, similar to results obtained in HOSUT tissues grown under field-like conditions. This scenario slightly changes in plants grown under *in vitro* N-deprived conditions (Table 11), where the sucrose content was significantly higher in root tissues of HOSUT, while shoot tissue just showed a tendency to increased values in glucose and sucrose.

The fact that more sugars are found in HOSUT root tissue under nutritional limiting conditions, might be linked to the necessity of the seedling to extend its root system in the search for nutrients and the potential of HOSUT lines to do so.

Sucrose and glucose are known signals for diverse developmental pathways. They are

important components not only at the structural level but also at the signalling level (Ruan, 2014). Consequently, their transporters along with its metabolizing enzymes are also important for plant growth and consequential for development (Rolland et al., 2006).

The increased lateral root formation in HOSUT might involve the use of sugars in a complex machinery for development, cell division and auxin synthesis, in order to increase the number of lateral roots. Detailed information about differential gene expression in HOSUT tissues is discussed in Chapter 3.

The higher content of aromatic amino acids (Trp, Tyr, Phe) in HOSUT lines suggests, that in HOSUT wheat root tissues the shikimate pathway might be more active than Certo. This pathway has been described to take place in plastids (mainly chloroplasts); however, it is also reported to be active in non-photosynthetic tissues such as roots and a key enzyme of the shikimate pathway is located also in the cytosol (Weaver and Herrmann, 1997).

Aromatic amino acids are precursors of a large number of compounds such as hormones, pigments and cell wall components. Moreover, through the shikimate pathway, the central carbohydrate metabolism and the aromatic amino acids metabolisms are linked (Maeda and Dudareva, 2012).

The increased content of sucrose in roots of HOSUT24 might have stimulated the activity of the shikimate pathway in comparison to that found in Certo. Furthermore, in shoot tissues, there is also a tendency to increased levels of aromatic amino acids (Table 13 and Table 17) that could indicate also higher activity of this pathway not only in roots but also in shoots.

Congruently with the result of an enhanced shikimate pathway and increased Trp content, in HOSUT24 IAA content and even the content of its analysed conjugates are found in greater amounts in roots and shoots of HOSUT24 as early as at 11BBCH. Increased auxin content enhances lateral root formation and reduces the primary root length (Woodward and Bartel, 2005), HOSUT lines present such phenotype. This result together with the hormone analysis of root and shoot tissues leads to the conclusion that either transport or biosynthesis of IAA is altered in HOSUT lines.



Taking together the compositional analyses of these tissues, rises the hypothesis that in HOSUT lines sucrose stimulates the Shikimate pathway which in turn stimulates auxin biosynthesis in a Trp-dependent way (Figure 21) as was found for maize kernels (Leclere et al., 2010).

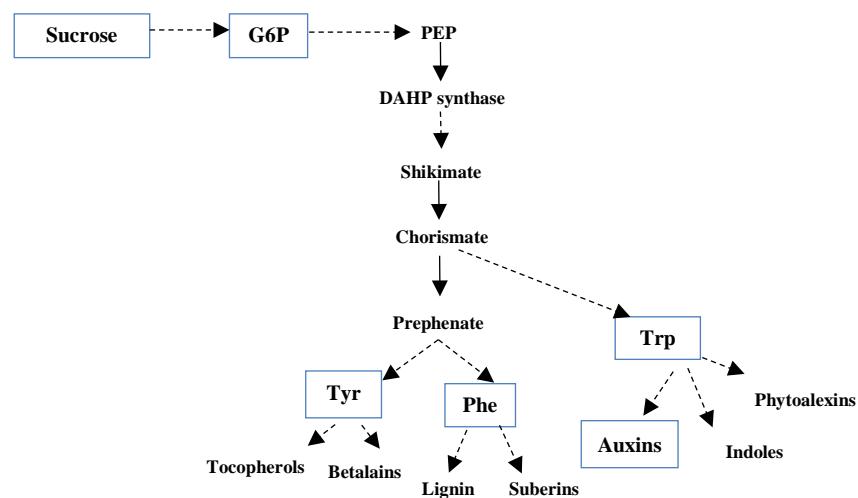


Figure 21. Metabolites involved in the auxin biosynthetic pathway found in increased contents in HOSUT seedlings (colour boxes). Modified from Maeda and Dudareva (2012). Dotted lines correspond to several steps in the metabolic pathway.

#### 2.4.3.2. Change in HOSUT's C/N ratio might be involved in lateral root formation

The changes in the C or N status in the tissues influence the C/N ratio. C/N balance signalling in plants has been linked to plant development as it indicates nutrient status in the plant; moreover, it has been linked also to diverse signalling pathways. Since changes in the content of IAA and its precursors were detected in HOSUT plants, it is possible that the C/N balance response could be part of the regulation of the auxin response genes (Zheng, 2009).

Increased lateral root number in HOSUT24 under N-deprived conditions might be an outcome of altered signalling pathways involving C/N ratio and its cross talk with hormones like auxin and cytokinins. Kiba et al. (2011) reported that N status and cytokinin contents are closely related and under N limitation, altering in this way, the root architecture.

### **3. Chapter. Influence of HvSUT1 on the transcriptome of early developing roots of winter wheat**

#### **3.1. Introduction**

Sucrose must be actively taken up by transporters to enter the phloem and continue its path through the plasmodesmata towards the sink cells (Braun and Slewinski, 2009). In symplastic isolated tissues, active transport is necessary to import sucrose against the osmotic potential in the phloem for long distance transport (Aoki et al., 2004; Truernit, 2001; Williams et al., 2000).

Carbohydrates are key molecules involved in key processes during plant growth and development as the backbones for biomass construction. Their role, however, is not restricted to structure and metabolism, they are also involved in diverse signalling pathways that also cross-talk with hormones like ABA, ethylene, cytokinin and auxin, regulating and controlling growth (Rolland et al. 2002; Rolland et al. 2006; Eveland and Jackson 2012).

HOSUT lines ectopically express the HvSUT1 gene under the control of a barley hordein B1 promoter (HO). Furtado et al. (2008; 2009) studied the expression of the GFP protein under the control of several seed specific promoters including hordein B1 promoter. In rice, the expression of the GFP protein was detected not only in the endosperm as expected, but also in maternally originated grain tissues as in leaf and root tissues.

Sucrose metabolism and therefore its transport are involved in key physiological pathways that regulate plant development (Mason et al., 2014; Rolland et al., 2006; Ruan, 2014; Wind et al., 2010). Expression of HvSUT1 in vegetative tissues may influence the sucrose uptake and/or partitioning into diverse sink tissues besides grains and therefore have an impact on gene expression. In this study, HvSUT1 effects were analysed based on the differences in the transcriptome of young root tissue comparing line HOSUT24 and the non-transgenic Certo as control.

## 3.2. Materials and methods

### 3.2.1. *qRT-PCR analysis of HvSUT1 expression in wheat seedlings at distinct developmental stages*

#### 3.2.1.1. *Plant material*

HOSUT24 and Certo plants were grown under N-depleted *in vitro* conditions in a climatic chamber, at 14°C day and 12°C night with 12 h photoperiod. Plant material was harvested at 11BBCH, 12BBCH and 13BBCH. For each of these stages, six pots were harvested; each pot contained five plants of each line.

The seedlings were harvested per pot and per line, then divided into root and shoot and placed into 50 mL Conical Centrifuge Tubes and immediately frozen in liquid N. Plant material was kept under deep freezing (-80°C).

Developing grains of HOSUT24 and Certo were harvested at 25 days after flowering (DAF) from plants grown under field-like conditions and kept at -80°C until further use. Three biological replications were harvested, each with five grains.

Plants grown under field-like conditions were harvested between the stages 25-32 according to the BBCH scale (tillering and early stem elongation). The developing spike of the main stem of 90 plants was harvested per line at four developmental stages identified according to the scaling of Vahamidis et al. (2014). Three biological replicates per line with 30 explants per replication represented each stage.

#### 3.2.1.2. *RNA isolation*

##### 3.2.1.2.1. *In vitro* seedlings

For total RNA extraction of the seedling material, the frozen tissue was grinded separately according to line and pot, during 50s using a MM 400 Retsch® mill. To assure that the tissue remained frozen, pre-chilled jar and milling balls were used. Grinded tissue was placed in cryotubes for storage at -80°C.

For RNA extraction three biological repetitions per tissue, line and developmental stage were used. Each biological repetition corresponded to the grinded tissue of two adjacent pots.

Total RNA was isolated from root or shoots tissue using TRIZOL reagent (Invitrogen GmbH, Karlsruhe, Germany). 100 mg of frozen grinded tissue was added to 1 ml of TRIZOL pre-warmed at 60°C and incubated at that same temperature during 5 min under

medium agitation in a thermomixer. Following this incubation, 200µl of Chloroform were added to each sample, which was then vortexed and incubated at room temperature for 2-3 min.

Samples were then centrifuged at 13000rpm 4°C during 12 min. The aqueous phase was transferred to a new 1,5 ml centrifuge tube, 0.6 volumes of isopropanol and 1/10 volumes of NaAC 3M (pH5) were added. Samples were then vortexed, incubated at room temperature for 2 min, and centrifuged at 13000rpm 4°C for 10 min. The pellet was washed with 1 ml of 70% EtOH and Centrifuged at 13000rpm 4°C for 10 min. Any remains of EtOH was carefully pipetted out and the samples were left to dry for 5-10 min. To initiate the cleansing of the samples, the pellet was dissolved in 100µl of nuclease free water. The cleansing procedure was performed with the RNeasy Plant mini kit from Qiagen according to manufacturer's protocol for on-column DNase digestion and RNA clean-up of samples.

#### 3.2.1.2.2. Developing grains

Due to the high starch content of the developing grain at 25 DAF, a phenol/chloroform extraction was performed using a modified protocol of Heim et al. (1993). Briefly, the frozen grain material was grinded with pestle and mortar in the presence of liquid N. 700 µl of extraction buffer (1% SDS, 1 M Tris pH 9.0 and 10mM EDTA) and 700µl Phenol/Chloroform/isoamyl alcohol (Ph/Ch/I, 25:24:1) were added to the grinded sample. The organic and aqueous phases were separated by centrifugation during 2-3 min at 4°C at 13000rpm, then the supernatant (aqueous phase) was transferred to a new centrifuge tube and 700µl Ph/Ch/I were added again. The samples were vortexed for 15sec and centrifuged again during 5-6 min at 4°C at 13000rpm. The supernatant was transferred again to a new centrifuge tube and 1/10vol of Na-acetate was added. To separate the nucleic acids by precipitation 1 ml EtOH was added to each sample. The samples were allowed to precipitate at -20°C for at least 1h.

After the latter incubation under freezing temperatures, samples were centrifuged at 13000rpm 4°C during 10-15 min. The resulting pellet was dissolved in 200µl cold water and 2,5µl RNaseOut (Invitrogen) were added. The pellet was dissolved overnight at 4°C. The samples were, then centrifuged 10 min at 4°C and to the supernatant 200µl of 4M LiCl were added. The samples precipitated overnight at 4°C and then centrifuged for 15min at 4°C at 13000rpm. The pellet that contains the RNA was then washed with 900µl

2M LiCl and then two times with 900 µl of cold 70% EtOH. The samples were centrifuged 5min at 4°C and the EtOH was removed by pipetting and drying.

To eliminate traces of DNA, a DNase treatment with Turbo DNA free kit (Ambion AM1907) was performed according to the manufacturer’s instructions. To increase purity, samples were washed with Vivaspin columns (Sartorius ®) according to manufacturer’s recommendations.

### 3.2.1.2.3. Developing spikes

RNA from developing spikes was isolated using the Agilent extraction kit “Absolutely RNA Microprep” following manufacturer’s instructions.

RNA quality from all samples was checked prior its use with the Agilent Bioanalyzer 2100.

### 3.2.1.3. *cDNA synthesis and qRT-PCR*

First-strand cDNA was synthesized with oligo(dT) primer and SuperScript III reverse transcriptase (Invitrogen) according to the manufacturer’s instructions.

qRT-PCR was performed using Power Sybr® Green PCR Mastermix, the amount of amplified cDNA use was of 25-30ng in each PCR reaction. HvSUT1 specific primers are given in Table 14. qRT-PCR was performed with ABI Prism 7900HT Sequence Detection System (Applied Biosystems). Cycling conditions were: 2 min at 50°C then 40 cycles of 10 min at 95°C, 15s at 95°C and 1 min at 60°C followed of a dissociation stage of 15s at 95°C, 15s at 60°C and 15s at 95°C.

Amplification efficiency was assessed with the LinRegPCR program. The wheat actin (accession no. AB181991) gene was used for normalization.

Table 14. Specific forward (F) and reverse (R) primers for qRT-PCR (5’ - 3’) oriented.

<b>Gene</b>	<b>F</b>	<b>R</b>
<b>TaAct1</b>	5’-GTG GAG GTT CTA CCA TGT TTC CTG-3’	5’-GCT AAG AGA GGC CAA AAT AGA GCC-3’
<b>HvSut1</b>	5’-CGG GCG GTC GCA GCT CGC GTC TAT T-3’	5’-CAT ACA GTG ACT CTG ACC GGC ACA CA-3’

### ***3.2.2. Transcriptome analysis of seedling's root tissue grown under control climatic conditions***

#### *3.2.2.1. RNA-labelling and array hybridization*

Labelling was performed using a Low Input Quick Amp Labelling Kit (Agilent Technologies) with a Cy3-labelling dye according to manufacturer's protocol. 200ng of RNA was used for cRNA synthesis. Quantification and quality of cRNA were obtained with an ND-1000 Spectrophotometer (NanoDrop Technologies, Wilmington, USA).

Prior to the hybridization, yield and specific activity were checked and calculated according to the manufacturer's recommendation. For hybridization 600ng of labelled cRNA were used for fragmentation. Gene Expression Hybridization Kit (Agilent Technologies) was used for fragmentation following the manufacturer's protocol. Hybridization was performed during 17h at 65°C in an Agilent 8×60K customized wheat array. Washing and drying were done using the Gene Expression Wash Buffer Kit (Agilent Technologies). Arrays were scanned at 3µm resolution using an Agilent Technologies Scanner G2505C. The data extraction was performed with Agilent Feature Extraction software 11.5v (Agilent Technologies). The gene annotation used in the analysis was prepared by OakLabs GmbH and Plant Genome and Systems Biology (PGSB).

Data evaluation was performed with GeneSpring 12.6v (Agilent Technologies). The experimental data was  $\log_2$  transformed and quantile normalized. Relative expression values were calculated using a baseline transformation. Removal of outliers and transcripts without significant expression was then performed. Statistical analysis was performed on the remaining data.

T-test ( $P < 0.05$ , FC: 1.5) was applied to the data and the p-value was corrected with the Multiple testing correction of Westfall and Young. Comparison of both lines was performed at each developmental stage. Pearson correlation ( $> 0.90$ , FC: 1.5) between chosen entities was also performed on the total entities that presented significant differences at least in one developmental stage.

### 3.3. Results

#### 3.3.1. *HvSUT1* expression is also found in vegetative tissues of *HOSUT24*

In order to identify whether the transgene was expressed in vegetative tissue during early development, analysis of *HvSUT1* expression by qRT-PCR at distinct developmental stages of roots and shoots of seedlings and in developing spikes was performed comparing it to that of the caryopses at 25 DAF, the time point when Weichert et al. (2010) found the highest expression.

The qRT-PCR analysis showed expression of the transgene in the vegetative seedling tissues analysed as well as in the developing spike. The expression found in the developing spikes at the 32BBCH and shoots was similar to that in the caryopsis at 25 DAF. The transgene was also expressed at relatively high level in young roots (Figure 22). This could indicate that the promoter used in the transgene, may not be controlled as it is in barley, where it is active specifically in the endosperm (Shewry and Halford, 2002; Weichert et al., 2010).

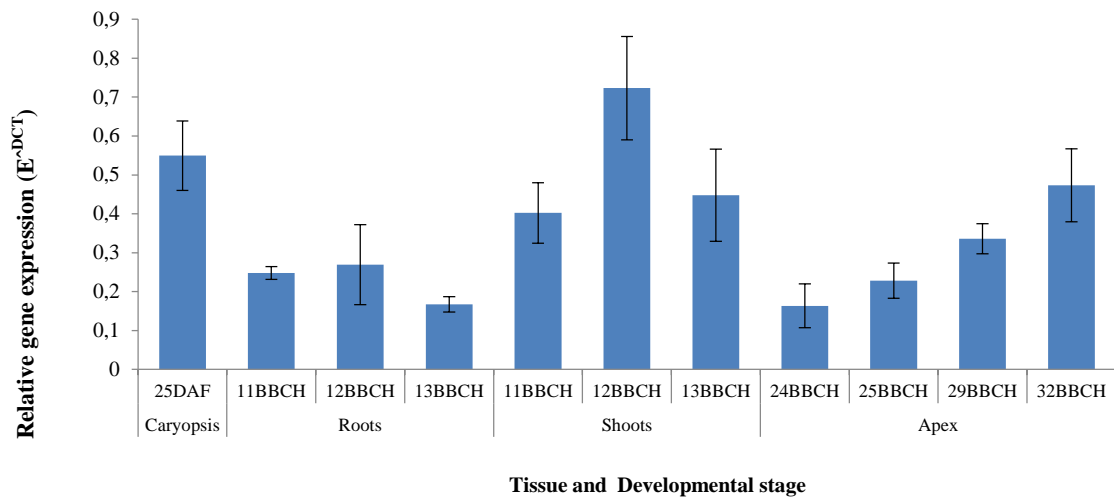


Figure 22. Relative expression of *HvSUT1* in distinct tissues of *HOSUT24*. Vertical bars:  $\pm$ SD.

#### 3.3.2. *Comparative gene expression analysis in the root system of seedlings*

Differences in gene expression in root tissue of *HOSUT24* and *Certo* at the 11-12 and 13BBCH developmental stages were analysed with 8x60k Agilent microarrays. Through statistical analysis (T-tests,  $P < 0.05$ , Westfall and Young Multiple testing correction), 2,649 transcripts were found differentially expressed between both lines in at least one developmental stage (Figure 23A).

Most of the differentially expressed transcripts were found at 13BBCH (1514 entities) followed by 964 transcripts at 12BBCH and at 11BBCH 530 (Top 460 entity list can be found in supplemental data, Table 19).

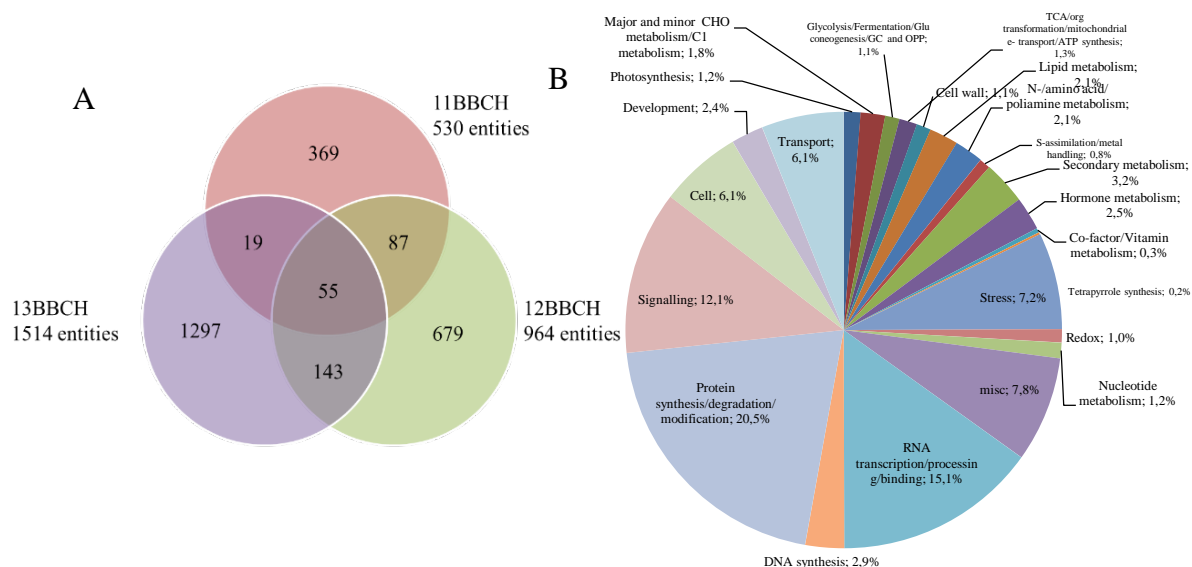


Figure 23. Differentially expressed transcripts between HOSUT24 and Certo. T-test  $P < 0.05$ , FC 1.5. Multiple testing correction: Westfall and Young. A. Venn diagram showing the number of transcripts differentially expressed in Certo and HOSUT24 evaluated at the 11, 12 and 13 BBCH stage of development. B. Percentage of differentially expressed transcripts of known function according to their Bincode classification. Partial list with top 460 significantly different entities available in Supplemental data Table 19.

From the 55 entities that were differentially expressed in all three stages (Figure 23A), eight were ANK repeat family proteins. These transcripts were found down regulated in HOSUT24 in all three stages. The best blast hit for wheat, given by the MIPS annotation, located these transcripts in chromosomes 2B, 2D, 4A, 4B, 4D, 5B and 5D. Proteins with ANK repeats are diverse in function, which ranges from signal transduction and cell cycle regulation to transcription regulation (Becerra et al., 2004; Kuhlmann et al., 2003).

From the known and/or characterized entities according to the Bincode classification and the annotation provided by the MIPS Plant DB and OakLabs, GmbH, 15.1% are involved in RNA processes *i.e.* transcription, transcriptional regulators or binding, 12.2% are transcripts involved in signalling pathways. Entities related to cell organization and development represented 6.0% and 2.4% respectively, whereas transport related entities 6.2%. Hormone metabolism entities differentially expressed in HOSUT24 corresponded to 2.4% of the known entities, carbohydrate metabolism had similar amount of differentially expressed entities (Figure 23B).



### 3.3.2.1. *Altered carbohydrate metabolism and cell division in roots of HOSUT*

In *Arabidopsis* it was shown that sugar signalling is important for root development since it promotes the root meristematic activity and the primary root growth (Ruan, 2014). This transcriptomic analysis revealed that transcripts involved in carbohydrate metabolism had a tendency to a higher expression in HOSUT24 especially evident at 11BBCH.

Among the entities found with differential gene expression, Trehalose phosphate synthase, *CWINV* and Hexokinase 1 (*HXK1*) (Figure 24) were detected with significantly different intensities in HOSUT24 roots. This result is of great interest due to the role that they have in the plant's metabolism.

Two trehalose-phosphate synthase genes were detected with increased expression in HOSUT at 12BBCH and later descending to a similar expression as found in Certo. Trehalose-phosphate synthase is involved in the synthesis of T6P, signalling molecule with critical roles in plant development and flowering (Rolland et al., 2006). Mutants deficient in T6P production have been reported to have an impaired use of available sugars as well as stunt seedling growth (O'Hara et al., 2013).

Higher expression of a *CWINV* was detected at 11 and 12BBCH. *CWINV* high activity in a given region might facilitate phloem unloading by cleaving sucrose in the apoplasm. Invertases have been reported to be induced by sugars at the transcript level and in parallel enhancing the sink strength of the tissue where they are expressed by increasing cell division (Roitsch and Ehneß, 2000).

*HXK1* was detected with higher expression in HOSUT24 at 11BBCH. At 12BBCH, expression was similar to that of Certo and then dropped down at 13BBCH. Besides their catalytic activity, hexokinases are also glucose sensors and modulators of gene expression (de Jong et al., 2014; Rolland et al., 2002).

Carbohydrate metabolism is highly regulated and changes could affect diverse developmental processes through sugar signalling. Increased content of sucrose and glucose detected in the developing seedlings of HOSUT wheat (Chapter 2) might stimulate events that are evident at the transcript level point of view as early as at 11BBCH, when alterations in important entities of the carbohydrate metabolism are detected with an altered profile, in general up regulated at 11BBCH with the exception of SnRK1-interacting protein1.

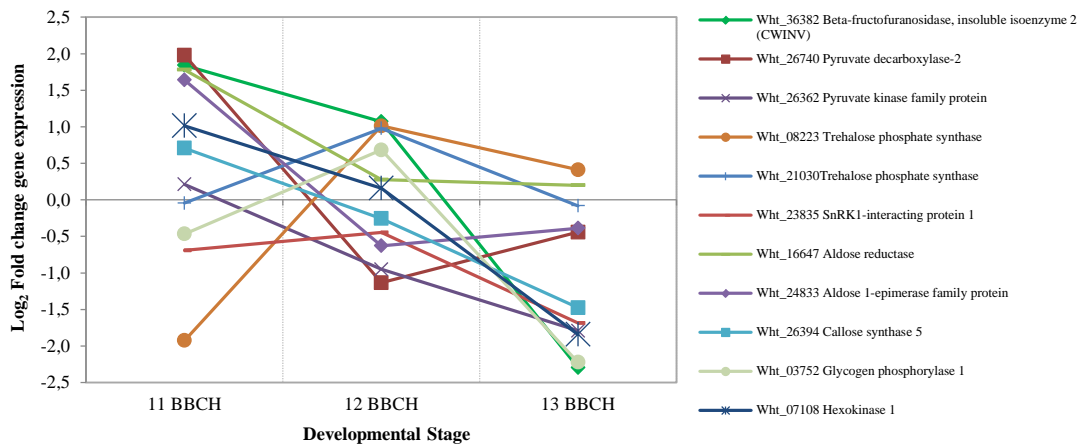


Figure 24. Differences in gene expression of Carbohydrate metabolism entities. Comparison of HOSUT: Certo (Values in  $\text{Log}_2$  of the gene expression fold change).

Higher expression of transcripts related to development, cell growth and cell division processes were found in HOSUT24 and were especially evident at stages 11 and 12 BBCH. Cyclins A2, B1, D4 showed higher expression at 11BBCH (Figure 25). Cyclin A2 and Cyclin D4 have been reported to act at the pericycle level and stimulate cell division (Inzé and De Veylder 2006; Malamy and Ryan 2001; Nieuwland et al. 2009). Callose synthase 5, two Cellulose Synthases and a Gamma-Tubulin complex component had also higher expression in HOSUT24 roots at 11BBCH. At this time point in development, the root system presented no visible lateral roots (Chapter 2), and so it could be the initiation moment of the lateral root primordia (priming), a moment of active cell division, and therefore higher activity of transcripts involved in cell division processes.

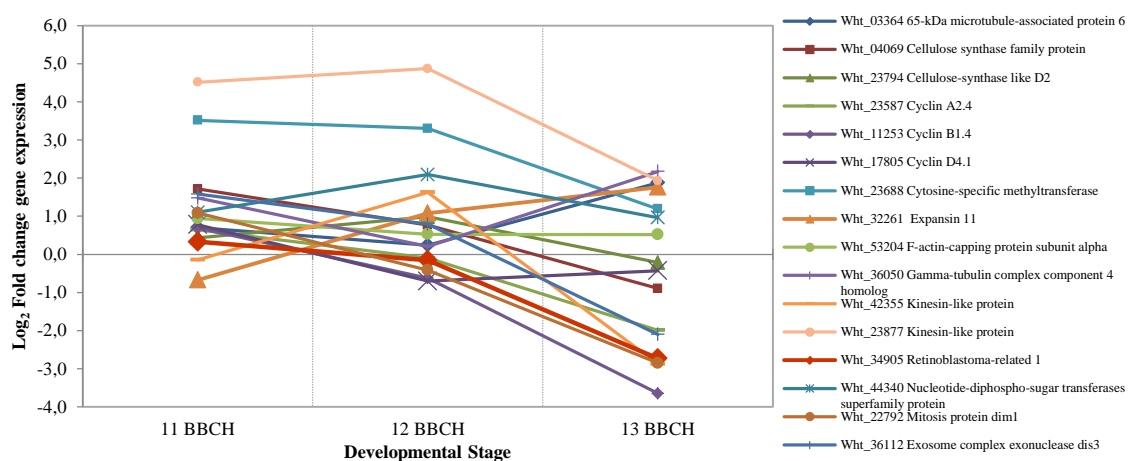


Figure 25. Differences in gene expression of transcripts related to processes in cellular organization and cell division. Comparison of HOSUT: Certo (Values in  $\text{Log}_2$  of the gene expression fold change).

Lateral root primordia (LRP) in order to extrude from inside of the primary root, must pass the endodermis, the cortex and the epidermis. This mechanism is regulated by auxin, which regulates the expression of diverse cell wall remodelling entities, among them expansins, which are the entities in charge of cell wall loosening, facilitating LR emergence by expanding the cells helping them protrude layers of cells and emerge (Cosgrove, 2005; Lavenus et al., 2013). In HOSUT24, this protrusion was visible at 12BBCH. Expansin 11 presented higher expression at the 12 and 13BBCH in HOSUT24 (Figure 25), just at the time when the cyclins' expression diminished and when the auxin content in the seedling was increased (Chapter 2).

#### 3.3.2.2. $Ca^{2+}$ and G-protein signalling pathways in HOSUT

Signal transduction pathways often involve secondary messengers as  $Ca^{2+}$  and DAG, which can be triggered by single molecules (Dodd et al., 2010; Kudla et al., 2010; Parre et al., 2007).

$Ca^{2+}$  signalling has been associated with diverse developmental processes in which CaM, CML proteins, Calcineurin B-like proteins, calcium-binding and calcium-dependent protein kinases have important roles. In HOSUT24 roots, two genes encoding Calcium-binding EF-family protein tend to have higher expression than Certo at 11BBCH and reducing its expression at 12BBCH, however during the stage 13BBCH expression increased again in HOSUT24 (Figure 26A).

CML proteins show a tendency to a higher expression in HOSUT24. CML-38 had an evident increase in expression at 12BBCH, CML-43, CML-23 and CML-37 were detected with higher expression values in HOSUT in all three stages (Figure 26A). CML-43 and CML37 have been related to stress responses in root tissues (Bouché et al., 2005; Tuteja and Mahajan, 2007; Vanderbeld and Snedden, 2007). Since these roots were grown under N-deprived conditions, once the grain was depleted, the plants could have suffered from nutritional stress, which could also have influenced transcription of stress responses.

Vanderbeld and Snedden (2007) through GUS reporter analysis suggested the involvement of CaM/CML in root development. They localized higher CML37::GUS activity during the emergence of lateral roots and at the root tip, where constant cell division is happening. CML38::GUS showed behaviour similar to CML37::GUS. CML38 in HOSUT24 had an increased expression level at 12BBCH; at this stage, there was a

tendency for entities involved in cell division to be expressed in higher amounts (*e.g.* kinesins, Figure 25). From these results, it could be suggested that at 12BBCH, there was a highly active cell division process controlled, at some extent, by  $\text{Ca}^{2+}$  signalling pathways, that could be related to the enhanced biomass production of HOSUT, which was previously documented in Chapter 2.

In HOSUT24, the G-protein complex had the tendency to be higher expressed at 11BBCH, whereas the GTP-dependent Elongation factor 1-alpha is higher expressed in HOSUT during all three developmental stages analysed (Figure 26B, C). The latter is reported to be active in the elongation of the amino acid chain during translation, also to be involved in signal transduction and to interact with CaMs, ubiquitins and tubulins (Suhandono et al., 2014), some of which had also a changed transcript profile in HOSUT24 root tissue. In plants, G-proteins are conformed by a hetero-trimeric complex of proteins that activates a response downstream through a signalling cascade. These proteins are formed by subunits named  $\alpha$ ,  $\beta$  and  $\gamma$ . This system is coupled to the inositol-lipid DAG transduction pathway (Rolland et al., 2006).

Brefeldin A-inhibited guanine nucleotide-exchange protein 1 (BIG1) is involved in the G-protein signalling pathway, through the activation of ADP-ribosylation factor proteins. It catalyses the conversion of GDP into GTP, which is then, a turn “on” signal for the subsequent signal transduction and cellular process. ADP-ribosylation factors and BIG1 are crucial for vesicle trafficking (Radchuk et al., 2007; Shen et al., 2006).

This “on” signal was higher expressed in HOSUT at 11BBCH and 12BBCH, but lower at 13BBCH. The “off” regulator is reported to be the Rho GTPase-activating protein 2, which is part of the small GTPase regulators (Chen and Friml, 2014). These transcripts had higher expression in HOSUT24 at 11 and at 12BBCH (Figure 26B); however, the overall expression of Rho GTPase-activating protein 2 at the raw signal level is lower than that of the BIG1. This leads to the speculation that the “on” signal that regulates vesicle trafficking is mostly active, at the time point when cell division transcripts reported a peak of expression in HOSUT24 root. The higher cell division rate that is postulated here for HOSUT24 roots would require intensive vesicle trafficking for cell wall formation.

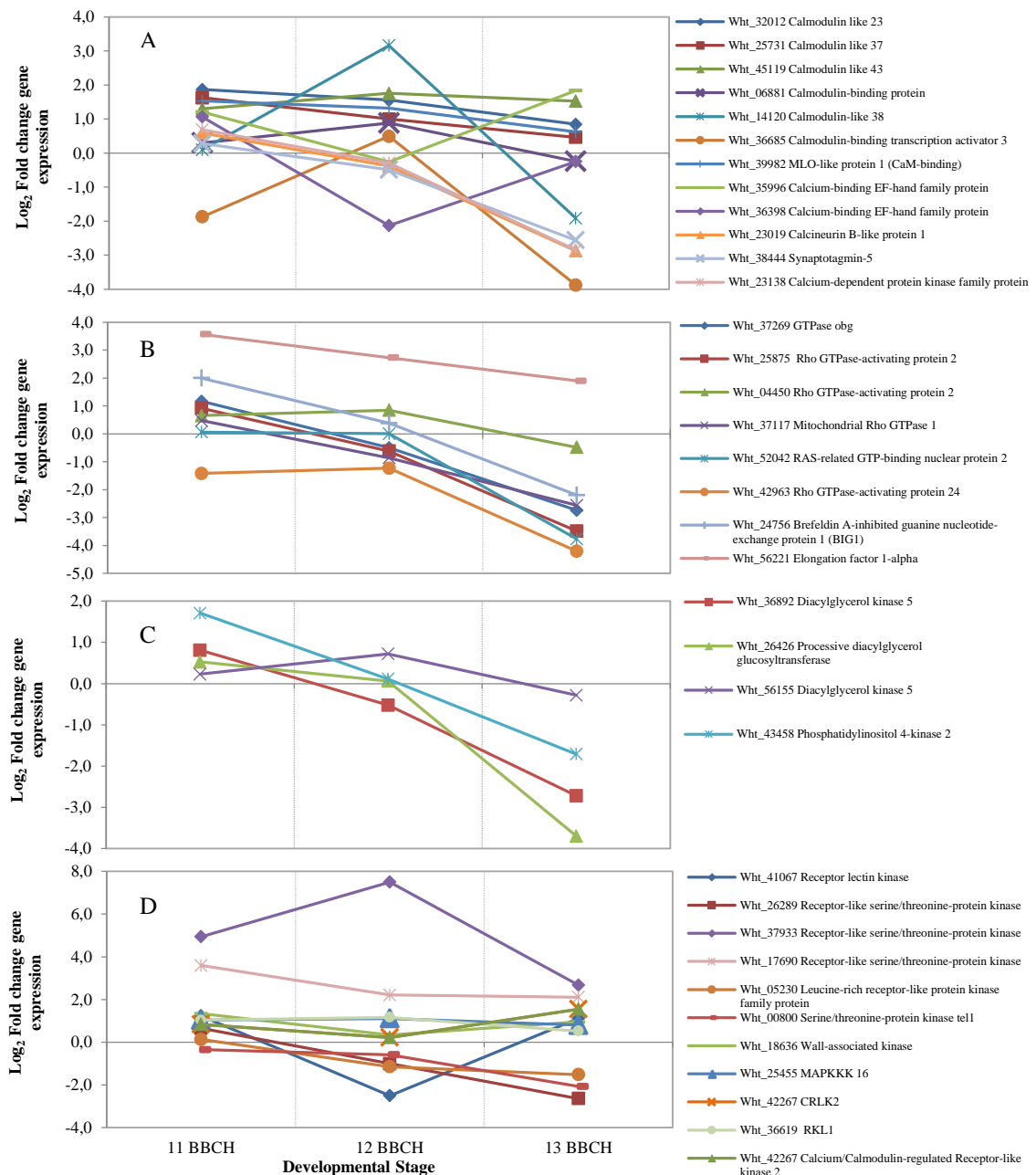


Figure 26. Differences in gene expression of transcripts related to signalling processes (A) calmodulin/Ca<sup>2+</sup> (B) G-proteins and GTPase (C) Inositol-Lipid/DAG/ signalling (D) Protein kinases. Comparison of HOSUT:Certo (Values in Log<sub>2</sub> of the gene expression fold change).

Coupled to the G-protein signalling complex is the Inositol-Lipid signalling pathway. The activated G-protein elicits a series of reactions in the plasma membrane with DAG as the resulting molecule. In this transcriptome analysis Phosphatidylinositol kinase, the starting enzyme of the pathway involved in the conversion of PI 4,5-bisphosphate (PIP<sub>2</sub>) to DAG and IP<sub>3</sub>, has higher expression in HOSUT at 11BBCH (Figure 26C). Furthermore, expression of DAG kinase 5 is higher at 11 and 12BBCH. This enzyme is in charge of the

phosphorylation of DAG into phosphatidic acid, also a secondary messenger in plants (Tuteja and Mahajan, 2007). Lanteri et al. (2008) showed in cucumber that phosphatidic acid formation was linked to auxin induction of adventitious roots. Moreover, IP3 is responsible for opening  $Ca^{2+}$  in the cell and so triggering a series of signalling cascades and changes (Hetherington and Brownlee 2004; Popescu et al. 2007).

Additionally, in HOSUT24 128 kinases had higher expression during all three developmental stages analysed. Seven are of particular interest due to the high signal intensity and the higher values in their fold change when compared to Certo. Two Receptor-like serine/threonine-protein kinases have significant higher expression in HOSUT24 (Figure 26D). MAPKKK16 and CRLK2 have constant higher expression in HOSUT24. The former is part of a complex signalling kinases cascade. This kind of signalling might be involved in defence mechanisms, cell cycle and development, this means a series of hormone signal transductions (Jonak et al., 2002; Woodward and Bartel, 2005).

#### 3.3.2.3. *Entities of the amino acid metabolism with changed gene expression*

In HOSUT24, there was a tendency to a higher expression of entities related to the amino acid metabolism at 11BBCH, which then tend to diminish. Alanine aminotransferase 2 had higher expression in HOSUT at 11BBCH as at 13BBCH, this entity synthesises pyruvate from L-alanine (Gaufichon et al., 2010).

L-asparaginase had a significantly high expression in HOSUT24 at both 11 and 12BBCH. This transcript corresponds to an enzyme involved in the catabolism of Asn. It converts this amino acid into L-aspartate and ammonia. Its increased activity has been related to sink tissues (Lea et al., 2007).

Indole-3-glycerol phosphate synthase is one of the enzymes involved in the production of Trp. The gene encoding this enzyme was significantly higher expressed in HOSUT24 at 11BBCH; at 12BBCH, its expression is higher than Certo's, although at this stage, the difference was not statistically different (Figure 27). This enhanced expression of Indole-3-glycerol phosphate synthase as well as that of Tryptophan aminotransferase related 2 could be indicative for the increased Trp production in diverse tissues of HOSUT24 (see compositional analyses Chapter 1 and Chapter 2).

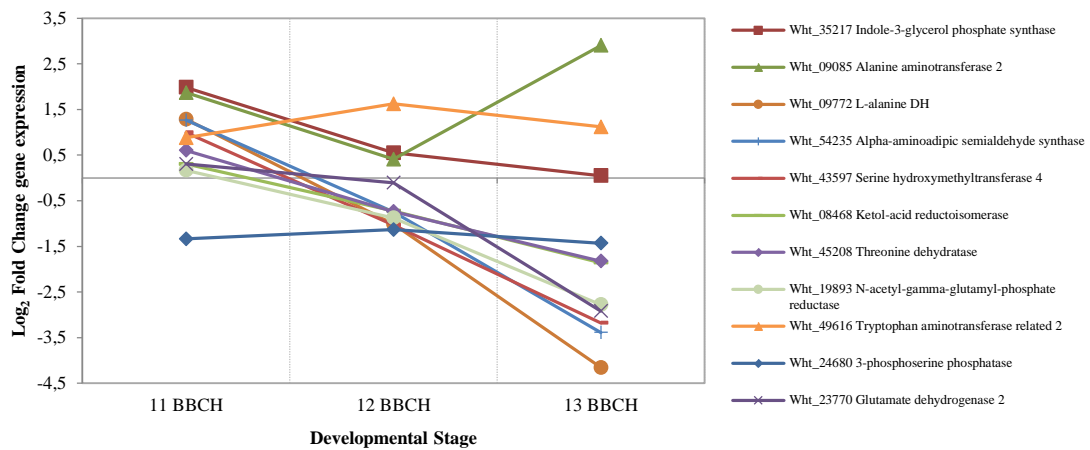


Figure 27. Differences in gene expression in the Amino acid metabolism. Comparison of HOSUT:Certo (Values in  $\text{Log}_2$  of the gene expression fold change).

#### 3.3.2.4. Hormone metabolism is altered in HOSUT24

Transcripts of the auxin transport protein BIG were higher at 11BBCH along with two SAUR-like auxin responsive proteins and Auxin Response Factor 1 (ARF1), IAA4 and Jasmonate-zim-domain protein 1 (JAZ1) (Figure 28). Moreover, an auxin efflux carrier showed an increased expression at early stages and at 13BBCH a significant drop down in its expression.

The two SAUR-like responsive proteins that showed higher expression at 11BBCH diminished their expression at 12BBCH, and one of these transcripts increased its expression at 13BBCH. This entities were reported to have early responsiveness to auxin stimuli (Bouché et al., 2005), and to be involved in the auxin mediated development in the plant. They belong to a broad protein family in which the exact function of each entity is not completely understood; nevertheless they have been related to developmental process in Arabidopsis (Fukaki et al., 2002; Overvoorde et al., 2010; McSteen, 2010).

SAUR-like proteins are responsive to auxin stimuli even in low amounts and the expression of this genes was related to the formation of lateral roots induced by ectopic application of IAA (Markakis et al., 2013). Furthermore, it has been reported for maize interaction between CaM and SAUR proteins in a  $\text{Ca}^{2+}$  dependent manner, coordinating diverse developmental processes (Galon et al., 2010; Bouché et al., 2005).

HOSUT24 showed higher expression of IAA amino acid hydrolase in the first two stages of development; at 12BBCH, this difference was statistically significant. This enzyme eliminates certain amino acid conjugation from IAA activating in this way the hormone (Campanella et al., 2004).

At 11BBCH also ARF1 was up regulated in HOSUT24 (Figure 28); however, was less expressed at 12 and 13BBCH, time point at which the differences in root biomass were evident between Certo and the transgenic lines (Chapter 2). Auxin responsive proteins IAA4 and IAA27 are Aux/IAA proteins, which interact with ARFs forming heterodimers and so modulating the gene expression response to auxin (Woodward and Bartel, 2005). IAA4 presented higher expression at 11BBCH meanwhile IAA27 highest expression was at 13BBCH.

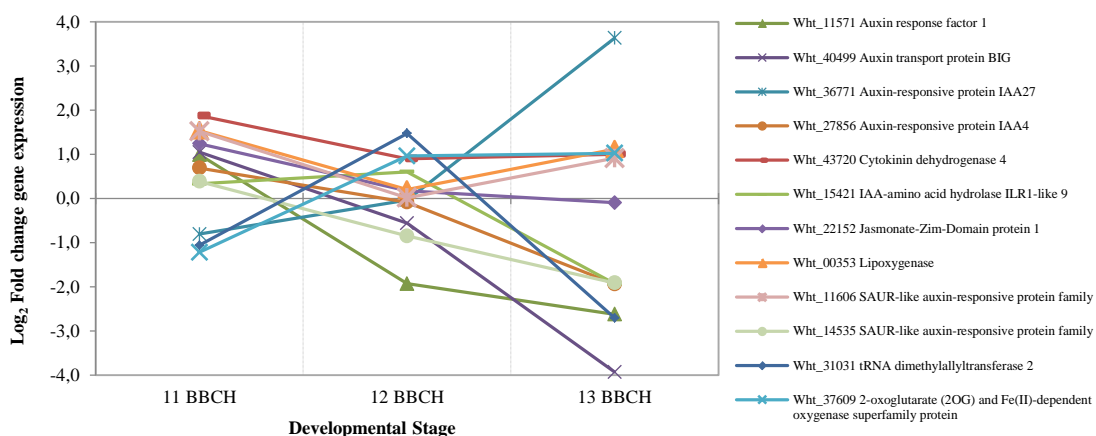


Figure 28. Differences in gene expression of transcripts involved in hormone metabolism. Comparison of HOSUT:Certo (Values in Log<sub>2</sub> of the gene expression fold change).

In this transcriptome analysis, the cytokinin dehydrogenase 4 had a constant higher expression at the transcript level in HOSUT24; this could have provoked the decrease of cytokinins in the root tissue reported in Chapter 2. Moreover, at 11BBCH, tRNA dimethylallyl transferase 2, an important enzyme involved in the first steps of the cytokinin biosynthesis (Sakakibara, 2006) was lower in HOSUT24 but later there was a significant increase in the expression at 12BBCH.

### 3.3.2.5. Transcription factors with altered expression levels in HOSUT24

A number of transcription factors revealed different expression levels between HOSUT24 and Certo. The expression of the LONESOME HIGHWAY (LHW) transcription factor was higher in HOSUT24 at 11 and 12BBCH. LHW has been reported as crucial for



lateral root development since it has been related to the initiation of the protoxylem of lateral roots (Iyer-Pascuzzi and Benfey, 2009; Ohashi-Ito and Bergmann, 2007; Ohashi-Ito et al., 2013; Péret et al., 2009).

Expression of LHW in HOSUT roots was highly correlated (Pearson >0.90) with 310 transcripts in HOSUT24 roots, among them Retinoblastoma-Related1, Processive diacylglycerol glucosyltransferase, the auxin transporter BIG, HXK1, Calcineurin B-like1 protein and Cyclin B1;4 (Table 20 in Supplemental data).

WRKY DNA-binding proteins 50 and 21 had higher expression in HOSUT24 in at least two developmental stages. WRKY DNA-binding proteins 46 and 57 showed a tendency to have increased expression in HOSUT24 only during the first two developmental stages. WRKY transcription factors are involved in a broad number of processes that englobe from seed development and germination to senescence (Ding et al., 2014; Kohl et al., 2015) and in the regulation of genes for the biotic and abiotic stress plant defence responses (Contento et al. 2004; Kim et al., 2008).

The interaction of CaM and CML proteins with distinct WRKY elements was addressed by Popescu et al. (2007) where it was shown how several CaM and CML proteins bind to WRKY transcription factors having in this way an important involvement in the responses governed by WRKYs. In this transcriptome analysis, there was a tendency for the CML entities 23, 37 and 43 for higher expression in all three evaluated developmental stages as the WRKY 50 and 46 did (Figure 26 and Figure 29).

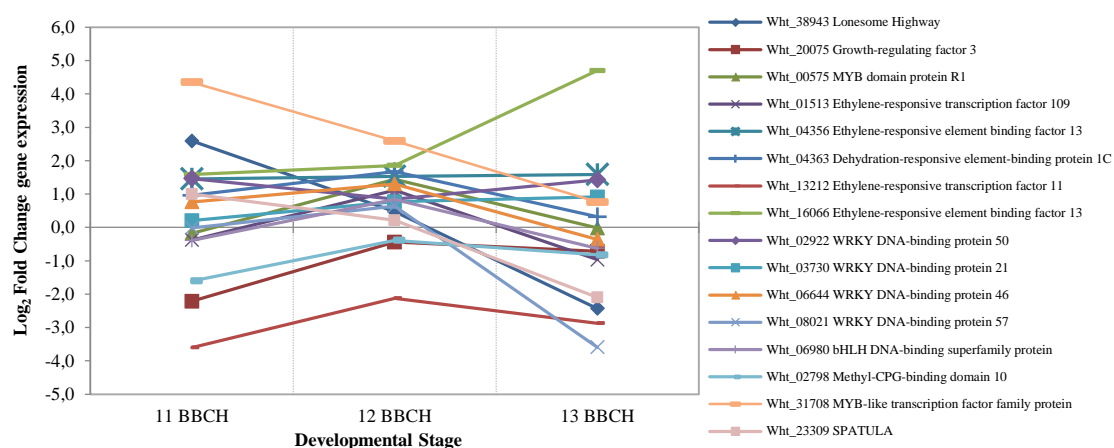


Figure 29. Transcription factors differentially expressed in HOSUT24 and Certo at least in one developmental stage. Comparison of HOSUT:Certo (Values in Log<sub>2</sub> of the gene expression fold change).

WRKY50 has been reported to directly repress JA derived defence responses in Arabidopsis (Gao et al., 2011). JA is not only involved in defence responses but also in several developmental processes (Cai et al. 2014; Mockaitis and Estelle 2008); moreover, Ethylene-Response Factor (ERF) 109 is highly sensitive to JA and is directly involved in lateral root formation by interacting with the auxin biosynthetic pathway (Cai et al., 2014). In roots of HOSUT24 ERF 109 was higher expressed at the 12BBCH (Figure 29). Lipoxygenase and JAZ1 are transcripts involved in the biosynthesis, the former, and in the signalling of JA the latter. HOSUT24 root transcriptome reported an increase in the expression of lipoxygenase and JAZ1 at the 11BBCH (Figure 28) preceding the emergence of lateral roots (Chapter 2) and followed by an increase of the ERF109.

### 3.3.2.6. Changes in gene expression of entities involved in transport processes

In HOSUT24 roots, ABC transporters had diverse expression profiles. ABCG28 had higher expression in all three stages of development. ABCC13 has a higher expression at 11BBCH diminishing at 12 and 13BBCH (Figure 30A). ABC transporters are important for diverse physiological processes and development. The ABC protein superfamily is a large family found in all living organisms and possess a large number of functions in the cell (Rea, 2007; Schulz and Kolukisaoglu, 2006; Theodoulou, 2000; Verrier et al., 2008).

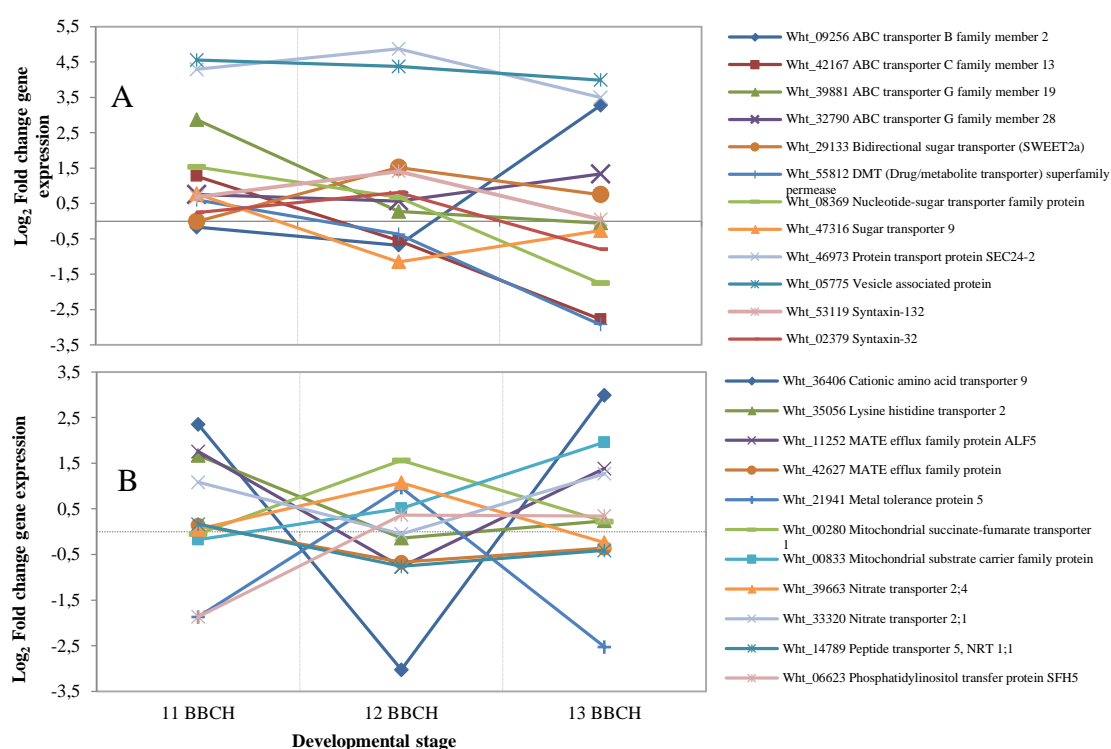


Figure 30. Expression pattern of entities involved in transport processes with differences in gene expression. Comparison of HOSUT:Certo (Values in Log<sub>2</sub> of the gene expression fold change).

Vesicle associated and SEC24-2 proteins are both involved in vesicle transport. Both transcripts had a higher expression in HOSUT24 in all three evaluated stages (Figure 30A). SEC 24-2 is a component of the coat protein complex that promotes the formation of transport vesicles from the endoplasmic reticulum (Conger et al., 2011). Enhanced production of vesicle transport in the cells relates with the higher expression of cell division and cell organization entities reported previously, transport of cell wall materials is done via exocytosis for which increased vesicle production is needed.

At 12BBCH, SWEET2a, Solute carrier family 2-facilitated glucose transporter member 3, two Syntaxins, Metal tolerance protein 5, Mitochondrial succinate-fumarate transporter 1, NTR 2;4 and Phosphatidylinositol transfer protein SFH5 had the tendency to an increased expression in HOSUT24.

In contrast to NRT2.4, NRT2.1 was detected with higher expression in 11 and 13BBCH (Figure 30B). The behaviour of these transcripts in HOSUT24 was similar to the one reported in Kiba et al. (2012), where this two NRT had complementary expression in the root tissue.

Two MATE efflux family proteins showed a decrease in their intensities at 12BBCH (Figure 30B) similarly as was found for the Peptide transporter 5. MATE family proteins are localized in the plasma and vascular membrane. They are a large group of transporters their involvement has been established among others with inter and intracellular transport of secondary metabolites and the extrusion of xenobiotics along with salicylic acid signalling (Seo et al., 2012). Moreover, in Arabidopsis the mutant phenotype for MATE efflux protein ALF5 is characterized by the inhibition of the lateral roots elongation (Diener et al., 2001). However, lateral root length was not measured in HOSUT lines.

### **3.4. Discussion**

Root architecture determines not only the anchorage capacity of a plant but also the capacity to reach nutrients and water from the soil (Orman-Ligeza et al., 2013). During wheat's vegetative development, roots are the largest sink organ.

Changes in the carbohydrate supply influence the metabolism. A comprehensive transcriptome analysis uncovers the difference in gene expression between the HOSUT24 and the non-transgenic line Certo and can be used to unravel the regulators responsible for the different phenotype between Certo and HOSUT24.

#### ***3.4.1. HvSUT1 expression in vegetative tissues leads to metabolic changes in the seedling***

It was previously described that overexpression of HvSUT1 in grains of HOSUT plants altered its metabolic status by increasing the assimilate supply to the grain which in turn influences the carbohydrate metabolism in the grain (Weichert et al., 2010).

In this study, HvSUT1 expression was detected in HOSUT24 seedlings and in developing apex/spikes. Root tissue of developing seedlings had a remarkable expression of the transgene in comparison to that of the grain at 25DAF, the time point described by Weichert et al. (2010) as the one with the highest expression (Figure 22). This result indicates that the hordein B1 promoter lost its specificity and expression of the transgene is leaky in HOSUT24. Similarly to this results Furtado et al. (2008, 2009) found in rice non-specific expression of the GFP protein controlled by the hordein B1 promoter.

Increased transport of assimilates to the developing tissues of seedlings might have an effect comparable to that of the one reported for developing grains. Changes in the expression of diverse transcripts of the carbohydrate metabolism, amino acid metabolism, cell division and cell organization, signalling, hormone metabolism, transport and transcription factor's expression will be discussed in the following sections.

Interestingly, it was also found that a number of ANK specific repeat family proteins are down regulated due to the metabolic changes induced by the expression of HvSUT1. ANK repeat family proteins have diverse functions in the cell and the ANK repeat is one of the most common protein domains (Becerra et al., 2004; Huang et al., 2009). Plant specific ANK repeat family could also act as a link between plant defence and carbohydrate metabolism (Wirdnam et al., 2004). There has been evidence of also sugars participating in the plant-pathogen interaction (Yadav et al., 2015). Given the changes in the CHO metabolism of HOSUT plants, it would be of interest challenging the HOSUT plants against diverse pathogens.

#### ***3.4.2. Enhanced sucrose-mediated signalling in HOSUT24 activates cell division in roots***

Carbohydrate metabolism in itself is a signalling network. Sucrose, glucose and other sugars are known signalling molecules with crucial effects on plant development (Eveland and Jackson, 2012). For this reason, it is likely that an enhanced assimilate supply into the root system influences the metabolism by deregulating the metabolic status of the tissue.

The ectopic expression of a sucrose transporter in the root tissue might be the reason for an increased delivery of sucrose to this tissue, but also for the increased expression of a cell wall invertase (CWINV) during the first two developmental stages. Invertases hydrolyse irreversibly sucrose into glucose and fructose. The products of the cleavage by CWINV had been proven to have a positive feedback on its up regulation (Roitsch and Ehneß, 2000; Roitsch and González, 2004). Increased expression of CWINV could increase the availability of glucose in the cells triggering diverse signalling cascades. Glucose is known to be an important signalling molecule and to be involved in IAA signalling and controlling its biosynthetic genes (Mishra et al., 2009).

Changes in glucose content are sensed by hexokinases (Rolland and Sheen, 2005). HXK1 had higher expression in HOSUT24 during the first developmental stages as did CWINV. This might enforce the hypothesis that there is an increased sucrose-glucose signalling in HOSUT24 root tissue, which also could have enhanced sink strength. The cleavage of sucrose by CWINV augments the pool of hexoses and diminish sucrose in the apoplasm, raising in this way the import of sucrose to the sink tissue (Peukert et al., 2016), in this case roots.

Sugar signalling is complex and interacts closely also with other known signalling pathways. Significant advances in its elucidation had been achieved recently (Barbier et al., 2015; Morkunas and Ratajczak, 2014; Ruan, 2014; Eveland and Jackson, 2012). Among signalling pathways related to sucrose, trehalose signalling pathway in plant development had been extensively analysed. Trehalose phosphate synthase (TPS) produces T6P from UDP-glucose and Glucose-6-phosphate. T6P serves as a signal for high sucrose availability (O'Hara et al., 2013).

T6P inhibits SnRK1, therefore the higher expression of TPS and lower expression of SnRK1 in HOSUT24, might infer that there might be changes in the trehalose sucrose-dependent signalling pathway in HOSUT24. O'Hara et al (2013) discuss the correlation of the complex T6P/SnRK1 with the hormonal regulation of plant growth. HOSUT24 has lower expression of Aux/IAA genes (*e.g.* IAA27 at early stages, IAA4 at a later stage, Figure 28), and a higher expression of TPS could mean an augmented T6P content, which in turn could have down regulated the Aux/IAA genes. In addition, ARF1 transcript was detected in higher magnitudes during the 11BBCH. ARF transcription factors could be involved in the regulation of cell division (Mockaitis and Estelle, 2008; Vanneste et al., 2005; Woodward and Bartel, 2005). The higher expression of ARF1 together with lower

expression of Aux/IAA during different developmental stages could be the responsible of triggering in HOSUT24 the expression of specific genes for cell division.

Roitsch and Ehneß (2000) discussed the cross talk between hormones and sugars, and the role of invertases in enlarging the sink size of the tissue where they are expressed by increasing cell division. The influence of sugar signalling pathways on cell division is detectable in HOSUT24 through the expression profile of transcripts involved in cell division and cellular organization such as cellulose synthases, cyclins and kinesins (Figure 25). In HOSUT, increased expression of vesicle-trafficking genes is evident, which would deliver to the cell wall biosynthetic materials as well as  $\text{Ca}^{2+}$ -dependent signalling transcripts which have been correlated with the expression of cyclins and the progression of cell cycle during abiotic stress conditions (Tuteja and Mahajan, 2007).  $\text{Ca}^{2+}$  can modulate proteins directly by attaching to them; membrane channels are an example of this.

Most of  $\text{Ca}^{2+}$  effects are through the  $\text{Ca}^{2+}$ /CaM complex, which are involved in a number of cellular processes, like the regulation of the progression of cell cycle by interacting with cyclins and the activation of  $\text{Ca}^{2+}$ /CaM-dependent protein kinases (Bouché et al., 2005; Winfield et al., 2010; Popescu et al., 2007).

$\text{Ca}^{2+}$ -activated CaM proteins are known to bind to SAUR proteins reported to accumulate rapidly in roots in response to auxin and had been previously correlated with cell division in the pericycle cells (Markakis et al., 2013). Auxin is involved in diverse developmental processes and its role in division of specific cells of the root system has been previously reported (Casimiro et al., 2001, 2003; De Smet et al., 2007).

Either auxin transport or its production are necessary to trigger the signalling required for the cellular divisions of the pericycle that give rise to functional lateral roots. Indole-3-glycerol phosphate synthase is the enzyme that synthesizes indole-3-glycerol phosphate, a precursor of Trp. The significantly higher expression of this transcript at 11BBCH and still augmented expression at 12BBCH in HOSUT24, together with the increased amounts of Trp found in HOSUT24 root tissues (Chapter 2), suggest that, in HOSUT24, the shikimate pathway could be potentiated towards indole production. As a consequence, there was an enhanced production not only of auxin, but also of products downstream of Trp such as defence products, proteins, and cell wall biosynthetic products (Ljung, 2013).

### ***3.4.3. Sucrose-dependent auxin signalling triggers GTPase and Ca<sup>2+</sup> signalling pathways in HOSUT wheat roots***

Auxin is produced in the root meristem, from there on, it is transported towards the rest of the organ. Diverse transcripts of auxin transporters presented differential expression in HOSUT24, among them the ABC transporters. These transporters are linked to auxin transport (Kaneda et al., 2011); moreover, the auxin transport protein BIG had an increased expression at 11BBCH. Coordinated synthesis and transport of auxin, its signalling process, plus cross talk with cytokinins signalling pathways are essential for lateral root priming and emergence (Casimiro et al., 2001, 2003; De Smet et al., 2007; Ruzicka et al., 2009). In HOSUT24 roots, cytokinin dehydrogenase was found with a steady higher expression. This entity degrades cytokinin, hence altering the contents of this hormone (hormone analyses, Chapter 2) and therefore its signalling pathway and cross talk with auxin.

As discussed previously, increase sucrose transport in HOSUT24 roots might trigger the shikimate pathway, which might be the reason of the increased auxin content in HOSUT.

Increased production of auxin and higher expression of auxin transporters at early stages of root development might trigger the auxin signalling pathways by activating the small GTPases signalling, which in turn unchains a series of kinases responses (MAPKKK) that will activate a series of transcription factors and modulating gene expression in this way (Mockaitis and Howell, 2000).

Another way in which auxin is involved in signalling is through the activation of the G-protein complex and latter interaction with the phospholipase signalling pathway. Inositol 1,4,5-triphosphate opens Ca<sup>2+</sup> channels in the endoplasmic reticulum or in the vacuole. The liberation of Ca<sup>2+</sup> and then activation of CaM/CML proteins has also an important contribution to delivering the message of auxin signalling. CaM and CML proteins were detected with higher expression in HOSUT roots. CaM and CML proteins interact with WRKY and MYB transcription factors (Dodd et al., 2010; Kudla et al., 2010) therefore regulating gene expression.

Furthermore, parallel to the involvement of Rho GTPase-activating proteins in vesicle trafficking is the trafficking and polarization of PIN auxin transporters (Chen and Friml, 2014). In roots, this polarization is important for the elongation of the root system to reach different nutrients in the soil, and this elongation will be defined by different hormonal signals (Zhang et al., 2007).

#### **3.4.4. LONESOME HIGHWAY (LHW) and auxin signalling and transport**

The LHW transcription factor has been tightly linked to lateral root formation (Ohashi-Ito et al., 2013). In HOSUT roots expression of the respective gene was detected with increased expression values at 11 and at 12BBCH.

The expression of LHW in Arabidopsis has been related to the initiation of the protoxylem of lateral roots and is therefore crucial for their development. It regulates the asymmetrical divisions in the pericycle for a proper vascular development. Auxin influences the development of the new vascular tissue and cellular divisions. In Arabidopsis *lhw* mutants, the auxin flow in the pericycle cells might be impaired (Iyer-Pascuzzi and Benfey 2009; Péret et al. 2009; Ohashi-Ito and Bergmann 2007; Ohashi-Ito et al. 2013).

The Pearson correlation (Pearson >0.90, Supplemental data Table 20) of Retinoblastoma-Related 1, BIG and HXK1 with LHW in HOSUT roots suggests that in these tissues LHW might also be related to cell division and given the developmental stage in which it is higher expressed, it could be suggested that it is involved in lateral root formation. Further investigation is necessary in order to understand the participation of LHW in the regulation of the cell cycle in HOSUT and if this transcription factor is influenced directly by glucose and/or sucrose, and if so, how this influence is given.



### III. General discussion

#### i. Seedling vigour in HOSUT goes beyond from a grain size effect

The increased vigour in HOSUT lines could be visualized as the increase in biomass and faster development during the crop's life cycle. All HOSUT lines showed accelerated development under *in vitro* and field-like conditions, resulting in earlier time of anthesis when grown under field-like conditions, a desirable trait in order to overcome the negative effects of climate change (Reynolds et al., 2012), as heat stress during anthesis negatively alters grain number in cereals (Ordóñez et al., 2015).

In cereals, seedling growth during early stages is influenced by their grain size/weight (Aparicio et al., 2002; Boyd et al., 1971; Evans and Bhatt, 1977; Gupta et al., 2006). In a large accession of spring barley cultivars, Neumann et al. (submitted) found medium-strength correlation between TGW and seedling biomass and only during early seedling stage. However, this kind of correlation has to be confirmed, since in sorghum, a significant correlation between grain weight and seedling vigour parameters was not found (Cisse and Ejeta, 2003).

Under *in vitro* N-deprived conditions, HOSUT and Certo seedlings depended mostly on assimilates and nutrients provided by the grain, and when emerging from grains of similar weight, little difference was found between the lines. This behaviour changed under field-like conditions, where increased vigour was found in HOSUT seedlings (Figure 14). Furthermore, regardless of the grain weight from which the seedling developed, there was no evidence of influence of grain weight over the increased chlorophyll content in HOSUT seedlings under field-like conditions. These results suggest that the increased chlorophyll content in HOSUT might not be simply a consequence of grain size, but could relate to the expression of HvSUT1 in the vegetative tissues and the metabolic changes that might relate to it.

An important point to consider is the heterogeneous grain weight distribution along the wheat spike, meaning that grain position significantly affects grain weight. The biggest grains are those that develop first and have better assimilate supply, changing also the composition of the macro and micronutrients of the grain (Calderini and Ortiz-Monasterio, 2003). While analysing the results of the experiments with grains of low and high weight of HOSUT24, this also must be taken into consideration. The comparison of HOSUT24 grains of 40-45 mg with Certo grains of the same weight range corresponds to

grains of different positions in the spike and the spikelet, and the effect of the difference in grain composition could influence the seedling vigour. In the previous example, it is likely that HOSUT24 seedlings were analysed in disadvantage, as grains of lower weight correspond to those developed later and have lesser assimilate supply. In spite of this, in those experiments HOSUT24 performance was similar to Certo.

The performed seedling vigour analysis of plantlets that germinate from grains of a weight close to the value of TGW of each line (Figure 10), gives a more accurate view of the actual seedling vigour and their potential in the field. These seedlings represent those developing from grains with a better assimilate supply, according to the sink strength of each line, which, due to their size will be the ones used for sowing in the fields according to the regular agronomical practices.

In HOSUT lines, the grain was depleted at 12BBCH ending its direct contribution to seedling growth. The increased nutrient availability in the endosperm of HOSUT lines might give an advantage to the seedling during early development. The seedling compositional analyses, the high expression of HvSUT1 in vegetative tissues and the results of the seedling transcriptome analyses suggest that seedling vigour in HOSUT might not be exclusively dependent on grain size and its reserves, but also by the alterations in the CHO metabolism reported in Chapter 3.

## **ii. HOSUT vigour and photosynthetic efficiency**

The increase in biomass of HOSUT could be related to an increased cell division rate not only in the root system as suggested from the transcriptome analysis, but also in the aboveground tissue. It has been reported that sucrose increases cell division (Tognetti et al., 2013), this will lead to increased cell number and in photosynthetic tissues also increased chloroplast number that will rise the absolute chlorophyll content. Additionally, the lower concentrations of free Asn and Gln in HOSUT24 in shoots and roots, at different developmental stages, might indicate a faster use of them for building-up of tissues of HOSUT24. These amino acids are fundamental for building-up of other N containing compounds including chlorophyll (Neuberg et al., 2010).

Direct effect of sucrose on chlorophyll biosynthesis in wheat seedlings can be examined further in the HOSUT lines by means of studying the transcriptome of the above ground tissues.

The SPAD values are an indirect yet proportional measurement of the chlorophyll content

by means of the leaf tissue transmittance detected in red (650nm) and infrared light (950nm) (Ling et al., 2011). Chlorophyll content has been correlated with the N status of the plant and the protons captured by the photosystems. Consequently, increased SPAD values have been directly and positively correlated with the quantum efficiency of the photosystem II ( $\Phi_{PSII}$ ) and therefore photosynthetic efficiency in both Arabidopsis and maize seedlings (Trachsel et al., 2010; Hund et al., 2004).

The results obtained in HOSUT plants suggest that the increased SPAD values might be related to a raise of the  $\Phi_{PSII}$ , giving in this way an early advantage to growth and vigour by enhancing the C fixation rate in HOSUT, which results in better supply of the dividing cells and aiding the biomass production. Further direct measurements of the C fixation rate or of the  $\Phi_{PSII}$  would be of great interest to confirm this hypothesis.

### **iii. Better HOSUT performance under limiting conditions might be related to increased N use efficiency**

The enhanced biomass production in roots and shoots of HOSUT at early developmental stages is advantageous for the early establishment of the crop as was described before in rice and maize by Cui et al. (2002) and Hund et al. (2004). A more vigorous shoot growth might help diminish the evaporation of water from the surface of the soil due to ground cover (Aparicio et al., 2002) and an development of more lateral roots increases the absorption volume of the root system, enlarging the potential to reach more nutrients and water in the soil (Werner et al., 2010).

The increased seedling vigour of HOSUT lines also under *in vitro* N-depleted medium, together with the increased yield of HOSUT grown under diminished fertilization, suggest that HOSUT lines might have a higher resistance to limiting nutritional conditions. This, is probably due to a greater nutrient and water extraction from the soil (Lilley and Kirkegaard, 2011), which might also result in increased N uptake.

Among all the nutrients applied as fertilizers, N is the most important for plant growth and yield (Kichey et al., 2007) and the one that is applied in greater amounts. Increased biomass and yield production in HOSUT lines in comparison to Certo, grown under the same fertilization regimes, suggests that HOSUT lines develop an increased N use efficiency (NUE). The NUE is described as the biomass produced per unit of applied fertilizer (Xu et al., 2012). According to this description, it is speculated that HOSUT lines have higher NUE, and an elevated NUE under nutritional limiting conditions, might

be the reason that HOSUT grains under diminished fertilization have comparable amounts of N in relation to Certo; however deeper evaluation of N remobilization in HOSUT plants is necessary to confirm this hypothesis.

N fertilization is one of the major costs in wheat crops, and production relies on it in a great extent. However, abuse in the application of fertilizers to the fields has strong consequences for the environment (Galloway et al., 2008; Masclaux-Daubresse et al., 2010). For this reason, cereals with increased NUE are desirable in breeding programs, since diminished N inputs result in unaltered or even increased output.

In this study, the TGW trait was stably increased in HOSUT under limiting conditions, the differences in grain weight between HOSUT and Certo remained ca. 20% regardless of the fertilization. Furthermore, tendency for increased plant biomass was also found under diminished fertilization (Figure 36 in Supplemental data). This might be interpreted as explained in Hermans et al. (2006), as a positive consequence of the altered C partitioning that promotes root development by altering the hormone metabolism.

The expression of the HvSUT1 gene in HOSUT seedlings and the increased amount of sucrose and glucose in shoots and roots linked with the results of the transcriptome analysis of seedling roots, might suggest an increased sucrose transport towards the vegetative tissues. Although no direct measurements of the sucrose flux was performed, increased expression of a CWINV in HOSUT roots was detected, the enzyme of this transcript hydrolyses apoplastic sucrose into fructose and glucose and its higher expression has been related to increased sucrose import into sink tissues (Albacete et al., 2014). Moreover, it has been determined that CWINVs are responsive to their own products. They are up-regulated by the sugar signal generated from their own action and increase the flow of assimilates to a given part of the plant and therefore increasing its sink strength (Koch, 2004; Roitsch et al., 2003; Roitsch and González, 2004).

This putatively increased sucrose transport towards the root system detected in HOSUT plants might change the root CHO metabolism stimulating a vast sucrose-glucose-responsive signalling network that also might include responses to the C/N ratio. In maize seedlings grown under N starvation, the nitrate uptake by roots is regulated by sugars from the aerial organs. Moreover, N uptake is linked to the C/N ratio signalling and mirror the photosynthetic capacity and growth activity of the plant (Trevisan et al., 2008).

HOSUT seedlings grown under N-deprived conditions had reduced C/N ratio in both

shoots and roots (Table 15 in Supplemental data), whereas seedlings grown under N-supplied or field-like conditions had higher values than Certo. Changes in the C/N balance might also play an important role for signalling towards increasing lateral root formation (Tognetti et al., 2013; Zheng, 2009).

C and N metabolism strongly interact, nitrate reductase (NTR) has been reported to be positively regulated at the transcriptional level by sugars and light (Xu et al., 2012). The changes in sucrose and glucose reported in HOSUT might be responsible for the higher expression of NRT2.1 and NRT2.4. Furthermore, there is evidence of the correlation in the expression of HXK1 and NTR2.1 (de Jong et al., 2014).

The activation of both high affinity NRTs in HOSUT might cause the better performance of HOSUT also under diminished fertilization, allowing the plants to not only produce more biomass, but also maintain their yield advantage by improving N uptake efficiency.

Additionally, the low affinity NRT1;1/PTR5 was found with lower expression in HOSUT roots. This transporter has been related also with auxin transport (Weichert et al., 2012). According to the transcriptome analysis, the BIG auxin transporter has higher expression at 11BBCH. This result together with the lower expression of NRT1;1/PTR5, specially at the 12BBCH, might be responsible first for the auxin transport towards the root from the shoot, that at early stages is the source, and later for the accumulation of auxin in the root tissues triggering the initiation of lateral roots (Krouk et al., 2010). The increased number of lateral roots reported in HOSUT could be a key characteristic of these lines to overcome nutritional-limiting and drought conditions.

The putative higher NUE in HOSUT might be responsible for the increased biomass accumulation in sink organs even under nutritional limiting conditions. With this accumulation, HOSUT lines could be able or remobilizing more matter to the developing grains augmenting their weight.

The higher expression of NRT2.1 and NRT2.4 during early seedling development under N-depleted conditions suggests that, under N limiting conditions and enhanced sucrose metabolism, wheat plants increase their NUE, with the subsequent positive influence over their yield and biomass.

Furthermore, the N status on the plant is an important signal to the cytokinin biosynthesis (Sakakibara, 2006); therefore, having also influence on the root system architecture. A tendency to lower levels of cytokinins was detected in both shoots and roots of

developing seedlings, this could point to such control. Whether it is due to N availability or an effect of the C/N itself is difficult to answer, but due to the cross talk between C and N metabolism to isolate the changes observed to only one of them is to have only a partial understanding of the physiological changes that occur.

#### **iv. Sucrose-induced tryptophan-dependent auxin biosynthetic pathway in HOSUT24**

Through free amino acid, targeted hormone and metabolite analyses was possible to detect in HOSUT seedlings increased contents of Trp, Tyr, Phe (Figure 21) as well as IAA, IAA-precursors, IAA-storage compounds and Glucose-6-phosphate (G-6-P) with the higher expression of CWINV and HXK1 at 11 and 12BBCH. The higher expression of pyruvate kinase at 11BBCH in HOSUT roots, and the amino acids and hormone results suggest changes not only in the shikimate pathway, but also suggests putative changes in glycolysis.

Higher expression of CHO metabolism transcripts, involved in the shikimate pathway, suggest that changes in the assimilate transport and its content in root tissues drives the shikimate pathway towards production of auxin in a Trp-dependent way in roots, the altered points in this pathway are represented in Figure 31. Similar scenario might take place in grains, since significantly increased Trp content was also found in grains of HOSUT24 plants grown in both complete and diminished fertilization.

In support of the hypothesis of a Trp-dependent auxin production IAN and IAM were found in HOSUT, both compounds are auxin precursors of the Trp-dependent pathway. IAN was reported as Brassicaceae specific pathway (Mano and Nemoto, 2012); however, there are other evidences that this Trp-dependent pathway is also expressed in monocots (Park et al., 2003; McSteen, 2010).

IAN was found only in roots, in both evaluated stages, while IAM precursor was found in both tissues with increased values (Figure 20). These results might indicate that in roots both Trp-dependent pathways are operational whereas in shoots only IAM.

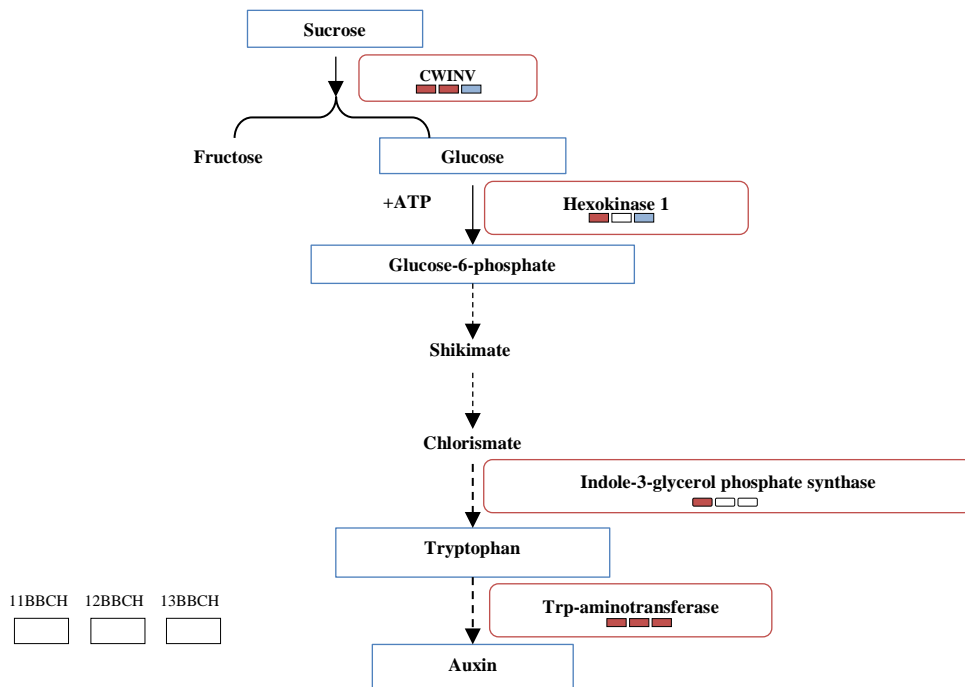


Figure 31. Proposed model for the shikimate pathway and auxin biosynthesis altered entities and metabolites in HOSUT roots. Red boxes are transcripts with higher expression at 11-13BBCH. Blue boxes metabolites found in higher concentration in roots or shoots. Small boxes describe higher expression in HOSUT according to developmental stage. Red, higher expression in HOSUT, white same level of expression and blue lower expression in HOSUT. Modified from Ljung (2013); Maeda and Dudareva (2012) and Tzin and Galili (2010).

Trp has been reported to be synthesized in chloroplasts, however there are also reports of expression of Trp-aminotransferase as well as other upstream biosynthesis enzymes in roots of legumes (Cho et al., 2000). In HOSUT, expression of Trp-aminotransferase was also detected in roots, which would also confirm the production of Trp in this tissue. Trp synthesis has been reported previously to be feedback regulated (Tzin and Galili, 2010), but evidence of that regulation was not found in this study.

#### v. Altered sucrose signalling in HOSUT root system plays a role in lateral root branching

Increased sucrose transport towards the growing root system, might help mitigating the effects of limiting nutritional environment by triggering a complex signalling network that subsequently stimulates lateral root branching.

Growth under N-limiting conditions, as the ones used in the *in vitro* N-deprived experiments, challenges the plant, stimulates changes in the root architecture by extending the root system in the search for N (Malamy, 2005; Smith and De Smet, 2012).

Results of the transcriptome analysis, supported by phenotype and compositional analyses, suggest that HOSUT seedlings under N-deprived conditions have altered signalling, stimulating cell division at 11BBCH. The altered signalling pathways in HOSUT (Figure 26) include auxin signalling, lipid/DAG, G-protein,  $\text{Ca}^{2+}$  and possibly Tre-6-P represented in Figure 32.

$\text{Ca}^{2+}$  is a secondary messenger involved in the transduction of diverse environmental signals. Although, in HOSUT roots  $\text{Ca}^{2+}$  was not directly measured, several CML proteins were detected with higher expression in HOSUT. CML-43, 37 and 23 had constantly higher expression in HOSUT roots, the first of these proteins has been described as a sensor that detects  $\text{Ca}^{+2}$  stimuli and transmits their signals (Bender et al., 2014). CML38 in the case of HOSUT had an increased expression level at 11BBCH but mostly at 12BBCH, at this stage of development, there is a tendency for entities involved in cell division to be expressed in higher intensities (*e.g.* kinesins, Figure 25).

Increased levels of sucrose and glucose, together with the higher expression of several entities of the G-protein, the DAG/lipid and  $\text{Ca}^{2+}$  signalling pathways, suggest a possible interaction between the G-protein signalling with glucose and auxin, which could trigger a signalling cascade involving the inositol/lipid signal-transduction pathway, and the CaM/CML proteins as represented Figure 32. The outcome of this signalling changes most likely is also accompanied by changes in transcription of entities related to development and cell division as reviewed earlier by other authors (Chen et al., 2006; Chen and Friml, 2014; Dodd et al., 2010; Tuteja and Mahajan, 2007; Wang and Ruan, 2013; Zhang et al., 2011).

WRKY transcription factors have been proposed to work in different developmental pathways in plants, that ranges from plant defence (Kim et al., 2008), senescence and N remobilization (Kohl et al., 2015) and hormone response in Arabidopsis (Cai et al., 2014; Ding et al., 2015) and to interact with CaM/CML proteins (Popescu et al., 2007). It is possible that in the HOSUT lines under the evaluated conditions, the signalling network towards increased lateral root production are enhanced involving also a series of transcription factors like WRKY and LONESOME HIGHWAY (LHW) (Figure 32). Therefore, altering the sugar signalling in roots under stress conditions proved beneficial for increasing root biomass *in vitro*.



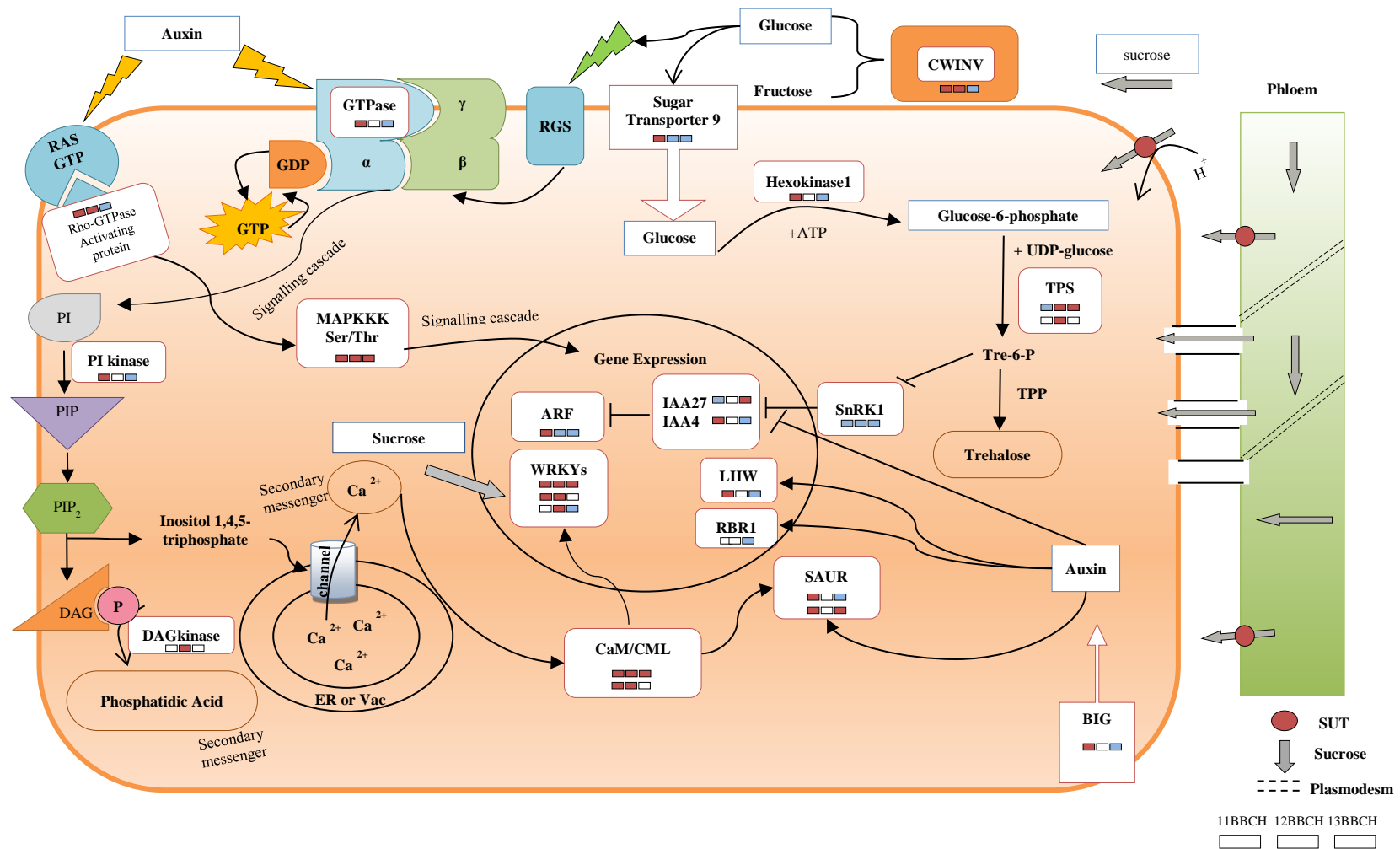


Figure 32. Proposed model of signalling pathways with changed expression in root tissues of HOSUT plants at the seedling stage under N limiting growing conditions. Metabolites in blue-framed boxes found in higher amounts in HOSUT plants. Transcripts are in red-framed boxes. Inner boxes describe expression in HOSUT according to developmental stage. Red boxes higher expressed in HOSUT, white same level of expression and blue lower expressed in HOSUT. Modified from (Dodd et al., 2010; Rolland et al., 2006; Ruan, 2014).

LHW transcription factor that has been related to the formation of lateral root by inducing auxin responses (Ohashi-Ito et al., 2013). LHW transcription factor has higher expression in HOSUT roots at 11-12BBCH. Its correlation with HXK1 and the higher expression of Tre-6-P synthase in HOSUT, might suggest a putative control of LHW over the shikimate pathway with the eventual outcome not only of increased auxin biosynthesis, but also of the production of Tre-6-P which serves as a signal for high sucrose availability (O'Hara et al., 2013).

Sucrose and glucose contents in HOSUT roots influence the biosynthesis, the signalling processes, perception and transport of auxin as described in Arabidopsis by Mishra et al. (2009) influencing cell division in the root system which is translated into higher number of root branching points. In HOSUT root transcriptome analysis, this effect is visible for entities involved in cell cycle and nucleotide metabolism (Figure 23B).

These results might suggest the involvement of LHW and WRKY with the hexokinase-dependent sugar signalling pathway regulating lateral root branching under stress conditions. Sugar signalling is complex, and closely interacts also with other known signalling pathways (Barbier et al., 2015; Morkunas and Ratajczak, 2014; Ruan, 2014; Eveland and Jackson, 2012).

The results of this study give novel information about the HOSUT phenotype. This results help unravel part of the molecular mechanisms, which might be responsible for the superior performance of the HOSUT wheat lines, and can be therefore considered as a valuable source of information for the future of modern wheat breeding programs as well as a model for research of the sucrose metabolism and its intricate network.

## IV. References

- Albacete, A.A., Martínez-Andújar, C., and Pérez-Alfocea, F.** (2014). Hormonal and metabolic regulation of source-sink relations under salinity and drought: From plant survival to crop yield stability. *Biotechnol. Adv.* **32**: 12–30.
- Aoki, N., Scofield, G.N., Wang, X.-D., Offler, C.E., Patrick, J.W., and Furbank, R.T.** (2006). Pathway of sugar transport in germinating wheat seeds. *Plant Physiol.* **141**: 1255–1263.
- Aoki, N., Scofield, G.N., Wang, X.D., Patrick, J.W., Offler, C.E., and Furbank, R.T.** (2004). Expression and localisation analysis of the wheat sucrose transporter TaSUT1 in vegetative tissues. *Planta* **219**: 176–184.
- Aparicio, N., Villegas, D., Araus, J.L., Blanco, R., and Royo, C.** (2002). Seedling development and biomass as affected by seed size and morphology in durum wheat. *J. Agric. Sci.* **139**: 143–150.
- Araus, J.L., Slafer, G. a., Royo, C., and Serret, M.D.** (2008). Breeding for Yield Potential and Stress Adaptation in Cereals. *CRC. Crit. Rev. Plant Sci.* **27**: 377–412.
- Bajguz, A. and Piotrowska, A.** (2009). Conjugates of auxin and cytokinin. *Phytochemistry* **70**: 957–69.
- Barbier, F. et al.** (2015). Sucrose is an early modulator of the key hormonal mechanisms controlling bud outgrowth in *Rosa hybrida*. *J. Exp. Bot.* **66**: 2569–2582.
- Becerra, C., Jahrmann, T., Puigdomènech, P., and Vicient, C.M.** (2004). Ankyrin repeat-containing proteins in Arabidopsis: Characterization of a novel and abundant group of genes coding ankyrin-transmembrane proteins. *Gene* **340**: 111–121.
- Bender, K.W., Dobney, S., Ogunrinde, A., Chiasson, D., Mullen, R.T., Teresinski, H.J., Singh, P., Munro, K., Smith, S.P., and Snedden, W. a** (2014). The calmodulin-like protein CML43 functions as a salicylic-acid-inducible root-specific Ca(2+) sensor in Arabidopsis. *Biochem. J.* **457**: 127–36.
- Bihmidine, S., Hunter, C.T., Johns, C.E., Koch, K.E., and Braun, D.M.** (2013). Regulation of assimilate import into sink organs: update on molecular drivers of sink strength. *Front. Plant Sci.* **4**: 177.
- Blanco, A., Mangini, G., Giancaspro, A., Giove, S., Colasuonno, P., Simeone, R., Signorile, A., De Vita, P., Mastrangelo, a. M., Cattivelli, L., and Gadaleta, A.** (2012). Relationships between grain protein content and grain yield components through quantitative trait locus analyses in a recombinant inbred line population derived from two elite durum wheat cultivars. *Mol. Breed.* **30**: 79–92.
- Blum, A., Mayer, J., Golan, G., Crops, F., Centre, T.V., and Dagan, B.** (1988). The Effect of Grain Number per Ear ( Sink Size ) on Source Activity and its Water-Relations in Wheat. *J. Exp. Bot.* **39**: 106–114.
- Bouché, N., Yellin, A., Snedden, W. a, and Fromm, H.** (2005). Plant-specific calmodulin-binding proteins. *Annu. Rev. Plant Biol.* **56**: 435–466.
- Boyd, W., Gordon, A., and LaCroix, L.** (1971). Seed Size, Germination and Seedling vigor in Barley. *Can. J. Plant Sci.* **51**: 93–99.

- Braun, D.M.** (2012). Plant science. SWEET! The pathway is complete. *Science* **335**: 173–4.
- Braun, D.M. and Slewinski, T.L.** (2009). Genetic control of carbon partitioning in grasses: roles of sucrose transporters and tie-dyed loci in phloem loading. *Plant Physiol.* **149**: 71–81.
- Cai, X.-T., Xu, P., Zhao, P.-X., Liu, R., Yu, L.-H., and Xiang, C.-B.** (2014). Arabidopsis ERF109 mediates cross-talk between jasmonic acid and auxin biosynthesis during lateral root formation. *Nat. Commun.* **5**: 5833.
- Calderini, D.F. and Ortiz-Monasterio, I.** (2003). Crop physiology & metabolism: Grain position affects grain macronutrient and micronutrient concentrations in wheat. *Crop Sci.* **43**: 141–151.
- Calderini, D.F., Savin, R., Abeledo, L.G., Reynolds, M.P., and Slafer, G.A.** (2001). The importance of the period immediately preceding anthesis for grain weight determination in wheat. *Euphytica* **119**: 199–204.
- Campanella, J.J., Olajide, A.F., Magnus, V., and Ludwig-Müller, J.** (2004). A novel auxin conjugate hydrolase from wheat with substrate specificity for longer side-chain auxin amide conjugates. *Plant Physiol.* **135**: 2230–2240.
- Casimiro, I., Beekman, T., Graham, N., Bhalerao, R., Zhang, H., Casero, P., Sandberg, G., and Bennett, M.J.** (2003). Dissecting Arabidopsis lateral root development. *Trends Plant Sci.* **8**: 165–171.
- Casimiro, I., Marchant, A., Bhalerao, R.P., Beekman, T., Dhooge, S., Swarup, R., Graham, N., Inzé, D., Sandberg, G., Casero, P.J., and Bennett, M.** (2001). Auxin transport promotes Arabidopsis lateral root initiation. *Plant Cell* **13**: 843–852.
- Chardon, F., Noël, V., and Masclaux-Daubresse, C.** (2012). Exploring NUE in crops and in Arabidopsis ideotypes to improve yield and seed quality. *J. Exp. Bot.* **63**: 3401–3412.
- Chen, J.-G., Gao, Y., and Jones, A.M.** (2006). Differential roles of Arabidopsis heterotrimeric G-protein subunits in modulating cell division in roots. *Plant Physiol.* **141**: 887–897.
- Chen, L.-Q., Qu, X.-Q., Hou, B.-H., Sosso, D., Osorio, S., Fernie, A.R., and Frommer, W.B.** (2012). Sucrose Efflux Mediated by SWEET Proteins as a Key Step for Phloem Transport. *Science* (80-. ). **335**: 207–211.
- Chen, X. and Friml, J.** (2014). Rho-GTPase-regulated vesicle trafficking in plant cell polarity. *Biochem. Soc. Trans.* **42**: 212–218.
- Cho, H.J., Brotherton, J.E., Song, H.S., and Widholm, J.M.** (2000). Increasing tryptophan synthesis in a forage legume *Astragalus sinicus* by expressing the tobacco feedback-insensitive anthranilate synthase (ASA2) gene. *Plant Physiol.* **123**: 1069–1076.
- Cisse, N. and Ejeta, G.** (2003). Genetic Variation and Relationships among Seedling Vigor Traits in Sorghum. *Crop Sci.* **43**: 824.
- Conger, R., Chen, Y., Fornaciari, S., Faso, C., Held, M.A., Renna, L., and Brandizzi, F.** (2011). Evidence for the involvement of the Arabidopsis SEC24A in male transmission. *J. Exp. Bot.* **62**: 4927–4936.

- Contento, A.L., Kim, S.-J., and Bassham, D.C.** (2004). Transcriptome profiling of the response of Arabidopsis suspension culture cells to Suc starvation. *Plant Physiol.* **135**: 2330–2347.
- Cosgrove, D.J.** (2005). Growth of the plant cell wall. *Nat. Rev. Mol. Cell Biol.* **6**: 850–861.
- Cui, H., Peng, B., Xing, Z., Xu, G., Yu, B., and Zhang, Q.** (2002). Molecular dissection of seedling-vigor and associated physiological traits in rice. *Theor. Appl. Genet.* **105**: 745–753.
- Cui, X., Lu, F., Li, Y., Xue, Y., Kang, Y., Zhang, S., Qiu, Q., Cui, X., Zheng, S., Liu, B., Xu, X., and Cao, X.** (2013). Ubiquitin-specific proteases UBP12 and UBP13 act in circadian clock and photoperiodic flowering regulation in Arabidopsis. *Plant Physiol.* **162**: 897–906.
- Diener, A.C., Gaxiola, R. a, and Fink, G.R.** (2001). Arabidopsis ALF5, a multidrug efflux transporter gene family member, confers resistance to toxins. *Plant Cell* **13**: 1625–1638.
- Ding, Z.J., Yan, J.Y., Li, C.X., Li, G.X., Wu, Y.R., and Zheng, S.J.** (2015). Transcription factor WRKY46 modulates the development of Arabidopsis lateral roots in osmotic/salt stress conditions via regulation of ABA signaling and auxin homeostasis. *Plant J.* **84**: 56–69.
- Ding, Z.J., Yan, J.Y., Xu, X.Y., Yu, D.Q., Li, G.X., Zhang, S.Q., and Zheng, S.J.** (2014). Transcription factor WRKY46 regulates osmotic stress responses and stomatal movement independently in Arabidopsis. *Plant J.* **79**: 13–27.
- Dodd, A.N., Kudla, J., and Sanders, D.** (2010). The Language of Calcium Signaling. *Annu. Rev. Plant Biol.* **61**: 593–620.
- Dolferus, R., Ji, X., and Richards, R. a.** (2011). Abiotic stress and control of grain number in cereals. *Plant Sci.* **181**: 331–341.
- Dreccer, M., Wockner, K., Palta, J., McIntyre, L., Borbogne, M., Bourgault, M., Reynolds, M., and Miralles, D.** (2014). More fertile florets and grains per spike can be achieved at higher temperature in wheat lines with high spike biomass and sugar content at booting. *Funct. Plant Biol.* **41**: 482–495.
- Dreccer, M.F., van Herwaarden, A.F., and Chapman, S.C.** (2009). Grain number and grain weight in wheat lines contrasting for stem water soluble carbohydrate concentration. *F. Crop. Res.* **112**: 43–54.
- Evans, L. and Bhatt, G.** (1977). Influence of seed size, protein content and cultivar on early seedling vigor in wheat. *Can. J. Plant Sci.* **57**: 929–935.
- Evans, L. and Fischer, R.** (1999). Yield Potential. *Crop Sci.* **39**: 1544.
- Eveland, A.L. and Jackson, D.P.** (2012). Sugars, signalling, and plant development. *J. Exp. Bot.* **63**: 3367–77.
- Evers, T. and Millar, S.** (2002). Cereal Grain Structure and Development: Some Implications for Quality. *J. Cereal Sci.* **36**: 261–284.
- FAO.** (2015). FAO Cereal Supply and Demand Brief. Release date: 05/03/2015. <http://www.fao.org/worldfoodsituation/csdb/en/>

- Ferrante, A., Savin, R., and Slafer, G.A.** (2010). Floret development of durum wheat in response to nitrogen availability. *J. Exp. Bot.* **61**: 4351–4359.
- Fischer, R.A.** (2008). The importance of grain or kernel number in wheat: A reply to Sinclair and Jamieson. *F. Crop. Res.* **105**: 15–21.
- Fisher, R.A.** (2007). Understanding the physiological basis of yield potential in wheat. *J. Agr. Sci.* **145**: 99–113.
- Foulkes, M.J., Slafer, G. a., Davies, W.J., Berry, P.M., Sylvester-Bradley, R., Martre, P., Calderini, D.F., Griffiths, S., and Reynolds, M.P.** (2011). Raising yield potential of wheat. III. Optimizing partitioning to grain while maintaining lodging resistance. *J. Exp. Bot.* **62**: 469–86.
- Fukaki, H., Tameda, S., Masuda, H., and Tasaka, M.** (2002). Lateral root formation is blocked by a gain-of-function mutation in the SOLITARY-ROOT/IAA14 gene of *Arabidopsis*. *Plant J.* **29**: 153–168.
- Furtado, A., Henry, R.J., and Pellegrineschi, A.** (2009). Analysis of promoters in transgenic barley and wheat. *Plant Biotechnol. J.* **7**: 240–253.
- Furtado, A., Henry, R.J., and Takaiwa, F.** (2008). Comparison of promoters in transgenic rice. *Plant Biotechnol. J.* **6**: 679–93.
- Galloway, J.N., Townsend, A.R., Erisman, J.W., Bekunda, M., Cai, Z., Freney, J.R., Martinelli, L. a, Seitzinger, S.P., and Sutton, M. a** (2008). Transformation of the Nitrogen Cycle: Recent Trends, Questions, and Potential Solutions. *Science* (80-. ). **320**: 889–892.
- Galon, Y., Aloni, R., Nachmias, D., Snir, O., Feldmesser, E., Scrase-Field, S., Boyce, J.M., Bouché, N., Knight, M.R., and Fromm, H.** (2010). Calmodulin-binding transcription activator 1 mediates auxin signaling and responds to stresses in *Arabidopsis*. *Planta* **232**: 165–178.
- Gao, Q.-M., Venugopal, S., Navarre, D., and Kachroo, A.** (2011). Low oleic acid-derived repression of jasmonic acid-inducible defense responses requires the WRKY50 and WRKY51 proteins. *Plant Physiol.* **155**: 464–476.
- García, G.A., Hasan, A.K., Puhl, L.E., Reynolds, M.P., Calderini, D.F., and Miralles, D.J.** (2013). Grain Yield Potential Strategies in an Elite Wheat Double-Haploid Population Grown in Contrasting Environments. *Crop Sci.* **53**: 2577–2587.
- Gaufichon, L., Reisdorf-Cren, M., Rothstein, S.J., Chardon, F., and Suzuki, A.** (2010). Biological functions of asparagine synthetase in plants. *Plant Sci.* **179**: 141–153.
- Gibson, S.I.** (2005). Control of plant development and gene expression by sugar signaling. *Curr. Opin. Plant Biol.* **8**: 93–102.
- González, F.G., Miralles, D.J., and Slafer, G.A.** (2011). Wheat floret survival as related to pre-anthesis spike growth. *J. Exp. Bot.* **62**: 4889–4901.
- Greenup, A.G., Sasani, S., Oliver, S.N., Walford, S.A., Millar, A.A., and Trevaskis, B.** (2011). Transcriptome analysis of the vernalization response in barley (*Hordeum vulgare*) seedlings. *PLoS One* **6**: e17900.

- Guo, Z. and Schnurbusch, T.** (2015). Variation of floret fertility in hexaploid wheat revealed by tiller removal. *J. Exp. Bot.* **66**: erv303.
- Gupta, P.K., Rustgi, S., and Kumar, N.** (2006). Genetic and molecular basis of grain size and grain number and its relevance to grain productivity in higher plants. *Genome* **49**: 565–571.
- Hawkesford, M.J., Araus, J.-L., Park, R., Calderini, D., Miralles, D., Shen, T., Zhang, J., and Parry, M.A.** (2013). Prospects of doubling global wheat yields. *Food Energy Secur.* **2**: 34–48.
- Herbers, K. and Sonnewald, U.** (1998). Molecular determinants of sink strength. *Curr. Opin. Plant Biol.* **1**: 207–216.
- Hermans, C., Hammond, J.P., White, P.J., and Verbruggen, N.** (2006). How do plants respond to nutrient shortage by biomass allocation? *Trends Plant Sci.* **11**: 610–617.
- Hetherington, A.M. and Brownlee, C.** (2004). The generation of Ca<sup>2+</sup> signals in plants. *Annu. Rev. Plant Biol.* **55**: 401–427.
- Howarth, J.R. et al.** (2008). Co-ordinated expression of amino acid metabolism in response to N and S deficiency during wheat grain filling. *J. Exp. Bot.* **59**: 3675–89.
- Huang, J., Zhao, X., Yu, H., Ouyang, Y., Wang, L., and Zhang, Q.** (2009). The ankyrin repeat gene family in rice: Genome-wide identification, classification and expression profiling. *Plant Mol. Biol.* **71**: 207–226.
- Hund, A., Fracheboud, Y., Soldati, A., Frascaroli, E., Salvi, S., and Stamp, P.** (2004). QTL controlling root and shoot traits of maize seedlings under cold stress. *Theor. Appl. Genet.* **109**: 618–629.
- Inzé, D. and De Veylder, L.** (2006). Cell cycle regulation in plant development. *Annu. Rev. Genet.* **40**: 77–105.
- Iyer-Pascuzzi, A.S. and Benfey, P.N.** (2009). Transcriptional networks in root cell fate specification. *Biochim. Biophys. Acta* **1789**: 315–325.
- Jansen, L., De Rybel, B., Vassileva, V., and Beeckman, T.** (2010). Plant Developmental Biology - Biotechnological Perspectives. In *Plant Developmental Biology - Biotechnological Perspectives*, E.C. Pua and M.R. Davey, eds (Springer Berlin Heidelberg: Berlin, Heidelberg), pp. 71–90.
- Ji, X., Shiran, B., Wan, J., Lewis, D.C., Jenkins, C.L.D., Condon, A.G., Richards, R.A., and Dolferus, R.** (2010). Importance of pre-anthesis anther sink strength for maintenance of grain number during reproductive stage water stress in wheat. *Plant. Cell Environ.* **33**: 926–42.
- Jonak, C., Ökrész, L., Bögre, L., and Hirt, H.** (2002). Complexity, cross talk and integration of plant MAP kinase signalling. *Curr. Opin. Plant Biol.* **5**: 415–424.
- De Jong, F., Thodey, K., Lejay, L. V., and Bevan, M.W.** (2014). Glucose Elevates NITRATE TRANSPORTER2.1 Protein Levels and Nitrate Transport Activity Independently of Its HEXOKINASE1-Mediated Stimulation of NITRATE TRANSPORTER2.1 Expression. *Plant Physiol.* **164**: 308–320.
- Kaneda, M., Schuetz, M., Lin, B.S.P., Chanis, C., Hamberger, B., Western, T.L., Ehltling, J., and Samuels, a. L.** (2011). ABC transporters coordinately expressed

- during lignification of *Arabidopsis* stems include a set of ABCBs associated with auxin transport. *J. Exp. Bot.* **62**: 2063–2077.
- Kiba, T., Feria-Bourrellier, A.-B., Lafouge, F., Lezhneva, L., Boutet-Mercey, S., Orsel, M., Bréhaut, V., Miller, A., Daniel-Vedele, F., Sakakibara, H., and Krapp, A.** (2012). The *Arabidopsis* nitrate transporter NRT2.4 plays a double role in roots and shoots of nitrogen-starved plants. *Plant Cell* **24**: 245–58.
- Kiba, T., Kudo, T., Kojima, M., and Sakakibara, H.** (2011). Hormonal control of nitrogen acquisition: Roles of auxin, abscisic acid, and cytokinin. *J. Exp. Bot.* **62**: 1399–1409.
- Kichey, T., Hirel, B., Heumez, E., Dubois, F., and Le Gouis, J.** (2007). In winter wheat (*Triticum aestivum* L.), post-anthesis nitrogen uptake and remobilisation to the grain correlates with agronomic traits and nitrogen physiological markers. *F. Crop. Res.* **102**: 22–32.
- Kim, K.-C., Lai, Z., Fan, B., and Chen, Z.** (2008). *Arabidopsis* WRKY38 and WRKY62 transcription factors interact with histone deacetylase 19 in basal defense. *Plant Cell* **20**: 2357–71.
- Koch, K.** (2004). Sucrose metabolism: Regulatory mechanisms and pivotal roles in sugar sensing and plant development. *Curr. Opin. Plant Biol.* **7**: 235–246.
- Kohl, S., Hollmann, J., Erban, A., Kopka, J., Riewe, D., Weschke, W., and Weber, H.** (2015). Metabolic and transcriptional transitions in barley glumes reveal a role as transitory resource buffers during endosperm filling. *J. Exp. Bot.* **66**: 1397–1411.
- Kojima, M., Kamada-Nobusada, T., Komatsu, H., Takei, K., Kuroha, T., Mizutani, M., Ashikari, M., Ueguchi-Tanaka, M., Matsuoka, M., Suzuki, K., and Sakakibara, H.** (2009). Highly sensitive and high-throughput analysis of plant hormones using MS-probe modification and liquid chromatography-tandem mass spectrometry: an application for hormone profiling in *Oryza sativa*. *Plant Cell Physiol.* **50**: 1201–14.
- Korasick, D.A., Enders, T.A., and Strader, L.C.** (2013). Auxin biosynthesis and storage forms. *J. Exp. Bot.* **64**: 2541–2555.
- Krouk, G. et al.** (2010). Nitrate-regulated auxin transport by NRT1.1 defines a mechanism for nutrient sensing in plants. *Dev. Cell* **18**: 927–937.
- Kudla, J., Batistic, O., and Hashimoto, K.** (2010). Calcium signals: the lead currency of plant information processing. *Plant Cell* **22**: 541–563.
- Kuhlmann, M., Horvay, K., Strathmann, A., Heinekamp, T., Fischer, U., Böttner, S., and Dröge-Laser, W.** (2003). The alpha-helical D1 domain of the tobacco bZIP transcription factor BZI-1 interacts with the ankyrin-repeat protein ANK1 and is important for BZI-1 function, both in auxin signaling and pathogen response. *J. Biol. Chem.* **278**: 8786–94.
- Kühn, C.** (2003). A comparison of the sucrose transporter systems of different plant species. *Plant Biol.* **5**: 215–232.
- Kühn, C. and Grof, C.P.L.** (2010). Sucrose transporters of higher plants. *Curr. Opin. Plant Biol.* **13**: 288–298.



- Lanteri, M.L., Laxalt, A.M., and Lamattina, L.** (2008). Nitric oxide triggers phosphatidic acid accumulation via phospholipase D during auxin-induced adventitious root formation in cucumber. *Plant Physiol.* **147**: 188–198.
- Lavenus, J., Goh, T., Roberts, I., Guyomarc'h, S., Lucas, M., De Smet, I., Fukaki, H., Beeckman, T., Bennett, M., and Laplaze, L.** (2013). Lateral root development in Arabidopsis: fifty shades of auxin. *Trends Plant Sci.* **18**: 450–458.
- Lea, P.J., Sodek, L., Parry, M. a J., Shewry, P.R., and Halford, N.G.** (2007). Asparagine in plants. *Ann. Appl. Biol.* **150**: 1–26.
- Leclere, S., Schmelz, E. a, and Chourey, P.S.** (2010). Sugar levels regulate tryptophan-dependent auxin biosynthesis in developing maize kernels. *Plant Physiol.* **153**: 306–18.
- Li, N. and Li, Y.** (2014). Ubiquitin-mediated control of seed size in plants. *Front. Plant Sci.* **5**: 332.
- Lilley, J.M. and Kirkegaard, J.A.** (2011). Benefits of increased soil exploration by wheat roots. *F. Crop. Res.* **122**: 118–130.
- Ling, Q., Huang, W., and Jarvis, P.** (2011). Use of a SPAD-502 meter to measure leaf chlorophyll concentration in Arabidopsis thaliana. *Photosynth. Res.* **107**: 209–214.
- Ljung, K.** (2013). Auxin metabolism and homeostasis during plant development. *Development* **140**: 943–950.
- Lizana, X.C. and Calderini, D.F.** (2013). Yield and grain quality of wheat in response to increased temperatures at key periods of grain number and grain weight determination: considerations for the climatic change scenarios of Chile. *J.Agr.Sci.* **151**: 209-221.
- López-Castañeda, C; Richards, R.A.; Farquhar, D.G.; Williamson, R.E.** (1996). Seed and Seedling Characteristics Contributing to Variation in Early Vigor among Temperate Cereals. *Crop Sci.* **36**: 125-1266.
- Ludwig-Müller, J.** (2011). Auxin conjugates: Their role for plant development and in the evolution of land plants. *J. Exp. Bot.* **62**: 1757–1773.
- MacGregor, D.R., Deak, K.I., Ingram, P. a, and Malamy, J.E.** (2008). Root system architecture in Arabidopsis grown in culture is regulated by sucrose uptake in the aerial tissues. *Plant Cell* **20**: 2643–60.
- Maeda, H. and Dudareva, N.** (2012). The Shikimate Pathway and Aromatic Amino Acid Biosynthesis in Plants. *Annu. Rev. Plant Biol.* **63**: 73–105.
- Malamy, J.E.** (2005). Intrinsic and environmental response pathways that regulate root system architecture. *Plant. Cell Environ.* **28**: 67–77.
- Malamy, J.E. and Ryan, K.S.** (2001). Environmental Regulation of Lateral Root Initiation in Arabidopsis 1. *Plant Physiol.* **127**: 899–909.
- Mano, Y. and Nemoto, K.** (2012). The pathway of auxin biosynthesis in plants. *J. Exp. Bot.* **63**: 2853–72.
- Manske, GGB; Vlek, PLG.** (2002). Root architecture – Wheat as a model plant. In Waisel, Y; Eshel, A; Kafkafi, U; eds. *Pant Roots: The hidden half.* Marcel Dekker, New York, pp 249-258.

- Marcelis, L.F.M.** (1996). Sink strength as a determinant of dry matter partitioning in the whole plant. *J. Exp. Bot.* **47**: 1281–1291.
- Markakis, M.N., Boron, A.K., Van Loock, B., Saini, K., Cirera, S., Verbelen, J.P., and Vissenberg, K.** (2013). Characterization of a small auxin-up RNA (SAUR)-like gene involved in *Arabidopsis thaliana* development. *PLoS One* **8**: 1–13.
- Masclaux-Daubresse, C., Daniel-Vedele, F., Dechorgnat, J., Chardon, F., Gaufichon, L., and Suzuki, A.** (2010). Nitrogen uptake, assimilation and remobilization in plants: challenges for sustainable and productive agriculture. *Ann. Bot.* **105**: 1141–1157.
- Mason, M.G., Ross, J.J., Babst, B. a., Wienclaw, B.N., and Beveridge, C.A.** (2014). Sugar demand, not auxin, is the initial regulator of apical dominance. *Proc. Natl. Acad. Sci.* **111**: 6092–6097.
- McSteen, P.** (2010). Auxin and monocot development. *Cold Spring Harb. Perspect. Biol.* **2**: a001479.
- Meier, U.** (2001). Growth stages of mono- and dicotyledonous plants. *BBCH Monographie.*: 166.
- Milberg, P., Pérez-Fernández, M.A., and Lamont, B.B.** (2014). Seedling growth response to added nutrients depends on seed size in three woody genera. *J. Ecol.* **86**: 624–632.
- Mishra, B.S., Singh, M., Aggrawal, P., and Laxmi, A.** (2009). Glucose and auxin signaling interaction in controlling *Arabidopsis thaliana* seedlings root growth and development. *PLoS One* **4**: e4502.
- Mockaitis, K. and Estelle, M.** (2008). Auxin receptors and plant development: a new signaling paradigm. *Annu. Rev. Cell Dev. Biol.* **24**: 55–80.
- Mockaitis, K. and Howell, S.H.** (2000). Auxin induces mitogenic activated protein kinase (MAPK) activation in roots of *Arabidopsis* seedlings. *Plant J.* **24**: 785–796.
- Moles, A.T. and Westoby, M.** (2004). Seedling survival and seed size: a synthesis of the literature. *J. Ecol.* **92**: 372–383.
- Morkunas, I. and Ratajczak, L.** (2014). The role of sugar signaling in plant defense responses against fungal pathogens. *Acta Physiol. Plant.* **36**: 1607–1619.
- Morris, P.C. and Bryce, J.H.** (2000). *Cereal biotechnology* P. Morris and J. Bryce, eds (Woodhead Publishing Limited: Cambridge).
- Neuberg, M., Pavlíková, D., Pavlík, M., and Balík, J.** (2010). The effect of different nitrogen nutrition on proline and asparagine content in plant. *Plant, Soil Environ.* **56**: 305–311.
- Neumann, K.; Zhao, Y.; Chu, J.; Waßermann, L.; Reif, J.; Kilian, B.; Graner, A.** (2016). The genetic architecture and temporal patterns of biomass accumulation in spring barley revealed by image analysis. (Manuscript Submitted).
- Nieuwland, J., Maughan, S., Dewitte, W., Scofield, S., Sanz, L., and Murray, J.A.** (2009). The D-type cyclin CYCD4;1 modulates lateral root density in *Arabidopsis* by affecting the basal meristem region. *Proc. Natl. Acad. Sci. U. S. A.* **106**: 22528–22533.

- O'Hara, L.E., Paul, M.J., and Wingler, A.** (2013). How Do Sugars Regulate Plant Growth and Development? New Insight into the Role of Trehalose-6-Phosphate. *Mol. Plant* **6**: 261–274.
- Ohashi-Ito, K. and Bergmann, D.C.** (2007). Regulation of the Arabidopsis root vascular initial population by LONESOME HIGHWAY. *Development* **134**: 2959–2968.
- Ohashi-Ito, K., Oguchi, M., Kojima, M., Sakakibara, H., and Fukuda, H.** (2013). Auxin-associated initiation of vascular cell differentiation by LONESOME HIGHWAY. *Development* **140**: 765–769.
- Ordóñez, R.A., Savin, R., Cossani, C.M., and Slafer, G.A.** (2015). Yield response to heat stress as affected by nitrogen availability in maize. *F. Crop. Res.* **183**: 184–203.
- Orman-Ligeza, B., Parizot, B., Gantet, P.P., Beeckman, T., Bennett, M.J., and Draye, X.** (2013). Post-embryonic root organogenesis in cereals: branching out from model plants. *Trends Plant Sci.* **18**: 459–67.
- Overvoorde, P., Fukaki, H., and Beeckman, T.** (2010). Auxin control of root development. *Cold Spring Harb. Perspect. Biol.* **2**: a001537.
- Park, W.J., Kriechbaumer, V., Möller, A., Piotrowski, M., Meeley, R.B., Gierl, A., and Glawischnig, E.** (2003). The Nitrilase ZmNIT2 converts indole-3-acetonitrile to indole-3-acetic acid. *Plant Physiol.* **133**: 794–802.
- Parre, E., Ghars, M.A., Leprince, A.-S., Thiery, L., Lefebvre, D., Bordenave, M., Richard, L., Mazars, C., Abdelly, C., and Saviouré, A.** (2007). Calcium signaling via phospholipase C is essential for proline accumulation upon ionic but not nonionic hyperosmotic stresses in Arabidopsis. *Plant Physiol.* **144**: 503–512.
- Pask, A., Sylvester-Bradley, R., Jamieson, P., and Foulkes, M.** (2012). Quantifying how winter wheat crops accumulate and use nitrogen reserves during growth. *F. Crop. Res.* **126**: 104–118.
- Peleg, Z., Reguera, M., Tumimbang, E., Walia, H., and Blumwald, E.** (2011). Cytokinin-mediated source/sink modifications improve drought tolerance and increase grain yield in rice under water-stress. *Plant Biotechnol. J.* **9**: 747–58.
- Péret, B., De Rybel, B., Casimiro, I., Benková, E., Swarup, R., Laplaze, L., Beeckman, T., and Bennett, M.J.** (2009). Arabidopsis lateral root development: an emerging story. *Trends Plant Sci.* **14**: 399–408.
- Peukert, M., Thiel, J., Mock, H.-P., Marko, D., Weschke, W., and Matros, A.** (2016). Spatiotemporal Dynamics of Oligofructan Metabolism and Suggested Functions in Developing Cereal Grains. *Front. Plant Sci.* **6**: 1–13.
- Popescu, S.C., Popescu, G. V., Bachan, S., Zhang, Z., Seay, M., Gerstein, M., Snyder, M., and Dinesh-Kumar, S.P.** (2007). Differential binding of calmodulin-related proteins to their targets revealed through high-density Arabidopsis protein microarrays. *Proc. Natl. Acad. Sci. U. S. A.* **104**: 4730–4735.
- Radchuk, R., Radchuk, V., Götz, K.-P., Weichert, H., Richter, A., Emery, R.J.N., Weschke, W., and Weber, H.** (2007). Ectopic expression of phosphoenolpyruvate carboxylase in *Vicia narbonensis* seeds: effects of improved nutrient status on seed maturation and transcriptional regulatory networks. *Plant J.* **51**: 819–839.

- Rea, P.A.** (2007). Plant ATP-binding cassette transporters. *Annu. Rev. Plant Biol.* **58**: 347–375.
- Reynolds, M., Foulkes, J., Furbank, R., Griffiths, S., King, J., Murchie, E., Parry, M., and Slafer, G.** (2012). Achieving yield gains in wheat. *Plant, Cell Environ.* **35**: 1799–1823.
- Reynolds, M., Foulkes, M.J., Slafer, G.A., Berry, P., Parry, M.A., Snape, J.W., and Angus, W.J.** (2009). Raising yield potential in wheat. *J. Exp. Bot.* **60**: 1899–918.
- Roitsch, T., Balibrea, M.E., Hofmann, M., Proels, R., and Sinha, a. K.** (2003). Extracellular invertase: Key metabolic enzyme and PR protein. In *Journal of Experimental Botany*, pp. 513–524.
- Roitsch, T. and Ehneß, R.** (2000). Regulation of source/sink relations by cytokinins. In *Plant Growth Regulation*, pp. 359–367.
- Roitsch, T. and González, M.C.** (2004). Function and regulation of plant invertases: Sweet sensations. *Trends Plant Sci.* **9**: 606–613.
- Rolland, F., Baena-Gonzalez, E., and Sheen, J.** (2006). Sugar sensing and signaling in plants: conserved and novel mechanisms. *Annu. Rev. Plant Biol.* **57**: 675–709.
- Rolland, F., Moore, B., and Sheen, J.** (2002). Sugar sensing and signaling in plants. *Plant Cell* **14 Suppl**: S185–S205.
- Rolland, F. and Sheen, J.** (2005). Sugar sensing and signalling networks in plants. *Biochem. Soc. Trans.* **33**: 269–271.
- Rosche, E., Blackmore, D., Tegeder, M., Richardson, T., Schroeder, H., Higgins, T.J. V, Frommer, W.B., Offler, C.E., Patrick, J.W., Of, C.E., Patrick, J.W., and Offler, C.E.** (2002). Seed-specific overexpression of a potato sucrose transporter increases sucrose uptake and growth rates of developing pea cotyledons. *Plant J.* **30**: 165–75.
- Ruan, Y.-L.** (2014). Sucrose metabolism: gateway to diverse carbon use and sugar signaling. *Annu. Rev. Plant Biol.* **65**: 33–67.
- Ruzicka, K., Simásková, M., Duclercq, J., Petrásek, J., Zazímalová, E., Simon, S., Friml, J., Van Montagu, M.C.E., and Benková, E.** (2009). Cytokinin regulates root meristem activity via modulation of the polar auxin transport. *Proc. Natl. Acad. Sci. U. S. A.* **106**: 4284–9.
- Saalbach, I., Mora-Ramírez, I., Weichert, N., Andersch, F., Guild, G., Wieser, H., Koehler, P., Stangoulis, J., Kumlehn, J., Weschke, W., and Weber, H.** (2014). Increased grain yield and micronutrient concentration in transgenic winter wheat by ectopic expression of a barley sucrose transporter. *J. Cereal Sci.* **60**: 75–81.
- Sakakibara, H.** (2006). Cytokinins: activity, biosynthesis, and translocation. *Annu. Rev. Plant Biol.* **57**: 431–49.
- Sauer, N.** (2007). Molecular physiology of higher plant sucrose transporters. *FEBS Lett.* **581**: 2309–17.

- Schroeder, J.I., Delhaize, E., Frommer, W.B., Guerinot, M. Lou, Harrison, M.J., Herrera-Estrella, L., Horie, T., Kochian, L. V, Munns, R., Nishizawa, N.K., Tsay, Y.-F., and Sanders, D.** (2013). Using membrane transporters to improve crops for sustainable food production. *Nature* **497**: 60–6.
- Schulz, B. and Kolukisaoglu, H.U.** (2006). Genomics of plant ABC transporters: the alphabet of photosynthetic life forms or just holes in membranes? *FEBS Lett.* **580**: 1010–6.
- Semenov, M.A., Stratonovitch, P., Alghabari, F., and Gooding, M.J.** (2014). Adapting wheat in Europe for climate change. *J. Cereal Sci.* **59**: 245–256.
- Seo, P.J., Park, J., Park, M.-J., Kim, Y.-S., Kim, S.-G., Jung, J.-H., and Park, C.-M.** (2012). A Golgi-localized MATE transporter mediates iron homeostasis under osmotic stress in Arabidopsis. *Biochem. J.* **442**: 551–61.
- Serrago, R. a., Alzueta, I., Savin, R., and Slafer, G. a.** (2013). Understanding grain yield responses to source–sink ratios during grain filling in wheat and barley under contrasting environments. *F. Crop. Res.* **150**: 42–51.
- Shen, X., Xu, K.-F., Fan, Q., Pacheco-Rodriguez, G., Moss, J., and Vaughan, M.** (2006). Association of brefeldin A-inhibited guanine nucleotide-exchange protein 2 (BIG2) with recycling endosomes during transferrin uptake. *Proc. Natl. Acad. Sci. U. S. A.* **103**: 2635–2640.
- Shewry, P.R.** (2009). Wheat. *J. Exp. Bot.* **60**: 1537–1553.
- Shewry, P.R. and Halford, N.G.** (2002). Cereal seed storage proteins: structures, properties and role in grain utilization. *J. Exp. Bot.* **53**: 947–58.
- Shewry, P.R., Tatham, A.S., and Halford, N.G.** (2001). Nutritional control of storage protein synthesis in developing grain of wheat and barley. *Plant Growth Regul.*
- Sinclair, T.R. and Jamieson, P.D.** (2008). Yield and grain number of wheat: A correlation or causal relationship?. Authors’ response to “The importance of grain or kernel number in wheat: A reply to Sinclair and Jamieson” by R.A. Fischer. *F. Crop. Res.* **105**: 22–26.
- Slafer, G. and Araus, J.** (2007). CHAPTER 12 PHYSIOLOGICAL TRAITS FOR IMPROVING WHEAT YIELD UNDER A WIDE RANGE OF CONDITIONS. In *Scale and Complexity in Plant Systems Research: Gene-Plant-Crop Relations*, P.S. and H. van L. JHL Spiertz, ed (Springer Berlin Heidelberg), pp. 147–156.
- Slafer, G.A. and Andrade, F.H.** (1993). Physiological attributes related to the generation of grain yield in bread wheat cultivars released at different eras. *F. Crop. Res.* **31**: 351–367.
- Slafer, G.A.; Calderini, D.F.; Miralles, D.J.** (1996). Yield Components and Compensation in Wheat: Opportunities for Further Increasing Yield Potential. In Reynolds, MP; Rajaram, S; McNab, A, eds. *Increasing Yield Potential in Wheat: Breaking the barriers*. CIMMYT, México. pp 101-133.
- De Smet, I. et al.** (2007). Auxin-dependent regulation of lateral root positioning in the basal meristem of Arabidopsis. *Development* **134**: 681–690.
- Smith, S. and De Smet, I.** (2012). Root system architecture: insights from Arabidopsis and cereal crops. *Philos. Trans. R. Soc. B Biol. Sci.* **367**: 1441–1452.

- Song, X., Ni, Z., Yao, Y., Xie, C., Li, Z., Wu, H., Zhang, Y., and Sun, Q.** (2007). Wheat (*Triticum aestivum* L.) root proteome and differentially expressed root proteins between hybrid and parents. *Proteomics* **7**: 3538–57.
- Suhandono, S., Apriyanto, A., and Ihsani, N.** (2014). Isolation and characterization of three cassava elongation factor 1 alpha (MeEF1A) promoters. *PLoS One* **9**: e84692.
- Theodoulou, F.L.** (2000). Plant ABC transporters (Review). *Biochim. Biophys. Acta* **1465**: 79–103.
- Tognetti, J.A., Pontis, H.G., and Martínez-Noël, G.M.** (2013). Sucrose signaling in plants: a world yet to be explored. *Plant Signal. Behav.* **8**: e23316.
- Trachsel, S., Messmer, R., Stamp, P., Ruta, N., and Hund, A.** (2010). QTLs for early vigor of tropical maize. *Mol. Breed.* **25**: 91–103.
- Trevaskis, B., Hemming, M.N., Dennis, E.S., and Peacock, W.J.** (2007). The molecular basis of vernalization-induced flowering in cereals. *Trends Plant Sci.* **12**: 352–7.
- Trevisan, S., Borsa, P., Botton, A., Varotto, S., Malagoli, M., Ruperti, B., and Quaggiotti, S.** (2008). Expression of two maize putative nitrate transporters in response to nitrate and sugar availability. *Plant Biol.* **10**: 462–475.
- Truernit, E.** (2001). Plant physiology: The importance of sucrose transporters. *Curr. Biol.* **11**: R169–71.
- Tuteja, N. and Mahajan, S.** (2007). Calcium signaling network in plants: an overview. *Plant Signal. Behav.* **2**: 79–85.
- Tzin, V. and Galili, G.** (2010). New Insights into the Shikimate and Aromatic Amino Acids Biosynthesis Pathways in Plants. *Mol. Plant* **3**: 956–972.
- Vahamidis, P., Karamanos, A., Economou, G., and Fasseas, C.** (2014). A new scale for the assessment of wheat spike morphogenesis. *Ann. Appl. Biol.* **164**: 220–231.
- Vanderbeld, B. and Snedden, W.A.** (2007). Developmental and stimulus-induced expression patterns of Arabidopsis calmodulin-like genes CML37, CML38 and CML39. *Plant Mol. Biol.* **64**: 683–697.
- Vanneste, S. et al.** (2005). Cell Cycle Progression in the Pericycle Is Not Sufficient for SOLITARY ROOT / IAA14-Mediated Lateral Root Initiation in Arabidopsis thaliana. *Plant Cell* **17**: 3035–3050.
- Verrier, P.J. et al.** (2008). Plant ABC proteins--a unified nomenclature and updated inventory. *Trends Plant Sci.* **13**: 151–9.
- Wakasa, K., Hasegawa, H., Nemoto, H., Matsuda, F., Miyazawa, H., Tozawa, Y., Morino, K., Komatsu, A., Yamada, T., Terakawa, T., and Miyagawa, H.** (2006). High-level tryptophan accumulation in seeds of transgenic rice and its limited effects on agronomic traits and seed metabolite profile. *J. Exp. Bot.* **57**: 3069–78.
- Wang, L. and Ruan, Y.-L.** (2013). Regulation of cell division and expansion by sugar and auxin signaling. *Front. Plant Sci.* **4**: 163.
- Weaver, L.M. and Herrmann, K.M.** (1997). Dynamics of the shikimate pathway in plants. *Trends Plant Sci.* **2**: 346–351.

- Weichert, A., Brinkmann, C., Komarova, N.Y., Dietrich, D., Thor, K., Meier, S., Suter Grottemeyer, M., and Rentsch, D.** (2012). AtPTR4 and AtPTR6 are differentially expressed, tonoplast-localized members of the peptide transporter/nitrate transporter 1 (PTR/NRT1) family. *Planta* **235**: 311–23.
- Weichert, N. et al.** (2010). Increasing sucrose uptake capacity of wheat grains stimulates storage protein synthesis. *Plant Physiol.* **152**: 698–710.
- Werner, T., Nehnevajova, E., Köllmer, I., Novák, O., Strnad, M., Krämer, U., and Schmülling, T.** (2010). Root-specific reduction of cytokinin causes enhanced root growth, drought tolerance, and leaf mineral enrichment in Arabidopsis and tobacco. *Plant Cell* **22**: 3905–20.
- Weschke, W., Panitz, R., Sauer, N., Wang, Q., Neubohn, B., Weber, H., and Wobus, U.** (2000). Sucrose transport into barley seeds: Molecular characterization of two transporters and implications for seed development and starch accumulation. *Plant J.* **21**: 455–467.
- Wheeler, T. and von Braun, J.** (2013). Climate Change Impacts on Global Food Security. *Science* (80-. ). **341**: 508–513.
- Williams, L.E., Lemoine, R., and Sauer, N.** (2000). Sugar transporters in higher plants-- a diversity of roles and complex regulation. *Trends Plant Sci.* **5**: 283–90.
- Wind, J., Smeekens, S., and Hanson, J.** (2010). Sucrose: metabolite and signaling molecule. *Phytochemistry* **71**: 1610–4.
- Winfield, M.O., Lu, C., Wilson, I.D., Coghill, J.A., and Edwards, K.J.** (2010). Plant responses to cold: Transcriptome analysis of wheat. *Plant Biotechnol. J.* **8**: 749–71.
- Wirdnam, C., Motoyama, A., Arn-Bouidoires, E., Van Eeden, S., Iglesias, A., and Meins, F.** (2004). Altered expression of an ankyrin-repeat protein results in leaf abnormalities, necrotic lesions, and the elaboration of a systemic signal. *Plant Mol. Biol.* **56**: 717–730.
- Woodward, A.W. and Bartel, B.** (2005). Auxin: regulation, action, and interaction. *Ann. Bot.* **95**: 707–35.
- Xu, G., Fan, X., and Miller, A.J.** (2012). Plant nitrogen assimilation and use efficiency. *Annu. Rev. Plant Biol.* **63**: 153–82.
- Yadav, U.P., Ayre, B.G., and Bush, D.R.** (2015). Transgenic approaches to altering carbon and nitrogen partitioning in whole plants: assessing the potential to improve crop yields and nutritional quality. *Front. Plant Sci.* **6**: 1–13.
- Zhang, H., Rong, H., and Pilbeam, D.** (2007). Signalling mechanisms underlying the morphological responses of the root system to nitrogen in Arabidopsis thaliana. *J. Exp. Bot.* **58**: 2329–2338.
- Zhang, J. et al.** (2011). Inositol trisphosphate-induced Ca<sup>2+</sup> signaling modulates auxin transport and pin polarity. *Dev. Cell* **20**: 855–866.
- Zheng, Z.-L.** (2009). Carbon and nitrogen nutrient balance signaling in plants. *Plant Signal. Behav.* **4**: 584–591.

## V. Supplemental Data

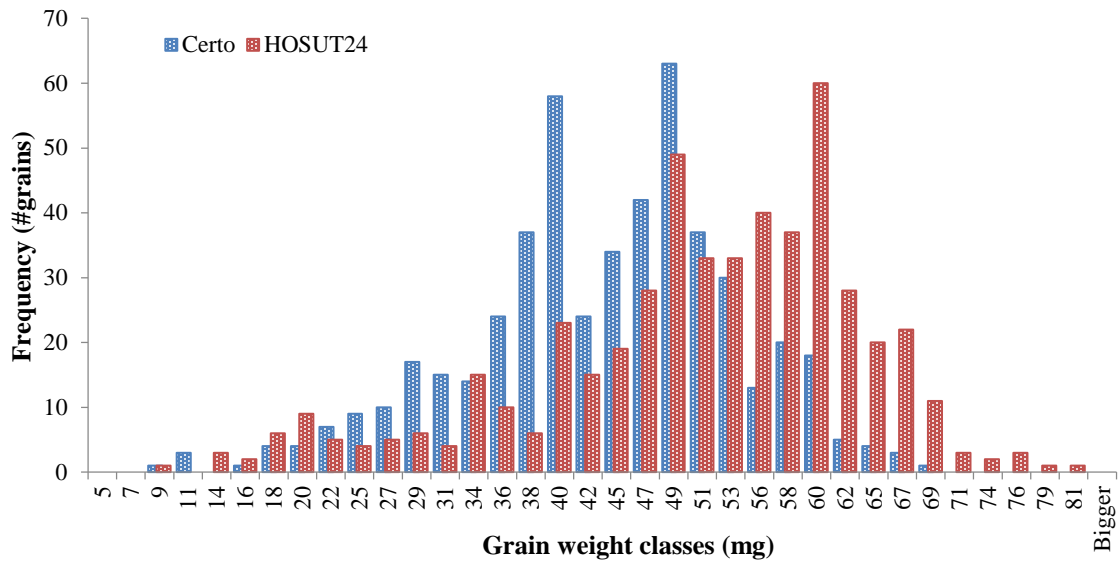


Figure 33. Distribution pattern of TGW. Growing season **2009-2010**. Certo grain weight distribution: Median value 44 mg, average value 42.6 mg. HOSUT24 grain weight distribution: Median value 52 mg, average value 50 mg.

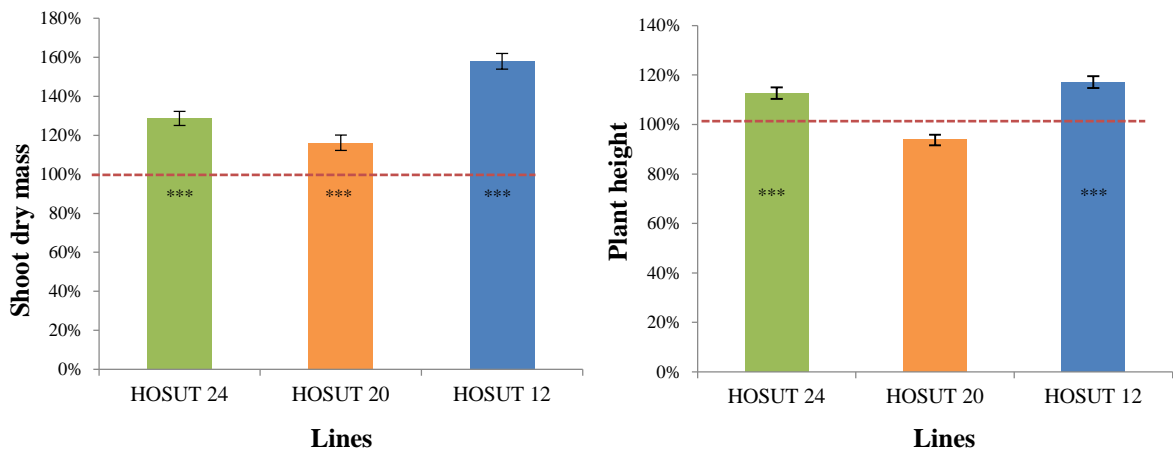


Figure 34. Shoot dry mass and plant height at 13 BBCH stage of development in three HOSUT lines. Comparison to Certo (100%, red dotted line). Plants were grown under near-field conditions. Vertical bars:  $\pm$  SE,  $P < 0.05$  (\*),  $P < 0.01$  (\*\*),  $P < 0.001$  (\*\*\*)



Table 15. Percentage of N, C and C/N in roots, shoots and grain rest during early seedling development of *in vitro* plants under N-deprived conditions. Comparison of HOSUT24 and Certo (Certo=100%).  $\pm$  SD. Analysis performed until the 13BBCH.

Day of growth	Plant part	C/N (%)	C (%)	N (%)
0	dried seed	87.1 $\pm$ 7.7	99.6 $\pm$ 0.1	114.7 $\pm$ 10.2
3	soaked seed	89.0 $\pm$ 3.3	99.0 $\pm$ 0.9	111.2 $\pm$ 4.4
7	grains	90.2 $\pm$ 5.7	99.6 $\pm$ 0.8	110.7 $\pm$ 7.9
	leaves	95.6 $\pm$ 0.6	101.1 $\pm$ 0.7	105.6 $\pm$ 0.1
	roots	100.0 $\pm$ 9.4	100.1 $\pm$ 1.2	100.4 $\pm$ 8.2
12	grains	82.5 $\pm$ 5.7	100.0 $\pm$ 0.9	121.2 $\pm$ 9.2
	leaves	92.3 $\pm$ 8.7	101.8 $\pm$ 1.9	110.8 $\pm$ 12.5
	roots	93.5 $\pm$ 25.9	90.9 $\pm$ 16.0	101.5 $\pm$ 45.0
17	grains	71.6 $\pm$ 9.9	98.1 $\pm$ 2.3	138.2 $\pm$ 22.4
	leaves	89.2 $\pm$ 10.0	101.2 $\pm$ 3.1	113.1 $\pm$ 16.0
	roots	98.0 $\pm$ 13.7	101.3 $\pm$ 4.9	104.6 $\pm$ 19.7
21	grains	83.5 $\pm$ 0.4	100.3 $\pm$ 1.9	119.7 $\pm$ 2.8
	leaves	90.3 $\pm$ 6.3	97.5 $\pm$ 0.8	107.0 $\pm$ 8.2
	roots	97.4 $\pm$ 15.3	100.5 $\pm$ 2.6	104.3 $\pm$ 19.4
26	grains	96.7 $\pm$ 7.1	100.1 $\pm$ 0.9	101.2 $\pm$ 6.7
	leaves	90.5 $\pm$ 1.0	101.1 $\pm$ 3.7	111.6 $\pm$ 2.6
	roots	109.5 $\pm$ 10.1	101.0 $\pm$ 2.6	91.2 $\pm$ 10.4
31	grains	95.5 $\pm$ 7.1	100.5 $\pm$ 1.3	105.1 $\pm$ 6.2
	leaves	94.9 $\pm$ 7.9	100.8 $\pm$ 3.4	106.7 $\pm$ 12.4
	roots	102.1 $\pm$ 9.4	100.7 $\pm$ 3.0	98.0 $\pm$ 12.2
35	grains	88.0 $\pm$ 3.8	101.8 $\pm$ 0.8	115.7 $\pm$ 6.1
	leaves	94.2 $\pm$ 9.3	100.5 $\pm$ 0.5	107.1 $\pm$ 11.4
	roots	92.5 $\pm$ 2.2	101.2 $\pm$ 1.8	108.7 $\pm$ 4.1

Table 16. N, C and sugars concentration in roots and shoots of HOSUT20 and HOSUT12 seedlings in comparison to Certo.  $\pm$  SD. T-test.  $P < 0.05$  (\*),  $P < 0.01$  (\*\*),  $P < 0.001$  (\*\*\*)

Growth condition	Metabolite	Root				Shoot			
		HOSUT20		HOSUT12		HOSUT20		HOSUT12	
		abs	% of Certo	abs	% of Certo	abs	% Certo	abs	% Certo
In vitro N-deprived	Glucose ( $\mu\text{mol/gDW}$ )	15.7 $\pm$ 3.7	96.7%	15.0 $\pm$ 2.3	106.8%	nd	nd	nd	nd
	Fructose ( $\mu\text{mol/gDW}$ )	19.2 $\pm$ 1.5	126.7%	14.4 $\pm$ 3.7	159.1%	nd	nd	nd	nd
	sucrose ( $\mu\text{mol/gDW}$ )	74.2 $\pm$ 2.5	102.2%	106.9 $\pm$ 8.0	111.8%	nd	nd	nd	nd
	Starch (mg/gDW)	16.8 $\pm$ 1.9	97.6%	18.8 $\pm$ 2.8	75.6%*	nd	nd	nd	nd
	Carbon (% of total mass)	42.6 $\pm$ 0.2	100.5%	41.4 $\pm$ 0.1	100.6%	nd	nd	nd	nd
	Nitrogen (% of total mass)	0.73 $\pm$ 0.03	112.3%*	0.7 $\pm$ 0.1	114.5%	nd	nd	nd	nd
	C:N	58.6 $\pm$ 2.5	89.8%*	58.8 $\pm$ 4.5	88.5%	nd	nd	nd	nd
Field-like	Glucose ( $\mu\text{mol/gDW}$ )	14.0 $\pm$ 2.5	83.8%	13.5 $\pm$ 2.1	68.5%*	55.2 $\pm$ 1.9	141.6%***	57.1 $\pm$ 5.9	153.5%*
	Fructose ( $\mu\text{mol/gDW}$ )	20.2 $\pm$ 2.9	80.4%**	22.7 $\pm$ 2.2	88.50%	160.4 $\pm$ 4.2	139.9%***	157.1 $\pm$ 4.4	110.7%*
	sucrose ( $\mu\text{mol/gDW}$ )	68.8 $\pm$ 11.3	93.4%	106.5 $\pm$ 1.4	114.5%*	25.9 $\pm$ 2.2	118.8%	75.6 $\pm$ 9.4	207.2%**
	Starch (mg/gDW)	22.8 $\pm$ 1.8	98.5%	29.9 $\pm$ 1.4	118.5%	15.0 $\pm$ 1.3	119.0%	18.2 $\pm$ 0.2	96.8%
	Carbon (% of total mass)	35.9 $\pm$ 1.4	106.7%*	34.8 $\pm$ 0.5	103.4%*	40.9 $\pm$ 0.5	100.3%	40.8 $\pm$ 0.0	101.2%***
	Nitrogen (% of total mass)	3.4 $\pm$ 0.3	90.60%	3.6 $\pm$ 0.1	96.50%	5.1 $\pm$ 0.1	93.9%***	5.0 $\pm$ 0.1	96.3%
	C:N	10.7 $\pm$ 0.9	107.4%***	9.8 $\pm$ 0.4	118.3%	8.1 $\pm$ 0.2	106.8%***	8.2 $\pm$ 0.1	105.1%*

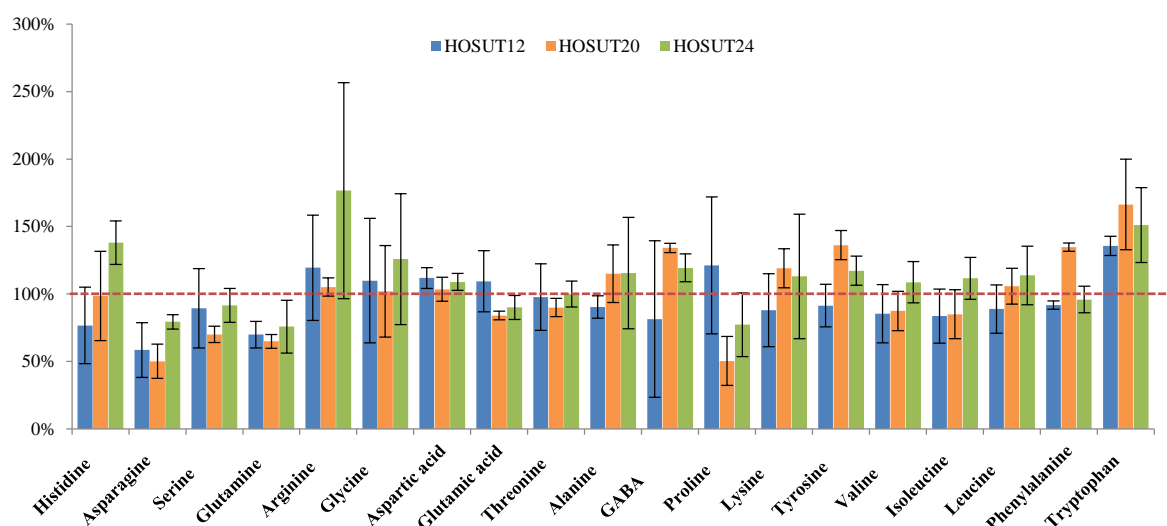


Figure 35. Free amino acids measured in lyophilised roots of HOSUT lines 24, 20 and 12 in comparison to Certo at the 13BBCH grown *in vitro* with N-deprived medium (XS medium). Certo =100% marked by a red dotted line. Vertical bars:  $\pm$ SD.

Table 17. Free amino acids in lyophilised shoots of HOSUT24 and Certo at the 13BBCH grown *in vitro* with N-supplied medium, *in vitro* with N-free medium and under field-like conditions (values: nmol/DWmg  $\pm$  SD, percentages are calculated with Certo as 100% T-test . P<0.05 (\*), P<0.01(\*\*), P<0.001(\*\*\*)).

Amino acid	N-free (abs)	% of Certo	N supplied (abs)	% of Certo	Field-like (abs)	% of Certo
Alanine	2.78 $\pm$ 0.28	117.7*	12.03 $\pm$ 1.26	103.5	14.41 $\pm$ 2.92	120.9
Arginine	0.70 $\pm$ 0.15	119.1	1.64 $\pm$ 0.47	93.2	1.76 $\pm$ 0.13	97.4
Asparagine	0.25 $\pm$ 0.06	100.0	12.35 $\pm$ 4.46	68.1*	5.42 $\pm$ 1.53	16.5***
Aspartic Acid	1.96 $\pm$ 0.21	103.0	13.32 $\pm$ 0.79	96.4	15.09 $\pm$ 2.23	105.0
GABA	2.97 $\pm$ 0.22	93.2	9.55 $\pm$ 2.55	89.7	19.08 $\pm$ 1.15	114.0*
Glutamic Acid	2.49 $\pm$ 0.82	118.8	18.02 $\pm$ 4.46	100.1	10.81 $\pm$ 1.25	96.7
Glutamine	0.54 $\pm$ 0.06	85.7	3.36 $\pm$ 0.50	74.7**	10.16 $\pm$ 2.57	65.5**
Glycine	0.67 $\pm$ 0.14	114.1	4.97 $\pm$ 0.86	224.4**	3.12 $\pm$ 0.40	112.9
Histidine	0.15 $\pm$ 0.02	136.9*	0.56 $\pm$ 0.22	135.4	0.65 $\pm$ 0.09	64.8**
Isoleucine	0.49 $\pm$ 0.08	112.6	1.35 $\pm$ 0.40	102.3	1.55 $\pm$ 0.15	111.1
Leucine	1.07 $\pm$ 0.22	111.7	1.95 $\pm$ 0.62	90.7	3.20 $\pm$ 0.29	122.4
Lysine	1.07 $\pm$ 0.18	117.2	1.29 $\pm$ 0.36	94.8	1.60 $\pm$ 0.19	123.5
Methionine	0 $\pm$ 0	0.0	0 $\pm$ 0	0.0	1.75 $\pm$ 0.43	120.5
Phenylalanine	0.61 $\pm$ 0.07	112.2	1.21 $\pm$ 0.35	97.8	1.74 $\pm$ 0.13	117.2*
Proline	0.46 $\pm$ 0.11	112.8	1.52 $\pm$ 0.35	88.8	9.08 $\pm$ 1.38	73.6**
Serine	2.00 $\pm$ 0.14	114.5**	12.52 $\pm$ 0.84	140.2***	11.24 $\pm$ 2.49	124.5
Threonine	0.76 $\pm$ 0.10	112.5	4.51 $\pm$ 0.51	114.2	3.50 $\pm$ 0.29	81.4
Tryptophan	0.47 $\pm$ 0.03	147.4***	0.35 $\pm$ 0.12	113.7	0.59 $\pm$ 0.07	170.8***
Tyrosine	0.62 $\pm$ 0.07	128.5**	1.21 $\pm$ 0.23	99.5	1.39 $\pm$ 0.21	117.9
Valine	0.95 $\pm$ 0.13	111.1	2.85 $\pm$ 0.65	103.5	3.76 $\pm$ 0.75	101.6

Table 18. Free amino acids in lyophilised root system of HOSUT24 and Certo at the 13BBCH grown *in vitro* with N-supplied medium, *in vitro* with N-free medium and under field-like conditions (values: nmol/DWmg  $\pm$  SD, percentages are calculated with Certo as 100% T-test . P<0.05 (\*), P<0.01(\*\*), P<0.001(\*\*\*)).

Amino acid	N-deprived (abs)	% of Certo	N supplied (abs)	% of Certo	Field-like (abs)	% of Certo
Alanine	0.51 $\pm$ 0.02	110.0	2.77 $\pm$ 0.31	90.2	3.12 $\pm$ 1.56	122.0
Arginine	0.27 $\pm$ 0.06	133.4	1.02 $\pm$ 0.13	138.5 *	0.47 $\pm$ 0.10	78.7
Asparagine	0.44 $\pm$ 0.13	78.6	22.41 $\pm$ 2.22	81.8 **	5.28 $\pm$ 2.02	38.4*
Aspartic Acid	1.07 $\pm$ 0.09	107.6	7.70 $\pm$ 0.67	87.3 *	10.62 $\pm$ 1.24	98.0
GABA	1.33 $\pm$ 0.10	112.1	2.30 $\pm$ 0.15	96.5	6.42 $\pm$ 0.80	100.6
Glutamic Acid	1.39 $\pm$ 0.17	100.2	6.42 $\pm$ 0.91	70.3 **	12.40 $\pm$ 2.53	96.8
Glutamine	0.82 $\pm$ 0.09	87.7	7.96 $\pm$ 0.67	80.0 **	20.03 $\pm$ 7.13	78.8
Glycine	0.33 $\pm$ 0.08	106.4	1.30 $\pm$ 0.21	58.1 ***	1.56 $\pm$ 0.31	95.8
Histidine	0.30 $\pm$ 0.09	186.6 *	0.48 $\pm$ 0.06	104.3	0.48 $\pm$ 0.07	95.2
Isoleucine	0.33 $\pm$ 0.03	108.3	1.18 $\pm$ 0.11	147.2 **	0.38 $\pm$ 0.12	87.3
Leucine	0.37 $\pm$ 0.03	112.6	0.94 $\pm$ 0.15	131.5 *	0.67 $\pm$ 0.14	95.4
Lysine	0.19 $\pm$ 0.03	130.6 **	0.49 $\pm$ 0.08	112.5	0.39 $\pm$ 0.10	105.9
Methionine	0.12 $\pm$ 0.03	154.1 *	0.43 $\pm$ 0.04	158.3 ***	0.67 $\pm$ 0.44	145.1
Phenylalanine	0.16 $\pm$ 0.02	112.6	0.40 $\pm$ 0.04	114.8	0.59 $\pm$ 0.09	120.0*
Proline	0.41 $\pm$ 0.09	97.2	0.42 $\pm$ 0.05	119.4 *	0.85 $\pm$ 0.22	138.1*
Serine	1.15 $\pm$ 0.11	112.1	3.01 $\pm$ 0.35	118.3 *	4.18 $\pm$ 3.61	151.6
Threonine	0.49 $\pm$ 0.05	121.8 **	1.96 $\pm$ 0.08	119.0 ***	1.17 $\pm$ 0.16	100.7
Tryptophan	0.24 $\pm$ 0.05	175.9 ***	0.16 $\pm$ 0.03	149.2 *	0.35 $\pm$ 0.10	95.8
Tyrosine	0.14 $\pm$ 0.02	119.2	0.43 $\pm$ 0.04	90.5	0.49 $\pm$ 0.20	127.8
Valine	0.48 $\pm$ 0.02	111.8 *	2.00 $\pm$ 0.18	126.6 **	1.37 $\pm$ 0.16	116.0*

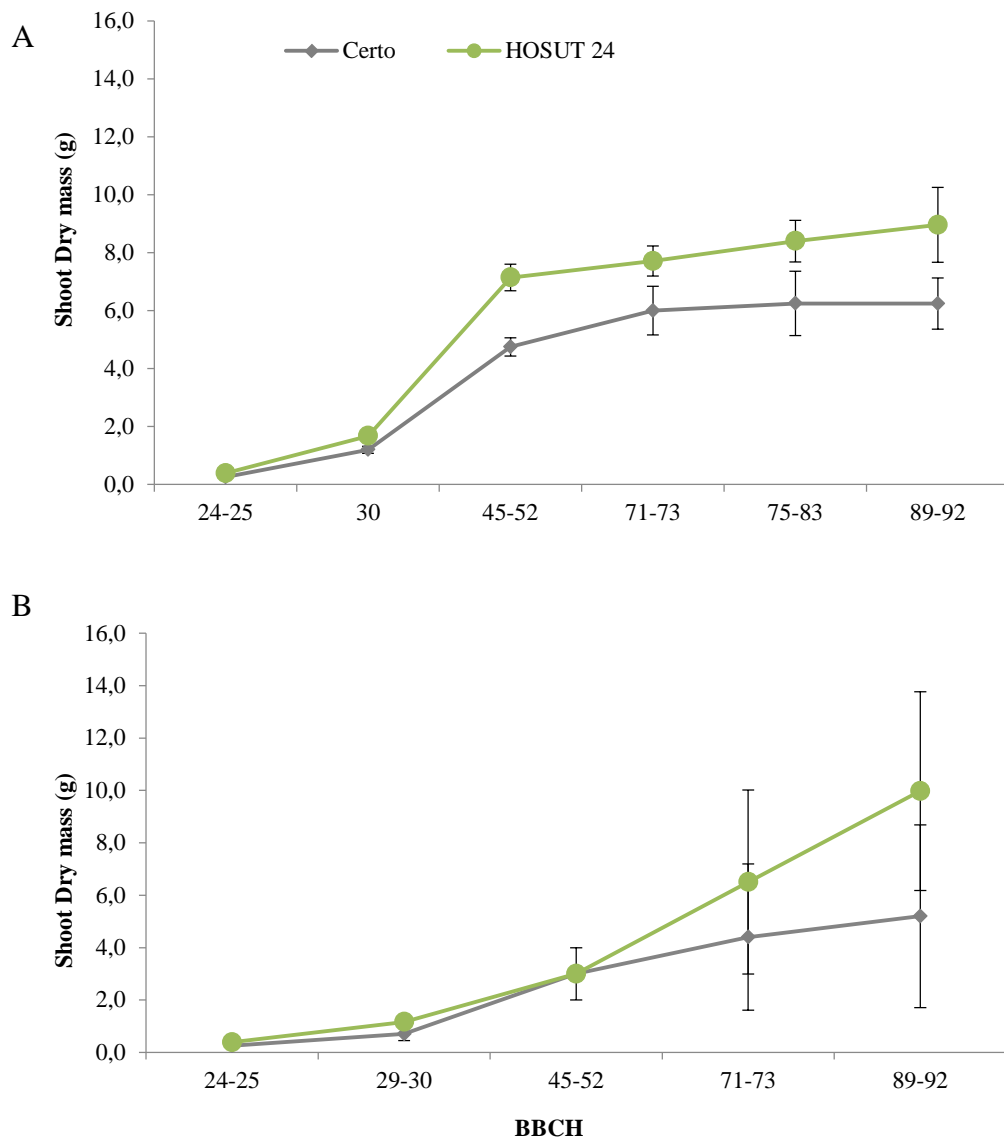


Figure 36. Biomass of above ground tissue of HOSUT24 and Certo plants during the growth cycle in the growing season 2012-2013. A. Complete fertilization. B. Diminished fertilization. Vertical bars:  $\pm$ SD.

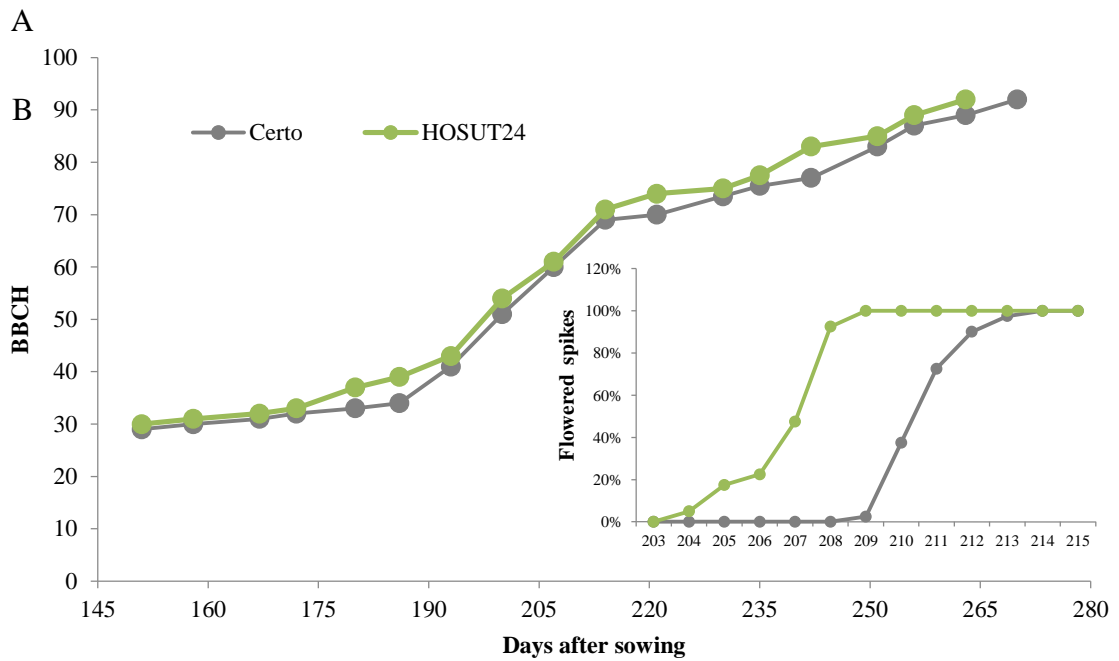
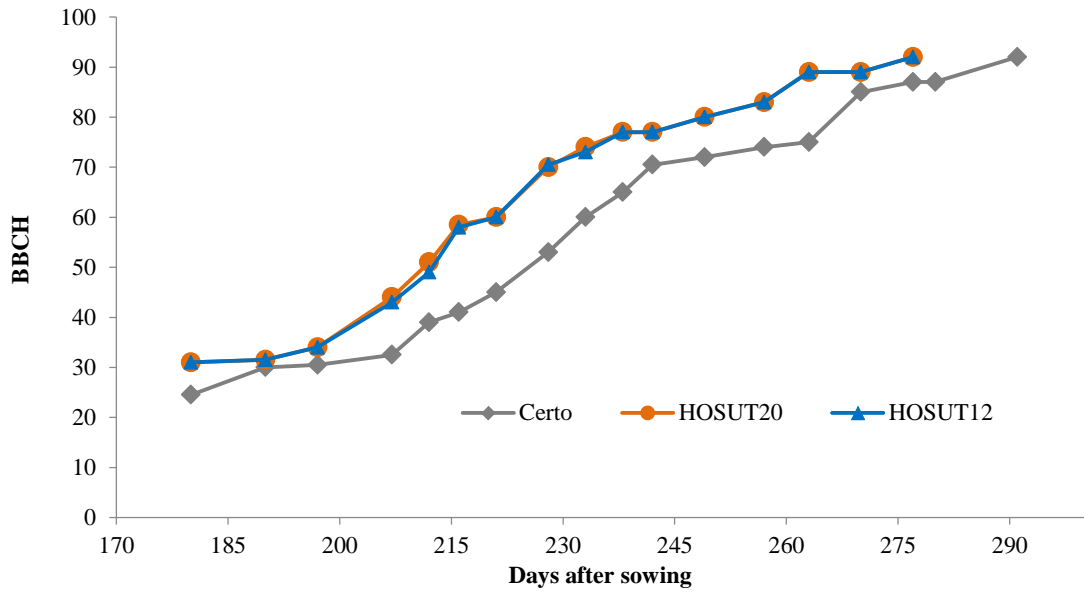


Figure 37. Phenological scale of HOSUT lines grown under field-like conditions with complete fertilization in comparison to their wild type Certo. A. HOSUT20 and 12, growing season 2012/2013. B. HOSUT24, growing season 2013/2014. Phenological phases given in the BBCH scale.

Table 19. Partial list of entities with statistical significant differences between HOSUT24 and Certo in root transcriptome analysis at 11, 12 and 13BBCH stage of development. (T-test P-value < 0.05, Multiple testing correction: Westfall and Young). Values correspond to the Log<sub>2</sub> of the gene-expression fold change between both lines. 460 entities with the highest values are presented. Coloured cells indicate statistical differences between the lines. Light blue significant differences at 11BBCH, medium blue at 12BBCH and dark blue at 13BBCH.

	ID-Code	Log <sub>2</sub> Fold Change HOSUT24:Certo			Description	Protein responsible for description	Best Blast Hit Wheat	InterPRO-IDs
		11BBCH	12BBCH	13BBCH				
N-metabolism								
	Wht_23770	0.30	-0.11	-2.92	Glutamate dehydrogenase 2	AT5G07440.1	Traes_2BL_A0FFC447F.1	IPR006097 (Glutamate/phenylalanine/leucine/valine dehydrogenase, dimerisation domain)
Amino acid metabolism								
	Wht_09772	1.29	-1.02	-4.16	L-alanine DH	UniRef100_Q1AW21		
	Wht_54235	1.27	-0.75	-3.39	Alpha-aminoadipic semialdehyde synthase / LYSINE-KETOGLUTARATE REDUCTASE	sp Q9SMZ4 AASS_ARATH	Traes_6AL_6D310D2B0.1	IPR005097 (Saccharopine dehydrogenase / Homospermidine synthase), IPR007545 (LOR/SDH bifunctional enzyme, conserved domain), IPR007698 (Alanine dehydrogenase/PNT, NAD(H)-binding domain), IPR007886 (Alanine dehydrogenase/pyridine nucleotide transhydrogenase, N-terminal)
	Wht_43597	1.00	-1.03	-3.18	serine hydroxymethyltransferase 4	AT4G13930.1	Traes_XX_19EBE5046.1	IPR01085 (Serine hydroxymethyltransferase), IPR015424 (Pyridoxal phosphate-dependent transferase)
	Wht_49616	0.88	1.62	1.12	Tryptophan aminotransferase related 2	AT4G24670.1	Traes_XX_20253E8101.1	IPR015424 (Pyridoxal phosphate-dependent transferase)
	Wht_45208	0.60	-0.74	-1.83	THREONINE DEHYDRATASE	UniRef100_Q7MAN2		
	Wht_19893	0.17	-0.88	-2.78	N-acetyl-gamma-glutamyl-phosphate reductase	sp Q2RRM4 ARGC_RHORT	Traes_4BS_A8F01CCC5.1	IPR000706 (N-acetyl-gamma-glutamyl-phosphate reductase, type 1), IPR012280 (Semialdehyde dehydrogenase, dimerisation domain), IPR016040 (NAD(P)-binding domain)
	Wht_11344	-0.27	-0.74	-3.28	Asparagine synthase	UniRef100_A6WDH3		
	Wht_23835	-0.69	-0.45	-1.69	cobalt ion binding, snRK1-interacting protein 1	AT1G71310.2	Traes_3B_58086CE35.1	
	Wht_38924	3.88	3.41	0.22	L-asparaginase	UniRef100_Q9FUG8		
	Wht_35217	1.98	0.55	0.05	Indole-3-glycerol phosphate synthase	sp B7K0H0 TRPC_CYAP8	Traes_7AL_38E309909.1	IPR013785 (Aldolase-type TIM barrel)
	Wht_09085	1.87	0.41	2.90	alanine aminotransferase 2	AT1G72330.3	Traes_5DS_3402EB8DF.1	IPR015424 (Pyridoxal phosphate-dependent transferase)
	Wht_44664	0.96	-0.23	-2.51	Ubiquitin carboxyl-terminal hydrolase 2	sp Q8W4N3 UBP2_ARATH	Traes_7BS_BAB63DC3B.1	IPR001394 (Ubiquitin carboxyl-terminal hydrolases family 2)
	Wht_51197	0.47	-0.86	-1.29	alanine aminotransferase 2	AT1G72330.3	Traes_XX_D42BFFEAC.1	IPR015424 (Pyridoxal phosphate-dependent transferase)
	Wht_06926	0.37	0.88	1.62	Chaperone protein dnaJ 72	sp Q0W7I8 DNJ72_ARATH	Traes_3B_8278F5E56.1	IPR001623 (DnaJ domain)
	Wht_08468	0.31	-0.72	-1.86	ketol-acid reductoisomerase	AT3G58610.1	Traes_XX_37E7587A9.1	IPR013023 (Acetohydroxy acid isomeroeductase), IPR016040 (NAD(P)-binding domain)
	Wht_24680	-1.34	-1.13	-1.43	3-phosphoserine phosphatase	AT1G18640.2	Traes_3AL_D5D0BF14D.1	IPR023190 (Phosphoserine phosphatase, domain 2)
	Wht_18507	-0.64	0.46	2.94	delta 1-pyrroline-5-carboxylate synthase 2	AT3G55610.1	Traes_3B_051B41DE3.1	

Cell and development									
	Wht_21163	5.37	5.13	4.42	BIGYIN, FIS1A	AT3G57090	Traes_4DL_1005826D8.2		
	Wht_46745	5.22	4.66	3.36	Cellulose synthase	UniRef100_Q4U0Z3			
	Wht_23877	4.51	4.87	1.93	kinesin 4	AT5G27000.1	Traes_4DL_3F6E62DAB.1	IPR001752 (Kinesin, motor domain), IPR021720 (Maleacin), IPR027325 (Kinesin-like protein KIFC3), IPR027417 (P-loop containing nucleoside triphosphate hydrolase), IPR027640 (Kinesin-like protein)	
	Wht_23688	3.51	3.30	1.19	Cytosine-specific methyltransferase	UniRef90_I1H7R2	Traes_4DS_A800BBB3B.1		
	Wht_41091	1.97	0.37	-0.51	UDP-Glycosyltransferase superfamily protein	AT1G05675.1	Traes_5DS_19AE064C1.1	IPR002213 (UDP-glucuronosyl/UDP-glucosyltransferase)	
	Wht_09948	1.81	1.09	1.34	Glycosyltransferase	UniRef100_Q50HV8			
	Wht_04069	1.72	0.77	-0.90	Cellulose synthase family protein	AT5G05170.1	Traes_2AS_665AF9500.1	IPR005150 (Cellulose synthase), IPR013083 (Zinc finger, RING/FYVE/PHD-type)	
	Wht_36050	1.48	0.20	2.17	Gamma-tubulin complex component 4 homolog	sp Q9M350 GCP4_ARATH	Traes_1DS_989E741CF.1	IPR007259 (Spc97/Spc98)	
	Wht_09096	1.35	-0.06	-2.96	kinesin-like protein 1	AT3G44730.1	Traes_3DL_DF48B3591.1	IPR001715 (Calponin homology domain), IPR001752 (Kinesin, motor domain), IPR027417 (P-loop containing nucleoside triphosphate hydrolase), IPR027640 (Kinesin-like protein)	
	Wht_44340	1.10	2.09	0.96	Nucleotide-diphospho-sugar transferases superfamily protein	AT1G27600.1	Traes_2AS_3D0A18D67.1	IPR005027 (Glycosyl transferase, family 43)	
	Wht_26189	1.10	1.67	-3.90	TRICHOME BIREFRINGENCE-LIKE 4	AT5G49340.1	Traes_6AL_E86F6B535.1	IPR026057 (PC-Esterase)	
	Wht_53204	0.94	0.53	0.52	F-actin-capping protein subunit alpha	sp O82631 CAPZA_ARATH	Traes_XX_CCF9E1938.1	IPR002189 (F-actin-capping protein subunit alpha)	
	Wht_04299	0.84	-0.69	0.06	Coatomer, beta' subunit LENGTH=970	AT1G52360.2	Traes_2DL_A4B16F05D.1	IPR015943 (WD40/YVTN repeat-like-containing domain)	
	Wht_14627	0.78	0.70	2.81	UDP-Glycosyltransferase superfamily protein	AT4G01070.1	Traes_XX_DA603566D.1	IPR002213 (UDP-glucuronosyl/UDP-glucosyltransferase)	
	Wht_17805	0.78	-0.70	-0.43	Cyclin D4;1	UniRef100_Q71FH0			
	Wht_54775	0.75	0.08	-1.93	Kinase interacting (KIP1-like) family protein	AT3G22790.1	Traes_1AL_E60FA09AE.1	IPR011684 (KIP1-like)	
	Wht_05740	0.71	-0.32	-2.55	myosin 1	AT3G19960.2	Traes_1AL_389AEC45B.1	IPR000048 (IQ motif, EF-hand binding site), IPR001609 (Myosin head, motor domain), IPR027401 (Myosin-like IQ motif-containing domain), IPR027417 (P-loop containing nucleoside triphosphate hydrolase)	
	Wht_03364	0.70	0.24	1.88	65-kDa microtubule-associated protein 6	sp Q9SIS3 MA656_ARATH	Traes_4DS_AFFD88C47.1	IPR007145 (Microtubule-associated protein, MAP65/Ase1/PRC1)	
	Wht_11253	0.69	-0.63	-3.65	Cyclin B1;4	AT2G26760.1	Traes_4AS_C381CB1A2.1	IPR013763 (Cyclin-like)	
	Wht_23587	0.65	-0.10	-1.99	Cyclin A2;4	AT1G80370.1	Traes_5AS_E9AC96395.1	IPR014400 (Cyclin A/B/D/E)	
	Wht_42648	0.50	-0.92	-0.96	Polyketide cyclase/dehydrase and lipid transport superfamily protein	AT3G11720.3	Traes_4AL_E35BCBB0D.1	IPR023393 (START-like domain)	
	Wht_39181	0.48	-1.29	-2.52	Sugar phosphate exchanger 2	sp Q8TED4 SPX2_HUMAN	Traes_7DL_F4972CA5C.1	IPR011701 (Major facilitator superfamily), IPR016196 (Major facilitator superfamily domain, general substrate transporter)	
	Wht_23794	0.44	0.99	-0.22	cellulose-synthase like D2	AT5G16910.1	Traes_XX_37E78F29C.1	IPR005150 (Cellulose synthase), IPR013083 (Zinc finger, RING/FYVE/PHD-type)	
	Wht_34905	0.33	-0.15	-2.73	retinoblastoma-related 1	AT3G12280.1	Traes_7BS_2CAF57700.1	IPR013763 (Cyclin-like), IPR024599 (Domain of unknown function DUF3452, retinoblastoma-associated)	
	Wht_43617	0.08	-0.07	-2.58	Neurobeachin-like protein 2	sp E7FAW3 NBEL2_DANRE	Traes_2BL_75EC2BDA9.1	IPR000409 (BEACH domain), IPR015943 (WD40/YVTN repeat-like-containing domain), IPR023362 (PH-BEACH domain)	



	Wht_02725	-0.09	-0.25	-2.54	kinesin 3	AT5G54670.1	Traes_1AS_62729A31C.1	IPR001752 (Kinesin, motor domain), IPR027417 (P-loop containing nucleoside triphosphate hydrolase), IPR027640 (Kinesin-like protein)
	Wht_19117	-0.14	-0.64	-4.01	Magnesium transporter MRS2-E	sp A2WXD3 MRS2E_ORYSI	Traes_3AL_04CD57FC2.1	IPR026573 (Magnesium transporter MRS2/LPE10)
	Wht_42355	-0.14	1.63	-2.87	kinesin 4	AT5G27000.1	Traes_1AL_EDCDB415C.1	IPR001752 (Kinesin, motor domain), IPR027417 (P-loop containing nucleoside triphosphate hydrolase), IPR027640 (Kinesin-like protein)
	Wht_37679	-0.43	-0.31	-1.97	kinesin-like protein 1	AT3G44730.1	Traes_7BL_463C0F2F8.1	IPR001752 (Kinesin, motor domain), IPR027417 (P-loop containing nucleoside triphosphate hydrolase), IPR027640 (Kinesin-like protein)
	Wht_32261	-0.67	1.08	1.76	Expansin 11	AT1G20190.1	Traes_4AS_A65DDCD05.1	IPR007118 (Expansin/Lol pl), IPR014733 (Barwin-like endoglucanase)
	Wht_24346	-1.01	-1.47	-3.47	Ankyrin repeat family protein	AT3G04710.1	Traes_5BL_DB68F86DB.1	IPR011990 (Tetratricopeptide-like helical), IPR020683 (Ankyrin repeat-containing domain)
	Wht_54685	-1.03	-0.44	-1.49	phragmoplast-associated kinesin-related protein, putative	AT3G23670.1	Traes_2AS_25568852C.1	IPR024658 (Kinesin-like, KLP2)
	Wht_32017	-1.18	0.59	-2.11	kinesin 4	AT5G27000.1	Traes_4AS_34DFBA49B.1	IPR001715 (Calponin homology domain), IPR001752 (Kinesin, motor domain), IPR027417 (P-loop containing nucleoside triphosphate hydrolase), IPR027640 (Kinesin-like protein)
	Wht_24397	-1.26	-0.49	-1.84	Ankyrin repeat family protein	AT3G04710.1	Traes_4DS_AC76653B6.1	IPR011990 (Tetratricopeptide-like helical), IPR020683 (Ankyrin repeat-containing domain)
	Wht_22258	-1.47	0.06	-2.39	Cyclin-P3-1	sp Q75HV0 CCP31_ORYSJ	Traes_1BL_49BF78501.1	IPR013763 (Cyclin-like), IPR013922 (Cyclin PHO80-like)
	Wht_23091	-1.50	-2.16	-3.02	Ankyrin repeat family protein	AT3G04710.1	Traes_4BS_16141A85E.1	IPR011990 (Tetratricopeptide-like helical), IPR020683 (Ankyrin repeat-containing domain)
	Wht_08020	-1.59	0.62	-5.18	regulatory protein (NPR1)	AT1G64280.1	Traes_3B_2380CD0DB.1	IPR011333 (BTB/POZ fold), IPR020683 (Ankyrin repeat-containing domain), IPR021094 (NPR1/NIM1-like, C-terminal), IPR024228 (Domain of unknown function DUF3420)
	Wht_08802	-2.22	-2.28	-1.84	Ankyrin repeat family protein	AT3G04710.1	Traes_5DS_6865B96FE.1	IPR011990 (Tetratricopeptide-like helical), IPR020683 (Ankyrin repeat-containing domain)
	Wht_06778	-2.62	-2.38	-2.89	Ankyrin repeat family protein	AT3G04710.1	Traes_5BL_4D20885CA.1	IPR011990 (Tetratricopeptide-like helical), IPR020683 (Ankyrin repeat-containing domain)
	Wht_23247	-2.90	-4.09	-5.07	Ankyrin repeat family protein	AT3G04710.1	Traes_4BS_ED5BCA38E.1	IPR011990 (Tetratricopeptide-like helical), IPR020683 (Ankyrin repeat-containing domain)
	Wht_17877	-3.00	-4.54	-4.94	Ankyrin repeat family protein	AT3G04710.1	Traes_2BL_0BE79ED40.1	IPR011990 (Tetratricopeptide-like helical), IPR020683 (Ankyrin repeat-containing domain)
	Wht_01120	-3.14	-0.91	-2.41	CYCLIN A3;4	AT1G47230.2	Traes_5DS_051F7E162.1	IPR014400 (Cyclin A/B/D/E)
	Wht_05335	-3.20	-3.76	-4.14	Ankyrin repeat family protein	AT3G04710.1	Traes_2DL_A29A5DFAA.1	IPR011990 (Tetratricopeptide-like helical), IPR020683 (Ankyrin repeat-containing domain)
	Wht_24356	-4.25	-0.73	-1.62	Ankyrin repeat family protein	AT3G04710.1	Traes_5DS_3D0E0BC00.1	IPR011990 (Tetratricopeptide-like helical), IPR020683 (Ankyrin repeat-containing domain)
	Wht_54255	-5.48	-6.62	-6.65	Ankyrin repeat family protein	AT3G04710.1	Traes_4AL_DF47C07FD.1	IPR020683 (Ankyrin repeat-containing domain)
	Wht_17727	1.94	-0.69	-4.22	microtubule-associated protein MAP65-1a	UniRef100_Q0J1C5		
	Wht_36050	1.48	0.20	2.17	Gamma-tubulin complex component 4 homolog	sp Q9M350 GCP4_ARATH	Traes_1DS_989E741CF.1	IPR007259 (Sp97/Sp98)
	Wht_04594	1.35	-1.58	-3.06	Kinesin heavy chain	UniRef100_Q93XF8		
	Wht_03364	0.70	0.24	1.88	65-kDa microtubule-associated protein 6	sp Q9SIS3 MA656_ARATH	Traes_4DS_AFFD88C47.1	IPR007145 (Microtubule-associated protein, MAP65/Asel/PRC1)
	Wht_56744	-0.37	0.80	-0.05	65-kDa microtubule-associated protein 3	sp Q9FHM4 MA653_ARATH	Traes_1BL_099B595EA.1	IPR007145 (Microtubule-associated protein, MAP65/Asel/PRC1)
	Wht_51938	2.58	0.56	-0.68	Tetraspanin family protein	AT5G46700.1	Traes_1BS_56CFEF3EA.1	IPR018499 (Tetraspanin/Peripherin)
	Wht_19970	-0.35	0.68	2.08	Embryogenesis transmembrane protein-like	UniRef90_Q5ZA60	Traes_XX_E2BC7859C.1	IPR026961 (PGG domain)

	Wht_34182	-0.36	-0.27	3.43	kinesin-like protein 1	AT3G44730.1	Traes_7BL_6590999C5.1	IPR001752 (Kinesin, motor domain), IPR027417 (P-loop containing nucleoside triphosphate hydrolase), IPR027640 (Kinesin-like protein)
	Wht_02184	-0.78	-0.22	3.41	pectinesterase family protein	AT3G14300.1	Traes_6AL_3EC6089A6.1	IPR011050 (Pectin lyase fold/virulence factor)
	Wht_00556	-1.33	0.33	2.84	Late embryogenesis abundant protein (LEA) family protein	AT4G21020.1	Traes_2DL_7E2FF7CF9.1	IPR004238 (Late embryogenesis abundant protein, LEA-3)
	Wht_10687	-1.33	0.05	3.30	Pectin lyase-like superfamily protein	AT3G07970.1	Traes_4DL_3E831AE39.1	IPR000743 (Glycoside hydrolase, family 28), IPR011050 (Pectin lyase fold/virulence factor)
	Wht_24102	-1.68	0.11	4.88	Potassium channel SKOR	sp Q9M8S6 SKOR_ARATH	Traes_7AS_48AE6B03F.1	IPR003938 (Potassium channel, voltage-dependent, EAG/ELK/ERG), IPR020683 (Ankyrin repeat-containing domain)
CHO metabolism								
	Wht_26740	1.98	-1.13	-0.44	pyruvate decarboxylase-2	AT5G54960.1	Traes_XX_6DDA59584.1	IPR011766 (Thiamine pyrophosphate enzyme, C-terminal TPP-binding), IPR012110 (Thiamine pyrophosphate (TPP)-dependent enzyme)
	Wht_36382	1.84	1.07	-2.30	Beta-fructofuranosidase, insoluble isoenzyme 2/ Cell wall invertase	sp Q01IS7 INV2_ORYSI/L0N6X6_WHEAT	Traes_2BL_3EDC425A7.1	IPR001362 (Glycoside hydrolase, family 32), IPR008985 (Concanavalin A-like lectin/glucanases superfamily), IPR023296 (Glycosyl hydrolase, five-bladed beta-propeller domain)
	Wht_16647	1.78	0.28	0.20	Aldose reductase	sp P23901 ALDR_HORVU	Traes_1BL_7BB61786E.1	IPR001395 (Aldo/keto reductase), IPR023210 (NADP-dependent oxidoreductase domain)
	Wht_24833	1.64	-0.63	-0.39	Aldose 1-epimerase family protein	AT3G47800		
	Wht_52894	1.04	-0.24	-2.71	Aldose reductase	sp P23901 ALDR_HORVU	Traes_1DL_B77C961EA.1	IPR001395 (Aldo/keto reductase), IPR023210 (NADP-dependent oxidoreductase domain)
	Wht_07108	1.01	0.16	-1.84	hexokinase 1	AT4G29130.1	Traes_3B_9F7731354.1	IPR001312 (Hexokinase)
	Wht_26394	0.71	-0.26	-1.48	Callose synthase 5	AT2G13680.1	Traes_4DL_FD4E98087.1	IPR003440 (Glycosyl transferase, family 48)
	Wht_26362	0.21	-0.95	-1.79	Pyruvate kinase family protein	AT5G56350.1	Traes_4DL_7AAB94AC2.1	IPR001697 (Pyruvate kinase)
	Wht_40811	-0.06	-0.82	-1.78	WD repeat-containing protein 89 homolog	sp Q54QU5 WDR89_DICDI	Traes_7DS_325AA8A34.1	IPR015943 (WD40/YVTN repeat-like-containing domain)
	Wht_53947	-0.08	0.06	-2.34	aldose 1-epimerase family protein	AT5G14500.1	Traes_2DL_94F3DAAE6.1	IPR008183 (Aldose 1-/Glucose-6-phosphate 1-epimerase), IPR011013 (Galactose mutarotase-like domain)
	Wht_56204	-0.29	-0.53	-3.35	Callose synthase 1	AT1G05570.1	Traes_3B_F154A6139.1	IPR003440 (Glycosyl transferase, family 48), IPR026953 (Callose synthase)
	Wht_03752	-0.47	0.68	-2.22	Glycogen phosphorylase 1	sp Q00766 PHS1_DICDI	Traes_5BL_CA33BB947.1	IPR000811 (Glycosyl transferase, family 35)
	Wht_08223	-1.92	1.01	0.41	trehalose phosphate synthase	AT1G60140.1	Traes_5BL_94F42F9A7.1	IPR001830 (Glycosyl transferase, family 20), IPR006379 (HAD-superfamily hydrolase, subfamily IIB), IPR023214 (HAD-like domain)
	Wht_34322	3.08	-0.75	-2.67	Protein kinase superfamily protein	AT4G32660.1	Traes_3B_DA7A8F4A2.1	IPR011009 (Protein kinase-like domain)
	Wht_54683	2.22	1.36	0.58	Fumarate hydratase class II	sp Q8KTE1 FUMC_METEA	Traes_4BL_C3267759F.1	IPR000362 (Fumarate lyase), IPR008948 (L-Aspartase-like), IPR024083 (Fumarase/histidase, N-terminal)
DNA synthesis								
	Wht_52105	2.50	0.50	-2.45	Regulator of telomere elongation helicase 1 homolog	sp Q16X92 RTEL1_AEDAE	Traes_5DL_3C9AAAE2D.1	IPR006555 (ATP-dependent helicase, C-terminal), IPR014013 (Helicase, superfamily 1/2, ATP-binding domain, DinG/Rad3-type), IPR027417 (P-loop containing nucleoside triphosphate hydrolase)
	Wht_42816	2.30	0.43	0.37	Mitochondrial substrate carrier family protein	AT1G74240.1	Traes_1AL_D5918162C.1	IPR018108 (Mitochondrial substrate/solute carrier), IPR023395 (Mitochondrial carrier domain)
	Wht_44365	2.18	0.25	-3.02	HAT family dimerization domain containing	UniRef90_Q8LNK9	Traes_5AL_57A6A5DEC.1	IPR008906 (HAT dimerisation domain, C-terminal), IPR012337 (Ribonuclease H-like domain), IPR025525 (Domain of unknown function DUF4413)
	Wht_06151	2.04	1.24	-0.25	DNA topoisomerase 2	sp Q24308 TOP2_PEA	Traes_1AL_E6A6C4E8F.1	IPR001241 (DNA topoisomerase, type IIA)

	Wht_20596	-1.39	-0.22	3.10	Tyrosine-sulfated glycopeptide receptor 1	UniRef90_M8AF42	Traes_7DL_F2EF2631B.1	
Hormones								
	Wht_43720	1.88	0.90	1.01	Cytokinin dehydrogenase 4	sp Q5JLP4 CKX4_ORYSJ	Traes_3B_B0CB736A0.1	IPR016164 (FAD-linked oxidase-like, C-terminal), IPR016166 (FAD-binding, type 2), IPR016170 (Vanillyl-alcohol oxidase/Cytokinin dehydrogenase C-terminal domain)
	Wht_36112	1.58	0.80	-2.10	Exosome complex exonuclease dis3	sp P37202 DIS3_SCHPO	Traes_5AL_CC6EE2ECC.1	IPR001900 (Ribonuclease II/R), IPR002716 (PIN domain), IPR012340 (Nucleic acid-binding, OB-fold), IPR022966 (Ribonuclease II/R, conserved site)
	Wht_00353	1.54	0.20	1.12	Lipoxygenase	UniRef90_UPI00032AB54D	Traes_5BL_245A319AD.1	
	Wht_11606	1.52	0.02	0.91	SAUR-like auxin-responsive protein family	AT1G56150.1	Traes_7DL_4ABF3A54D.1	IPR003676 (Auxin-induced protein, ARG7)
	Wht_22152	1.24	0.17	-0.10	Jasmonate-zim-domain protein 1	AT1G19180.1	Traes_4DL_7564D43A9.1	IPR010399 (Tify), IPR018467 (CO/COL/TOC1, conserved site)
	Wht_40499	1.05	-0.56	-3.93	auxin transport protein (BIG)	AT3G02260.1	Traes_5BL_C9FD62D61.1	IPR003126 (Zinc finger, N-recogin), IPR017986 (WD40-repeat-containing domain)
	Wht_40499	1.05	-0.56	-3.93	auxin transport protein (BIG)	AT3G02260.1	Traes_5BL_C9FD62D61.1	IPR003126 (Zinc finger, N-recogin), IPR017986 (WD40-repeat-containing domain)
	Wht_11571	0.99	-1.93	-2.62	auxin response factor 1	AT1G59750.1	Traes_7DS_204F82E02.1	
	Wht_05379	0.70	1.20	-1.92	O-fucosyltransferase family protein	AT1G51630.1	Traes_XX_334131283.1	IPR019378 (GDP-fucose protein O-fucosyltransferase)
	Wht_27856	0.69	-0.08	-1.93	Auxin-responsive protein IAA4	sp A2WNM0 IAA4_ORYSI	Traes_1DS_CA4185D11.1	IPR003311 (AUX/IAA protein)
	Wht_14535	0.39	-0.85	-1.91	SAUR-like auxin-responsive protein family	AT1G29430.1	Traes_5DL_B98E6F9A5.1	IPR003676 (Auxin-induced protein, ARG7)
	Wht_15421	0.33	0.61	-1.93	IAA-amino acid hydrolase ILR1-like 9	sp Q8H3C7 ILL9_ORYSJ	Traes_5AL_C057EFB98.1	IPR002933 (Peptidase M20)
	Wht_37270	0.02	-0.08	-3.04	O-fucosyltransferase family protein	AT1G20550.1	Traes_5AL_A94EEDB30.1	IPR019378 (GDP-fucose protein O-fucosyltransferase)
	Wht_43719	-0.52	0.25	3.57	Cytokinin dehydrogenase 2	sp Q4ADV8 CKX2_ORYSJ	Traes_XX_4AEA0946E.1	IPR016164 (FAD-linked oxidase-like, C-terminal), IPR016166 (FAD-binding, type 2), IPR016170 (Vanillyl-alcohol oxidase/Cytokinin dehydrogenase C-terminal domain)
	Wht_36771	-0.81	-0.03	3.64	Auxin-responsive protein IAA27	sp P0C129 IAA27_ORYSJ	Traes_4DS_03ABB2A80.1	IPR003311 (AUX/IAA protein)
	Wht_30408	-1.04	-0.58	-0.28	Protein of unknown function (DUF604)	AT5G41460.1	Traes_XX_7F53DF39C.1	IPR006740 (Protein of unknown function DUF604)
	Wht_31031	-1.06	1.48	-2.70	tRNA dimethylallyltransferase 2	sp Q9ZUX7 IPT2_ARATH	Traes_2AL_53F78F455.1	IPR002627 (tRNA isopentenyltransferase), IPR022755 (Zinc finger, double-stranded RNA binding)
	Wht_37609	-1.22	0.96	1.02	2-oxoglutarate (2OG) and Fe(II)-dependent oxygenase superfamily protein	AT1G52820.1	Traes_4DL_FFF7A4E01.1	IPR005123 (Oxoglutarate/iron-dependent dioxygenase), IPR027443 (Isopenicillin N synthase-like)
	Wht_04165	-1.23	-0.88	-0.03	2-oxoglutarate (2OG) and Fe(II)-dependent oxygenase superfamily protein	AT5G20400.1	Traes_5BL_EB04B5379.1	IPR002283 (Isopenicillin N synthase), IPR026992 (Non-haem dioxygenase N-terminal domain), IPR027443 (Isopenicillin N synthase-like)
	Wht_15639	2.31	1.24	0.03	Terpenoid cyclases/Protein prenyltransferases superfamily protein	AT1G79460.1	Traes_2DL_A9384D6C8.1	IPR008949 (Terpenoid synthase)
	Wht_44920	2.10	-0.66	0.10	GEM-like protein 6	sp Q9FMW6 GEML6_ARATH // AT5G23350	Traes_1DL_23B562CE2.1	IPR004182 (GRAM domain)
	Wht_12729	-1.82	-0.29	3.21	12-oxophytodienoate reductase 2	AT1G76690.1	Traes_7DS_D7F6AF9811.1	IPR013785 (Aldolase-type TIM barrel)
Lipid metabolism								
	Wht_45099	0.10	-0.79	3.89	sulfotransferase 2A	AT5G07010.1	Traes_6AS_80A7B44EA.1	IPR000863 (Sulfotransferase domain), IPR027417 (P-loop containing nucleoside triphosphate hydrolase)

Metal handling								
	Wht_27160	0.14	-1.32	3.57	Heavy metal transport/detoxification superfamily protein	AT5G27690.1	Traes_7DL_2F413CF0E.1	IPR006121 (Heavy metal-associated domain, HMA)
	Wht_32841	-1.12	-0.66	3.24	Heavy metal transport/detoxification superfamily protein	AT1G22990.1	Traes_4DS_C46F11B44.1	IPR006121 (Heavy metal-associated domain, HMA)
Miscellaneous								
	Wht_34062	7.48	7.00	2.83	GDSL esterase/lipase	sp Q9FJ45 GDL83_ARATH	Traes_2AS_1959B026B.1	IPR001087 (Lipase, GDSL)
	Wht_27883	3.06	0.62	-1.34	Cytochrome P450 superfamily protein	AT5G07990.1	Traes_4BL_42305EC28.1	IPR001128 (Cytochrome P450)
	Wht_53151	2.58	0.29	1.42	2-oxoglutarate (2OG) and Fe(II)-dependent oxygenase superfamily protein	AT4G16770.1	Traes_XX_1B16119D5.1	IPR002283 (Isopenicillin N synthase), IPR026992 (Non-haem dioxygenase N-terminal domain), IPR027443 (Isopenicillin N synthase-like)
	Wht_34449	2.20	0.34	0.01	Bifunctional inhibitor/lipid-transfer protein/seed storage 2S albumin superfamily protein	AT2G48140.1	Traes_2BL_5F0630367.1	IPR016140 (Bifunctional inhibitor/plant lipid transfer protein/seed storage helical domain)
	Wht_28775	2.17	2.74	0.30	Cytochrome P450 superfamily protein	AT5G07990.1	Traes_XX_B9FA2E4EE.1	IPR001128 (Cytochrome P450)
	Wht_40090	2.15	-0.99	0.78	Glutathione S-transferase family protein	AT1G10370.1	Traes_3B_2E0C9F193.1	IPR010987 (Glutathione S-transferase, C-terminal-like), IPR012336 (Thioredoxin-like fold)
	Wht_11006	-0.39	1.09	2.77	GDSL esterase/lipase	sp Q94F40 GDL9_ARATH	Traes_XX_C86B726A8.1	IPR001087 (Lipase, GDSL)
	Wht_32361	-0.44	-0.52	4.02	C-glucosyltransferase	UniRef90_C3W7B0	Traes_1BL_615BF0555.1	
	Wht_14098	-0.81	-0.31	4.06	Glucan endo-1,3-beta-glucosidase 13	sp Q9FU9 E1313_ARATH	Traes_XX_5D7AD6097.1	IPR000490 (Glycoside hydrolase, family 17), IPR012946 (X8), IPR017853 (Glycoside hydrolase, superfamily)
	Wht_32023	-0.95	-0.77	3.97	Peroxidase superfamily protein	AT3G21770.1	Traes_1BL_488EB8124.1	IPR010255 (Haem peroxidase)
Mitochondrial electron transport								
	Wht_37738	2.04	2.01	-3.26	Double-strand-break repair protein rad21 homolog	sp O93310 RAD21_XENLA	Traes_3B_5E153DF63.1	IPR006910 (Rad21/Rec8-like protein, N-terminal), IPR023093 (Rad21/Rec8-like protein, C-terminal)
Not classified								
	Wht_21107	4.10	4.03	4.64	30S ribosomal protein S10	sp P28079 RS10_THEAC	Traes_7DS_304EAFD6B.1	IPR001848 (Ribosomal protein S10), IPR027486 (Ribosomal protein S10 domain)
	Wht_19352	3.74	3.42	3.54	Disease resistance protein (CC-NBS-LRR class) family	AT1G53350.1	Traes_7BL_96F7FCE87.1	IPR000767 (Disease resistance protein), IPR027417 (P-loop containing nucleoside triphosphate hydrolase)
	Wht_22354	3.65	1.14	0.46	Expressed protein	UniRef90_Q10DP3	Traes_2DS_182B8C5C4.1	IPR011676 (Domain of unknown function DUF1618)
	Wht_43889	3.58	4.18	3.46	Kinesin heavy chain isolog	UniRef90_B6TA17	Traes_XX_7ED372AF9.1	IPR006839 (Ribosome-associated, YjgA), IPR023153 (PSP04464-like domain)
	Wht_36889	3.46	-0.12	-3.25	Pentatricopeptide repeat-containing protein	sp Q9LFL5 PP390_ARATH // AT5G16860	Traes_3AS_A7027CC25.1	IPR002885 (Pentatricopeptide repeat), IPR011990 (Tetratricopeptide-like helical)
	Wht_40825	3.16	2.75	0.49	beta glucosidase 43	AT3G18070.1	Traes_3B_94CC5F2C2.1	IPR001360 (Glycoside hydrolase, family 1), IPR017853 (Glycoside hydrolase, superfamily)
	Wht_10620	3.04	1.33	0.34	zinc-finger protein 2	AT3G19580.1	Traes_5DL_4B4927090.1	IPR015880 (Zinc finger, C2H2-like)
	Wht_47487	2.99	-1.09	-1.05	Ribonuclease H2 subunit C	sp Q9CQ18 RNH2C_MOUSE	Traes_6DS_11583F62A.1	IPR013924 (Ribonuclease H2, subunit C)
	Wht_16067	2.89	1.39	1.82	Ethylene-responsive transcription factor 4	sp Q9LW49 ERF4_NICSY	Traes_XX_8A7E755F7.1	IPR016177 (DNA-binding domain)
	Wht_04901	2.79	0.68	-0.43	Expressed protein	UniRef90_Q7G4F2	Traes_5BL_94C5B581B.1	IPR022059 (Protein of unknown function DUF3615)

Wht_24310	2.78	-1.52	-0.77	NADH:cytochrome B5 reductase 1	AT5G17770.1	Traes_1AL_F7AEB9163.1	IPR001433 (Oxidoreductase FAD/NAD(P)-binding), IPR001834 (NADH:cytochrome b5 reductase (CBR)), IPR017938 (Riboflavin synthase-like beta-barrel)
Wht_21963	2.77	0.49	-0.70	Peptidoglycan-binding LysM domain-containing protein	AT5G23130.1	Traes_7AL_1522CB55B.1	
Wht_50037	2.74	1.28	-0.16	Embryogenesis transmembrane protein-like	UniRef90_Q5Z577	Traes_XX_AE43A669A.1	IPR026961 (PGG domain)
Wht_35367	2.55	0.02	1.95	Pentatricopeptide repeat-containing protein	sp Q9ZUW3 PP172_ARATH // AT2G27610	Traes_7DS_32EFB7CD0.1	IPR002885 (Pentatricopeptide repeat), IPR011990 (Tetratricopeptide-like helical)
Wht_16704	2.52	-0.77	-2.02	Helicase-like protein	UniRef90_Q9AYF0	Traes_7DS_C3466EAD6.1	IPR010285 (DNA helicase Pif1), IPR027417 (P-loop containing nucleoside triphosphate hydrolase)
Wht_57282	2.52	-0.07	-0.05	Plant protein of unknown function (DUF868)	AT2G27770.1	Traes_2BL_98BE793F0.1	IPR008586 (Protein of unknown function DUF868, plant)
Wht_43796	2.52	-1.24	-3.95	Ubiquitin carboxyl-terminal hydrolase 9	sp Q93Y01 UBP9_ARATH	Traes_1DS_B75D2A1E3.1	IPR001394 (Ubiquitin carboxyl-terminal hydrolases family 2), IPR006615 (Peptidase C19, ubiquitin-specific peptidase, DUSP domain)
Wht_15659	2.45	-1.06	1.14	Protein FAR1-RELATED SEQUENCE 3	UniRef90_M8BGQ5	Traes_2DL_724E8A49F.1	IPR001878 (Zinc finger, CCHC-type)
Wht_57354	2.43	0.07	-0.21	Pentatricopeptide repeat-containing protein	sp Q9SY02 PP301_ARATH // AT4G02750	Traes_4AL_15A19D331.1	IPR002885 (Pentatricopeptide repeat), IPR011990 (Tetratricopeptide-like helical)
Wht_44473	2.43	-0.15	-2.50	Phosphoribosylglycinamide formyltransferase 2	sp A5GX22 PURT_SYNR3	Traes_3DS_90E0B2BE9.1	IPR005875 (Phosphoribosylaminoimidazole carboxylase, ATPase subunit), IPR016185 (Pre-ATP-grasp domain)
Wht_35417	2.34	1.77	-1.66	Integral membrane HPP family protein	AT5G62720.1	Traes_XX_1A9B2CE22.1	IPR007065 (HPP)
Wht_42315	2.29	-0.26	-2.59	ATP-dependent DNA helicase PIF1	UniRef90_G7IGJ3	Traes_2BL_9EA1D4DEE.1	IPR010285 (DNA helicase Pif1)
Wht_38442	2.27	-0.35	-0.60	Pentatricopeptide repeat-containing protein	sp Q9ZVX5 PP156_ARATH	Traes_1AS_C7A81EC64.1	IPR002885 (Pentatricopeptide repeat)
Wht_44337	2.24	1.39	-0.49	Basic blue protein	sp Q8LG89 BABL_ARATH	Traes_4AL_E9B779879.1	IPR008972 (Cupredoxin)
Wht_35624	2.24	0.98	-0.30	Expressed protein	UniRef90_Q7G241	Traes_XX_61BD9A6E5.1	
Wht_37399	2.13	-0.77	-1.60	Zinc finger MYM-type protein	UniRef90_G7IY07	Traes_2AL_D887348D3.1	IPR008906 (HAT dimerisation domain, C-terminal), IPR012337 (Ribonuclease H-like domain)
Wht_13754	2.13	0.52	-0.55	B3 domain-containing protein	sp Q0DXB1 Y2641_ORYSJ	Traes_3B_174B7D5D2.1	IPR015300 (DNA-binding pseudobarrel domain)
Wht_36053	2.09	-0.13	-3.07	protein kinase family protein	AT1G51870.1	Traes_1DL_3EE5BBEA1.1	IPR001611 (Leucine-rich repeat), IPR003591 (Leucine-rich repeat, typical subtype), IPR011009 (Protein kinase-like domain), IPR013320 (Concanavalin A-like lectin/glucanase, subgroup), IPR024788 (Malectin-like carbohydrate-binding domain)
Wht_41586	2.09	0.53	-0.45	Disease resistance RPP13-like protein 4	UniRef90_M8B3Z4	Traes_1AS_1975A8E52.1	IPR002182 (NB-ARC), IPR027417 (P-loop containing nucleoside triphosphate hydrolase)
Wht_33511	2.08	1.41	-0.18	Casparian strip membrane protein 1	sp P0DI33 CASP1_PANVG	Traes_7AS_8EB52BB31.1	IPR006702 (Uncharacterised protein family UPP0497, trans-membrane plant)
Wht_35907	2.06	-0.67	-0.45	pentatricopeptide repeat 336	AT1G61870.1	Traes_2BL_52EB2A092.1	IPR002885 (Pentatricopeptide repeat), IPR011990 (Tetratricopeptide-like helical)
Wht_40042	2.05	-0.65	-2.21	adenylate kinase family protein	AT5G35170.1	Traes_3B_FE5FD27C7.1	IPR000850 (Adenylate kinase), IPR027417 (P-loop containing nucleoside triphosphate hydrolase)
Wht_39934	2.05	0.08	-0.80	Retrotransposon protein, putative, unclassified	UniRef90_Q2QQV8	Traes_2BL_9ED22B27E.1	IPR000477 (Reverse transcriptase)
Wht_37685	2.02	-0.43	-3.45	ubiquitin protein ligase 6	AT3G17205.1	Traes_1BS_D11AB25D6.1	IPR000569 (HECT)
Wht_09033	2.02	1.05	-1.36	Tudor/PWWP/MBT domain-containing protein	AT3G63070.1	Traes_2DS_39C68EED9.1	IPR006569 (CID domain)
Wht_04388	2.01	-0.17	-2.64	Phospholipid-transporting ATPase 10	sp Q9L183 ALA10_ARATH	Traes_7AS_5BBC303CA.1	IPR001757 (Cation-transporting P-type ATPase), IPR023214 (HAD-like domain)
Wht_43016	2.00	0.31	-0.39	PHD and RING finger domain-containing protein	sp A6H619 PHRF1_MOUSE	Traes_2DS_D0991BCED.1	IPR013083 (Zinc finger, RING/FYVE/PHD-type)

					1			
Wht_01423	1.31	-2.72	2.77	Maf-like protein	AT5G42770.2	Traes_4DL_27B98B01B.1	IPR003697 (Maf-like protein)	
Wht_14867	1.17	0.14	4.35	alpha/beta-Hydrolases superfamily protein	AT2G36290.1	Traes_XX_8054DED02.1		
Wht_01633	1.10	1.45	2.05	UPI000234EBF1 related cluster	UniRef90_UPI000234EBF1	Traes_2DS_15F609E06.1		
Wht_24207	0.70	-1.03	4.01	Tetraspanin family protein	AT5G46700.1	Traes_7DL_DD3E13ED3.1	IPR018499 (Tetraspanin/Peripherin)	
Wht_07155	0.69	-0.30	2.31	zinc finger protein-related	AT3G18290.1	Traes_1BL_467D0EA6B.1	IPR008913 (Zinc finger, CHY-type), IPR012312 (Haemerythrin/HHE cation-binding motif)	
Wht_18927	0.56	0.60	2.27	Lachrymatory-factor synthase	sp P59082 LFS_ALLCE	Traes_3B_216EC5695.1	IPR019587 (Polyketide cyclase/dehydrase), IPR023393 (START-like domain)	
Wht_21036	0.42	-0.64	3.32	Disease resistance protein	sp Q9T048 DRL27_ARATH	Traes_7BL_E337D9181.1	IPR000767 (Disease resistance protein), IPR027417 (P-loop containing nucleoside triphosphate hydrolase)	
Wht_52219	0.04	0.03	2.73	Transmembrane protein 115	sp Q12893 TM115_HUMAN	Traes_XX_DC44730CD.1	IPR013861 (Protein of unknown function DUF1751, integral membrane, eukaryotic), IPR022764 (Peptidase S54, rhomboid domain)	
Wht_12398	0.01	0.68	2.52	O-methyltransferase 1	AT5G54160.1	Traes_XX_7D898111C.1	IPR016461 (Caffeate O-methyltransferase (COMT) family)	
Wht_07515	-0.10	0.52	2.13	Aminotransferase-like, plant mobile domain family protein	AT1G50830.1	Traes_5DL_7986CD831.1	IPR019557 (Aminotransferase-like, plant mobile domain)	
Wht_49808	-0.16	-0.51	3.02	Ureide permease 2	AT2G03530.1	Traes_XX_0030D7427.1	IPR009834 (Ureide permease)	
Wht_04092	-0.49	0.75	2.35	Proactivator polypeptide	sp P07602 SAP_HUMAN	Traes_1DL_BF298DBEC.1	IPR011001 (Saposin-like)	
Wht_14666	-0.51	-0.02	2.51	Pentatricopeptide repeat-containing protein	sp Q9SN85 PP267_ARATH	Traes_4AL_D347DF000.1	IPR002885 (Pentatricopeptide repeat)	
Wht_00804	-0.54	0.12	2.03	UPI0002B43D8F related cluster	UniRef90_UPI0002B43D8F	Traes_3DS_44695941E.1	IPR019331 (NEFA-interacting nuclear protein NIP30, N-terminal)	
Wht_09018	-0.58	0.65	2.77	WD-40 repeat family protein	AT5G67320.1	Traes_2BL_54B562A79.1	IPR015155 (PLAA family ubiquitin binding, PFU), IPR015943 (WD40/YVTN repeat-like-containing domain), IPR020472 (G-protein beta WD-40 repeat)	
Wht_20403	-0.61	-0.08	2.41	Disease resistance protein	sp Q9T048 DRL27_ARATH	Traes_7AL_4916AD518.1	IPR000767 (Disease resistance protein), IPR001611 (Leucine-rich repeat), IPR025875 (Leucine rich repeat 4), IPR027417 (P-loop containing nucleoside triphosphate hydrolase)	
Wht_52973	-0.64	0.18	2.12	Mitochondrial glycoprotein family protein	AT3G55605.1	Traes_XX_0D0887679.1	IPR003428 (Mitochondrial glycoprotein)	
Wht_41380	-0.79	0.24	2.41	UPI0002C31F2A related cluster	UniRef90_UPI0002C31F2A	Traes_1AL_B3161C4EC.1	IPR003386 (Lecithin:cholesterol/phospholipid:diacylglycerol acyltransferase)	
Wht_07232	-0.85	0.90	2.48	Cell division cycle-associated 7-like protein	sp Q96GN5 CDA7L_HUMAN	Traes_3B_56B9E0EE6.1	IPR018501 (DDT domain superfamily), IPR018866 (Zinc-finger domain of monoamine-oxidase A repressor R1)	
Wht_24444	-0.86	0.53	3.51	Tubby like protein 8	AT1G16070.2	Traes_6BS_5C281F303.1	IPR025659 (Tubby C-terminal-like domain)	
Wht_56615	-0.93	-1.47	4.37	exoribonuclease 4	AT1G54490.1	Traes_5DL_0A7A22BEB.1	IPR027073 (5'-3' exoribonuclease)	
Wht_52059	-0.93	-0.71	4.59	Nucleotide-diphospho-sugar transferase family protein	AT1G28710.1	Traes_4AL_4B6CDE112.1	IPR005069 (Nucleotide-diphospho-sugar transferase)	
Wht_02129	-1.01	0.62	3.82	Gamma-gliadin B	sp P06659 GDBB_WHEAT	Traes_1DS_67B7153A8.1	IPR001954 (Gliadin/LMW glutenin), IPR016140 (Bifunctional inhibitor/plant lipid transfer protein/seed storage helical domain)	
Wht_22255	-1.03	-0.32	2.78	Protein yippee-like	sp P59234 YIPL_SOLTU	Traes_5AS_D8D79E99E.1	IPR004910 (Yippee/Mis18)	
Wht_08838	-1.14	-0.18	2.45	ATP-dependent zinc metalloprotease FtsH	sp B8H444 FTSH_CAUCN	Traes_5DL_90507FDAC.1	IPR005936 (Peptidase, FtsH), IPR027417 (P-loop containing nucleoside triphosphate hydrolase)	
Wht_31836	-1.17	-0.17	5.38	FAD-dependent oxidoreductase family protein	AT3G56840.1	Traes_3B_91AED5BAA.1	IPR006076 (FAD dependent oxidoreductase)	

	Wht_50209	-1.18	0.11	3.70	Disease resistance protein	sp Q9T048 DRL27_ARATH	Traes_6BS_43649D0E4.1	IPR000767 (Disease resistance protein), IPR027417 (P-loop containing nucleoside triphosphate hydrolase)
	Wht_00482	-1.43	-0.21	2.96	beta-1,4-N-acetylglucosaminyltransferase family protein	AT3G27540.1	Traes_2AL_A1F33894A.1	IPR006813 (Glycosyl transferase, family 17)
	Wht_50072	-1.45	0.21	3.18	CASP-like protein	sp Q84WP5 CSPL8_ARATH //AT2G36330	Traes_3B_9E2101666.1	IPR006702 (Uncharacterised protein family UPPF0497, trans-membrane plant)
	Wht_47170	-1.47	-0.96	2.72	Cysteine--tRNA ligase	sp B3E1P0 SYC_GEOLS	Traes_XX_D7B8ABF77.1	IPR009080 (Aminoacyl-tRNA synthetase, class 1a, anticodon-binding), IPR024909 (CysteinyI-tRNA synthetase/mycothiol ligase)
	Wht_50305	-2.55	-0.06	2.07	RING-H2 finger protein 2B	AT2G01150.1	Traes_2BL_8CD63FE77.1	IPR013083 (Zinc finger, RING/FYVE/PHD-type)
Nucleotide metabolism								
	Wht_36898	0.66	-0.19	-3.24	adenylate kinase family protein	AT5G35170.1	Traes_3B_FE5FD27C7.1	IPR000850 (Adenylate kinase), IPR027417 (P-loop containing nucleoside triphosphate hydrolase)
	Wht_39189	2.01	-0.26	-1.60	uridine kinase-like 5	AT3G27440.1	Traes_5AS_9E5FCDEC5.1	IPR006083 (Phosphoribulokinase/uridine kinase), IPR027417 (P-loop containing nucleoside triphosphate hydrolase)
	Wht_08750	0.25	0.76	3.81	Ribose-phosphate pyrophosphokinase 1	sp Q9XG98 KPRS1_SPIOL	Traes_XX_BE9292A82.1	IPR005946 (Ribose-phosphate diphosphokinase)
	Wht_31934	-1.54	-0.30	3.07	cytidine deaminase 1	AT2G19570.1	Traes_XX_49DF7722C.1	IPR006263 (Cytidine deaminase, homodimeric)
Protein								
	Wht_32217	3.55	0.22	-0.18	40S ribosomal protein S19 (RPS19A)	AT3G02080		
	Wht_26871	3.54	2.14	-0.12	26S proteasome regulatory subunit, putative (RPN5)	AT5G09900.3	Traes_5DL_C8AC411F1.1	IPR000717 (Proteasome component (PCI) domain)
	Wht_37290	3.32	2.38	-0.02	ATP-dependent Clp protease ATP-binding subunit clpA homolog	sp Q1XDF4 CLPC_PYRYE	Traes_5BL_3971D82BB.1	IPR001270 (ClpA/B family), IPR019489 (Clp ATPase, C-terminal), IPR027417 (P-loop containing nucleoside triphosphate hydrolase)
	Wht_27065	3.08	1.26	1.86	Transcription factor MYC2	sp Q39204 RAP1_ARATH //AT1G32640	Traes_XX_AD241834D.1	IPR011598 (Myc-type, basic helix-loop-helix (bHLH) domain), IPR025610 (Transcription factor MYC/MYB N-terminal)
	Wht_14843	3.07	-0.28	-1.34	Nucleoporin autopeptidase	AT1G10390.1	Traes_4DS_5CEB4DB49.1	
	Wht_41187	2.76	0.20	-2.21	protein kinase family protein	AT1G51870.1	Traes_1DL_38ABC82C0.1	IPR011009 (Protein kinase-like domain), IPR013320 (Concanavalin A-like lectin/glucanase, subgroup), IPR024788 (Malectin-like carbohydrate-binding domain), IPR025875 (Leucine rich repeat 4)
	Wht_08195	2.71	0.01	-1.87	F-box domain containing protein, expressed	UniRef90_Q2R9A5	Traes_2AL_2AA0872A7.1	
	Wht_54465	2.63	-0.06	-3.67	FBD-associated F-box protein	AT4G13985.1	Traes_1DL_780AD681F.1	IPR001810 (F-box domain)
	Wht_16566	2.56	0.74	-2.16	F-box and associated interaction domains-containing protein	AT3G17280.1	Traes_6BS_D4D509ACB.1	IPR001810 (F-box domain)
	Wht_28762	2.56	0.79	-0.17	E3 ubiquitin-protein ligase PUB23	sp Q84TG3 PUB23_ARATH	Traes_3B_0B86BCF93.1	
	Wht_51508	2.55	-1.01	0.91	Proteasome subunit alpha type-2	sp A2YVR7 PSA2_ORYSI //AT1G16470	Traes_XX_2DA2BA453.1	IPR000426 (Proteasome, alpha-subunit, N-terminal domain), IPR001353 (Proteasome, subunit alpha/beta)
	Wht_23542	2.39	0.85	1.84	Protein kinase superfamily protein	AT5G01020.1	Traes_4DS_EA656FA48.1	IPR011009 (Protein kinase-like domain), IPR013320 (Concanavalin A-like lectin/glucanase, subgroup)
	Wht_32227	2.14	0.05	-0.25	ADP-ribosylation factor 1	AT1G23490.1	Traes_5BL_A8CB3ACF6.1	IPR003579 (Small GTPase superfamily, Rab type), IPR003225 (Small GTP-binding protein domain), IPR006689 (Small GTPase superfamily, ARF/SAR type), IPR027417 (P-loop containing nucleoside triphosphate hydrolase)
	Wht_14583	2.08	1.43	1.58	U-box domain-containing protein 21	sp Q5PNY6 PUB21_ARATH	Traes_XX_196FB4025.1	IPR013083 (Zinc finger, RING/FYVE/PHD-type), IPR016024 (Armadillo-type fold)

	Wht_29845	2.02	0.51	-0.18	methionine aminopeptidase 2B	AT3G59990.1	Traes_XX_21EFDC039.1	IPR000994 (Peptidase M24, structural domain), IPR001714 (Peptidase M24, methionine aminopeptidase)
	Wht_39250	2.00	0.24	-0.40	ADP-ribosylation factor 1	AT1G23490.1	Traes_6DL_DF084B211.1	IPR005225 (Small GTP-binding protein domain), IPR006689 (Small GTPase superfamily, ARF/SAR type), IPR027417 (P-loop containing nucleoside triphosphate hydrolase)
	Wht_00675	1.52	-0.67	2.97	Protein disulfide-isomerase LQY1	sp Q8GSJ6 LQY1_ARATH	Traes_4DL_1233D47E2.1	IPR001305 (Heat shock protein DnaJ, cysteine-rich domain)
	Wht_34754	0.93	-0.06	2.27	Protein phosphatase 2C family protein	AT5G36250.1	Traes_6DS_50C17FF00.1	IPR001932 (Protein phosphatase 2C (PP2C)-like domain), IPR015655 (Protein phosphatase 2C)
	Wht_30689	0.64	0.33	4.52	RING finger protein 38	sp Q9H0F5 RNF38_HUMAN	Traes_1AL_772113B31.1	IPR013083 (Zinc finger, RING/FYVE/PHD-type)
	Wht_51221	-0.09	-0.05	3.78	E3 ubiquitin-protein ligase RNF170	sp Q7SZN2 RN170_DANRE	Traes_5DL_D0E16F980.1	IPR010652 (Protein of unknown function DUF1232), IPR013083 (Zinc finger, RING/FYVE/PHD-type)
	Wht_56150	-0.10	-1.01	2.21	Eukaryotic aspartyl protease family protein	AT5G22850.1	Traes_3B_4D30CDD12.1	IPR001461 (Peptidase A1), IPR021109 (Aspartic peptidase)
	Wht_13618	-0.27	0.20	3.53	UPI000234E3B7 related cluster	UniRef90_UPI000234E3B7	Traes_7BL_D3C5528D9.1	IPR006566 (FBD domain)
	Wht_43105	-0.28	-0.12	3.52	protein kinase family protein	AT5G26150.1	Traes_6DS_7CDC74412.1	IPR011009 (Protein kinase-like domain), IPR013083 (Zinc finger, RING/FYVE/PHD-type)
	Wht_07853	-0.49	-1.66	3.36	Ankyrin repeat family protein	AT3G04710.1	Traes_3DS_46B7839BF.1	IPR020683 (Ankyrin repeat-containing domain)
	Wht_13252	-0.53	-0.90	3.93	Single-stranded nucleic acid binding R3H domain protein	UniRef90_B7K2D2	Traes_7AS_D867B319B.1	
	Wht_32665	-0.94	-0.20	2.15	Protein kinase superfamily protein	AT1G68690.1	Traes_7DS_F2A50E14F.1	IPR011009 (Protein kinase-like domain), IPR013320 (Concanavalin A-like lectin/glucanase, subgroup)
	Wht_29091	-1.46	-0.80	3.01	RING/U-box superfamily protein	AT5G24870.1	Traes_6DS_D6F9F10D8.1	IPR013083 (Zinc finger, RING/FYVE/PHD-type)
	Wht_37684	-1.50	-0.63	4.42	Histidine--tRNA ligase	sp P93422 SYH_ORYSJ	Traes_1AS_880B9AC92.1	IPR004516 (Histidine-tRNA ligase/ATP phosphoribosyltransferase regulatory subunit)
	Wht_52322	-3.74	-1.67	2.12	serine carboxypeptidase-like 45	AT1G28110.1	Traes_6DS_6C2C902AB.1	IPR001563 (Peptidase S10, serine carboxypeptidase)
Secondary metabolism								
	Wht_42746	6.96	6.27	4.88	Aldehyde dehydrogenase	sp P12693 ALDH_PSEOL	Traes_2AS_1002418B1.1	IPR016161 (Aldehyde/histidinol dehydrogenase)
	Wht_24318	6.80	7.83	3.91	HXXXD-type acyl-transferase family protein	AT5G67150.1	Traes_2AS_347B43C78.1	IPR003480 (Transferase), IPR023213 (Chloramphenicol acetyltransferase-like domain)
	Wht_18548	5.61	3.44	2.42	Betaine aldehyde dehydrogenase	sp O24174 BADH_ORYSJ	Traes_XX_2CF36FAAB.1	IPR016161 (Aldehyde/histidinol dehydrogenase)
	Wht_52307	2.87	1.35	0.95	Terpenoid cyclases/Protein prenyltransferases superfamily protein	AT1G70080.1	Traes_2DS_E11E98E1A.1	IPR008930 (Terpenoid cyclases/protein prenyltransferase alpha-alpha toroid), IPR008949 (Terpenoid synthase)
	Wht_53560	2.18	0.84	1.75	2-oxoglutarate (2OG) and Fe(II)-dependent oxygenase superfamily protein	AT1G78550.1	Traes_1BL_2DC5F0295.1	IPR005123 (Oxoglutarate/iron-dependent dioxygenase), IPR026992 (Non-haem dioxygenase N-terminal domain), IPR027443 (Isopenicillin N synthase-like)
	Wht_21992	1.11	0.67	2.66	phenylalanine ammonia-lyase 2	AT3G53260.1	Traes_1DS_A21FCBA3D.1	IPR001106 (Aromatic amino acid lyase), IPR023144 (Phenylalanine ammonia-lyase, shielding domain), IPR024083 (Fumarase/histidase, N-terminal)
	Wht_02056	-0.57	0.06	2.11	1-deoxy-D-xylulose 5-phosphate synthase 1	AT3G21500.2	Traes_XX_995EA1A53.1	IPR005477 (Deoxyxylulose-5-phosphate synthase), IPR009014 (Transketolase, C-terminal/Pyruvate-ferredoxin oxidoreductase, domain II)
Signalling and kinases								
	Wht_21030	-0.04	0.98	-0.08	trehalose phosphate synthase	AT1G60140.1	Traes_XX_9E0498F68.1	IPR001830 (Glycosyl transferase, family 20), IPR006379 (HAD-superfamily hydrolase, subfamily 1B), IPR023214 (HAD-like domain)
	Wht_43584	6.22	6.61	2.25	receptor kinase 2	AT1G65800.1	Traes_7DL_F0110933B.1	IPR011009 (Protein kinase-like domain)
	Wht_37933	4.94	7.50	2.67	receptor kinase 2	AT1G65800.1	Traes_7BL_2D6DB297B.1	IPR011009 (Protein kinase-like domain), IPR013320 (Concanavalin A-like lectin/glucanase, subgroup),



								IPR021864 (Protein of unknown function DUF3475)
	Wht_05775	4.55	4.37	3.99	vesicle associated protein	AT3G60600.1	Traes_2DS_8E56CA0E3.1	IPR008962 (PapD-like)
	Wht_17690	3.59	2.21	2.11	receptor kinase 2	AT1G65800.1	Traes_2AS_09E707C65.1	IPR11009 (Protein kinase-like domain)
	Wht_56221	3.58	2.73	1.90	Elongation factor 1-alpha GTP-dependent	sp A1RXW9 EF1A_THEPD	Traes_2AS_55BD046C1.1	IPR000795 (Elongation factor, GTP-binding domain), IPR009000 (Translation elongation/initiation factor/Ribosomal, beta-barrel), IPR009001 (Translation elongation factor EF1A/initiation factor IP2gamma, C-terminal), IPR027417 (P-loop containing nucleoside triphosphate hydrolase)
	Wht_15806	2.62	1.11	-0.39	Leucine-rich repeat receptor-like protein kinase family protein	AT4G08850.1	Traes_3AL_CE3238869.1	IPR13210 (Leucine-rich repeat-containing N-terminal, type 2), IPR025875 (Leucine rich repeat 4)
	Wht_24756	2.00	0.38	-2.19	Brefeldin A-inhibited guanine nucleotide-exchange protein 1	sp F4JSZ5 BIG1_ARATH	Traes_6BS_5A77A3321.1	IPR000904 (SEC7-like), IPR016024 (Armadillo-type fold), IPR023394 (SEC7-like, alpha orthogonal bundle)
	Wht_22287	1.91	-0.92	-2.52	Leucine-rich repeat receptor-like protein kinase family protein	AT2G33170.1	Traes_XX_174C6FD13.1	IPR001611 (Leucine-rich repeat), IPR013210 (Leucine-rich repeat-containing N-terminal, type 2), IPR025875 (Leucine rich repeat 4)
	Wht_32012	1.87	1.56	0.84	calmodulin like 23	AT1G66400.1	Traes_3B_41EE9C1AA.1	IPR011992 (EF-hand domain pair)
	Wht_43458	1.71	0.11	-1.71	Phosphatidylinositol 4-kinase 2	sp Q0WPX9 P4KB2_ARATH	Traes_4DS_4B325101D.1	IPR015433 (Phosphatidylinositol Kinase), IPR016024 (Armadillo-type fold)
	Wht_25731	1.62	1.00	0.46	calmodulin like 37	AT5G42380.1	Traes_7DL_0484503F1.1	IPR011992 (EF-hand domain pair)
	Wht_37902	1.60	-0.13	2.19	receptor lectin kinase	AT2G37710.1	Traes_6DL_544B74CBB1.1	IPR008985 (Concanavalin A-like lectin/glucanases superfamily), IPR011009 (Protein kinase-like domain)
	Wht_42346	1.59	1.22	-0.20	FAR1-related sequence 5	AT4G38180.1	Traes_2BL_2ECC216F7.1	IPR004330 (FAR1 DNA binding domain), IPR007527 (Zinc finger, SWIM-type), IPR018289 (MULE transposase domain)
	Wht_30977	1.59	-1.78	0.30	Cytochrome P450 superfamily protein	AT3G28740.1	Traes_3B_268CA8C4D.1	IPR001128 (Cytochrome P450)
	Wht_25720	1.54	1.25	0.77	calmodulin like 37	AT5G42380.1	Traes_7DL_6BD95FEAB.1	IPR011992 (EF-hand domain pair)
	Wht_39982	1.53	1.32	0.62	MLO-like protein 1	sp O49621 MLO1_ARATH	Traes_2AS_E92C7ABDF.1	IPR004326 (Mlo-related protein)
	Wht_15522	1.47	0.76	0.34	glutamate receptor 2.5	AT5G11210.1	Traes_6DL_12CD9ACC0.1	IPR001320 (Ionotropic glutamate receptor), IPR001638 (Extracellular solute-binding protein, family 3)
	Wht_18636	1.33	0.34	0.95	wall-associated kinase	AT3G25490.1	Traes_6DL_9FAE3F08F.1	IPR011009 (Protein kinase-like domain)
	Wht_45119	1.30	1.75	1.53	calmodulin like 43	AT5G44460.1	Traes_1AL_D7A903FD2.1	IPR011992 (EF-hand domain pair)
	Wht_41067	1.23	-2.51	1.11	receptor lectin kinase	AT2G37710.1	Traes_3AS_80B17F967.1	IPR008985 (Concanavalin A-like lectin/glucanases superfamily), IPR011009 (Protein kinase-like domain)
	Wht_35996	1.21	-0.26	1.84	Calcium-binding EF-hand family protein	AT2G15680.1	Traes_5DL_09EEB473D.1	IPR011992 (EF-hand domain pair)
	Wht_01300	1.18	-0.78	-1.35	calcium-dependent protein kinase 13	AT3G51850.1	Traes_3AL_0360C0D50.1	IPR011009 (Protein kinase-like domain), IPR011992 (EF-hand domain pair)
	Wht_37269	1.17	-0.50	-2.74	GTPase obg	sp B7GIR2 OBG_ANOFW	Traes_1AS_C10C60219.1	IPR014100 (GTP-binding protein Obg/CgtA), IPR027417 (P-loop containing nucleoside triphosphate hydrolase)
	Wht_17602	1.15	0.17	-1.45	receptor kinase 3	AT4G21380.1	Traes_6DL_6214806F8.1	IPR000742 (Epidermal growth factor-like domain), IPR011009 (Protein kinase-like domain), IPR025287 (Wall-associated receptor kinase galacturonan-binding domain)
	Wht_36398	1.07	-2.13	-0.25	Calcium-binding EF-hand family protein	AT4G38810.2	Traes_4AS_056805E40.1	IPR011992 (EF-hand domain pair)
	Wht_40499	1.05	-0.56	-3.93	Auxin transport protein BIG	AT3G02260.1	Traes_5BL_C9FD62D61.1	IPR003126 (Zinc finger, N-recognition), IPR017986 (WD40-repeat-containing domain)

Wht_36619	1.03	1.16	0.52	RECEPTOR-LIKE KINASE 1, RKL1	AT1G48480.1	Traes_2AS_5810DD9381.1	IPR001611 (Leucine-rich repeat), IPR003591 (Leucine-rich repeat, typical subtype), IPR011009 (Protein kinase-like domain), IPR013210 (Leucine-rich repeat-containing N-terminal, type 2), IPR013320 (Concanavalin A-like lectin/glucanase, subgroup)
Wht_25455	1.03	1.11	0.80	mitogen-activated protein kinase kinase kinase 16	AT4G26890.1	Traes_3B_B5C69DB4A.1	IPR011009 (Protein kinase-like domain)
Wht_54583	0.94	-0.64	-3.90	Mitochondrial Rho GTPase	Q6ATR5 - Q6ATR5_ORYSJ		
Wht_25875	0.92	-0.62	-3.48	Rho GTPase-activating protein 2	sp F4JI46 RGAP2_ARATH	Traes_5BS_C643C10BA.1	IPR000095 (CRIB domain), IPR008936 (Rho GTPase activation protein)
Wht_42267	0.83	0.22	1.54	ATCRLK2, CALCIUM/CALMODULIN-REGULATED RECEPTOR-LIKE KINASE 2, CRLK2	AT5G15730.2	Traes_XX_3C69724A2.1	IPR011009 (Protein kinase-like domain), IPR013320 (Concanavalin A-like lectin/glucanase, subgroup)
Wht_36892	0.81	-0.52	-2.72	diacylglycerol kinase 5	AT2G20900.1	Traes_XX_60CBDEEDD.1	IPR000756 (Diacylglycerol kinase, accessory domain), IPR001206 (Diacylglycerol kinase, catalytic domain), IPR016064 (ATP-NAD kinase-like domain)
Wht_42489	0.77	-1.31	-2.85	Wall-associated receptor kinase 2	sp Q9LMP1 WAK2_ARATH	Traes_4DS_5334FB296.1	IPR025287 (Wall-associated receptor kinase galacturonan-binding domain)
Wht_23138	0.69	-0.29	-2.85	Calcium-dependent protein kinase family protein	AT2G17290.1	Traes_6DL_4DA973768.1	IPR011009 (Protein kinase-like domain), IPR011992 (EF-hand domain pair)
Wht_04450	0.66	0.85	-0.48	Rho GTPase-activating protein 2	sp F4JI46 RGAP2_ARATH	Traes_2DS_1208A147B.1	IPR000095 (CRIB domain), IPR008936 (Rho GTPase activation protein)
Wht_26289	0.65	-1.00	-2.64	receptor kinase 2	AT1G65800.1	Traes_7DS_BC9426B0F.1	IPR011009 (Protein kinase-like domain), IPR013320 (Concanavalin A-like lectin/glucanase, subgroup), IPR020946 (Flavin monooxygenase-like)
Wht_38282	0.60	1.42	-0.87	receptor kinase 1	AT1G65790.1	Traes_2BL_D7E37D22E.1	IPR008973 (C2 calcium/lipid-binding domain, CaLB), IPR011009 (Protein kinase-like domain), IPR013320 (Concanavalin A-like lectin/glucanase, subgroup)
Wht_23019	0.59	-0.38	-2.87	Calcineurin B-like protein 1	AT4G17615.1	Traes_1AL_4AB2BF02A.1	IPR001125 (Recoverin)
Wht_26426	0.53	0.06	-3.70	Processive diacylglycerol glucosyltransferase	sp A8FED1 UGTP_BACP2	Traes_5AL_C1E3FCB4F.1	IPR007235 (Glycosyl transferase, family 28, C-terminal), IPR009695 (Diacylglycerol glucosyltransferase, N-terminal)
Wht_36909	0.50	-0.92	-1.12	Protein kinase superfamily protein	AT5G24080.1	Traes_5DL_91EFA6E79.1	IPR000742 (Epidermal growth factor-like domain), IPR000858 (S-locus glycoprotein), IPR001480 (Bulb-type lectin domain), IPR003609 (Apple-like), IPR011009 (Protein kinase-like domain), IPR013320 (Concanavalin A-like lectin/glucanase, subgroup), IPR024171 (S-receptor-like serine/threonine-protein kinase)
Wht_37117	0.48	-0.86	-2.56	Mitochondrial Rho GTPase 1	sp P0CO79 GEM1_CRYNB	Traes_XX_73F3EA5A7.1	IPR001806 (Small GTPase superfamily), IPR011992 (EF-hand domain pair), IPR027417 (P-loop containing nucleoside triphosphate hydrolase)
Wht_56313	0.45	-0.25	-2.96	Pre-mRNA 3'-end-processing factor FIP1	sp Q5XJD3 FIP1_DANRE	Traes_4AS_C5EDC65CD.1	IPR007854 (Pre-mRNA polyadenylation factor Fip1)
Wht_34471	0.41	1.35	-0.35	Protein kinase superfamily protein	AT1G67000.1	Traes_3AL_B27A64367.1	IPR011009 (Protein kinase-like domain), IPR013320 (Concanavalin A-like lectin/glucanase, subgroup), IPR025287 (Wall-associated receptor kinase galacturonan-binding domain)
Wht_17932	0.36	-0.46	-2.78	receptor kinase 2	AT1G65800.1	Traes_5BL_3DC0729AB.1	IPR011009 (Protein kinase-like domain)
Wht_43794	0.34	-0.80	-1.54	B-cell receptor-associated 31-like	AT5G42570.1	Traes_1AL_FB0EAB102.1	IPR008417 (B-cell receptor-associated 31-like)
Wht_10456	0.33	-0.79	3.01	Leucine-rich repeat receptor-like protein kinase family protein	AT5G06940.1	Traes_2AL_34786C78C.1	IPR001611 (Leucine-rich repeat), IPR013210 (Leucine-rich repeat-containing N-terminal, type 2)
Wht_23770	0.30	-0.11	-2.92	glutamate dehydrogenase 2	AT5G07440.1	Traes_2BL_A0FFC447F.1	IPR006097 (Glutamate/phenylalanine/leucine/valine dehydrogenase, dimerisation domain)
Wht_06881	0.30	0.88	-0.24	Calmodulin-binding protein	AT4G25800.1	Traes_4BL_84961FD37.1	IPR012416 (Calmodulin binding protein-like)

Wht_38444	0.28	-0.49	-2.56	Synaptotagmin-5	sp Q8L706 SYT5_ARATH	Traes_3B_D7DBFB914.1	IPR008973 (C2 calcium/lipid-binding domain, CaLB)
Wht_06191	0.27	-0.04	-1.85	Receptor protein kinase-related	UniRef100_Q0J3C6		
Wht_40045	0.25	-0.76	-3.25	receptor kinase 2	AT1G65800.1	Traes_2DS_B2BE54C63.1	IPR011009 (Protein kinase-like domain)
Wht_56155	0.23	0.72	-0.28	diacylglycerol kinase 5	AT2G20900.1	Traes_2BL_F9E12C3E4.1	IPR016064 (ATP-NAD kinase-like domain), IPR016961 (Diacylglycerol kinase, plant)
Wht_08335	0.20	-0.51	-3.40	Leukocyte receptor cluster member 8 homolog	sp Q32NW2 LENG8_XENLA	Traes_3B_05F1B7D47.1	IPR005062 (SAC3/GANP/Nin1/mts3/eIF-3 p25)
Wht_43640	0.18	-0.27	-1.72	Phosphatidylinositide phosphatase SAC1	sp Q9NTJ5 SAC1_HUMAN	Traes_1DS_8965FF182.1	IPR002013 (Synaptotagmin, N-terminal)
Wht_05230	0.13	-1.15	-1.52	Leucine-rich receptor-like protein kinase family protein	AT5G46330.1	Traes_7DS_7E5E07181.1	IPR001611 (Leucine-rich repeat), IPR003591 (Leucine-rich repeat, typical subtype), IPR011009 (Protein kinase-like domain), IPR013210 (Leucine-rich repeat-containing N-terminal, type 2), IPR013320 (Concanavalin A-like lectin/glucanase, subgroup)
Wht_56539	0.10	-0.78	-0.04	Expressed protein / Calmodulin binding protein	UniRef90_Q10Q34	Traes_4DL_64508CBF1.1	
Wht_14120	0.10	3.16	-1.91	calmodulin-like 38	AT1G76650.1	Traes_5DL_FCB8BFE07.1	IPR011992 (EF-hand domain pair)
Wht_52042	0.07	0.01	-3.76	RAS-related GTP-binding nuclear protein 2	AT5G20020.1	Traes_7BS_2FE819546.1	
Wht_21030	-0.04	0.98	-0.08	trehalose phosphate synthase	AT1G60140.1	Traes_XX_9E0498F68.1	IPR001830 (Glycosyl transferase, family 20), IPR006379 (HAD-superfamily hydrolase, subfamily IIB), IPR023214 (HAD-like domain)
Wht_43583	-0.14	-0.45	-2.83	receptor kinase 2	AT1G65800.1	Traes_1DL_32C9B45A0.1	IPR011009 (Protein kinase-like domain)
Wht_26105	-0.25	-0.86	-1.24	protein kinase family protein	AT1G51870.1	Traes_4DL_D0237CA32.1	IPR001611 (Leucine-rich repeat), IPR011009 (Protein kinase-like domain), IPR013320 (Concanavalin A-like lectin/glucanase, subgroup), IPR024788 (Malectin-like carbohydrate-binding domain)
Wht_00800	-0.35	-0.59	-2.07	Serine/threonine-protein kinase tel1	sp O74630 ATM_SCHPO	Traes_1BL_8F3BBD25E.1	IPR011009 (Protein kinase-like domain), IPR015519 (ATM/Tel1), IPR016024 (Armillo-type fold)
Wht_00873	-0.46	1.38	1.08	Core-2/I-branching beta-1,6-N-acetylglucosaminyltransferase family protein	AT1G10280.1	Traes_7AL_C77279230.1	IPR003406 (Glycosyl transferase, family 14)
Wht_03753	-0.53	-0.78	-1.43	Protein kinase superfamily protein	AT5G38260.1	Traes_1BS_32E191808.1	IPR011009 (Protein kinase-like domain)
Wht_27013	-1.01	-0.20	-1.61	Protein FAR1-RELATED SEQUENCE 3	UniRef90_M8BGQ5	Traes_3DL_F28E6CE46.1	
Wht_35322	-1.03	0.74	-1.45	Leucine-rich repeat receptor-like protein kinase family protein	AT4G08850.1	Traes_XX_D9CCD3E10.1	IPR001611 (Leucine-rich repeat), IPR011009 (Protein kinase-like domain), IPR013210 (Leucine-rich repeat-containing N-terminal, type 2), IPR025875 (Leucine-rich repeat 4)
Wht_42963	-1.42	-1.23	-4.21	Rho GTPase-activating protein 24	sp Q8C4V1 RHG24_MOUSE	Traes_XX_29A8482C7.1	IPR008936 (Rho GTPase activation protein)
Wht_31680	-1.72	0.87	2.85	Leucine-rich receptor-like protein kinase family protein	AT3G28040.1	Traes_XX_850FB0601.1	IPR001611 (Leucine-rich repeat), IPR003591 (Leucine-rich repeat, typical subtype), IPR011009 (Protein kinase-like domain), IPR013210 (Leucine-rich repeat-containing N-terminal, type 2), IPR025875 (Leucine-rich repeat 4)
Wht_36685	-1.87	0.49	-3.88	Calmodulin-binding transcription activator 3	sp Q8GSA7 CMTA3_ARATH	Traes_XX_16C919FDB.1	IPR000048 (IQ motif, EF-hand binding site), IPR005559 (CG-1 DNA-binding domain), IPR013783 (Immunoglobulin-like fold), IPR014756 (Immunoglobulin E-set), IPR020683 (Ankyrin repeat-containing domain), IPR027417 (P-loop containing nucleoside triphosphate hydrolase)
Wht_15607	-1.95	-1.40	-2.64	Protein kinase family protein	AT5G38250.1	Traes_1DS_DC2DCED34.1	IPR011009 (Protein kinase-like domain)
Wht_38023	-2.04	0.73	-3.71	receptor-like protein kinase 2	AT3G02130.1	Traes_6AS_AFEEDC190.1	IPR001611 (Leucine-rich repeat), IPR025875 (Leucine-rich repeat 4)
Wht_26286	-2.14	-0.33	-4.32	mitogen-activated protein kinase kinase kinase 5	AT5G66850.1	Traes_7DS_4D3DBF10A.1	IPR011009 (Protein kinase-like domain)

	Wht_35884	2.39	0.61	-0.51	CRIB domain-containing protein RIC5	sp F4J424 RIC5_ARATH // AT3G23380	Traes_6DL_A1DE6A54F.1	IPR000095 (CRIB domain)
	Wht_37509	2.26	0.02	-1.09	FAR1-related sequence 5	AT4G38180.1	Traes_5AL_50D72F0A4.1	IPR007527 (Zinc finger, SWIM-type)
	Wht_05664	2.16	-0.27	-1.24	IQ-domain 5	AT3G22190.1	Traes_5DS_A19DCED87.1	IPR000048 (IQ motif, EF-hand binding site)
	Wht_25154	0.29	-0.49	3.65	Pentapeptide repeat-containing protein	AT1G12250.1	Traes_3B_B12420403.1	IPR001646 (Pentapeptide repeat)
	Wht_02593	-1.00	-0.38	2.38	calcineurin B-like protein 1	AT4G17615.1	Traes_5AL_F2D4ACCA3.1	IPR001125 (Recoverin)
	Wht_19736	-1.22	1.13	2.03	calmodulin like 23	AT1G66400.1	Traes_1AL_80931BE4C.1	IPR011992 (EF-hand domain pair)
	Wht_03983	-1.36	-1.24	2.57	Protein kinase superfamily protein	AT5G24080.1	Traes_7BL_CA3361FCD.1	IPR011009 (Protein kinase-like domain), IPR013320 (Concanavalin A-like lectin/glucanase, subgroup)
Stress biotic or abiotic								
	Wht_37996	6.82	6.89	5.53	Disease resistance protein (CC-NBS-LRR class) family	AT5G48620.1	Traes_2AS_6BC67DD45.1	
	Wht_09959	4.01	1.21	0.96	Stress responsive alpha-beta barrel domain protein	AT2G31670.1	Traes_2DS_F1F7FE1D2.1	IPR011008 (Dimeric alpha-beta barrel)
	Wht_36596	3.69	0.05	-0.11	S-adenosyl-L-methionine-dependent methyltransferases superfamily protein	AT2G40280.1	Traes_1BL_1557A6E94.1	IPR004159 (Putative S-adenosyl-L-methionine-dependent methyltransferase)
	Wht_15292	3.23	2.98	0.64	Disease resistance protein RPP13	sp Q9M667 RPP13_ARATH // AT3G46530	Traes_2AS_3947F19A9.1	IPR002182 (NB-ARC), IPR027417 (P-loop containing nucleoside triphosphate hydrolase)
	Wht_36591	2.77	1.10	1.68	Disease resistance protein (CC-NBS-LRR class) family	AT1G59620.1	Traes_2AS_9D1FC09D7.1	IPR002182 (NB-ARC), IPR027417 (P-loop containing nucleoside triphosphate hydrolase)
	Wht_28734	2.58	0.22	1.18	Disease resistance-responsive (dirigent-like protein) family protein	AT2G21100.1	Traes_2DS_99B8F339A.1	IPR004265 (Plant disease resistance response protein)
	Wht_35761	2.12	-0.61	-3.21	Chaperone protein dnaJ 3	sp Q94AW8 DNAJ3_ARATH // AT3G44110.1	Traes_XX_7B6FC358A.1	IPR001623 (DnaJ domain), IPR002939 (Chaperone DnaJ, C-terminal)
	Wht_40768	0.99	-0.72	2.85	Disease resistance protein	sp Q9T048 DRL27_ARATH // AT4G27190	Traes_6BS_E6BD652E0.1	IPR000767 (Disease resistance protein), IPR027417 (P-loop containing nucleoside triphosphate hydrolase)
	Wht_20097	-0.52	-0.28	2.82	PHD-finger family protein	UniRef90_M4Q9V5	Traes_7BS_B0F581FF2.1	
	Wht_41391	-0.60	0.40	3.24	Disease resistance protein (CC-NBS-LRR class) family	AT1G58400.1	Traes_6BL_E6F4E90A5.1	IPR000767 (Disease resistance protein), IPR027417 (P-loop containing nucleoside triphosphate hydrolase)
	Wht_48641	-0.66	0.23	2.34	Disease resistance protein (CC-NBS-LRR class) family	AT1G58390.1	Traes_5BL_33D83A0CB.1	IPR000767 (Disease resistance protein), IPR027417 (P-loop containing nucleoside triphosphate hydrolase)
	Wht_12131	-1.19	-0.82	2.59	Disease resistance protein RPM1	sp Q39214 RPM1_ARATH // AT3G07040	Traes_5DL_87561F7C6.1	
	Wht_41200	-1.32	-1.26	4.39	Disease resistance protein	sp Q9T048 DRL27_ARATH // AT4G27190	Traes_1BS_70B733D34.1	IPR000767 (Disease resistance protein), IPR027417 (P-loop containing nucleoside triphosphate hydrolase)
Tetrapyrrole synthesis								
	Wht_14983	2.72	-1.32	-1.30	Putrescine aminotransferase	sp Q0TD34 PAT_ECOL5	Traes_7BL_95CF78A1C.1	IPR005814 (Aminotransferase class-III), IPR015424 (Pyridoxal phosphate-dependent transferase)
Transcription factors								
	Wht_31708	4.35	2.59	0.76	myb-like transcription factor family protein	AT1G70000.1	Traes_XX_41DC51E73.1	IPR009057 (Homeodomain-like)
	Wht_38943	2.59	0.47	-2.43	LHW, LONESOME HIGHWAY	AT2G27230.1	Traes_6AL_D20E70F28.1	IPR011598 (Myc-type, basic helix-loop-helix (bHLH) domain), IPR025610 (Transcription factor MYC/MYB N-terminal)

Wht_13938	2.56	1.56	0.59	Unknown protein		Traes_2BL_BAC6CF5B8.1	
Wht_47455	2.49	1.34	-0.05	Basic helix-loop-helix (bHLH) family protein	UniRef100_Q0JEB7		
Wht_31779	2.05	0.68	-1.75	Transcription elongation factor A protein 3	sp O75764 TCEA3_HUMAN	Traes_XX_4169E71C4.1	IPR017923 (Transcription factor IIS, N-terminal)
Wht_56348	2.02	0.40	-4.16	Lysine-specific demethylase 5C	sp A1YVX4 KDM5C_PIG	Traes_XX_3A7EB4DC8.1	IPR013083 (Zinc finger, RING/FYVE/PHD-type)
Wht_16066	1.59	1.86	4.70	ethylene-responsive element binding factor 13	AT2G44840.1	Traes_5BL_6647931E2.1	IPR016177 (DNA-binding domain)
Wht_02922	1.46	0.85	1.43	WRKY DNA-binding protein 50	AT5G26170.1	Traes_3B_7F3B35623.1	IPR003657 (DNA-binding WRKY)
Wht_04356	1.46	1.53	1.59	ethylene-responsive element binding factor 13	AT2G44840.1	Traes_XX_C3D316A93.1	IPR016177 (DNA-binding domain)
Wht_25925	1.36	-0.69	0.39	RNA-binding (RRM/RBD/RNP motifs) family protein	AT1G33470.1	Traes_XX_B0F66B990.1	
Wht_34808	1.11	1.47	-0.22	WRKY DNA-binding protein 46	AT2G46400.1	Traes_3AL_6E92D4E1F.1	IPR003657 (DNA-binding WRKY)
Wht_23309	1.00	0.21	-2.10	Transcription factor SPATULA	sp Q9FUA4 SPT_ARATH	Traes_6BL_5AA3D02B3.1	IPR011598 (Myc-type, basic helix-loop-helix (bHLH) domain), IPR024097 (Basic helix-loop-helix leucine zipper transcription factor)
Wht_04363	0.96	1.67	0.32	Dehydration-responsive element-binding protein 1C	sp A2Y8S6 DRE1C_ORYSI	Traes_XX_5919BAADA.1	IPR016177 (DNA-binding domain)
Wht_06644	0.76	1.30	-0.36	WRKY DNA-binding protein 46	AT2G46400.1	Traes_7BL_53AA25AA1.1	IPR003657 (DNA-binding WRKY)
Wht_15017	0.53	0.99	0.07	Nucleolar protein 56	sp O00567 NOP56_HUMAN	Traes_2AS_4CB8AF22D.1	IPR002687 (Nop domain), IPR012974 (NOP5, N-terminal), IPR012976 (NOSIC)
Wht_41280	0.41	-0.71	0.95	UPI000234EEC8 related cluster	UniRef90_UPI000234EEC8	Traes_2AL_349EF5B5D.1	
Wht_33207	0.41	0.72	1.10	UPI00023B2DC4 related cluster	UniRef90_UPI00023B2DC4	Traes_2AS_7BAFA2CA8.1	IPR003604 (Zinc finger, U1-type)
Wht_09842	0.34	-1.05	-1.24	CCR4-NOT transcription complex subunit 2	UniRef90_R7W1V9	Traes_5AS_329D02E70.1	
Wht_28746	0.32	0.67	1.19	Arabinanase/levansucrase/invertase	AT1G26761.1	Traes_XX_FFEE0BB9D.1	IPR023296 (Glycosyl hydrolase, five-bladed beta-propeller domain)
Wht_05913	0.28	0.22	-2.42	histone acetyltransferase of the CBP family 1	AT1G79000.2	Traes_6DS_620B85F1B.1	IPR000197 (Zinc finger, TAZ-type), IPR000433 (Zinc finger, ZZ-type), IPR013083 (Zinc finger, RING/FYVE/PHD-type), IPR013178 (Histone H3-K56 acetyltransferase, RTT109)
Wht_37585	0.26	-2.00	-2.17	DNA damage-binding protein 2	sp Q66JG1 DDB2_XENTR	Traes_3B_1763E055A.1	IPR015943 (WD40/YVTN repeat-like-containing domain)
Wht_03730	0.20	0.77	0.91	WRKY DNA-binding protein 21	AT2G30590.1	Traes_5AL_A3653B781.1	IPR003657 (DNA-binding WRKY), IPR018872 (Zn-cluster domain)
Wht_21108	0.20	-0.45	-1.95	rcd1-like cell differentiation protein	AT3G20800		
Wht_22661	0.19	1.28	0.88	tRNA-splicing endonuclease	sp Q97ZY3 ENDA_SULSO	Traes_3AS_D9E1E4F70.1	IPR006678 (tRNA intron endonuclease, N-terminal), IPR011856 (tRNA endonuclease-like domain)
Wht_18384	0.18	-0.34	-3.04	UPI0002C315D6 related cluster	UniRef90_UPI0002C315D6	Traes_6BL_A512096D7.1	IPR008906 (HAT dimerisation domain, C-terminal), IPR012337 (Ribonuclease H-like domain)
Wht_08433	0.17	0.69	0.67	C2H2-like zinc finger protein	AT1G75710.1	Traes_3B_9E2CA92E7.1	
Wht_04358	0.08	-0.92	1.09	Dehydration-responsive element-binding protein 1B	sp Q8GUW4 DRE1B_ORYSI	Traes_5BL_8D6C8E27F.1	IPR016177 (DNA-binding domain)
Wht_08839	0.02	0.89	-1.39	arginine/serine-rich splicing factor 35	AT4G25500.1	Traes_XX_B21BC2692.1	IPR012677 (Nucleotide-binding, alpha-beta plait)
Wht_56324	0.00	-0.61	-0.52	molecular function unknown	AT2G40820.1	Traes_3AL_0E507A045.1	

Wht_08021	-0.02	0.64	-3.59	WRKY DNA-binding protein 57	AT1G69310.1	Traes_XX_117F5C06F.1	IPR003657 (DNA-binding WRKY)
Wht_16242	-0.12	-0.83	-3.92	Unknown protein		Traes_3AL_1E22507C0.1	
Wht_01535	-0.18	-0.59	-1.76	Transcription factor-like	UniRef100_Q6H7J8		
Wht_00575	-0.18	1.44	-0.02	myb domain protein r1	AT5G67300.1	Traes_XX_B8E67F1C8.1	IPR009057 (Homeodomain-like)
Wht_15754	-0.21	-0.67	0.09	ABSCISIC ACID-INSENSITIVE 5-like protein 2	sp Q9LES3 A15L2_ARATH	Traes_5AL_521868848.1	IPR004827 (Basic-leucine zipper domain)
Wht_15926	-0.28	-0.90	-0.70	Eukaryotic aspartyl protease family protein	AT5G10770.1	Traes_7DL_BD3BB9CB3.1	IPR001461 (Peptidase A1), IPR021109 (Aspartic peptidase)
Wht_01513	-0.38	1.11	-0.97	Ethylene-responsive transcription factor ERF109	sp Q9SZ06 EF109_ARATH	Traes_1AL_A16202A31.1	
Wht_06980	-0.39	0.84	-0.63	basic helix-loop-helix (bHLH) DNA-binding superfamily protein	AT4G37850.1	Traes_4BS_34AF89ACE.1	IPR011598 (Myc-type, basic helix-loop-helix (bHLH) domain)
Wht_43921	-0.42	0.76	0.16	basic helix-loop-helix (bHLH) DNA-binding superfamily protein	AT1G26945.1	Traes_6DL_3F9FA4887.1	IPR011598 (Myc-type, basic helix-loop-helix (bHLH) domain)
Wht_36528	-0.55	-0.38	-4.32	Unknown protein with aspartic-type endopeptidase activity		Traes_XX_C1FAAF0.1	IPR001461. Aspartic_peptidase. IPR001969. Aspartic_peptidase_AS. IPR021109. Peptidase_aspartic_dom.
Wht_27241	-1.18	0.55	-0.33	tRNA (guanine(26)-N(2))-dimethyltransferase	sp Q3TX08 TRM1_MOUSE	Traes_4AS_7C72912D0.1	IPR002905 (tRNA (guanine(26)-N(2))-dimethyltransferase)
Wht_54180	-1.27	0.35	0.52	histone deacetylase 6	AT5G63110.1	Traes_6DS_08E9A4EDB.1	IPR000286 (Histone deacetylase superfamily), IPR023801 (Histone deacetylase domain)
Wht_02798	-1.61	-0.39	-0.82	methyl-CPG-binding domain 10	AT1G15340.1	Traes_5BS_19E54A2E0.1	IPR016177 (DNA-binding domain)
Wht_00649	-1.62	-2.73	-2.43	Zinc finger CCCH domain-containing protein 8	sp Q5ZDJ6 C3H8_ORYSJ	Traes_1DL_AD1D08A18.1	IPR000571 (Zinc finger, CCCH-type)
Wht_08765	-1.64	-0.96	0.24	Zinc finger A20 and AN1 domain-containing stress-associated protein 9	sp Q7Y1W9 SAP9_ORYSJ	Traes_2DL_C9D102B1D.1	IPR000058 (Zinc finger, AN1-type), IPR002653 (Zinc finger, A20-type)
Wht_36685	-1.87	0.49	-3.88	Calmodulin-binding transcription activator 3	sp Q8GSA7 CMTA3_ARATH	Traes_XX_16C919FDB.1	IPR000048 (IQ motif, EF-hand binding site), IPR005559 (CG-1 DNA-binding domain), IPR013783 (Immunoglobulin-like fold), IPR014756 (Immunoglobulin E-set), IPR020683 (Ankyrin repeat-containing domain), IPR027417 (P-loop containing nucleoside triphosphate hydrolase)
Wht_23848	-1.94	-4.42	-5.84	Ankyrin repeat family protein	AT3G04710.1	Traes_4DS_D39C3F0D2.1	IPR020683 (Ankyrin repeat-containing domain)
Wht_09849	-2.07	0.37	0.52	Zinc finger CCCH domain-containing protein 14	sp Q7F8R0 C3H14_ORYSJ	Traes_7BL_342CAC6CE.1	IPR000571 (Zinc finger, CCCH-type), IPR004087 (K Homology domain)
Wht_20075	-2.22	-0.44	-0.72	growth-regulating factor 3	AT2G36400.1	Traes_XX_4CBABEE02.1	IPR014977 (WRC), IPR014978 (Glutamine-Leucine-Glutamine, QLQ)
Wht_07567	-2.56	0.72	-1.81	Mitochondrial transcription termination factor family protein	AT5G07900.1	Traes_6DS_5878FA87F.1	IPR003690 (Mitochondrial transcription termination factor-related)
Wht_13212	-3.60	-2.12	-2.87	Ethylene-responsive transcription factor 11	sp Q9C5I3 ERF76_ARATH	Traes_3B_82E1F5484.1	IPR016177 (DNA-binding domain)
Wht_52321	3.56	2.35	1.94	NAC domain-containing protein 68	UniRef100_Q339F9		IPR003441. NAC-dom.
Wht_14606	3.54	1.25	0.54	Ethylene-responsive transcription factor 9	sp Q9FE67 ERF80_ARATH	Traes_6DL_7B2EC9B84.1	IPR016177 (DNA-binding domain)
Wht_13766	2.83	1.02	1.41	Dehydration-responsive element-binding protein 1E	sp A2XWL6 DRE1E_ORYSI	Traes_2BL_6FDBA749E.1	
Wht_54507	2.25	-0.22	-0.97	XH/XS domain-containing protein	AT1G15910.1	Traes_5DS_871545FA1.1	IPR005379 (Uncharacterised domain XH)
Wht_13696	2.03	0.76	-0.64	basic helix-loop-helix (bHLH) DNA-binding family protein	AT5G56960.1	Traes_3DL_2795DC25B.1	IPR011598 (Myc-type, basic helix-loop-helix (bHLH) domain)

	Wht_28146	0.92	3.59	1.07	zinc-finger protein 2	AT3G19580.1	Traes_5DL_9D713AD9C.1	IPR015880 (Zinc finger, C2H2-like)
	Wht_09571	0.51	0.27	2.78	UPF0496 protein	sp Q9LT84 U496M_ARATH // AT3G19330	Traes_XX_41D93A6EA.1	
	Wht_45191	0.10	-0.86	2.24	Retrotransposon protein, putative, unclassified	UniRef90_Q2QPU3	Traes_2BL_D441EBFA4.1	IPR012337 (Ribonuclease H-like domain)
	Wht_28511	0.01	1.15	2.48	Transcription factor MYC2	sp Q39204 RAP1_ARATH	Traes_XX_AD241834D.1	IPR011598 (Myc-type, basic helix-loop-helix (bHLH) domain), IPR025610 (Transcription factor MYC/MYB N-terminal)
	Wht_16615	-0.13	0.09	2.11	Mitochondrial transcription termination factor family protein	AT5G64950.1	Traes_6AS_3AFC735F7.1	IPR003690 (Mitochondrial transcription termination factor-related)
	Wht_48392	-0.38	0.52	2.50	RNA binding	AT2G43410.2	Traes_XX_973DAA47F.1	IPR012677 (Nucleotide-binding, alpha-beta plait)
	Wht_05310	-1.71	-0.08	3.65	Transcription factor bHLH36	UniRef90_M8CFX8	Traes_4BL_BEF6AF501.1	IPR011598 (Myc-type, basic helix-loop-helix (bHLH) domain)
	Wht_06337	-1.78	-1.54	2.70	MADS-box transcription factor 5	sp A2Y9P0 MADS5_ORYSI	Traes_7BS_7C0E94DFE.1	IPR002487 (Transcription factor, K-box)
	Wht_03507	-2.04	-0.44	3.59	Transcription factor bHLH95	sp Q9FXA3 BH095_ARATH // AT1G49770	Traes_6BS_C53202201.1	IPR011598 (Myc-type, basic helix-loop-helix (bHLH) domain)
Transport and vesicle traffic								
	Wht_36603	1.54	-0.54	-0.84	Vacuolar protein sorting-associated protein 27	sp Q2GS33 VPS27_CHAGB	Traes_1AL_0CF11612B.1	IPR004152 (GAT), IPR008942 (ENTH/VHS)
	Wht_37111	6.55	7.56	6.25	Expressed protein	UniRef100_Q2QVD9		
	Wht_05775	4.55	4.37	3.99	vesicle associated protein	AT3G60600.1	Traes_2DS_8E56CA0E3.1	IPR008962 (PapD-like)
	Wht_46973	4.29	4.87	3.49	Protein transport protein SEC24-2	sp Q875V7 SC242_NAUCC	Traes_1AL_6F832D98C.1	IPR002035 (von Willebrand factor, type A), IPR006895 (Zinc finger, Sec23/Sec24-type), IPR006896 (Sec23/Sec24, trunk domain), IPR006900 (Sec23/Sec24, helical domain)
	Wht_39881	2.87	0.27	-0.06	ABC transporter G family member 19	sp Q9M3D6 AB19G_ARATH	Traes_5BL_3E1A739FF.1	IPR013525 (ABC-2 type transporter), IPR027417 (P-loop containing nucleoside triphosphate hydrolase)
	Wht_36406	2.35	-3.03	2.99	cationic amino acid transporter 9	AT1G05940.1	Traes_6AL_1E68C6606.1	IPR002293 (Amino acid/polyamine transporter I)
	Wht_31240	2.14	2.37	1.58	90 kDa actin-associated protein palladin	UniRef90_UPI000234E381	Traes_2DS_3C2330209.1	
	Wht_39609	2.09	0.24	-0.73	Actin-3	UniRef100_A2XNS1		
	Wht_11252	1.76	-0.78	1.38	MATE efflux family protein	AT3G23560.1	Traes_1DS_4D4EBDB6F.1	IPR002528 (Multi antimicrobial extrusion protein)
	Wht_35056	1.67	-0.14	0.24	lysine histidine transporter 2	AT1G24400.1	Traes_2AL_D952549E8.1	IPR013057 (Amino acid transporter, transmembrane)
	Wht_36112	1.58	0.80	-2.10	Exosome complex exonuclease dis3	sp P37202 DIS3_SCHPO	Traes_5AL_CC6EE2ECC.1	IPR001900 (Ribonuclease II/R), IPR002716 (PIN domain), IPR012340 (Nucleic acid-binding, OB-fold), IPR022966 (Ribonuclease II/R, conserved site)
	Wht_36603	1.54	-0.54	-0.84	Vacuolar protein sorting-associated protein 27	sp Q2GS33 VPS27_CHAGB	Traes_1AL_0CF11612B.1	IPR004152 (GAT), IPR008942 (ENTH/VHS)
	Wht_08369	1.53	0.67	-1.76	Nucleotide-sugar transporter family protein	AT3G11320.1	Traes_2AL_77F3E5201.1	IPR000620 (Drug/metabolite transporter), IPR004853 (Triose-phosphate transporter domain)
	Wht_04681	1.36	-1.50	-1.03	Cycloartenol synthase 1	AT2G07050.1	Traes_6BS_4B87EDB1A.1	IPR018333 (Squalene cyclase)
	Wht_34419	1.35	1.41	0.74	Disease resistance protein (CC-NBS-LRR class) family	AT5G43470.1	Traes_2AS_3478D9D66.1	IPR000767 (Disease resistance protein), IPR027417 (P-loop containing nucleoside triphosphate hydrolase)
	Wht_42167	1.27	-0.55	-2.77	ABC transporter C family member 13	sp Q9SKX0 AB13C_ARATH	Traes_7BS_A38FF94BD.1	IPR011527 (ABC transporter, transmembrane domain, type 1), IPR027417 (P-loop containing nucleoside triphosphate hydrolase)
	Wht_39384	1.16	0.24	-1.07	Plasma membrane ATPase	UniRef100_P83970		

Wht_33320	1.08	-0.05	1.27	nitrate transporter 2:1	AT1G08090.1	Traes_XX_7D456E213.1	IPR011701 (Major facilitator superfamily), IPR016196 (Major facilitator superfamily domain, general substrate transporter)
Wht_49899	0.96	-1.68	-3.07	Extensin	UniRef100_Q41645		
Wht_04299	0.84	-0.69	0.06	Coatomer, beta' subunit	AT1G52360.2	Traes_2DL_A4B16F05D.1	IPR015943 (WD40/YVTN repeat-like-containing domain)
Wht_47316	0.78	-1.15	-0.27	sugar transporter 9	AT1G50310.1	Traes_2AL_E9BFA084F.1	IPR005828 (General substrate transporter), IPR016196 (Major facilitator superfamily domain, general substrate transporter)
Wht_32790	0.75	0.57	1.33	ABC transporter G family member 28	sp Q9FF46 AB28G_ARATH	Traes_2AS_537A8D6B5.1	IPR027417 (P-loop containing nucleoside triphosphate hydrolase)
Wht_20977	0.73	0.17	-3.41	Sulfate ABC transporter	UniRef100_A4Y0H8		
Wht_53119	0.69	1.41	0.05	Syntaxin-132	sp Q8VZU2 SY132_ARATH	Traes_2DS_4299C702E.1	IPR010989 (t-SNARE)
Wht_23461	0.65	-0.02	-2.44	EIN2 (ETHYLENE INSENSITIVE 2); transporter	AT5G03280		
Wht_18851	0.64	-0.78	-2.96	DNA replication helicase, putative	AT1G08840.2	Traes_5DL_F7D935FAF.1	IPR026852 (Probable helicase MAGATAMA 3), IPR027417 (P-loop containing nucleoside triphosphate hydrolase)
Wht_56167	0.64	-0.95	-2.30	Syntaxin-71	sp Q9SF29 SYP71_ARATH	Traes_1AL_12FE5575D.1	IPR000727 (Target SNARE coiled-coil domain)
Wht_55812	0.60	-0.37	-2.92	DMT(Drug/metabolite transporter) superfamily permease	UniRef90_L8M2I2	Traes_4AL_B674B528F.1	IPR000620 (Drug/metabolite transporter)
Wht_32813	0.56	-0.34	-3.35	ABC transporter C family member 9	sp Q9M1C7 AB9C_ARATH	Traes_2DL_E79ECCBC9.1	IPR011527 (ABC transporter, transmembrane domain, type 1), IPR027417 (P-loop containing nucleoside triphosphate hydrolase)
Wht_03984	0.49	-2.31	-1.21	Phosphatidylinositol transfer protein SFH5	sp A5DEQ9 SFH5_PICGU	Traes_1AL_EB198861F.1	IPR001251 (CRAL-TRIO domain), IPR009038 (GOLD)
Wht_39181	0.48	-1.29	-2.52	Sugar phosphate exchanger 2	sp Q8TED4 SPX2_HUMAN	Traes_7DL_F4972CA5C.1	IPR011701 (Major facilitator superfamily), IPR016196 (Major facilitator superfamily domain, general substrate transporter)
Wht_05471	0.42	-0.02	-3.77	ABC transporter G family member 33	sp Q9ZUT8 AB33G_ARATH // AT2G37280	Traes_5DL_35D4870E.1	IPR013525 (ABC-2 type transporter)
Wht_23155	0.27	-0.44	-2.52	ABC transporter, ATP-binding/permease protein	UniRef100_Q73R47		
Wht_02379	0.25	0.81	-0.79	Syntaxin-32	sp Q9LK09 SYP32_ARATH	Traes_3B_247453D3B.1	IPR000727 (Target SNARE coiled-coil domain)
Wht_18384	0.18	-0.34	-3.04	UPI0002C315D6 related cluster	UniRef90_UPI0002C315D6	Traes_6BL_A512096D7.1	IPR008906 (HAT dimerisation domain, C-terminal), IPR012337 (Ribonuclease H-like domain)
Wht_14789	0.16	-0.76	-0.41	Peptide transporter 5 / Nitrate transporter 1;1	AT5G01180.1	Traes_3B_C8389D284.1	IPR000109 (Proton-dependent oligopeptide transporter family), IPR016196 (Major facilitator superfamily domain, general substrate transporter)
Wht_42627	0.14	-0.67	-0.36	MATE efflux family protein	AT3G21690.1	Traes_3DL_529B9DEC3.1	IPR002528 (Multi antimicrobial extrusion protein)
Wht_42670	0.08	-0.74	0.24	Syntaxin/t-SNARE family protein	AT1G27700.1	Traes_4AS_D70D3CAC6.1	IPR010989 (t-SNARE)
Wht_32674	0.06	-0.71	-2.53	Pyruvate kinase family protein	AT3G22960.1	Traes_1AL_0815BD32E.1	IPR001697 (Pyruvate kinase)
Wht_39663	0.05	1.07	-0.24	Nitrate transporter 2.4	AT5G60770.1	Traes_6DS_4F3D1F2D3.1	IPR011701 (Major facilitator superfamily), IPR016196 (Major facilitator superfamily domain, general substrate transporter)
Wht_22985	0.00	-1.06	0.01	Potassium-transporting ATPase B chain 2	sp Q8YSD5 ATKB2_NOSS1	Traes_7DL_DF97DD324.1	IPR001757 (Cation-transporting P-type ATPase), IPR023214 (HAD-like domain)
Wht_17701	0.00	-1.10	-4.57	pleiotropic drug resistance 11	AT1G66950.1	Traes_4DL_7B2DDE265.1	
Wht_29133	-0.01	1.52	0.75	Bidirectional sugar transporter N3	sp P93332 NOD3_MEDTR	Traes_6DS_FABB8D540.1	IPR004316 (SWEET sugar transporter)
Wht_00280	-0.05	1.56	0.22	Mitochondrial substrate carrier family protein / Mitochondrial succinate-fumarate transporter 1	AT5G01340.1	Traes_4BL_2847E4F04.1	IPR002067 (Mitochondrial carrier protein), IPR023395 (Mitochondrial carrier domain)



Wht_18092	-0.06	-0.71	0.05	chloride channel C	AT5G49890.1	Traes_3AS_AA4DE445B.1	IPR001807 (Chloride channel, voltage gated)
Wht_04239	-0.13	2.47	1.22	Solute carrier family 2, facilitated glucose transporter member 3	sp P47843 GTR3_SHEEP	Traes_XX_2AA10F27D.1	IPR005828 (General substrate transporter), IPR016196 (Major facilitator superfamily domain, general substrate transporter)
Wht_05721	-0.15	-0.61	-0.34	UPI0002C3602A related cluster	UniRef90_UPI0002C3602A	Traes_5AS_74806186E.1	IPR022227 (Protein of unknown function DUF3754)
Wht_09256	-0.17	-0.68	3.27	ABC transporter B family member 2	sp Q8LPK2 AB2B_ARATH	Traes_6DL_BA6F2BE81.1	IPR011527 (ABC transporter, transmembrane domain, type 1), IPR027417 (P-loop containing nucleoside triphosphate hydrolase)
Wht_00833	-0.17	0.51	1.96	Mitochondrial substrate carrier family protein /SHS1 (SODIUM HYPERSENSITIVE 1)	AT4G32400.1	Traes_6DS_CA5464FC5.1	IPR002067 (Mitochondrial carrier protein), IPR023395 (Mitochondrial carrier domain)
Wht_05050	-0.26	-0.08	-2.00	Proton-translocating inorganic pyrophosphatase	UniRef100_O82680		
Wht_22676	-0.42	-0.88	-0.48	UPI000234E39F related cluster	UniRef90_UPI000234E39F	Traes_3DS_EA3E17291.1	
Wht_04780	-0.46	-0.37	-1.75	V-type proton ATPase subunit a	sp O13742 VPH1_SCHPO	Traes_2AL_3E61D4DE2.1	IPR002490 (ATPase, V0 complex, subunit 116kDa)
Wht_02386	-0.46	0.26	-2.07	Potassium channel AKT1	sp P0C550 AKT1_ORYSI	Traes_3AL_D426C4603.1	IPR003938 (Potassium channel, voltage-dependent, EAG/ELK/ERG), IPR020683 (Ankyrin repeat-containing domain)
Wht_36102	-1.01	1.77	-5.90	Mitochondrial substrate carrier family protein	AT5G48970.1	Traes_1BL_6F0399802.1	IPR002067 (Mitochondrial carrier protein), IPR023395 (Mitochondrial carrier domain)
Wht_04944	-1.21	-0.27	-1.07	zinc induced facilitator-like 2	AT3G43790.3	Traes_3AS_C25151458.1	IPR011701 (Major facilitator superfamily), IPR016196 (Major facilitator superfamily domain, general substrate transporter)
Wht_14243	-1.30	0.37	-0.03	Magnesium transporter MRS2-C	sp A2XV81 MRS2C_ORYSI	Traes_2BL_E96264564.1	IPR026573 (Magnesium transporter MRS2/LPE10)
Wht_06623	-1.87	0.36	0.35	Phosphatidylinositol transfer protein SFH5	sp Q6C9R9 SFH5_YARLI	Traes_7DL_63118F92C.1	IPR001251 (CRAL-TRIO domain), IPR011074 (CRAL/TRIO, N-terminal domain)
Wht_21941	-1.87	0.96	-2.53	Metal tolerance protein 5	sp Q5NA18 MTP5_ORYSJ	Traes_1BL_3E65FFB6B.1	IPR002524 (Cation efflux protein), IPR027469 (Cation efflux protein transmembrane domain), IPR027470 (Cation efflux protein cytoplasmic domain)
Wht_37398	-2.52	-1.99	-0.73	Glucose/galactose transporter	UniRef100_A3QBZ2		
Wht_04765	2.29	-0.32	-3.27	AP-3 complex subunit beta-2	sp Q9JME5 AP3B2_MOUSE	Traes_3AL_E0ED003C5.1	IPR002553 (Clathrin/coatomer adaptor, adaptin-like, N-terminal), IPR016024 (Armadillo-type fold), IPR026739 (AP complex subunit beta)
Wht_23001	-0.22	-0.98	4.20	exocyst subunit exo70 family protein D1	AT1G72470.1	Traes_5DL_4A78B3650.1	IPR004140 (Exocyst complex protein Exo70), IPR016159 (Cullin repeat-like-containing domain)
Wht_28119	-0.88	-0.13	2.93	Major facilitator superfamily protein	AT4G36790.1	Traes_2DL_559BABFD8.1	IPR011701 (Major facilitator superfamily), IPR016196 (Major facilitator superfamily domain, general substrate transporter)
Wht_27597	-1.84	0.62	3.19	Magnesium transporter NIPA2	sp Q8N8Q9 NIPA2_HUMAN	Traes_XX_8D9A50C0D.1	IPR008521 (Magnesium transporter NIPA)

Table 20. Top 48 entity list with a correlation >0.90 to LHW and a value of Log<sub>2</sub> Fold Change higher than 1.0 at the 11BBCH and lower than -2 at 13BBCH. All entities shown have significant differences between HOSUT24 and Certo at least in one developmental stage according to the transcriptome analysis. Coloured cells indicate statistical differences between the lines. Light blue significant differences at 11BBCH, medium blue at 12BBCH and dark blue at 13BBCH.

ID-code	Similarity	Log <sub>2</sub> gene expression fold change			Description	Protein responsible for description	Best Blast Hit Wheat	InterPRO-IDs
		11BBCH	12BBCH	13BBCH				
Wht_38943	1.00	2.59	0.47	-2.43	LHW, LONESOME HIGHWAY	AT2G27230.1	Traes_6AL_D20E70F28.1	IPR011598 (Myc-type, basic helix-loop-helix (bHLH) domain), IPR025610 (Transcription factor MYC/MYB N-terminal)
Wht_52117	0.99	1.05	0.08	-2.85	multipolar spindle 1	AT5G57880.1	Traes_7DS_35BA212D4.1	
Wht_53483	0.98	1.20	-0.67	-4.45	Zinc finger MYM-type	UniRef90_G7IY07	Traes_4AL_F6A43DB43.1	IPR008906 (HAT dimerisation domain, C-terminal), IPR012337 (Ribonuclease H-like domain), IPR025398 (Domain of unknown function DUF4371)
Wht_43271	0.98	1.73	-0.32	-2.74	Tetratricopeptide repeat (TPR)-like superfamily protein	AT3G04240.1	Traes_5BS_F0734AFDD.1	
Wht_56025	0.98	1.02	0.53	-2.30	histone deacetylase 1	AT4G38130.1	Traes_6DS_402EC38AD.1	IPR000286 (Histone deacetylase superfamily), IPR023801 (Histone deacetylase domain)
Wht_53665	0.98	1.01	0.20	-2.35	NAD-dependent protein deacetylase	sp Q8PQK3 NPD_XANAC	Traes_5DL_84C49FB59.1	IPR003000 (Sirtuin family), IPR026590 (Sirtuin family, catalytic core domain), IPR026591 (Sirtuin family, catalytic core small domain)
Wht_52105	0.98	2.50	0.50	-2.45	Regulator of telomere elongation helicase 1 homolog	sp Q16X92 RTEL1_AEDAE	Traes_5DL_3C9AAAE2D.1	IPR006555 (ATP-dependent helicase, C-terminal), IPR014013 (Helicase, superfamily 1/2, ATP-binding domain, DinG/Rad3-type), IPR027417 (P-loop containing nucleoside triphosphate hydrolase)
Wht_11253	0.97	0.69	-0.63	-3.65	Cyclin B1;4	AT2G26760.1	Traes_4AS_C381CB1A2.1	IPR013763 (Cyclin-like)
Wht_09024	0.97	1.19	0.19	-2.78	Translation initiation factor eIF-2B subunit epsilon	sp P47823 EI2BE_RABIT	Traes_6BL_2B18C9CAD.1	IPR011004 (Trimeric LpxA-like), IPR016024 (Armadillo-type fold)
Wht_23019	0.96	0.59	-0.38	-2.87	Calcineurin B-like protein 1	AT4G17615.1	Traes_1AL_4AB2BF02A.1	IPR001125 (Recoverin)
Wht_33981	0.96	1.41	-0.18	-2.30	Importin subunit beta-4	sp P40069 IMB4_YEAST	Traes_4DL_874B7B04D.1	IPR016024 (Armadillo-type fold)
Wht_26426	0.96	0.53	0.06	-3.70	Processive diacylglycerol glucosyltransferase	sp A8FED1 UGTP_BACP2	Traes_5AL_C1E3FCB4F.1	IPR007235 (Glycosyl transferase, family 28, C-terminal), IPR009695 (Diacylglycerol glucosyltransferase, N-terminal)
Wht_56478	0.96	1.75	0.65	-2.21	General transcription factor IIH subunit I	sp P32780 TF2H1_HUMAN	Traes_XX_D291FC5F8.1	IPR005607 (BSD), IPR027079 (TFIIH subunit Tfb1/p62)
Wht_36550	0.96	1.81	-0.11	-2.98	telomere repeat binding factor 1	AT1G49950.3	Traes_5AS_8756ECB5A.1	IPR009057 (Homeodomain-like), IPR011991 (Winged helix-turn-helix DNA-binding domain)
Wht_02369	0.96	0.15	0.36	-1.82	Cytochrome P450 superfamily protein	AT5G07990.1	Traes_5DS_B9BFD5BEC.1	IPR001128 (Cytochrome P450)
Wht_40499	0.96	1.05	-0.56	-3.93	Auxin transport protein BIG	AT3G02260.1	Traes_5BL_C9FD62D61.1	IPR003126 (Zinc finger, N-recogin), IPR017986 (WD40-repeat-containing domain)
Wht_08338	0.96	0.94	0.13	-1.64	Arf-GAP with GTPase, ANK repeat and PH domain-containing protein 3	sp Q8VHH5 AGAP3_MOUSE	Traes_6DS_E0A326AEE.1	IPR001164 (Arf GTPase activating protein), IPR008973 (C2 calcium/lipid-binding domain, CaLB)
Wht_34905	0.96	0.33	-0.15	-2.73	Retinoblastoma-related 1	AT3G12280.1	Traes_7BS_2CAF57700.1	IPR013763 (Cyclin-like), IPR024599 (Domain of unknown function DUF3452, retinoblastoma-associated)
Wht_22792	0.96	1.08	-0.41	-2.85	Mitosis protein dim1	sp P87215 DIM1_SCHPO	Traes_2AL_FBC16DECF1.1	IPR004123 (mRNA splicing factor, thioredoxin-like U5 snRNP), IPR012536 (Thioredoxin-like fold)
Wht_09096	0.96	1.35	-0.06	-2.96	kinesin-like protein 1	AT3G44730.1	Traes_3DL_DF48B3591.1	IPR001715 (Calponin homology domain), IPR001752 (Kinesin, motor domain), IPR027417 (P-loop containing nucleoside triphosphate hydrolase), IPR027640 (Kinesin-like protein)
Wht_23247	0.95	-2.90	-4.09	-5.07	Ankyrin repeat family protein	AT3G04710.1	Traes_4BS_ED5BCA38E.1	IPR011990 (Tetratricopeptide-like helical), IPR020683 (Ankyrin repeat-containing domain)

Wht_45189	0.95	1.23	-0.06	-3.10	NAD(P)-binding Rossmann-fold superfamily protein	AT5G58490.1	Traes_5BL_D5FFA0E4D.1	IPR01509 (NAD-dependent epimerase/dehydratase), IPR016040 (NAD(P)-binding domain)
Wht_02368	0.95	-0.70	0.58	-2.08	Cytochrome P450 superfamily protein	AT5G07990.1	Traes_5AS_D06CE8CE5.1	IPR001128 (Cytochrome P450)
Wht_05307	0.95	0.45	-0.04	-2.95	Cell division cycle and apoptosis regulator protein 1	sp Q8IX12 CCAR1_HUMAN	Traes_4BL_4D49C13C4.1	IPR01992 (EF-hand domain pair), IPR025224 (DBC1/CARP1), IPR025954 (DBC1/CARP1 catalytically inactive NUDIX hydrolase domain)
Wht_22164	0.95	1.36	-0.26	-2.50	Acetyl-coenzyme A synthetase	sp Q4ZQG8 ACSA_PSEU2	Traes_5BL_DAE1BD995.1	IPR000873 (AMP-dependent synthetase/ligase)
Wht_15147	0.95	1.09	-0.03	-2.95	DCD (Development and Cell Death) domain protein	AT2G35140.1	Traes_4AS_6C3B8858F.1	IPR013989 (Development/cell death domain)
Wht_51867	0.95	1.51	-0.14	-2.86	Mitotic checkpoint protein BUB3	sp Q1JQB2 BUB3_BOVIN	Traes_2BS_B4CB084ED.1	IPR015943 (WD40/YVTN repeat-like-containing domain)
Wht_23811	0.95	0.54	0.37	-3.03	ATP-citrate synthase subunit 1	sp O93988 ACL1_SORMK	Traes_3AS_205DD4791.1	IPR005810 (Succinyl-CoA ligase, alpha subunit), IPR016102 (Succinyl-CoA synthetase-like)
Wht_51449	0.94	1.07	-0.26	-3.12	Leucine Rich Repeat family protein, expressed	UniRef90_Q7XF95	Traes_XX_6500F2384.1	IPR001611 (Leucine-rich repeat), IPR003591 (Leucine-rich repeat, typical subtype), IPR025875 (Leucine rich repeat 4)
Wht_08771	0.94	1.48	0.13	-2.60	Haloacid dehalogenase-like hydrolase (HAD) superfamily protein	AT3G62040.1	Traes_2AS_341ED2581.1	IPR006439 (HAD hydrolase, subfamily IA), IPR010237 (Pyrimidine 5-nucleotidase), IPR023214 (HAD-like domain)
Wht_14632	0.94	-0.25	0.04	-1.89	H(+)-ATPase 11	AT5G62670.1	Traes_5BS_7DDBE5B89.1	IPR001757 (Cation-transporting P-type ATPase), IPR023214 (HAD-like domain), IPR023298 (P-type ATPase, transmembrane domain)
Wht_52954	0.93	1.10	0.44	-2.64	Transcription initiation factor TFIID subunit 5	UniRef90_M8AQM1	Traes_7BL_E0DACEF5E.1	
Wht_41616	0.93	0.69	-0.62	-2.46	Callose synthase 1	AT1G05570.1	Traes_5AL_1EDC5886C.1	IPR003440 (Glycosyl transferase, family 48), IPR023175 (Vacuolar protein sorting-associate protein Vta1/Callose synthase, N-terminal domain), IPR026899 (1,3-beta-glucan synthase subunit FKS1-like, domain-1), IPR026953 (Callose synthase)
Wht_30355	0.93	1.01	0.46	-3.21	RING finger protein 157	sp Q3TEL6 RN157_MOUSE	Traes_7BL_DA1722C8E.1	IPR013083 (Zinc finger, RING/FYVE/PHD-type)
Wht_26927	0.93	1.24	0.11	-2.45	Chromodomain-helicase-DNA-binding protein Mi-2 homolog	sp O97159 CHDM_DROME	Traes_5DL_52B952D4F.1	IPR027417 (P-loop containing nucleoside triphosphate hydrolase)
Wht_37471	0.93	1.18	0.38	-2.14	serine carboxypeptidase-like 19	AT5G09640.1	Traes_4DS_605378143.1	IPR001563 (Peptidase S10, serine carboxypeptidase)
Wht_25169	0.93	1.14	0.01	-2.19	Lysine-specific demethylase 5B	sp Q80Y84 KDM5B_MOUSE	Traes_7AL_6B05A3754.1	IPR003347 (JmjC domain), IPR004198 (Zinc finger, C5HC2-type), IPR013083 (Zinc finger, RING/FYVE/PHD-type), IPR013637 (Lysine-specific demethylase-like domain)
Wht_01405	0.92	1.00	-0.44	-1.97	LHW, LONESOME HIGHWAY	AT2G27230.1	Traes_4DS_07F394006.1	IPR011598 (Myc-type, basic helix-loop-helix (bHLH) domain), IPR025610 (Transcription factor MYC/MYB N-terminal)
Wht_07108	0.92	1.01	0.16	-1.84	hexokinase 1	AT4G29130.1	Traes_3B_9F7731354.1	IPR001312 (Hexokinase)
Wht_18682	0.92	1.05	-0.43	-3.13	Katanin p80 (WD40-containing) subunit B 1-like protein	UniRef90_Q5ZCG1	Traes_7BS_97AB520FD.1	
Wht_54235	0.91	1.27	-0.75	-3.39	Alpha-aminoadipic semialdehyde synthase	sp Q9SMZ4 AASS_ARATH	Traes_6AL_6D310D2B0.1	IPR005097 (Saccharopine dehydrogenase / Homospermidine synthase), IPR007545 (LOR/SDH bifunctional enzyme, conserved domain), IPR007698 (Alanine dehydrogenase/PNT, NAD(H)-binding domain), IPR007886 (Alanine dehydrogenase/pyridine nucleotide transhydrogenase, N-terminal)
Wht_05471	0.91	0.42	-0.02	-3.77	ABC transporter G family member 33	sp Q9ZUT8 AB33G_ARATH // AT2G37280.1	Traes_5DL_35D48707E.1	IPR013525 (ABC-2 type transporter)
Wht_44473	0.91	2.43	-0.15	-2.50	Phosphoribosylglycinamide formyltransferase 2	sp A5GX22 PURT_SYNR3	Traes_3DS_90E0B2BE9.1	IPR005875 (Phosphoribosylaminoimidazole carboxylase, ATPase subunit), IPR016185 (Pre-ATP-grasp domain)
Wht_25946	0.91	1.39	0.21	-2.10	Chromatin accessibility complex protein 1	sp Q9NRG0 CHRC1_HUMAN	Traes_4AL_14A81F225.1	IPR009072 (Histone-fold)
Wht_20940	0.90	0.61	-0.15	-2.13	myb domain protein 4	AT4G38620.1	Traes_4AL_CC5803BED.1	IPR009057 (Homeodomain-like)

Wht_51317	0.90	0.96	-0.71	-1.78	Callose synthase 1	AT1G05570.1	Traes_3B_798C724AC.1	IPR023175 (Vacuolar protein sorting-associate protein Vta1/Callose synthase, N-terminal domain), IPR026899 (1,3-beta-glucan synthase subunit FKS1-like, domain-1), IPR026953 (Callose synthase)
Wht_55977	0.90	0.17	-0.57	-4.49	SKP1-like protein 4	UniRef90_M8BQZ8	Traes_2AL_E1050558D.1	
Wht_21807	0.90	0.47	1.24	-2.91	Quinone oxidoreductase putative, PIG3	UniRef90_E4PGX7	Traes_4DL_8ED725A6C.1	IPR011032 (GroES-like)
Wht_51217	0.90	1.74	-0.23	-3.47	deoxyhypusine synthase	AT5G05920.1	Traes_3AS_2BB8731EB.1	IPR002773 (Deoxyhypusine synthase)

## VI. Curriculum vitae

### Personal Information

**Name:** María Isabel Mora Ramírez  
**Gender:** Female  
**Marital status:** Married  
**Telephone:** 0176-71054970 (mobile)  
039482-796117 (residence)  
**Nationality:** Costa Rican  
**Place of birth:** Costa Rica  
**Date of birth:** April 8th 1982  
**Address:** Finkenweg 2, 06466 Stadt Seeland OT Gatersleben  
**e-mail:** moram@ipk-gatersleben.de  
isamora@gmail.com

### Education

**IPK-GATERSLEBEN** PhD in the topic: “Impact of increased sucrose uptake  
October 2011-to date capacity on plant development and productivity-  
Ag. Seed Development comprehensive characterization of HOSUT transgenic  
winter wheat lines”

**UNIVERSITY OF COSTA  
RICA** M.Sc. Agricultural Sciences and Natural Resources -  
2005-2010 Biotechnology (hon.). Thesis: Isolation and *in vitro*  
culture of viable *Ficus carica* L. protoplasts

**COSTA RICA INSTITUTE OF  
TECHNOLOGY** B.Sc. Biotechnology Engineering  
2000-2004

**SCIENTIFIC HIGH SCHOOL  
OF COSTA RICA** High School degree (hon.)  
1998-1999

### Professional experience

**CIGRAS** (Grains and Seeds Research Centre) Lecturer in the courses Plant physiology  
University of Costa Rica, 2010-2011 (laboratory) and Agricultural technology

**CIGRAS** (Grains and Seeds Research Centre) Laboratory technician and research assistant  
University of Costa Rica, 2006-2010 for the Biotechnology area of the research  
centre

## Peer reviewed publications

**Isolde Saalbach, Isabel Mora-Ramírez, Nicola Weichert; Franka Andersch, Georgia Guild, Herbert Wieser, Peter Koehler, James Stangoulis, Jochen Kumlehn, Winfriede Weschke, Hans Weber.** (2014). Increased grain yield and micronutrient concentration in transgenic winter wheat by ectopic expression of a barley sucrose transporter. *Journal of Cereal Science*. **60**:75-81.

## Participation in scientific conferences during the PhD study

### Oral presentation

Isabel Mora-Ramírez, Isolde Saalbach, Hans Weber, Udo Seiffert, Jochen Kumlehn, Winfriede Weschke. February 09-12, 2014. Transgenic winter wheat ectopically expressing a barley sucrose transporter exhibits enhanced root growth accelerated development and increased yield. *Translational Cereal Genomics VISCEA*, Vienna, Austria.

### Poster presentations

Isabel Mora-Ramírez, Isolde Saalbach, Hans Weber, Udo Seiffert, Jochen Kumlehn, Winfriede Weschke. September, 2013. Vegetative growth characteristics of transgenic winter wheat lines with ectopic expression of a barley sucrose transporter. Institute's Day, IPK-Gatersleben, Germany.

Isabel Mora-Ramírez, Isolde Saalbach, Hans Weber, Jochen Kumlehn, Winfriede Weschke. June 29-July 3, 2014. Transgenic winter wheat expressing a barley sucrose transporter exhibits increased grain yield and accelerated plant development. *EUCARPIA Cereal Section and I•T•M•I Conference*, Wernigerode, Germany.

Isabel Mora-Ramírez, Isolde Saalbach, Mohammed-Reza Hajirezaei, Udo Seiffert, Jochen Kumlehn, Hans Weber, Winfriede Weschke. October, 2015. Altered sucrose metabolism and auxin signalling are responsible for increased lateral root branching in HOSUT winter wheat seedlings. Institute's Day, IPK-Gatersleben, Germany.

\*Underlined author was presenting the work

María Isabel Mora Ramírez  
Gatersleben, den 31.03. 2016

## **VII. Declaration (Eklärung)**

I, María Isabel Mora Ramírez, declare that the submitted scientific work has been completed by me and, that I have not used any other than permitted reference sources or materials or engaged any plagiarism. All the references and the other sources used in the presented work have been appropriately acknowledged in the work. I further declare that the work has not been previously submitted for the purpose of academic examination, either in its original or similar form, anywhere else.

Ich, María Isabel Mora Ramírez, erkläre hiermit, dass die eingereichte wissenschaftliche Arbeit von mir verfasst wurde und ich keine anderen als die erlaubten Quellen oder Hilfsmittel verwendet habe oder irgendein Plagiat begangen habe. Alle Quellen und Literaturangaben wurden als solche in der Arbeit korrekt kenntlich gemacht. Desweiteren erkläre ich, dass die vorliegende Arbeit vorher noch nie zur Begutachtung eingereicht wurde, weder in ihrer jetzigen Form noch in einer ähnlichen. Ich bewerbe mich damit zum ersten Mal um einen Doktorgrad.

María Isabel Mora Ramírez  
Gatersleben, den 31.03.2016

## **VIII. Acknowledgments**

The accomplishment of my PhD project would not have become true without the help of several colleagues, friends and family who offered me their support, guidance and trust.

In first place, I would like to thank Dr. Winfriede Weschke, Dr. Hans Weber and Prof. Thomas Altmann for accepting me as a PhD student in the Seed Development group and Molecular Genetic Department and for providing a productive and trustful environment, in which, together with their tutoring, I developed my project

I would like to thank the DAAD, IPK-Gatersleben and the University of Costa Rica for financing my PhD project.

My most sincere gratitude to Dr. Isolde Saalbach for her guidance and support during most of my project. I would also like to thank Petra Hoffmeister, who gave me excellent technical assistantship during the first stages of my work. I am also very grateful for the support provided by Dr. Jochen Kumlehn also during the early stages of my work.

I would like to thank Dr. Johannes Thiel, Dr. Volodymyr Radchuk, Dr. Ruslana Radchuk, Dr. Götz Hensel, Dr. Mohammad-Reza Hajirezaei, Dr. David Riewe and Dr. Stephan Kohl, for their advices, training and help. I am most grateful with Prof. Dr. Udo Seiffert and his Research group at the Fraunhofer IFF in Magdeburg for their help in the lateral root analysis of my wheat plants.

I would also like to thank the technical assistants of the Seed Development, Stress Genomics and Plant Reproduction groups who helped me and guided me through several techniques and helped me performed them. Thank you Heiko, Katrin, Sussane, Angela Stegman, Angela Schwarz, Mandy and Andreas.

I want to express my gratitude to Mr. Enk Geyer and the gardeners for their excellent care of my wheat plants.

I would also like to thank my special people, my family in Costa Rica whose love and support always cheer up my life, Paride who is always in my heart and whose unconditional love and support keeps me going and I would also like to thank my new family in Italy for their support.

Thanks to my friends from who I have learned so much and laughed so much, and hope to continue doing so.